AD NUMBER

AD881769

NEW LIMITATION CHANGE

TO

Approved for public release, distribution unlimited

FROM

Distribution authorized to U.S. Gov't. agencies only; Proprietary Information; 15 DEC 1970. Other requests shall be referred to Naval Air Systems Command, Washington, DC 20360.

AUTHORITY

NAVAIR ltr, 3 Oct 1973

RDR 1626-5

Hot Corrosion of Coated Superalloys in a Gas Turbine Environment

Final Report

15 December 1970

V.S. Moore
A.R. Stetson

Prepared For
Department of the Navy
Naval Air Systems Command (AIR-53674)
Contract No. N00019-68-C-0532
Washington, D.C.

~~Distribution of this document is unlimited.~~

SOLAR
DIVISION OF INTERNATIONAL HARVESTER COMPANY
2200 PACIFIC HIGHWAY SAN DIEGO, CALIFORNIA 92112

NOTICE

This report was prepared as an account of Government sponsored work. Neither the United States, nor the Department of the Navy, Naval Air Systems Command (NASC), nor any person acting on behalf of NASC:

A.) Makes any warranty or representation, expressed or implied, with respect to the accuracy, completeness, or usefulness of the information contained in this report, or that the use of any information, apparatus, method, or process disclosed in this report may not infringe privately owned rights; or

B.) Assumes any liabilities with respect to the use of, or for damages resulting from the use of any information, apparatus, method or process disclosed in this report.

As used above, "person acting on behalf of NASC" includes any employee or contractor of NASC, or employee of such contractor, to the extent that such employee or contractor of NASC, or employee of such contractor prepares, disseminates, or provides access to, any information pursuant to his employment or contract with NASC, or his employment with such contractor.

RDR 1626-5

Hot Corrosion of Coated Superalloys in a Gas Turbine Environment

Final Report

15 December 1970

V.S. Moore
A.R. Stetson

Prepared For
Department of the Navy
Naval Air Systems Command (AIR-53674)
Contract No. N00019-68-C-0532
Washington, D.C.

~~Distribution of this document is unlimited~~

SOLAR
DIVISION OF INTERNATIONAL HARVESTER COMPANY
2200 PACIFIC HIGHWAY SAN DIEGO, CALIFORNIA 92112

FOREWORD

This report was prepared in the Research Laboratories of the Solar Division of International Harvester Company, San Diego, California under United States Naval Air Systems Command Contract N00019-68-C-0532 and covers all work performed between 3 July 1968 and 30 November 1970.

Mr. Samuel Goldberg of the Naval Air Systems Command is the technical program manager. Solar professional personnel participating in the program are Mr. Victor S. Moore, Principal Engineer; Mr. Harold A. Cook, Support Engineer; Mrs. M. E. Gulden, Examination of Fracture Surfaces; and Mr. Alvin R. Stetson, Program Director.

Special recognition is given to the Misco Division of the Howmet Corporation, Allvac Corporation and to the Special Metals Corporation who are supplying the alloys to be used in the program and to the following companies who have agreed to permit the evaluation of their coatings in the program:

- Misco Division of Howmet
- General Electric Company, Large Jet Engine Division
- Pratt & Whitney Division of United Aircraft Corporation
- Allison Division of General Motors Corporation
- Chromizing Corporation, a subsidiary of Chromalloy American Corporation
- Alloy Surfaces Company, Inc.

The Solar program reference number is RP 6-3019-7 and report reference number is RDR 1626-5.

ABSTRACT

The final results of a Hot Corrosion Rig Test Evaluation of 45 coating-alloy combinations are presented. Alloys included in the program were B1900, Inco 713C, IN-100, Rene' 41, SEL-15, U-700, U-710, MAR-M-246, WI-52 and X-40. Rig tests were performed for up to 150 hours at 1650°F and 1800°F on nickel-base alloys and 1800°F and 2000°F on cobalt-base alloys in a high-velocity environment obtained from the combustion of JP-5 fuel and air and ingestion of 35 parts sea salt per one million parts air.

The coatings tested (1) were commercially available, (2) were essentially βNiAl or βCoAl with numerous secondary phases, and (3) were formed from the combination of the reaction of aluminum with the substrate and with elements codeposited with aluminum. One exception was a coating (K) on B1900 which appeared to be a silicide.

Under the conditions of the test, protection could be afforded by at least one of the coatings on the nickel-base alloys for 150 hours at 1650°F and 100 hours at 1800°F. At 1800°F the relatively thin coatings on cobalt-base alloys exhibited poorer protection than coated nickel-base alloys at this temperature. At 2000°F the coatings on WI-52 could not afford protection beyond 60 hours. Performance was only slightly better on the higher-chromium X-40 alloy. The life of coatings closely correlated with thickness on both nickel- and cobalt-base alloys and was strongly influenced by the chromium content of the substrate. Minor additives to the aluminides, notably silicon, also significantly enhanced the performance of the aluminide coatings on nickel-base alloys.

The effects of coatings, processing conditions, and long term high temperature exposures on the mechanical properties of the nickel- and cobalt-base alloys were also evaluated. Data are presented on (1) the low-cycle fatigue life of the ten alloys uncoated as-received, uncoated and coated after 500 hours exposure at high temperature, and, (2) the elevated temperature stress rupture properties of the coated alloys after long term exposures and after coating stripping and recoating operations to simulate repair of used blades and vanes.

A single best coating was selected for each alloy based on a combination of hot corrosion resistance, stress rupture and low-cycle fatigue data.

CONTENTS

CONTENTS (Cont)

CONTENTS (Cont)

ILLUSTRATIONS

ILLUSTRATIONS (Cont)

ILLUSTRATIONS (Cont)

ILLUSTRATIONS (Cont)

ILLUSTRATIONS (Cont)

ILLUSTRATIONS (Cont)

ILLUSTRATIONS (Cont)

ILLUSTRATIONS (Cont)

ILLUSTRATIONS (Cont)

ILLUSTRATIONS (Cont)

TABLES

1

INTRODUCTION

The Navy is currently using a large variety of alloys and coatings for turbine blades and vanes in operational aircraft gas turbine engines. Unbiased data is generally lacking which compared (1) the efficacy of the various alloy-coating combinations in resisting a hot corrosion environment, (2) the influence of the coatings on critical mechanical properties, and (3) the potential for reworking or recoating of the components after use. Need for such data is particularly critical at the Naval Air Rework Facilities (NARF), which have the responsibility to rework the engines. To have available all of the potential combinations of alloys and coatings (45 are evaluated in this program) for the numerous engines creates an unbearable burden on inventory costs of the NARF.

An approach that has been used at NARF with notable success in the compressor end of the gas turbine engine has been to inventory coating materials, only, and not coated components. In rework, three types of coatings - silicone, cermet and ceramic - can be used to recoat reworked or new components. Anticipated as an outgrowth of this program will be a similar approach for the turbine end of the engine. A single best coating for cobalt- and nickel-base alloys has been selected in the program. Use of these coatings will markedly reduce alloy-coating combinations required in inventory at the NARF or for logistic reasons, the coating processes can be set up at the NARF.

In this program, ten alloys - Rene' 41, Udimet 700, Inco 713C, B1900, IN-100, U-710, MAR-M-246, SEL-15, X-40 and WI-52 - and three to five coatings per alloy from the generic group - PWA 47, ALPAK, CODEP, UC, MDC, HI-15 and on a limited basis Chromalloy 870 - were evaluated in a series of tests designed to quantitatively differentiate between the coatings and yield the one best overall coating per alloy or alloy type. The program was divided into two phases as noted:

- Phase I - Screening of all coating-alloy combinations in hot corrosion-erosion rig testing

- Phase II - Screening of selected coatings for each alloy in stress-rupture and low-cycle fatigue. In addition, the influence of the recoat operation on mechanical properties was determined.

This final report presents the results of the hot corrosion tests at two temperature levels on all 45 coating-alloy combinations included in the program. From the results of the tests, two coatings per alloy were selected for mechanical property testing in Phase II. Data are also presented to show the effects of the two selected coatings on the mechanical properties of the alloys as-coated, after thermal exposures, and after re-coating operations.

A single best coating was selected for each alloy based on a combination of hot corrosion resistance, stress rupture and low-cycle fatigue data.

2

SUMMARY

The hot corrosion resistance of ten commercially available coatings on eight nickel- and two cobalt-base superalloys under simulated gas turbine operating conditions were determined in this program. Tests were performed at 1650°F and 1800°F on the nickel-base alloys and at 1800°F and 2000°F on the cobalt-base alloys in a high gas velocity (>2000 ft/sec) environment obtained from the combustion of standard grade JP-5 fuel and air, and the ingestion of 35 parts sea salt per one million parts air. All cycles presented in this report were constant at 60 minutes in the flame and 3 minutes in a cool air blast. Specimens were tested for a maximum of 150 hours exposure. Evaluation of coating performance was established by weight change, surface appearance, changes in microstructure and thickness, surface X-ray diffraction and electron beam microprobe analysis.

Eight nickel-base alloys -- B1900, Inco 713C, IN-100, Rene' 41, SEL-15, U-700, U-710, MAR-M-246 and two cobalt-base alloys -- WI-52, X-40 were evaluated. Three to five coatings per alloy from the generic group -- PWA47, ALPAK, CODEP, UC, MDC, HI-15 and on a limited basis, Chromalloy 870 -- were applied to the alloys and subjected to the hot corrosion tests. From these tests, two coatings per alloy were selected for mechanical property testing, i.e., low cycle fatigue and stress rupture tests.

At the request of the NASC Program Manager, a letter code system was assigned to the program coatings. This code is used throughout the program in discussing performance of the coating systems. The alloy and coatings are identified as shown in Table II (Section 3.1.1).

The coatings tested were essentially βNiAl or βCoAl with numerous secondary phases. The coatings were formed from the reaction of coating elements with the substrate and codeposited elements. One coating appeared to be a silicide.

The J coating was evaluated on six of the eight nickel-base alloys and was found to be the best coating for protecting five of these alloys in the hot corrosion environment. The coating was found to consist of aluminum deficient βNiAl, Cr_3Al_2, α-Cr and carbides in the outer area, mainly βNiAl in the denuded zone and βNiAl, $\gamma' Ni_3Al$, carbides

and sigma phase in the diffusion zone. Remnants of the grain boundry carbides from the substrate were observed in the βMAl matrix all the way out to the surface of the coating.

The J coating was the most stable of any of the coatings from a diffusion point of view and was selected for further evaluation in mechanical property tests on six of the eight nickel-base alloys.

The second most hot corrosion resistant coating on the nickel-base alloys was the A coating. This coating was evaluated on all ten of the program alloys in hot corrosion tests. For the nickel-base alloys, the coating was found to consist of βNiAl + Cr_2Al in the outer area, mainly βNiAl in the denuded zone and βNiAl, $\gamma'Ni_3Al$, carbides and finger-like sigma phase in the diffusion zone. At the diffusion zone-substrate interface, a continuous dark band of γ solid solution had developed for the different alloys. This γ band was quite pronounced for IN-100 and SEL-15 alloys.

On the cobalt-base alloys, the A coating was very uniform with white etching, irregular shaped particles dispersed throughout the β-CoAl matrix. A hard white phase had formed at the β-CoAl/substrate interface, which was continuous with some of the carbide phase in the substrate. The coating failed early in the hot corrosion test on WI-52 alloy but exhibited satisfactory performance on the X-40 alloy in these tests. The coating on X-40 alloy was selected for inclusion in the low-cycle fatigue and stress rupture test program.

The thickness of the A coating increased considerably as a consequent of the hot corrosion tests at 1650°F and 1800°F on most of the nickel-base alloys indicating that diffusion instability is the main problem with this coating system. The performance of the A coating, however, was surpassed mainly by the J coating on several alloys and also by the K coating on B1900 and the G coating on Inco 713C. Overall, this coating was rated second best and was selected for mechanical property evaluation on seven of the ten program alloys.

The G coating was tested on only four of the nickel-base alloys, viz., Inco 713C, IN-100, Rene' 41 and SEL-15. The outer layer of the coating consisted of βNiAl matrix, large α-Al_2O_3 inclusions and α-Cr precipitates. The diffusion zone consisted of βNiAl matrix, γ' phase, carbides and sigma phase. At the interface, the predominant phase was γ' with sigma phase platelets.

As a result of the hot corrosion tests, the G coating was rated as the third best coating. The coating exhibited best performance on the Inco 713C and Rene' 41 alloys only and was selected for low-cycle fatigue and stress rupture mechanical property testing on these two alloys.

Coating F was rated fourth in the hot corrosion test program. The coating was applied and tested on six of the eight nickel-base alloys but performance was poor on all alloys except SEL-15 and Rene' 41. On the Rene' 41 alloy, the coating was rated as fair, whereas on SEL-15 alloy, the coating exhibited slightly better performance than coatings C and G.

The coating consisted of βNiAl + large α-Al_2O_3 inclusions and α- Cr precipitates in the outer zone, a line of titanium-rich precipitates near the center of the coating and βNiAl, carbides, and lamellar sigma phase oriented perpendicular to the base-metal interface in the diffusion zone. On the Inco 713C, the presence of a hard, white phase, most likely Ni_2Al_3 was present at the surface of the coating, indicating a high aluminum activity during the coating application cycle. The structure of this coating was similar to that of the G coating except that the line of titanium-rich precipitates in the F coating was not present in the G coating. Also, the α-Al_2O_3 inclusions were somewhat larger in the G coating than in the F coating system.

The F coating was selected for mechanical property testing on the SEL-15 alloy only.

The I coating was evaluated on only two alloys -- B1900 and U-700. This coating was applied extremely thin (0.0018 inch) on both alloys and as a consequence the life obtained in hot corrosion testing was very short. The coating consisted of a βNiAl matrix, refractory metal-rich precipitates and some partially dissolved carbides. There was a tendency to form γ' phase at the interface. This coating was not selected for further evaluation in the mechanical property testing phase of the program.

The C coating was evaluated on six of the eight nickel-base alloys and on both cobalt-base alloys. The microstructure on nickel-base alloys consisted of βNiAl (the major phase) with a very fine dispersion of a chromium rich phase. Carbides were present in the diffusion zone and a fine acicular sigma phase precipitated at the interface. The chromium content of the substrate alloy was largely responsible for observed variations in the phase morphology in the diffusion zone.

In hot corrosion testing, the performance of the C coating on the nickel-base alloys was poor. The predominant failure modes were coating spalling and pinholes. The coating was not selected for further evaluation on the nickel-base alloys in the program.

On the cobalt-base alloys, the C coating consisted of an outer zone of βCoAl matrix with small amounts of a dispersed white phase. The diffusion zone appeared to consist of a γCo matrix, β phase carbides and oxide. In hot corrosion tests, the coating provided excellent protection to the WI-52 alloy at 1800°F, however,

on X-40 alloy the coating exhibited excessive pinhole type failures and was not selected for mechanical property testing on this alloy.

Coating K was evaluated only on B1900 alloy. The phases Cr_3Si and Cr_3Al_2 in a βNiAl matrix were found to be present in the outer area of the coating based on X-ray diffraction analysis. EMP analysis indicated the presence of predominantly a $NiSi_x$ matrix. The silicides in the coating resulted in an extremely high hardness ranging from 1075 KHN in the diffusion zone to 1020 to 1315 KHN in the outer zone of the coating.

The K coating exhibited only fair diffusional stability after the hot corrosion tests. The coating did, however, provide protection on the B1900 alloy comparable to the J coating and was selected for inclusion in the mechanical property test phase of the program.

The B, D and H coatings on the two cobalt-base alloys were similar and consisted of βCoAl, carbides from the substrate, and a chromium-rich, white phase. The coatings on WI-52 all exhibited interface oxides or voids that were not observed in the coatings on X-40 alloy.

Coatings B and C on WI-52 alloy and coatings A and D on X-40 alloy exhibited best overall performance in hot corrosion testing. Coatings D and H on WI-52 and B and H on X-40 alloy were over 80 percent consumed as a result of the 150-hour hot corrosion test at 1800°F. Coating A on WI-52 and C on X-40 were found to spall-off, especially at the trailing edges of the test specimens.

The results of low-cycle fatigue and stress rupture tests performed on the eight nickel-base alloys after exposure in air for 500 hours at 1800°F showed a significant loss in strength due to the coating and oxidation exposures. For the fatigue tests, loss in strength ranged from a low of about 2 percent on MAR-M-245 and B1900 alloys to a high of 30-45 percent on Rene' 41 and U-700 alloys. The other nickel-base alloys all exhibited a decrease in strength of approximately 10 to 15 percent.

The A coating, which exhibited a large amount of sigma phase formation after the long term oxidation exposure, also caused the greatest loss in fatigue life of the six nickel-base alloys on which it was applied. This decrease in life was particularly observed for the Rene' 41 alloy (-45%), U-700 alloy (-33%), and IN-100 alloy (-31%).

The two cobalt-base alloys, WI-52 and X-40, did not show any appreciable loss in fatigue strength due to the coating and long term thermal exposure.

In stress rupture testing, most of the coated nickel-base alloys exhibited a decrease in time to rupture due to the long-term exposure. At 1800°F, the Inco 713C

and B1900 alloys exhibited a decrease after coating and exposing with the average time to rupture (for the two different coatings on each alloy) dropping to about 50 percent of baseline data. The two coatings on IN-100 and U-710 alloys decreased the rupture life by approximately 28 percent, whereas the coated MAR-M-246 and U-700 alloys exhibited a stress rupture life of only 30 percent of the baseline uncoated data.

All coating vendors were able to strip the coatings, either partially or completely, and recoat with the original coating system. The stripping and recoating operations on the alloys after the 500-hour thermal exposure did not appear to have any appreciable added detrimental effects on the stress rupture lives of the nickel-base alloys. Some coating-alloy combinations exhibited an increase in the stress rupture life after the stripping and recoating and others showed a decrease in the rupture life after this recoating operation. No real trend was apparent to show that the one additional thermal cycle from recoating was significantly harmful to the nickel-base alloys, however, the two cobalt-base alloys both exhibited an additional decrease in rupture life due to the stripping and recoating operation.

Based on performance in the hot corrosion tests, stress rupture and low-cycle fatigue tests, the best overall performing coating was selected for each of the substrate alloys. These coating alloy combinations were:

Alloy	Best Coating	Alloy	Best Coating
B1900	J	U-710	J
713C	J	Rene' 41	G
IN-100	J	SEL-15	A
MAR-M-246	J	X-40	D
U-700	J	WI-52	B or C

The J coating was selected as the best performing coating on six of the eight nickel-base alloys. (The coating vendor declined to apply the coating to Rene' 41 and SEL-15 alloys due to lack of performance data on these two alloys.) The hot corrosion resistance was excellent on U-710, U-700, MAR-M-246, and Inco 713C and good on IN-100 and B1900 alloys. The coating also had the lease affect on the mechanical properties of the alloys.

The A coating, which was initially selected and tested on all ten of the program alloys provided very good protection in the hot corrosion test environment (probably due to the fact it was thicker than the other coatings). However, diffusion instability was more severe than with the other coatings evaluated in the program, and extensive formation of sigma phase was also apparent after long term oxidation exposure. The A coating also caused the largest drop in fatigue life of the six nickel-

base alloys on which it was evaluated. Performance was best in the hot corrosion and stress rupture tests and rated good in the low-cycle fatigue tests on SEL-15 alloy only.

The G coating was selected for Rene' 41 alloy based mainly on performance in the low-cycle fatigue tests. The coating caused less reduction in mechanical properties than the A coating system.

On the cobalt-base alloys, the D coating was selected for the X-40 alloy and the B or C coatings for the WI-52 alloy. The D coating on X-40 was below the specified minimum thickness, only 0.0011 inch, however, performance in the hot corrosion test environment was rated fair to good. The coating had less influence on the mechanical properties of the alloy than the A coating and was therefore selected as the better coating system.

Both the B and C coatings were selected as the best coatings for WI-52 alloy. Performance in the hot corrosion tests was slightly better for the C coating, but in the stress rupture tests the B coating was rated somewhat higher. In low-cycle fatigue, neither coating had an adverse effect on the fatigue life of the alloy. Both B and C coated WI-52 alloy specimens exhibited approximately the same fatigue strength as the uncoated-exposed alloy specimens.

3

PHASE I - HOT CORROSION TESTING

Phase I was organized and divided into several work tasks. These tasks were:

- Procurement of test specimens (alloys and coatings)
- Receiving inspection tests
- Hot corrosion tests
- Diagnostic evaluation of specimens
- Selection of two best coatings per alloy for Phase II testing

A detailed discussion of these items is presented in the following paragraphs.

3.1 TEST SPECIMENS AND TESTING TECHNIQUES

3.1.1 Test Specimens

A simulated airfoil specimen (Fig. 1) was selected for the hot corrosion tests in Phase I. The blade design simulates the dimensions of a turbine blade much more closely than the commonly used wedge, yet it is only slightly more difficult to investment cast.

Based on competitive bidding, delivery, and availability of casting patterns, Misco Division of Howmet Corporation was selected as the casting vendor for all ten program alloys.

The cast alloys did not receive any heat treatment and were used in the as-cast condition throughout the program.

The chemical compositions of these alloys are shown in Table I.

Selection of the protective coatings for use in this program was made by the NASC. The coatings ranged from a maximum of six (on B1900 alloy) to three on MAR-M-246 and U-710 alloys.

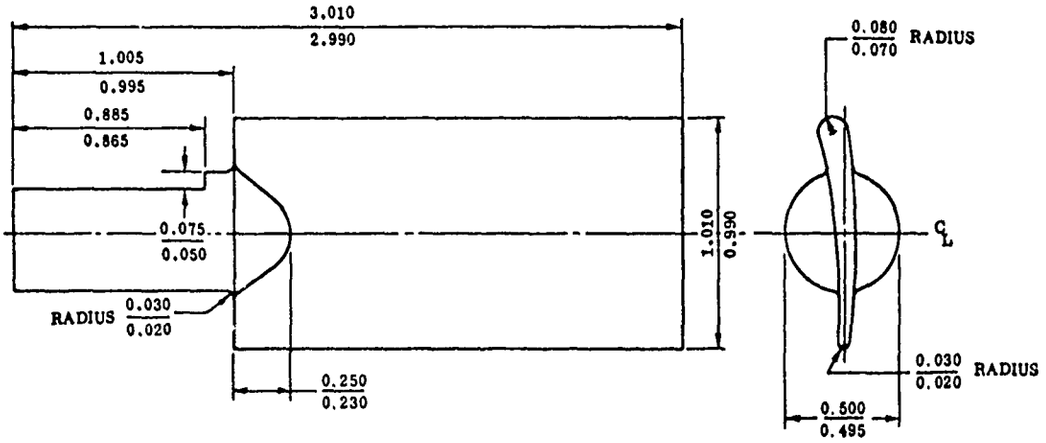

ALL DIMENSIONS IN INCHES

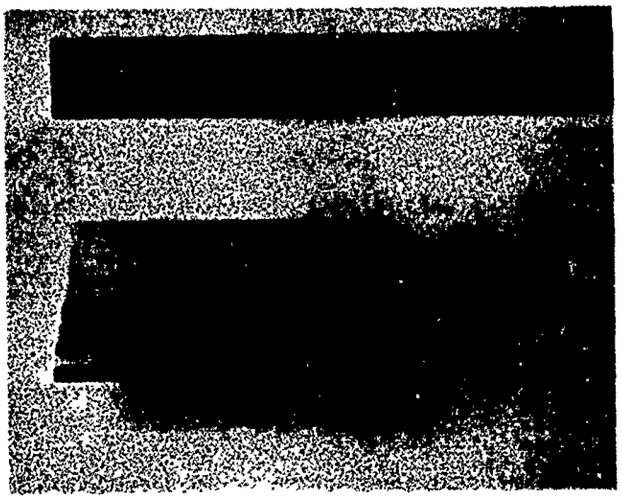

FIGURE 1. SIMULATED AIRFOIL SPECIMEN

TABLE I

CHEMICAL ANALYSES OF PROGRAM ALLOYS

Cast Alloys[1]	Heat No.	Composition (Weight Percent)												
		Ni	Co	W	Mo	Ta	Cb	Cr	V	C	Al	Ti	Zr	B	Other
B1900	MG/RG 224	Bal	9.99	---	6.00	4.48	---	8.26	---	.081	6.07	1.00	.09	.010	.18 Fe
B1900	MG 245	Bal	10.30	---	5.95	4.23	0.1	8.50	---	.093	5.85	1.02	.09	.011	.21 Fe
713C	RW 551	Bal	0.22	---	4.55	---	2.27	13.80	---	.135	5.85	0.78	.10	.010	.12 Fe
713C	RW 553	Bal	0.20	---	4.57	---	2.35	13.80	---	---	5.74	0.79	.10	.007	---
IN-100	UB 026	Bal	15.40	---	3.17	---	---	10.50	.76	.16	5.49	4.34	.16	.013	.12 Fe
IN-100	UB 030	Bal	15.30	---	3.16	---	---	10.50	.76	.178	5.27	4.38	.06	.012	.11 Fe
MAR-M246	KB 001	Bal	10.10	10.00	2.69	1.39	---	8.69	---	.144	5.47	1.52	.05	.011	.08 Fe
René 41	RP 106	Bal	11.30	---	9.79	---	---	19.20	---	.078	1.56	3.30	---	.006	.35 Fe
SEL-15	KA 004	Bal	13.70	1.9	6.18	---	0.45	10.70	---	.057	5.51	2.18	.10	.014	.15 Fe
U-700	RJ 200	Bal	14.90	---	4.10	---	---	14.30	---	.06	4.25	3.42	.04	.015	.22 Fe
U-710	KC 001	Bal	14.60	---	3.10	---	---	17.90	---	.07	2.50	4.84	---	.020	.10 Fe
WI-52	MF 268	0.47	Bal	10.90	---	---	1.81	20.70	---	.488	---	---	---	---	2.09 Fe
WI-52	MF 272	0.37	Bal	11.00	---	---	1.82	20.80	---	.452	---	---	---	---	2.13 Fe
X-40	CB 007	10.70	Bal	7.54	---	---	---	25.80	---	.487	---	---	.06	.003	.21 Fe
Wrought Alloys[2]															
U-700	6-3270	Bal	18.70	---	4.95	---	---	15.10	---	.06	4.49	3.44	.05	.014	.15 Fe
René 41	6711	Bal	11.05	---	9.73	---	---	18.90	---	.08	1.53	3.13	---	.005	1.17 Fe

(1) Cast specimens analyses by Misco

(2) Wrought alloys analyses by Special Metals Corp. (U-700), and Allvac (René 41)

TABLE II

SPECIMEN IDENTIFICATION CODE*

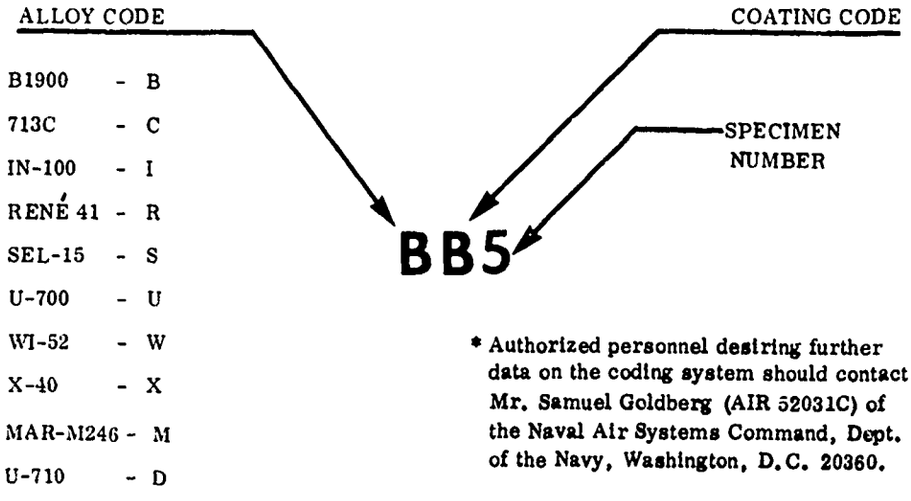

* Authorized personnel desiring further data on the coding system should contact Mr. Samuel Goldberg (AIR 52031C) of the Naval Air Systems Command, Dept. of the Navy, Washington, D.C. 20360.

At the request of the NASC Program Manager, a letter and code system was assigned to the program coatings. This system will henceforth be used throughout the report in discussing performance of the coating systems. The alloys and coatings are identified as shown in Table II.

Surface Finish and General Appearance of Coatings

The simulated airfoil blades were supplied to the coating vendors ready for coating, i.e., all burrs and casting lines were removed and the sharp edges well radiused. This was accomplished by tumbling the specimens for 24 hours in a large SWECO vibrating finisher using several sizes of coarse tumbling aggregate and water. After tumbling, the specimens were weighed at Solar and shipped to the coating vendors. It was assumed that the vendor's cleaning process would introduce a negligible error in the coating weight gain measurements.

A summary of the results of the profilometer surface finish measurements made on all specimens before and after coating in shown in Table III. Also included in the table is the mean change in surface roughness due to the application of the coating.

The average surface finish of the cast alloys ranged from 12 to 20 microinches. These surfaces are considerably smoother than most as-cast surfaces (60 microinches) because of the tumbling operation previously performed.

TABLE III

SUMMARY OF SURFACE FINISH

Alloy	Spec. Ident. Code	SURFACE FINISH (μin. rms)						Average Change (μin. rms)
		Before Coating			After Coating			
		Max.	Min.	Avg.	Max.	Min.	Avg.	
B1900	BA	16	15	15.3	50	35	42.5	+27.2
	BC	17	13	15.3	37	28	32.8	+17.5
	BF	17	14	15.3	65	60	60.8	+45.3
	BI	17	15	15.7	60	45	50.0	+33.7
	BJ	17	14	15.0	90	50	67.5	+52.5
	BK	16	15	15.5	180	150	159	+143
713C	CA	18	15	16.2	45	35	40.0	+23.8
	CC	20	15	16.7	48	42	44.8	+28.1
	CF	18	13	16.3	70	60	65.0	+48.7
	CG	18	15	15.8	65	50	58.1	+42.0
	CJ	17	16	16.7	125	40	64.2	+47.5
IN-100	IA	17	15	16.7	40	35	36.6	+20.0
	IC	18	15	16.5	45	36	38.0	+21.5
	IF	18	13	16.0	60	45	51.7	+35.7
	IG	17	12	14.5	65	50	58.1	+43.5
	IJ	17	15	15.5	90	40	64.2	+48.7
René 41	RA	20	17	19.2	40	35	38.0	+18.7
	RC	20	17	18.5	50	40	45.8	+27.3
	RF	20	15	17.0	65	55	61.7	+44.7
	RG	20	16	18.3	80	70	75.8	+57.5
SEL-15	SA	15	12	13.8	45	32	37.8	+25.7
	SC	15	12	13.3	42	32	37.8	+24.5
	SF	15	12	13.5	55	50	51.6	+38.2
	SG	16	14	15.0	80	70	76.7	+60.8
U-700	UA	15	12	13.0	75	40	46.6	+35.3
	UC	16	13	14.7	40	32	35.3	+20.6
	UF	15	15	15.0	65	55	59.2	+44.2
	UI	15	13	14.2	55	45	49.0	+35.7
	UJ	15	13	14.7	125	50	64.1	+49.4
WI-52	WA	20	17	18.2	75	50	60.8	+42.7
	WB	19	15	17.5	47	38	41.7	+24.2
	WC	20	17	17.7	40	33	36.3	+18.6
	WD	18	16	17.2	50	45	49.2	+32.0
	WH	19	17	17.8	70	45	55.0	+39.0
X-40	XA	20	15	17.5	70	55	62.5	+44.8
	XB	20	17	19.2	45	37	39.3	+20.1
	XC	20	17	19.2	34	28	32.3	+13.1
	XD	20	18	19.3	55	50	53.3	+34.0
	XH	20	17	19.2	100	60	72.0	+53.0
U-710	DA	15	12	15.2	45	38	40.2	+25.0
	DG	16	12	14.1	80	70	72.2	+58.1
	DJ	15	13	14.5	60	40	46.5	+32.0
M246	MA	18	15	15.5	40	30	35.0	+29.5
	MG	16	14	15.2	90	60	80.2	+65.0
	MJ	15	15	14.8	50	40	45.8	+31.0

Note: + denotes increase in surface roughness

A large increase in surface roughness was exhibited by the G coating on the six nickel-base alloys and the K coating on B1900 alloy. For the G coating, the surface finish ranged from 80 microinches on the MAR-M-246 alloy to 58 microniches on the Inco 713C alloy. The K coating was extremely rough, with several specimens exhibiting a surface finish of 180 microinches. The J coating was also quite rough due to numerous small surface nodules of coating on both the concave and convex surfaces of the blade. The smoothest surface on most of the alloys was exhibited by the C coating.

In general, only the K coating was considered to be excessively rough. As mentioned previously, the as-cast surface roughness averaged 60 microinches for all eight alloys. Only 14 of the 45 coating-alloy combinations exhibited a surface finish slightly greater than the as-cast finish.

With the exception of the J coated specimens, all 270 blades appeared to be adequately coated. There was no spalling observed on any of the specimens; edges and flat surfaces appear extremely well coated. The J coating on 713C, IN-100, B1900 and U-700 alloys exhibited a rough surface with numerous small surface nodules. Several specimens of the H coating on X-40 alloy (XH combination) had a few particles of the pack media adhering to the surfaces.

With the exception of the J coated blades, all other coated specimens appeared to be coated "all over" using a pack process, i.e., the airfoil sections and the round shanks of the blades were coated. The J coating appears to be a slurry spray or dip process. Most of the blade shank was not coated.

Weight Gain Due to Coating

All coating vendors were advised that the coating thickness should be controlled within the following limits:

- Nickel-base alloys: 0.0020 to 0.0035 inch
- Cobalt-base alloys: 0.0015 to 0.0025 inch

Coating thickness was measured on the one specimen submitted for metallographic analysis. This specimen was selected (based on weight gain measurements) as being representative of the average of the six coated specimens of each coating-alloy combination.

A summary of the results of the weight-gain measurements made on all coating-alloy combinations is contained in Table IV. All coating vendors were advised that the specimens were weighed at Solar prior to shipment and would also be reweighed after the coating operation. The B coating vendor notified Solar that their cleaning operation (a dry 100 mesh aluminum oxide blast) removed a substantial amount of

TABLE IV

SUMMARY OF WEIGHT GAIN AND COATING THICKNESS

Specimen Identification Code		Average Coating Thickness (mils) (1)	Average Weight Gain (mg/cm^2) (2)
B1900 Alloy -	BA	3.4	8.3
	BC	2.4	8.1
	BK	3.9	11.1
	BF	2.0	5.5
	BI	1.7	3.8
	BJ (3)	3.0	5.9
713C Alloy -	CA	3.3	7.5
	CC	2.5	8.2
	CF	2.4	5.8
	CG	2.2	2.5
	CJ (3)	3.0	5.9
IN-100 Alloy -	IA	3.0	6.5
	IC	2.3	7.2
	IF	2.0	5.1
	IG	1.6	0.8
	IJ (3)	2.6	5.4
Rene 41 Alloy-	RA	1.9	3.3
	RC	2.9	8.0
	RF (3)	2.2	4.8
	RG	2.0	-2.1
SEL-15 Alloy-	SA	3.3	8.0
	SC	2.7	7.9
	SF	2.0	5.2
	SG	2.0	-1.2
U-700 Alloy -	UA	4.5	6.8
	UC	2.4	7.4
	UF	2.0	5.0
	UI	1.8	6.1
	UJ (3)	2.3	5.5
WI-52 Alloy -	WA	2.2	4.0
	WB (3)	1.8	7.5
	WC	1.9	5.9
	WD	1.4	3.0
	WH	1.4	3.1
X-40 Alloy -	XA	2.6	1.9
	XB (3)	1.5	7.2
	XC	1.3	4.4
	XD	1.1	-19.9
	XH	1.1	3.6
MAR-M-246 Alloy -	MA	2.5	3.3
	MG (3)	2.3	6.6
	MJ (3)	2.9	6.9
U-710 Alloy-	DA	3.0	7.0
	DG (3)	1.7	5.6
	DJ (3)	2.4	6.8

1. Measured metallographically
2. Six specimens per each alloy-coating combination
3. Weight gains supplied by coating vendor
- Denotes specimens lost weight

material (up to 50 milligrams). Therefore, this coating vendor reweighed the specimens after cleaning and prior to the coating operation. The F coating vendor reweighed the Rene' 41 specimens after a coating error and also submitted the adjusted initial weights to Solar along with the coated specimens. The J and K coating vendors also submitted "before coating" weights of the test specimens. Therefore, the data shown in Table III for the WB, XB, RF, BJ, CJ, IJ, UJ, BK, MG, MJ, DG and DJ coating-alloy combinations are considered very valid. All other weight gains may be lower than actual values depending upon the amount of substrate material removed by their cleaning operation. It is apparent that specimens in the CG, IG, RG, SG, MA, and XD coating-alloy combinations had quite a bit of substrate material removed in the cleaning operation. The weight gains were very low and, in three cases (RG, SG and XD), the specimens weighed less after coating than when they were shipped from Solar to the coating vendors. Coating-alloy combination XD must have been coated, stripped and recoated several times in order to exhibit an average weight loss of 20 mg/cm^2 per specimen.

Prior to initiation of the hot corrosion tests, the C coating vendor advised us that this coating had not been optimized for the B1900 alloy and recommended the substitution of another coating (Code K) which had been tested on this alloy. Both the C and K coatings were included in the program after approval by NASC program manager.

3.1.2 Turbine Environmental Simulators

The two Solar gas turbine environmental simulators (burner rigs) used throughout this program are shown in Figures 2 and 3. Design details of these burners are similar in features to those of Solar's modern small commercial gas turbine combustors. A straight-through, can-type combustor is used with atomization from a single fuel nozzle. A water cooled, one-inch diameter stainless steel nozzle is used for long-time trouble-free operation. The combustion chamber inner liner is fabricated from Hastelloy X.

The control console for the simulators is shown in Figure 2. Duplicate controls and measuring equipment are provided for independent operation of each simulator. The major items used to ensure reproducible operation of each rig are:

- Synthetic sea water flowmeters
- Fuel flowmeters
- Airflow measuring equipment
- Slip rings for thermocouple temperature control

Figure 3 shows a close-up of the two simulators. In this setup, note that the two combustors are mounted vertically while the specimen holder rotation motor, drive shaft,

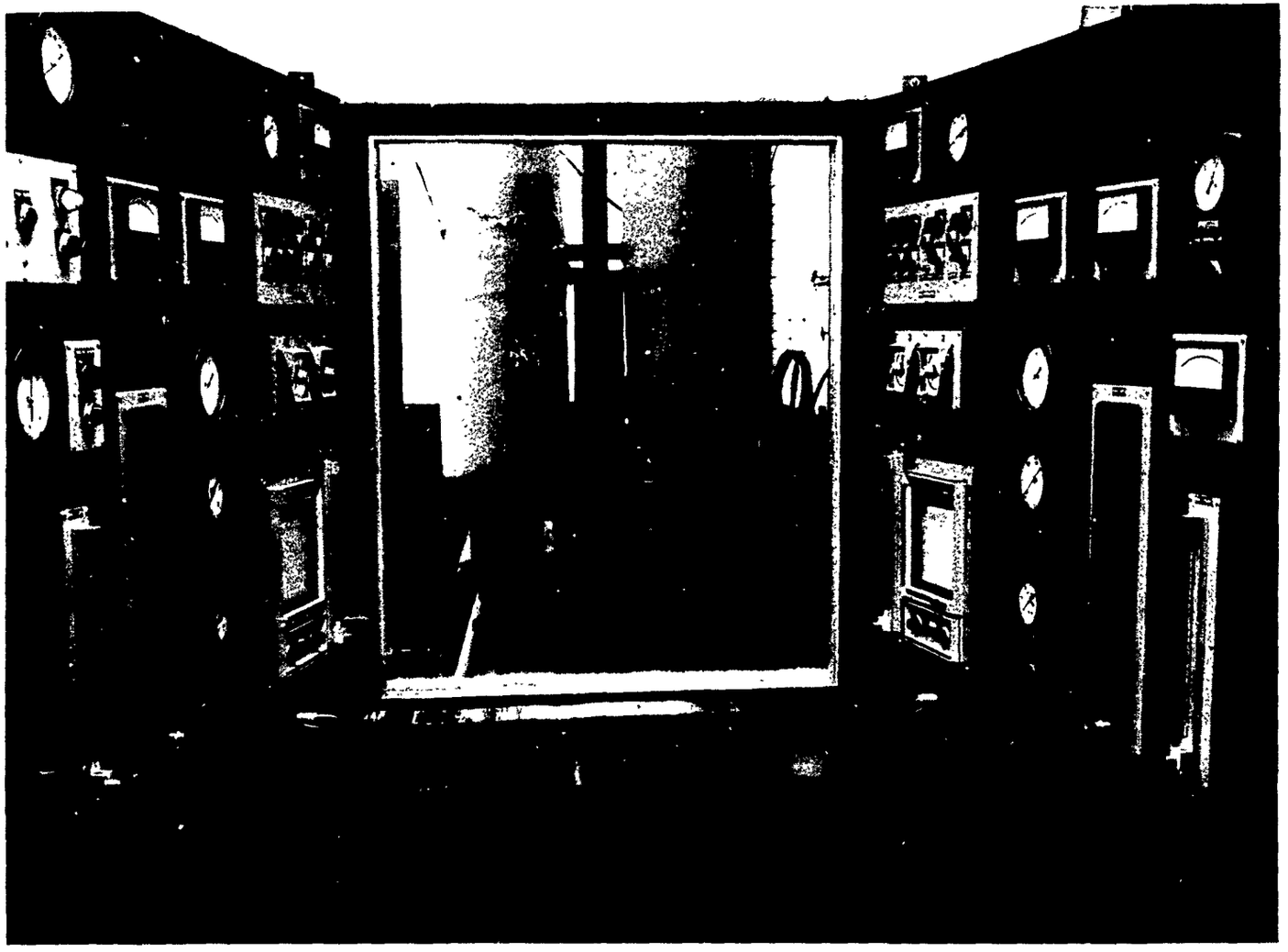

FIGURE 2. CONTROL CONSOLE FOR GAS TURBINE ENVIRONMENTAL SIMULATORS

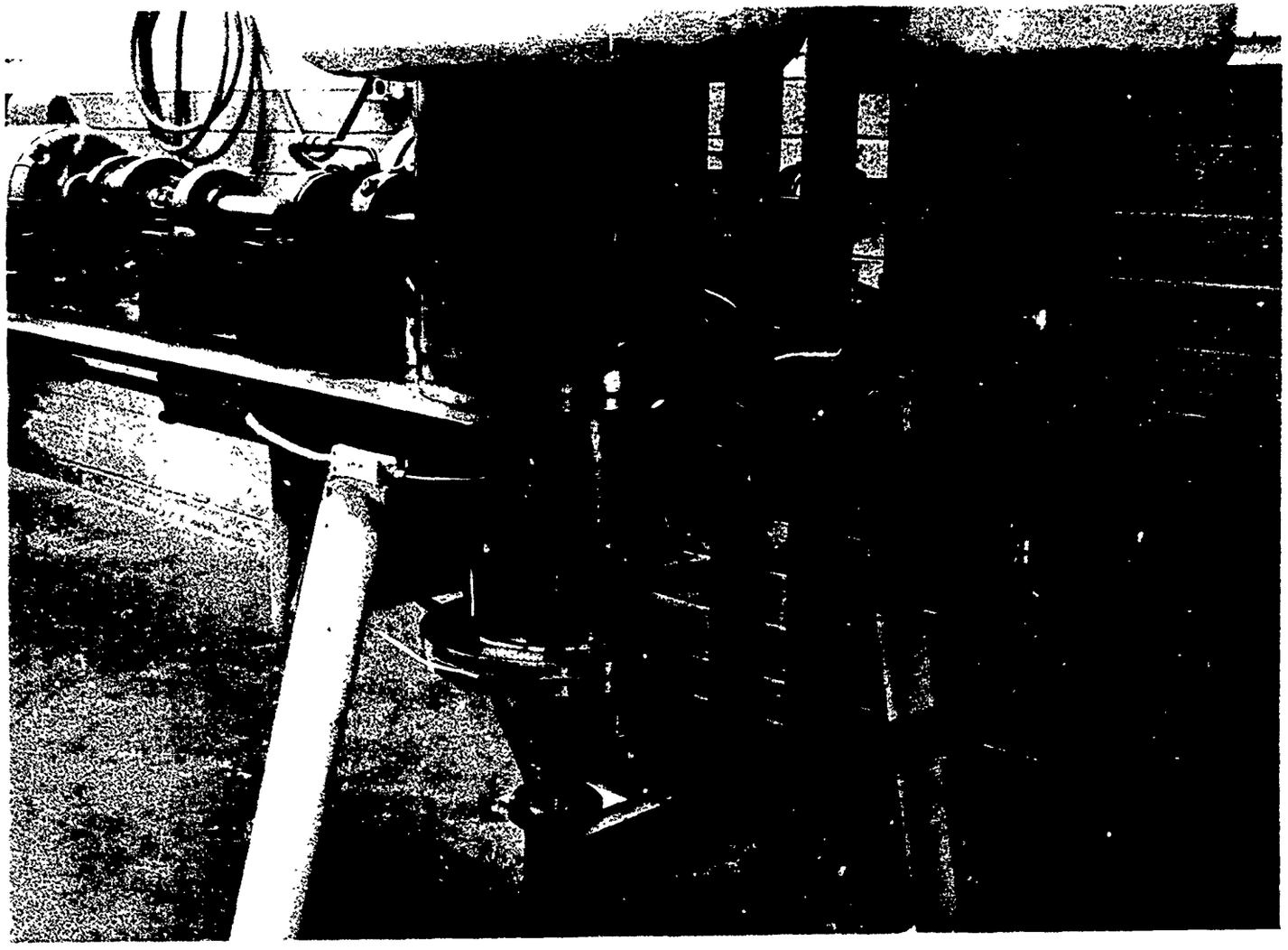

FIGURE 3. GAS TURBINE ENVIRONMENTAL SIMULATORS

and the slip ring assembly are mounted horizontally. The pneumatic piston that cycles the specimen in and out of the hot gas stream are mounted horizontally underneath the table top.

During the rig tests, eight specimens were mounted in a holder which rotated at 1725 rpm. Rotation in the gas stream was required to ensure that all specimens experienced the same test environment. The holder was positioned so that the leading edge of the specimen was one inch from the exit of the nozzle. Tests were performed as follows:

- Standard grade JP-5 fuel (MIL-J-5624G) was used for all tests.
- A synthetic sea water was made (per Federal Test Method Standard No. 151, Method 812), and 35 parts sea salt per one million parts air was injected into the combustion gases.
- Duplicate specimens of uncoated and coated nickel-base alloys were tested at 1650°F and 1800°F. The cobalt-base alloys (both coated and uncoated) were tested at 1800°F and 2000°F. The nozzle exit gas velocity was maintained at Mach 0.85 minimum (>2000 ft/sec) for all tests.

One-hour thermal cycles were used for a total of 150 hours maximum at temperature for each test. Initially, specimens were removed at the end of each 20-hour exposure (20 cycles) for visual examination, cleaning and weighing. This interval was subsequently changed to 30 hours for the coated specimens and 10 to 20 hours for most of the uncoated alloys due to early failures. Photographs of the surface appearance and final weight changes were obtained at the completion of each test.

3.1.3 Temperature Calibrations and Control Methods

Temperature is the major parameter that must be carefully controlled to obtain quantitative, reproducible test results. In the hot corrosion rig tests, control of the specimen metal temperature was effected by automatically adjusting and regulating the fuel flow to the combustor nozzle. Air flow was held constant by means of dome loading, diaphragm-type, high-capacity air regulators.

Specimen metal temperature was continuously monitored, recorded and controlled throughout the test period by means of a thermocouple inserted into a small hole in a test specimen. This hole was electrical discharge machined (EDM) to a diameter of 0.042 inch by 2.0 inches deep through the base of the blade so that the thermocouple tip was at the center of the test section. One specimen in each group of blades (in the holder) was instrumented in this manner with an 0.040-inch diameter

Inconel sheathed, magnesium oxide insulated, chromel-alumel thermocouple. Output of the thermocouple was fed to a slip-ring assembly and then to a potentiometer-type strip chart temperature recorder and three-mode temperature controller. Any deviation between the temperature set point and the specimen temperature was sensed in the temperature recorder-controller, which continuously activated an electric-to-pneumatic converter thereby controlling a pneumatic-operated fuel-flow control valve. Fuel flow was increased or decreased automatically as required to maintain the set temperature.

To determine the temperature distribution and the temperature gradient along the length and width of the airfoil-type specimens, uncoated test specimens were initially instrumented with small thermocouples spot tacked to the concave surface of the blade. This method of temperature calibration did have limitations on accuracy, however, and best results were obtained by actually imbedding a small thermocouple into the airfoil section at a known location. Internal thermocouples were installed in the test blades in the following manner.

- A small groove 0.050 inch wide by 0.050 inch deep was chemically milled into the concave surface of a blade so that the measuring junction of the thermocouple was at a precisely known location (Fig. 4A).

- A 0.040 inch diameter Inconel sheathed thermocouple was inserted into this groove (Fig. 4B).

- The thermocouple junction was spot tacked in place and the entire groove containing the thermocouple sheath was filled by plasma arc spraying with Nichrome powder (Ni-20Cr) (Fig. 4C).

- The concave surface was then reground to the original surface contour (Fig. 4D).

The results of the blade temperature measurements made to establish calibration data for the 1650°F, 1800°F and 2000°F hot corrosion tests are shown in Figures 5, 6, and 7. In these figures, surface temperatures are shown at eleven different locations on the concave surface of a specimen. Prior to initiation of a hot corrosion test, these data were used to determine the temperature gradient across the airfoil and the location of the hottest area of the blade for placement of the internal thermocouple.

In Figure 5B, the data from the internal thermocouples show that the center of the hot zone on the airfoil surface is 3/4 inch down from the tip of the blades. The thermocouple control temperature for this turbine simulator for the 1650°F hot

A

Chem Mill Groove

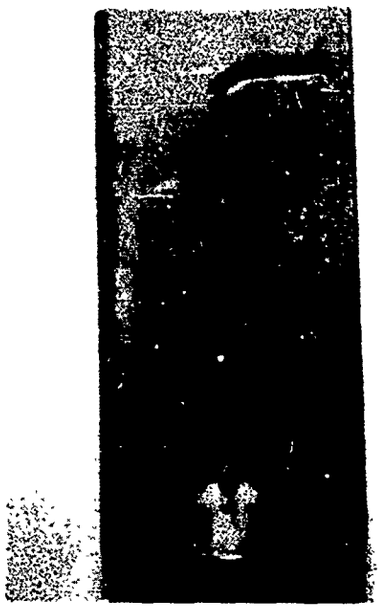

B

Install Thermocouple

C

Plasma Arc Spray Ni-Cr

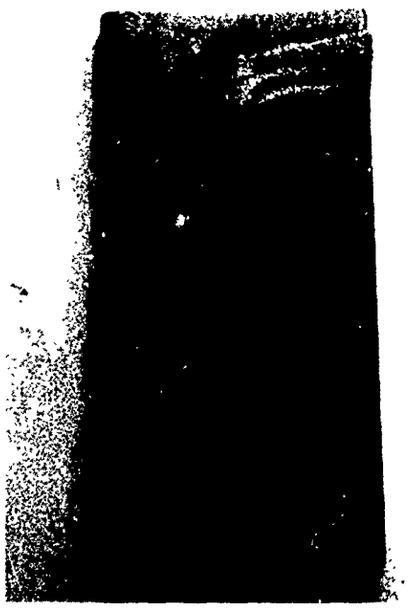

Magnification: 1.5X

D

Clean-Up Surface

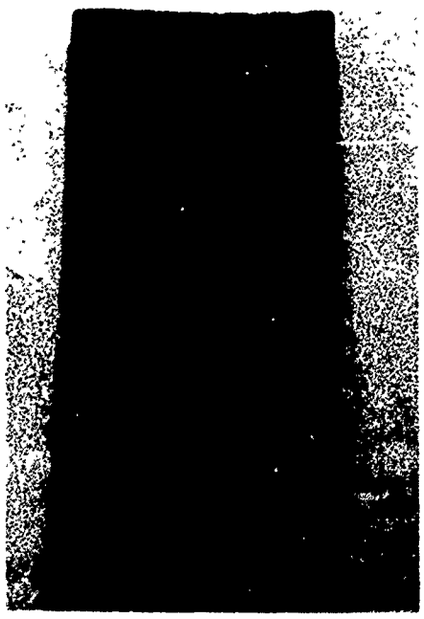

FIGURE 4. METHOD OF IMBEDDING THERMOCOUPLE IN SPECIMEN FOR TEMPERATURE CALIBRATION

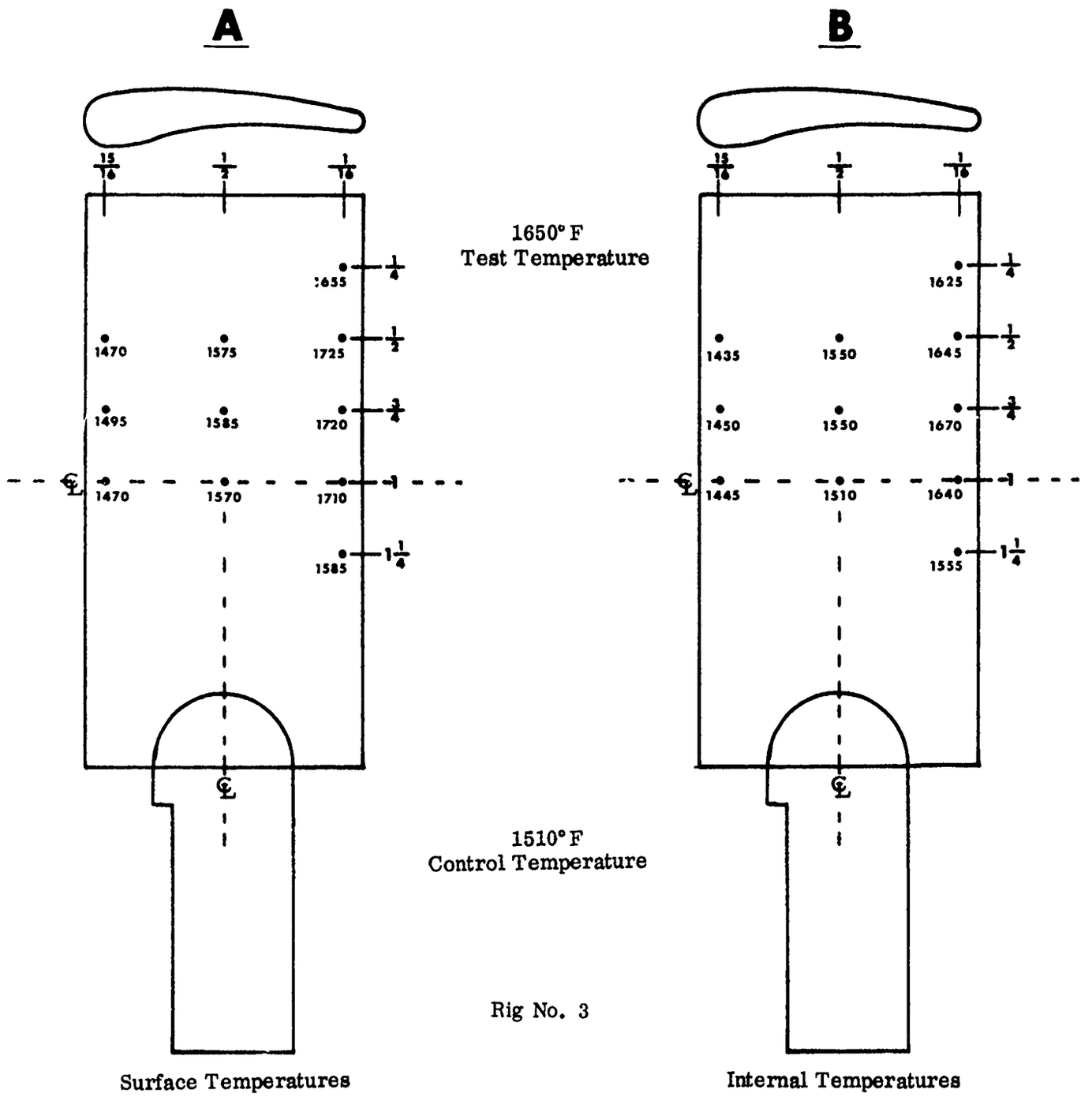

FIGURE 5. SPECIMEN TEMPERATURE DISTRIBUTION FOR 1650° F HOT CORROSION TESTS

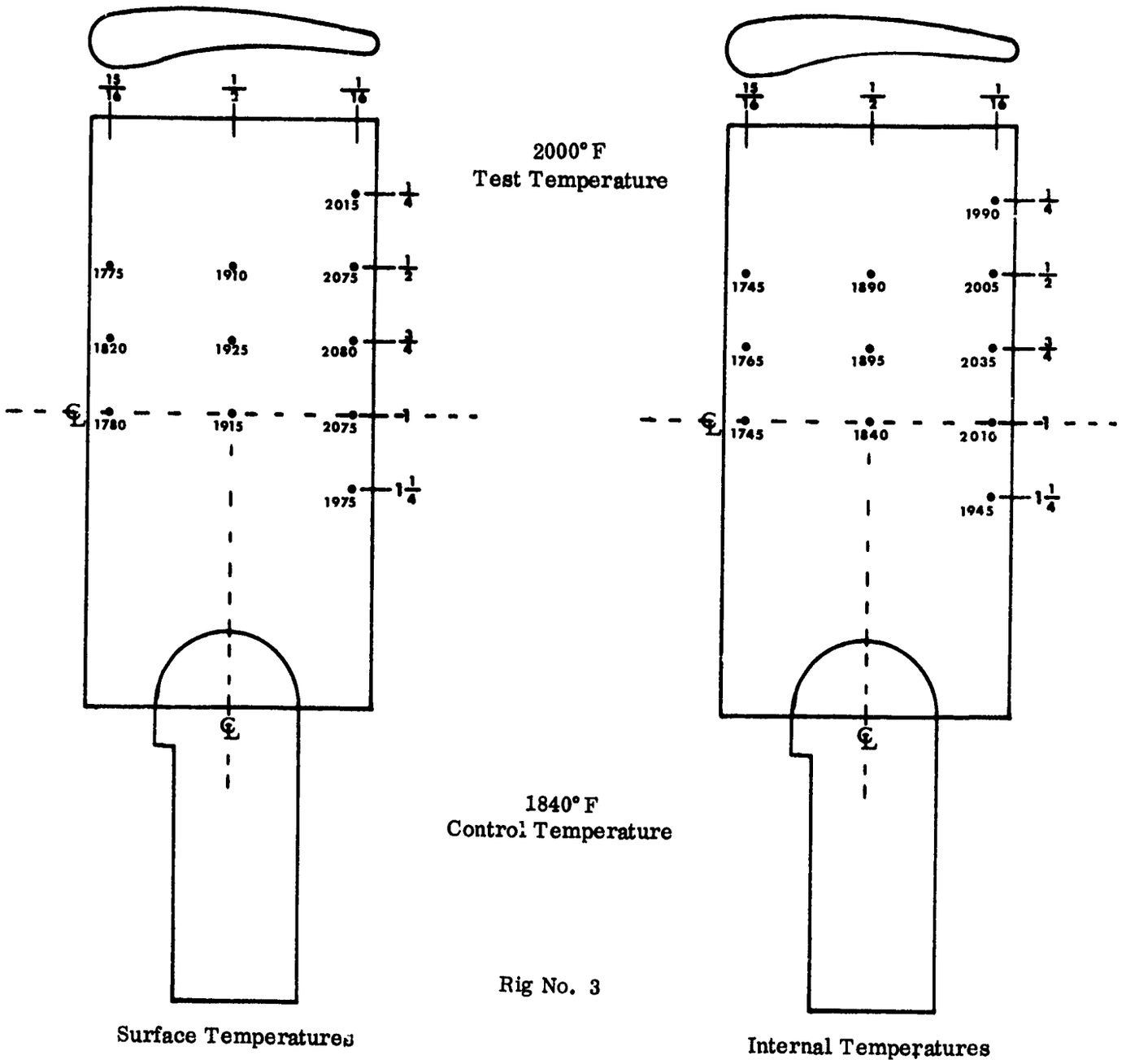

FIGURE 6. SPECIMEN TEMPERATURE DISTRIBUTION FOR 2000° F HOT CORROSION TESTS

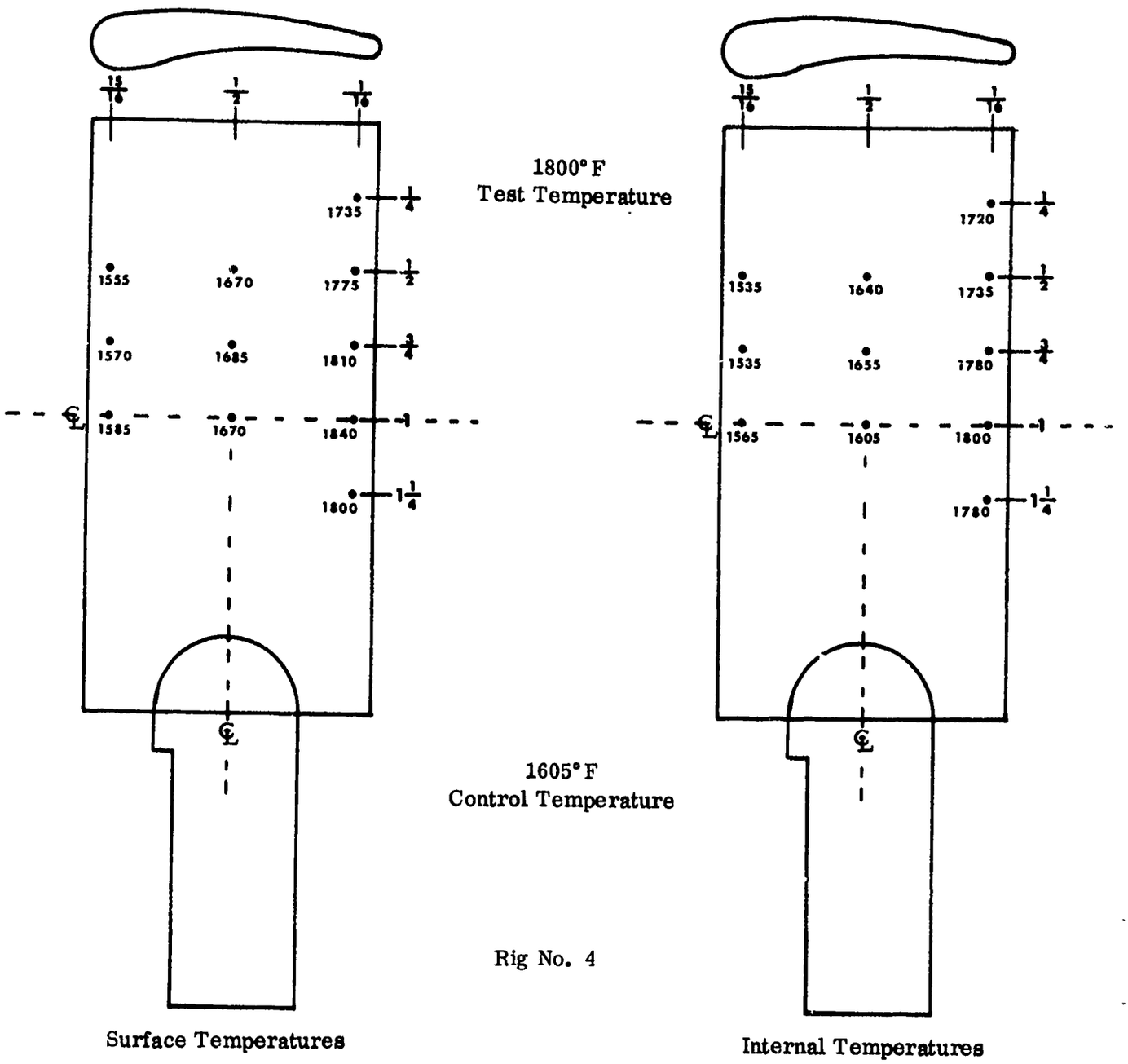

FIGURE 7. SPECIMEN TEMPERATURE DISTRIBUTION FOR 1800° F HOT CORROSION TESTS

corrosion tests was therefore established as 1510°F. (Note that the peak temperature was actually determined to be 1670°F after initiation of the tests.)

The internal and external temperature distribution for tests at the 2000°F temperature level in this same simulator are shown in Figure 6. For these tests the peak temperature determined during the calibration tests was 2035°F.

Figure 7 shows the specimen temperature distribution for the 1800°F hot corrosion tests. In this turbine simulator test rig, a thermocouple control temperature of 1605°F produced peak metal temperature of 1800°F.

3.1.4 Specimen Cleaning

At regular intervals in the hot corrosion tests the sea salt residue was cleaned from the surfaces of the coated specimens for visual inspection and weight gain measurements. Specimens were cleaned by soaking in distilled water (160-190°F) for 15 minutes and hand scrubbed with a fine wire stainless steel brush (Osborne No. 254 SV-3). This cleaning method did not appear to be detrimental to the coatings and removed most of the accumulated salt deposit.

3.1.5 Sulfur Content of Fuel

The specification for JP-5 grade aviation turbine fuel (MIL-J-5624) allows a sulfur content maximum of 0.040 percent by weight.

At Solar, JP-5 fuel is stored in large 5,000 and 10,000 gallon production facility tanks. Fuel for the turbine simulators (burner rigs) was withdrawn from these storage tanks and transported in 500 gallon lots to a small supply tank located adjacent to the simulator test cell. To ensure proper control of test conditions, the sulfur content of the JP-5 fuel was determined at regular intervals. The fuel sample was obtained at the combustor fuel nozzle in order to include any possible pickup from the portable 500-gallon tank, storage tank, transfer lines, and test cell filters.

The sulfur content of 35 samples taken at regular intervals over the last year ranged from 0.02 weight percent to a maximum of 0.10 weight percent. Average sulfur content for the 35 samples was 0.08 weight percent and was significantly less than the specification maximum (0.40%). The sulfur level of the fuel is approximately equal to the quantity of sulfur found in over 50 percent of the JP-5 fuel produced in the United States (Ref. 1).

3.1.6 Hot Corrosion Evaluation Techniques

All hot corrosion tests were terminated at 150 hours exposure, or at the first visual evidence of substrate oxidation.

Curves of cumulative weight change plotted as a function of exposure time are presented for all test specimens. These graphs contain the data points for both specimens included in the test. Generally, the weight change curves are a good indication of coating performance during testing. Major inflections in the curves (large weight gains or losses) usually indicate onset of coating failure. The cumulative weight changes during testing are summarized in the tables in Appendix II.

Photographs of the surface appearance after test of a typical exposed specimen are included for each coating tested at each temperature level. Photographs are taken after lightly glass bead blasting the surfaces of the specimens in order to clearly show the extent of coating loss and/or substrate corrosion.

The various substrate-coating combinations before and after hot corrosion rig testing were sectioned and examined metallographically. In all cases, the specimens were sectioned through the hottest area on the blade. Standard metallographic techniques were used. Final polishing with chromium sesqui oxide was standard and edge retention was effected by using a linen-phenolic supporting collar around each specimen embedded within the bakelite mount. An electrolytic etchant (2% aqueous solution of CrO_3) was used throughout. The use of a single etchant allowed coating structure evaluations to be made without the confusing effects of variations in etching rate and staining characteristics. In all cases, a low magnification (40X) photograph of the blade trailing edge and a high magnification (1000X) photograph of the representative area along the trailing edge of the coating are shown. The metallographic structures of the coatings are discussed in the different sections corresponding to each substrate alloy.

3.2 HOT CORROSION TEST RESULTS OF UNCOATED ALLOYS

3.2.1 Weight Change and Appearance

Figures 8 through 18 show the surface appearance of uncoated specimens after the hot corrosion tests. The cumulative weight change during testing are summarized in the tables in Appendix II.

Nickel-Base Alloys

The weight change data for the uncoated alloys at 1650°F are used to indicate alloy performance in these tests. Large, sudden weight changes (gains and losses) indicated initiation of hot corrosion attack to the alloy. For example, the B1900 alloy specimen number B2 showed a weight gain of 54.6 mg at the conclusion of 10 hours exposure. Visual examination of the specimen showed a major portion of the concave surface of the specimen to be severely corroded (Fig. 8A), accounting for this large weight gain. After lightly glass bead blasting to remove the surface corrosion products,

Text Continued on Page 33

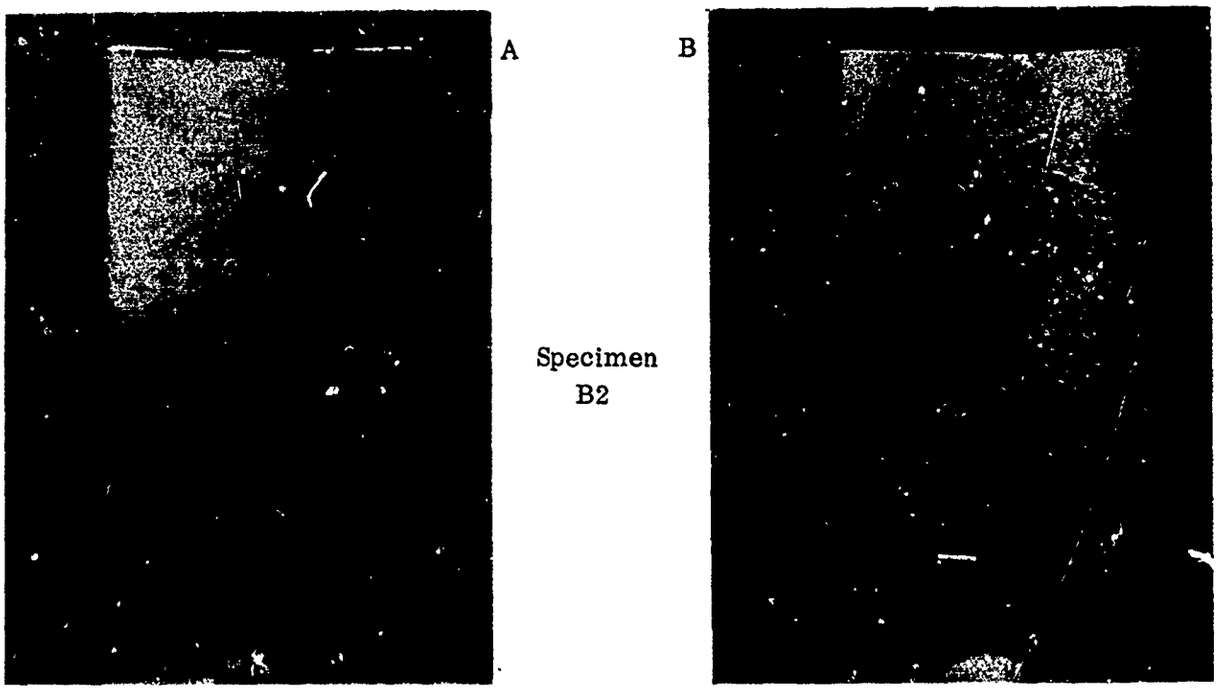

Surface Wire Brushed — After Glass Bead Blast Clean

1650°F Test, 10 Hours Exposure

FIGURE 8. SURFACE APPEARANCE OF UNCOATED B1900 ALLOY AFTER TEST AT 1650°F; Magnification: 2X

Specimen B29
1800°F Test
17 Hours Exposure

FIGURE 9. SURFACE APPEARANCE OF UNCOATED B1900 ALLOY AFTER TEST AT 1800°F; Magnification: 2X

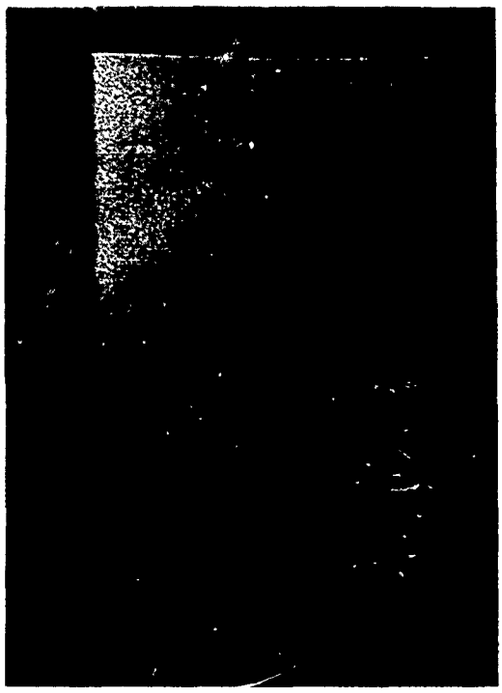

Specimen C2
1650°F Test, 60 Hours Exposure

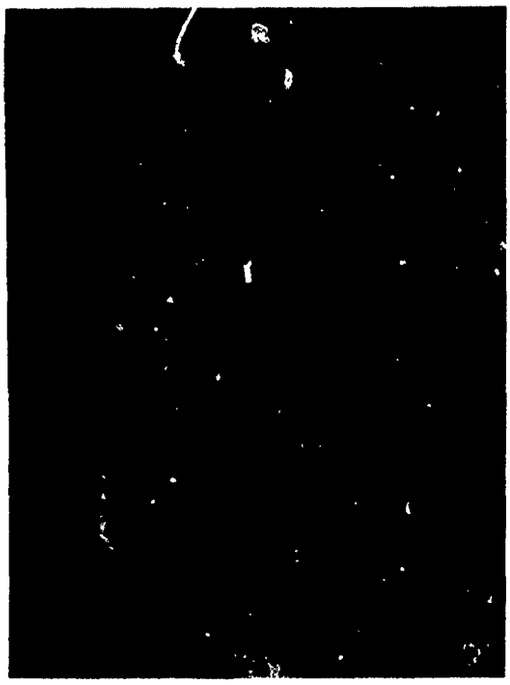

Specimen C3
1800°F Test, 10 Hours Exposure

FIGURE 10. SURFACE APPEARANCE OF UNCOATED INCO 713C ALLOY AFTER TEST; Magnification: 2X

Specimen I2
1650°F Test, 10 Hours Exposure

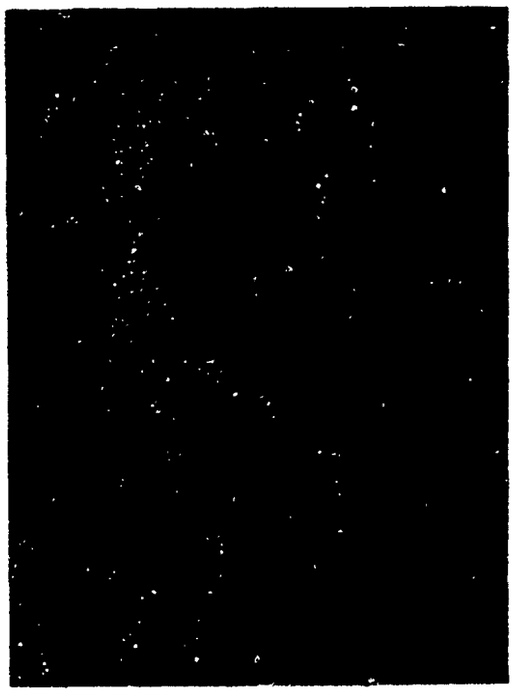

Specimen I25
1800°F Test, 17 Hours Exposure

FIGURE 11. SURFACE APPEARANCE OF UNCOATED IN-100 ALLOY AFTER TEST; Magnification: 2X

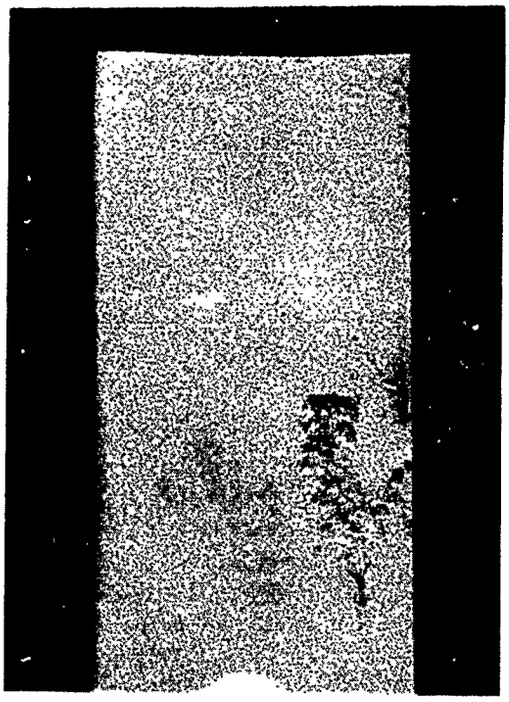

Specimen R1
1650°F Test, 150 Hours Exposure

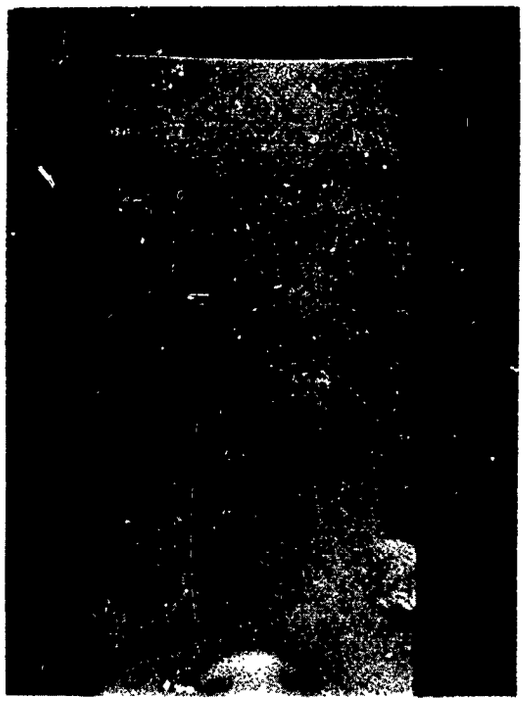

Specimen R3
1800°F Test, 70 Hours Exposure

FIGURE 12. SURFACE APPEARANCE OF UNCOATED RENE' 41 ALLOY AFTER TEST; Magnification: 2X

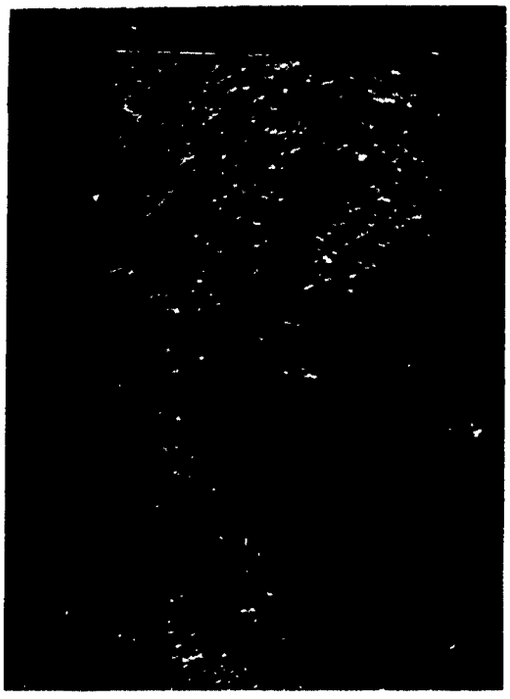

Specimen S1
1650°F Test, 10 Hours Exposure

Specimen S4
1800°F Test, 20 Hours Exposure

FIGURE 13. SURFACE APPEARANCE OF UNCOATED SEL-15 ALLOY AFTER TEST; Magnification: 2X

Specimen U1
1650°F Test
110 Hours Exposure

Specimen U3
1800°F Test
150 Hours Exposure

FIGURE 14. SURFACE APPEARANCE OF UNCOATED U-700 ALLOY AFTER TEST; Magnification: 2X

Specimen M2
1650°F Test, 20 Hours Exposure

Specimen M4
1800°F Test, 20 Hours Exposure

FIGURE 15. SURFACE APPEARANCE OF UNCOATED MAR-M-246 ALLOY AFTER TEST; Magnification: 2X

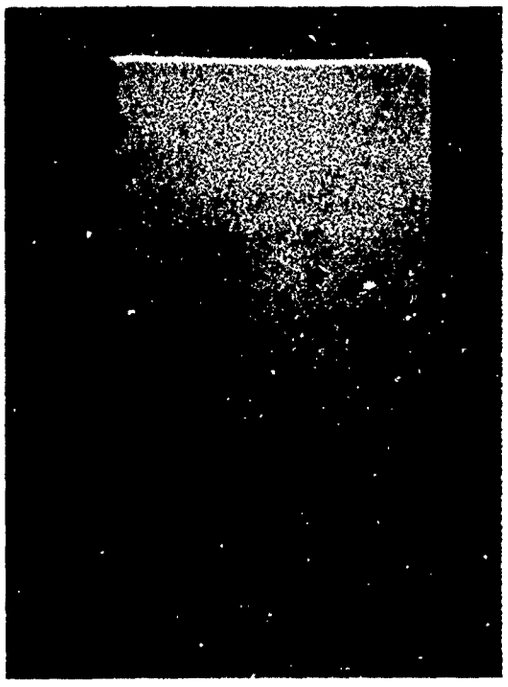

Specimen D1
1650°F Test, 160 Hours Exposure

Specimen D4
1800°F Test, 150 Hours Exposure

FIGURE 16. SURFACE APPEARANCE OF UNCOATED U-710 ALLOY AFTER TEST; Magnification: 2X

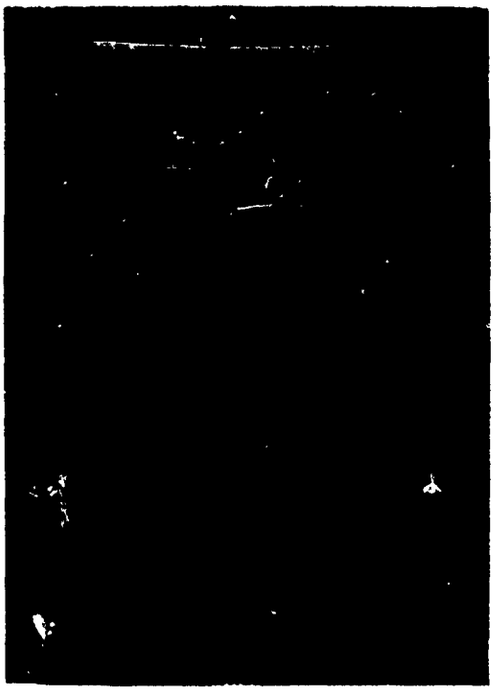

Specimen W25
1800°F Test, 17 Hours Exposure

Specimen W23
2000°F Test, 10 Hours Exposure

FIGURE 17. SURFACE APPEARANCE OF UNCOATED WI-52 ALLOY AFTER TEST; Magnification: 2X

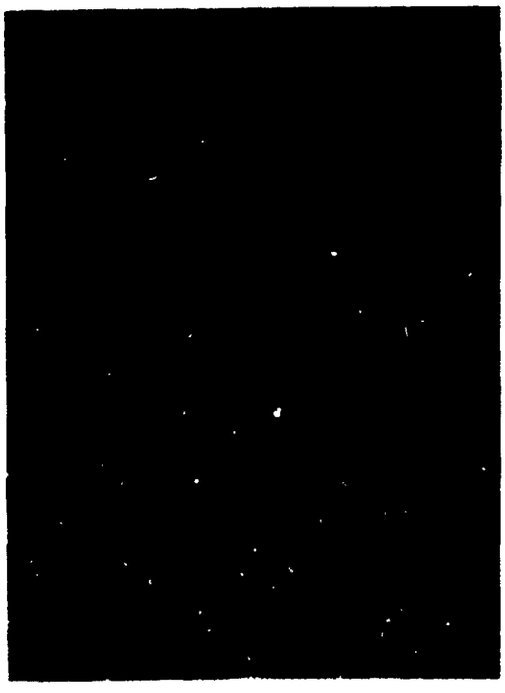

Specimen X68
1800°F Test, 17 Hours Exposure

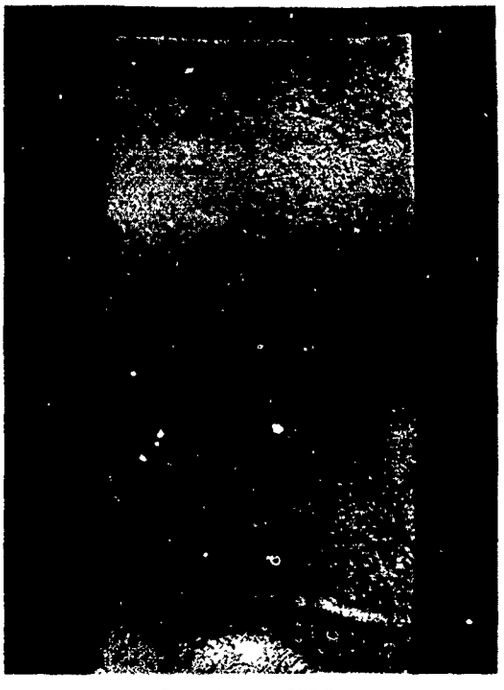

Specimen X98
2000°F Test, 50 Hours Exposure

FIGURE 18. SURFACE APPEARANCE OF UNCOATED X-40 ALLOY AFTER TEST; Magnification: 2X

the depth of substrate attack is clearly shown in Figure 8B. The surfaces of all other specimens after test are shown after lightly glass bead blasting to indicate the magnitude of the substrate corrosion.

As expected, the chemistries of the alloys had a strong influence on the resistance to hot corrosion. The Rene' 41, U-700 and U-710 alloys with their high chromium content showed best performance at T_{max} of 1650 and 1800°F. The U-700 and U-710 alloys (15 and 18% Cr) exhibited better performance than the Rene' 41 alloy (19% Cr), probably due to the lower molybdenum content (10% Mo in Rene' 41 versus 5% Mo in U-700 and 3% Mo in U-710).

Cobalt-Base Alloys

Figures 17 and 18 show the surface appearance of typical X-40 and WI-52 alloy specimens after hot corrosion testing at 1800°F and 2000°F.

The X-40 alloy with its high chromium content (25% Cr) exhibited best performance at both temperature levels. Tests at 1800°F were terminated after a total of 17 hours exposure due to the extremely rapid hot corrosion of the alloys. Corrosion of both of the cobalt-base alloys, however, was not as severe at this temperature as the B1900, Inco 713C, SEL-15, and IN-100 alloys.

At 2000°F, the X-40 alloy specimens were continued in test for a total of 50 hours. At the conclusion of testing, both specimens exhibited an identical weight loss of approximately 2 grams. Corrosion attack was uniformly centered along the trailing edge of the blades on the concave surfaces.

3.2.2 Metallographic Analyses

The B1900 alloy is reported to contain about 63 w/oγ' (Ref. 2) and exhibited a large grain structure made up of cored dendrites with interdendritic carbides and primary γ' or $\gamma + \gamma'$ eutectic (Ref. 2). The carbides had the "script" morphology which is caracteristic of the MC-type carbides and, since the B1900 alloy contains Ti and Ta, they are most probably TiC and TaC (Ref. 3). Examination under higher magnification showed the typical fine dispersions of γ' in the f.c.c. matrix and islands of $\gamma + \gamma'$ eutectic in the interstices of the dendrites.

The uncoated B1900 alloy specimen was found to fail on hot corrosion testing at 1650°F after only 20 hours. Microscopic examination revealed oxidation and formation of an alloy depletion layer (Fig. 19). The maximum thickness of the alloy depletion layer was 0.0025 inch. The depletion layer is most probably depleted of C, Cr, Al, Ti, etc. Internal oxide spots can be seen in the outer layer.

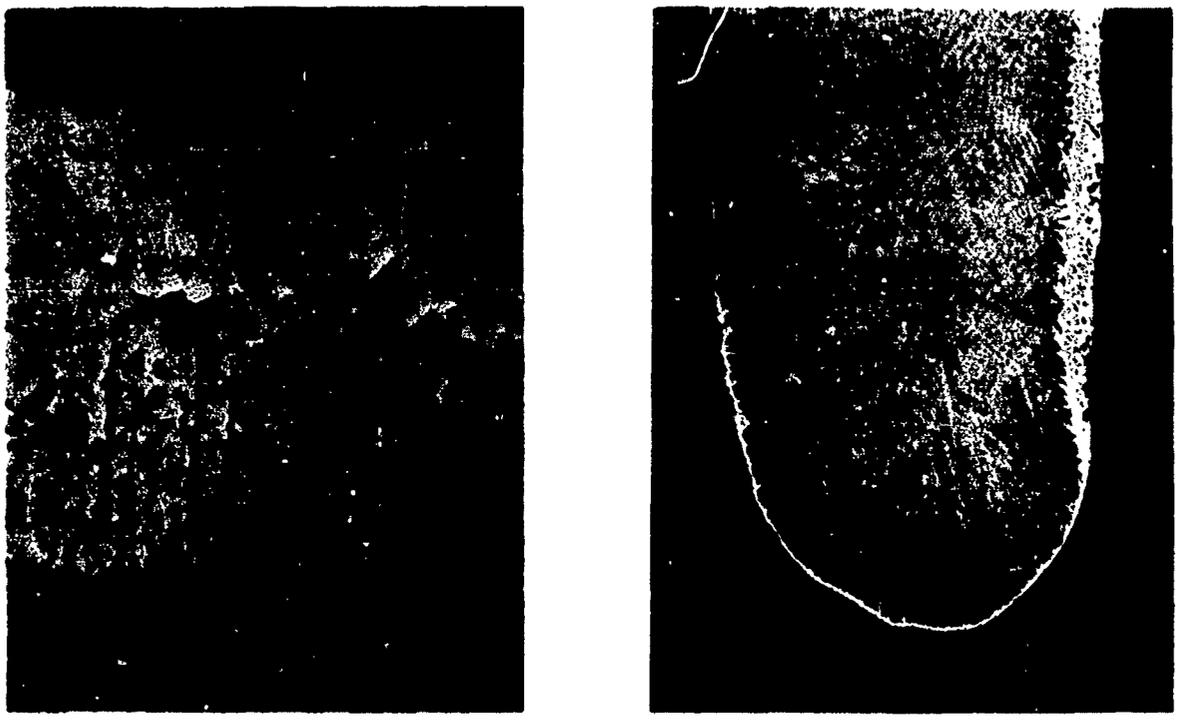

Magnification: 1000X Specimen B 26 Magnification: 40X

FIGURE 19. MICROSTRUCTURE OF UNCOATED B1900 ALLOY AFTER HOT CORROSION TESTS AT 1650°F FOR 20 HOURS

The uncoated Inco 713C lasted longer (60 hours) in hot corrosion testing than the B1900 during hot corrosion testing at 1650°F. The higher Cr content (13.8%) in Inco 713C than in B1900 (8.5% Cr) is probably responsible. An alloy depletion layer (0.0005 inch thick) developed all along the specimen (Fig. 20). Depletion in C, Cr, Ti and Al is most likely. The alloy 713C contains 2 percent Cb, which would favor the formation of MC carbide in addition to $M_{23}C_6$ carbides. These phases are relatively immobile and dissolve very slowly in the aluminide coatings. During hot corrosion testing, some decarburization occurred.

The uncoated IN-100 alloy specimens failed after 20 and 17 hours testing at 1650°F and 1800°F, respectively. The hot corrosion resistance of IN-100 was poor and was about the same as that of B1900. The hot corrosion testing at 1650°F for 20 hours caused oxidation and the formation of a thin alloy depletion layer (0.0005 inch thick) along the specimen (Fig. 21). The hot corrosion testing at 1800°F for 17 hours resulted in more than 60 percent loss in cross-section at the trailing edge (Fig. 22).

Magnification: 1000X

Specimen C1

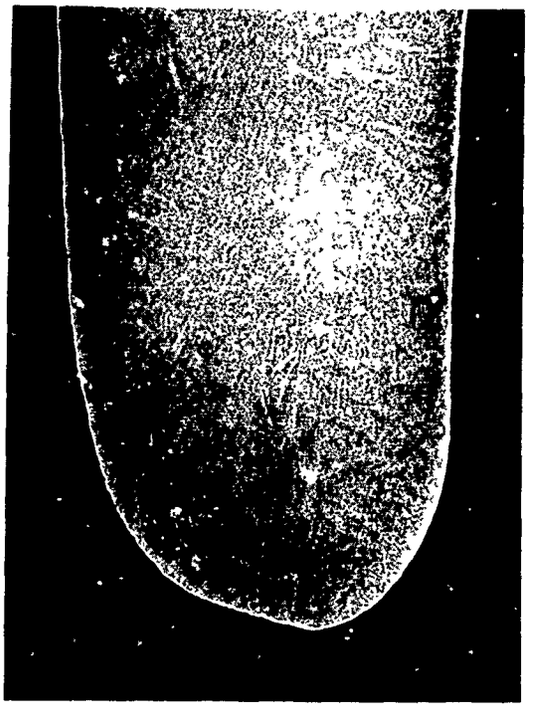

Magnification: 40X

FIGURE 20. MICROSTRUCTURE OF UNCOATED INCO 713C AFTER HOT CORROSION TESTS AT 1650° F FOR 60 HOURS

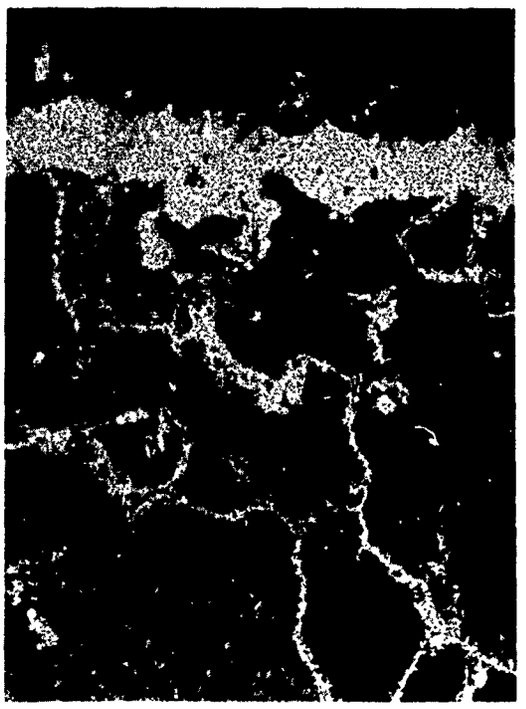

Specimen

I28

Magnification: 1000X

Magnification: 40X

FIGURE 21. MICROSTRUCTURE OF UNCOATED IN-100 ALLOY AFTER HOT CORROSION TESTS AT 1650° F FOR 20 HOURS

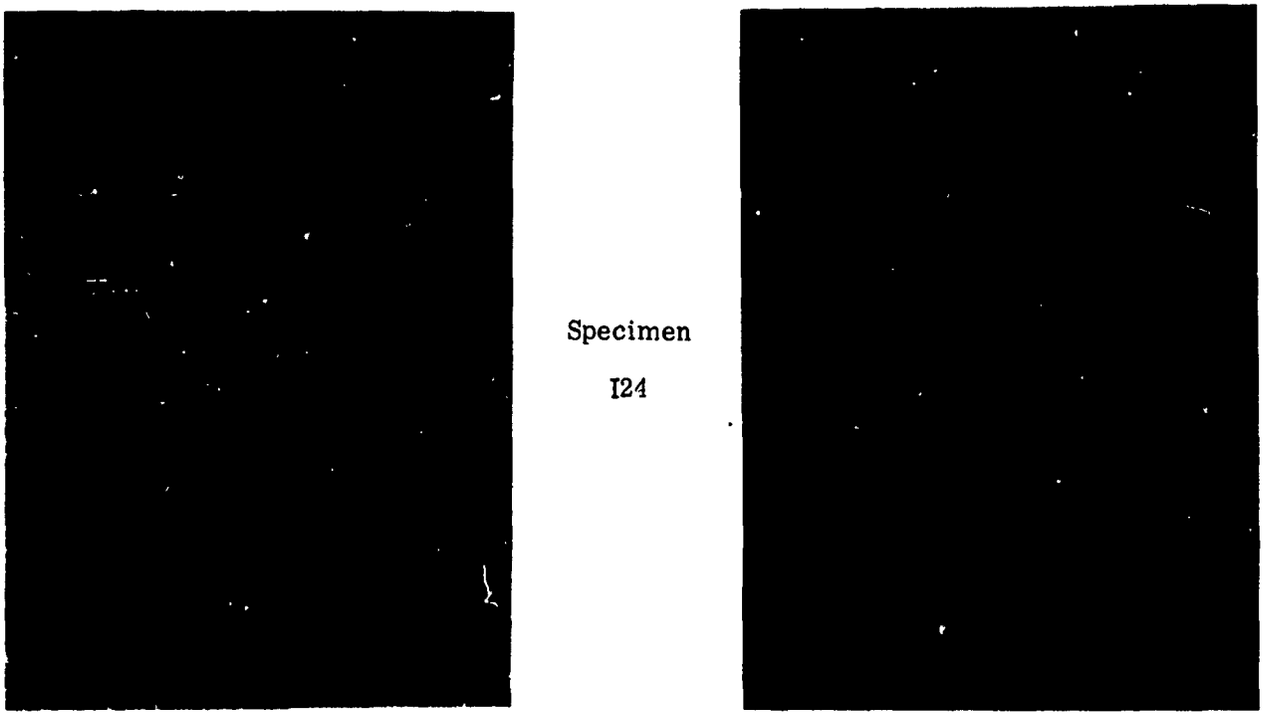

Magnification: 1000X Magnification: 40X

FIGURE 22. MICROSTRUCTURE OF UNCOATED IN-100 ALLOY AFTER HOT CORROSION TESTS AT 1800° F FOR 17 HOURS

Although the uncoated Rene' 41 alloy was maintained in HCR testing at 1650°F for 150 hours, surface appearance and metallographic examination indicated that this alloy is perhaps less resistant than U-710 and U-700. The microstructure after test (Fig. 23) showed extensive intergranular oxidation and alloy depletion.

The uncoated SEL-15 alloy failed after 9.5 hours in hot corrosion testing at 1650°F. This alloy contains 10.7 percent Cr and 6.18 percent Mo. The hot corrosion test exposure resulted in oxidation, decarburization and formation of an alloy depleted layer.

Udimet-700 alloy (Fig. 24) failed after 110 hours in hot corrosion testing at 1650°F. There was no severe intergranular oxidation. Hot corrosion testing resulted in decarburization and formation of an alloy depletion layer (0.001 inch thick).

Hot corrosion resistance of the MAR-M-246 alloy was extremely poor ranking with B1900, IN-100 and SEL-15. Specimens were removed from test after only 20 hours at 1650°F. Severe attack of the alloy had occurred which can be seen in the microstructure shown in Figure 25. Approximately 40 percent of the alloy had been penetrated primarily from the concave side. Both intergranular and transgranular attack was in evidence.

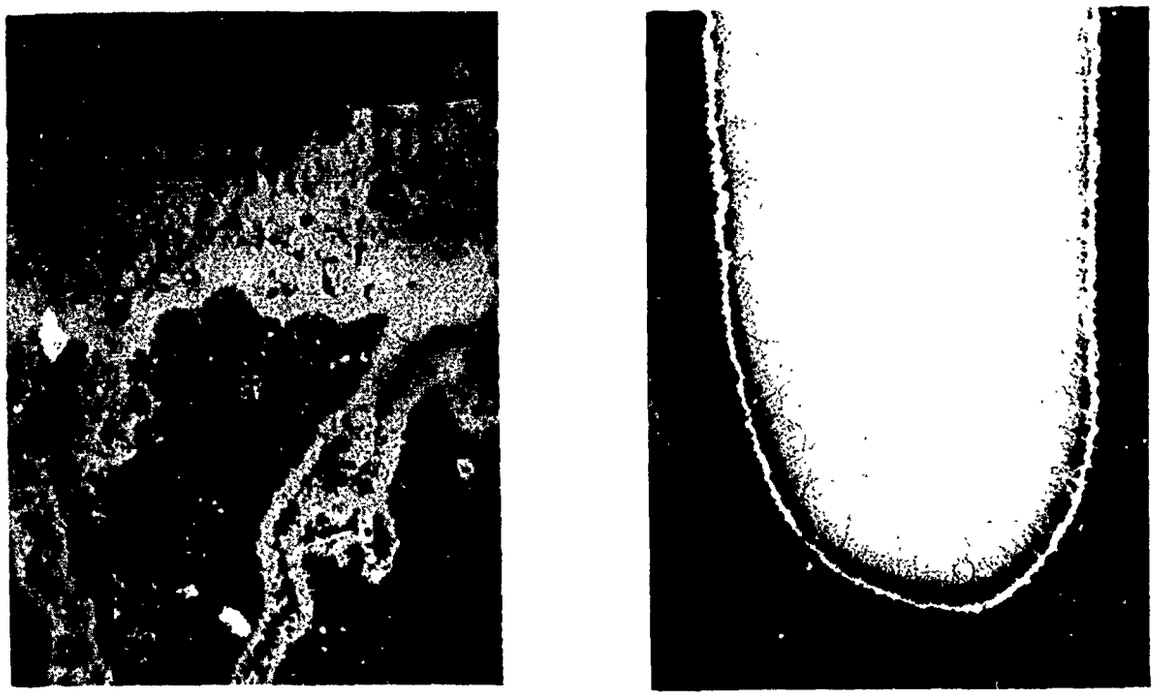

Magnification: 1000X Specimen R2 Magnification: 40X

FIGURE 22. MICROSTRUCTURE OF UNCOATED RENE' 41 AFTER HOT CORROSION TESTS AT 1650° F FOR 150 HOURS

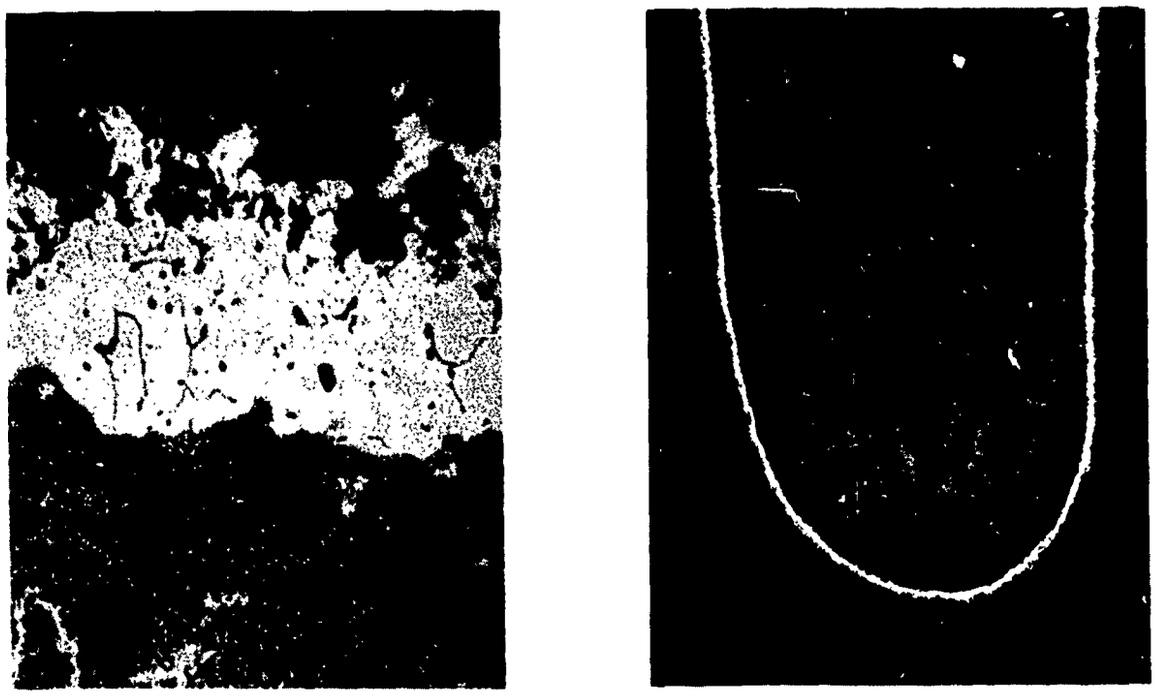

Magnification: 1000X Specimen U2 Magnification: 40X

FIGURE 24. MICROSTRUCTURE OF UNCOATED U-700 ALLOY AFTER HOT CORROSION TESTS AT 1650° F FOR 150 HOURS

Magnification: 1000X

Magnification: 40X

Specimen M2

FIGURE 25. MICROSTRUCTURE OF UNCOATED MAR-M-246 AFTER HOT CORROSION TESTS AT 1650°F FOR 20 HOURS

The most hot corrosion resistant alloy evaluated in the program was U-710. After testing for 160 hours at 1650°F only a relatively thin surface alloy depletion zone developed (0.0005 inch) (Fig. 26). Intergranular alloy depletion and internal oxidation extended the overall alloy penetration to 0.0025 inch in the period of test.

Metallographic examination of uncoated WI-52 and X-40 alloys after hot corrosion testing revealed decarburization and oxidation of the cobalt-base alloys. Tests were of such short duration at 1800°F (17 hours prior to removal) that uncoated testing only showed that the alloys cannot be used at this temperature or higher without effective coatings.

Magnification: 1000X

Specimen D2

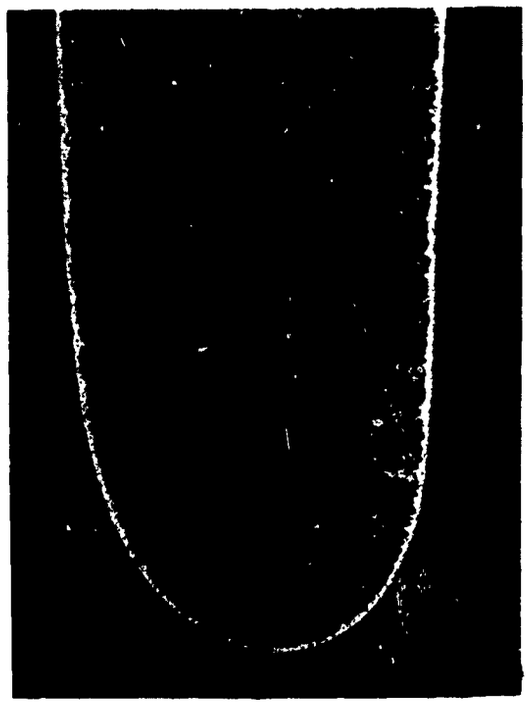

Magnification: 40X

FIGURE 26. MICROSTRUCTURE OF UNCOATED U-710 AFTER HOT CORROSION TESTS AT 1650°F FOR 160 HOURS

The ranking of the six uncoated nickel-base alloys after hot corrosion testing is shown in Figure 27. For comparison purposes, also included are the results of a Round-Robin Test Program sponsored by the ASTM Gas Turbine Panel.

The Solar data are in good agreement with the results of the Round-Robin tests. The B1900, SEL-15, IN-100 and MAR-M-246 alloys had by far the worst hot corrosion resistance, with 713C alloy only slightly better. The U-700, Rene' 41, and U-710 alloys exhibited significantly better hot corrosion resistance at both temperature levels.

3.3 HOT CORROSION TEST RESULTS OF COATED B1900 ALLOY

3.3.1 Weight Change and Appearance

Curves of cumulative weight change plotted as a function of exposure time at 1650°F and 1800°F are presented in Figures 28, 29 and 30 for the B1900 alloy. In addition, a photograph is included showing the surface appearance after test of a typical exposed specimen of each group.

Text Continued on Page 44.

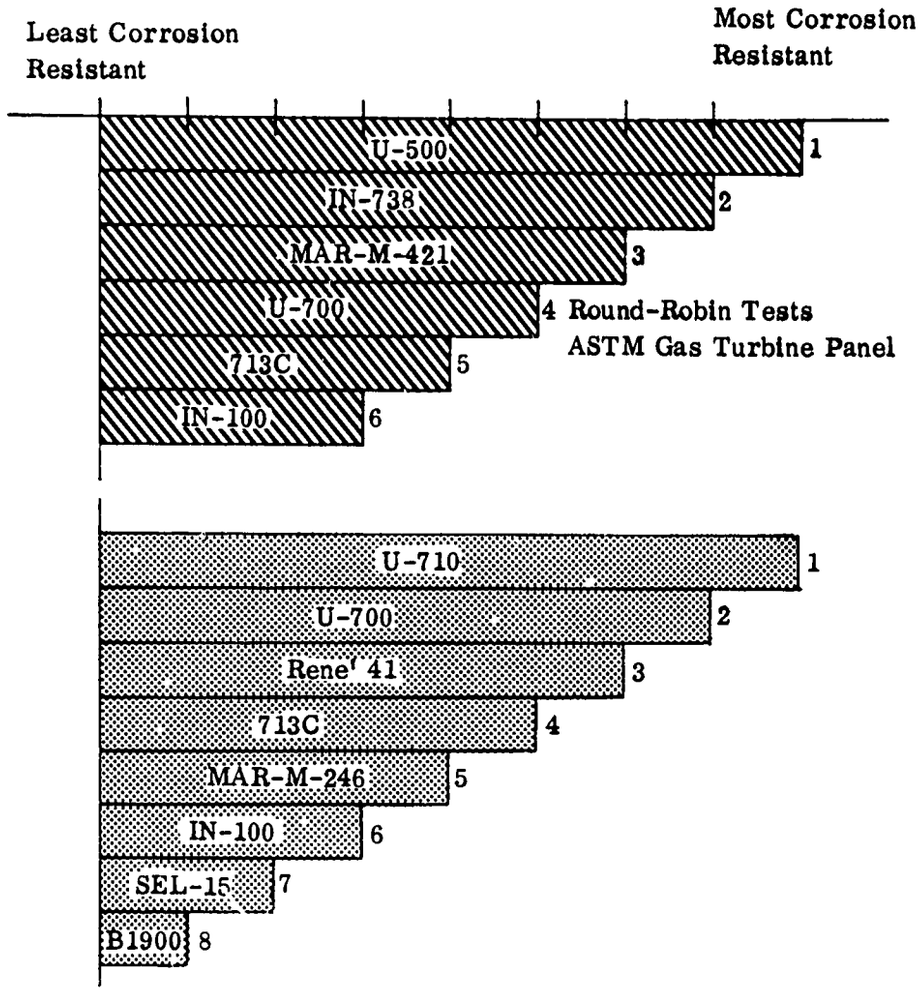

FIGURE 27. RANKING OF UNCOATED NICKEL-BASE ALLOYS

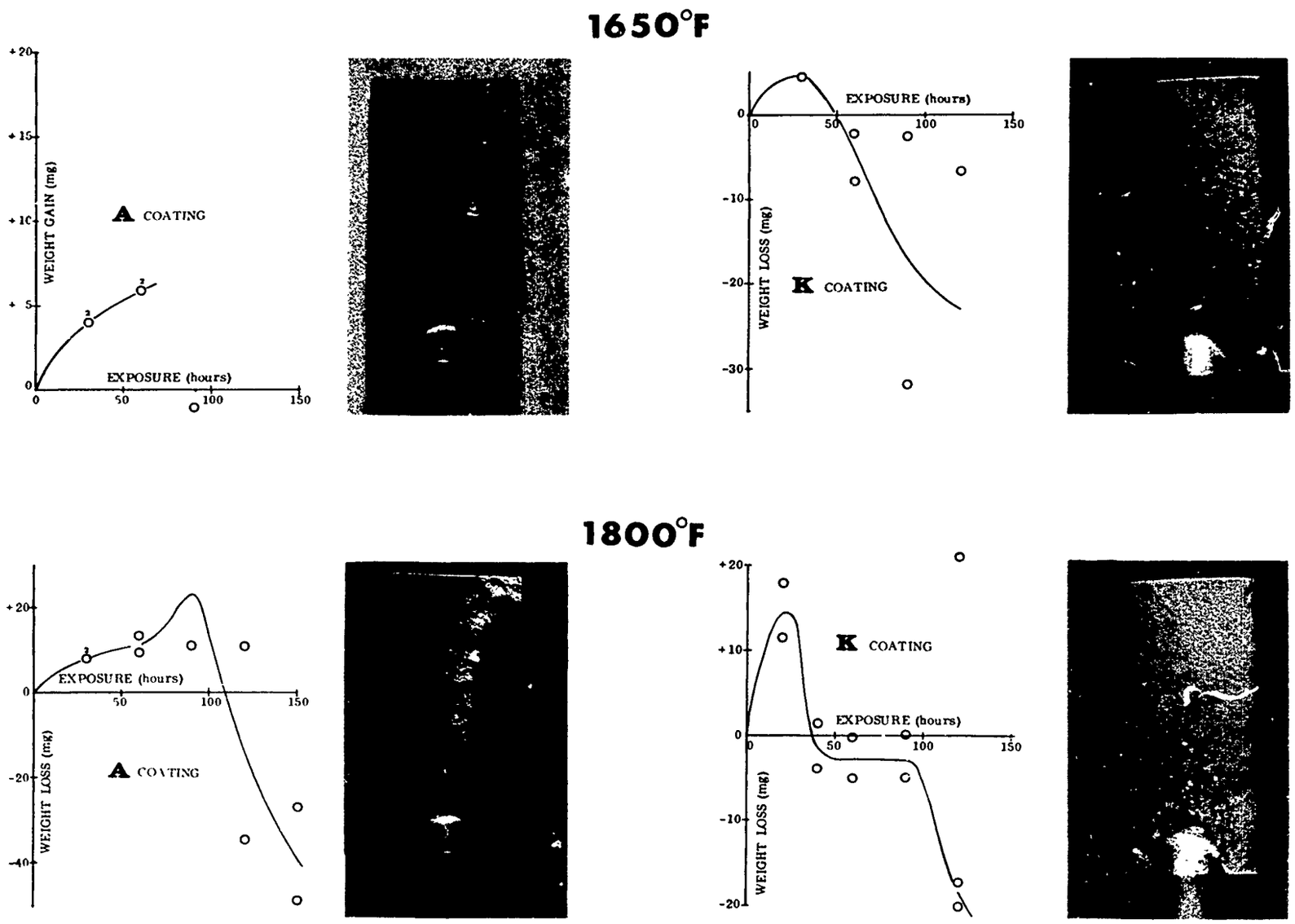

FIGURE 28. WEIGHT CHANGE AND APPEARANCE OF COATINGS A AND K ON B1900 ALLOY TESTED AT 1650° F AND 1800° F

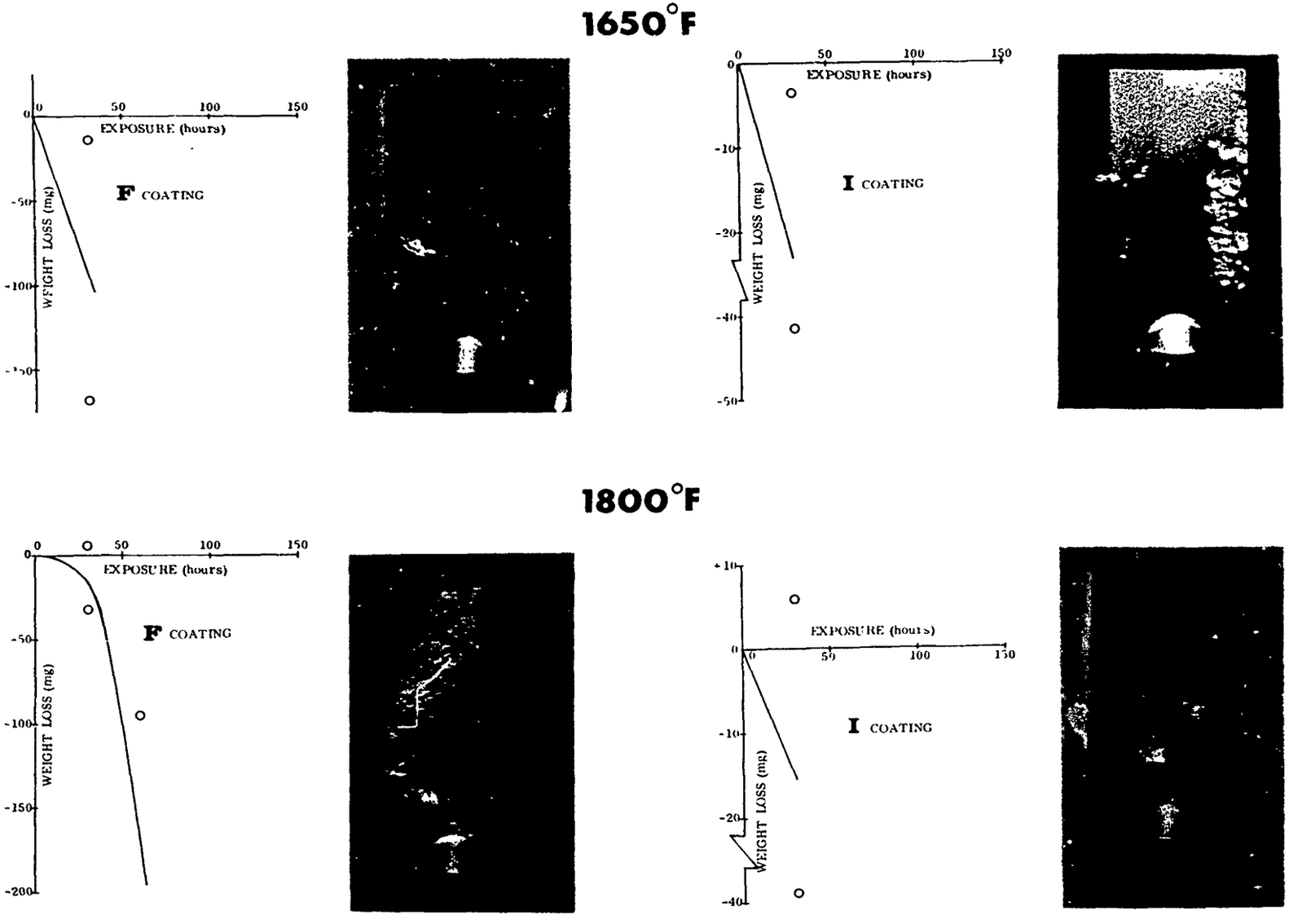

FIGURE 29. WEIGHT CHANGE AND APPEARANCE OF COATINGS F AND I ON B1900 ALLOY TESTED AT 1650° F AND 1800° F

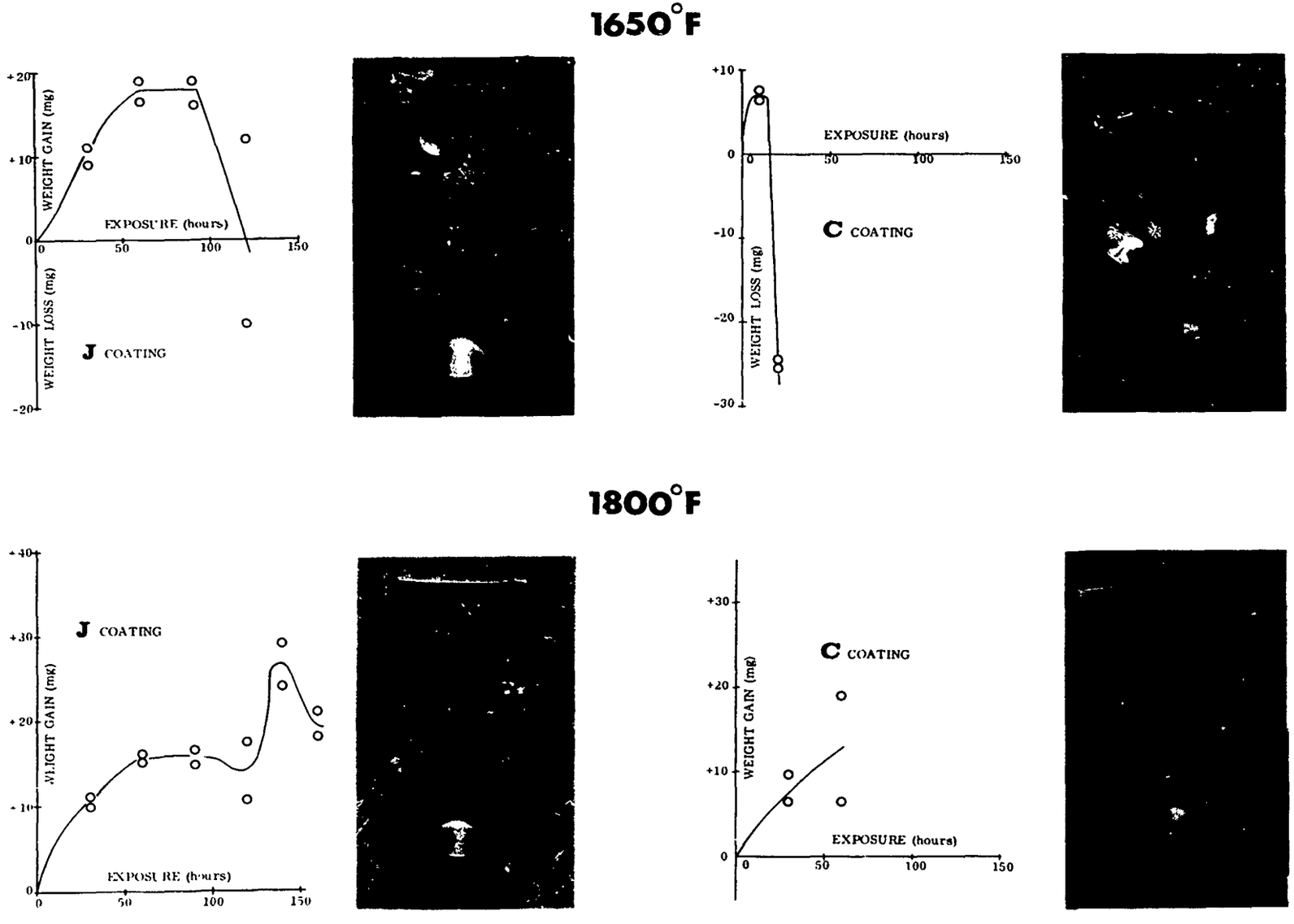

FIGURE 30. WEIGHT CHANGE AND APPEARANCE OF COATINGS J AND C ON B1900 ALLOY TESTED AT 1650°F AND 1800°F

This alloy proved to be the most difficult of the eight nickel-base alloys to protect from hot corrosion. Only the J coating (in the 1800°F test) survived 150 hours exposure without evidence of coating degradation or substrate oxidation. All of the other coatings showed major signs of failure ranging from a low of 20 hours (the C coating) to a maximum of 150 hours for the A coating. With the exception of the K and I coatings, all failures were of the pinhole type occurring on either the concave or convex surfaces of the specimens, generally away from the trailing edge towards the cooler areas of the blades. The I coating tested at 1650°F exhibited numerous pinhole type coating failures which were concentrated in the hot zone along the trailing edge of the blades. The K coating exhibited second best overall performance in the hot corrosion test at both temperature levels. The heavy K coating spalled, and specimens showed a weight loss in the tests after 30 hours exposure; but substrate oxidation was apparent on only one specimen in the 1650°F test. On this specimen, oxidation occurred on the sharp tip of the blade near the base which must have been an uncoated area or damaged during coating or testing operations.

3.3.2 Metallographic Analyses of Coatings on B1900 Alloy

Coating A As-Coated

The microstructure of the A coating is shown in Figure 31. The thickness of the A coating was 0.0034 inch, i.e., thicker than all other coatings on B1900 except K. The coating was very uniform in appearance. The structure of the outer area of the coating was found to consist of βNiAl + Cr_2Al white phase based on X-ray diffraction analyses (Table V). Partially dissolved carbide particles from the substrate were evident in the outer layer of the coating indicating that the coating was formed by predominant inward diffusion of Al (i.e., high Al activity pack and/or high process temperature). The hardness of this zone was 597 KHN and was greater than that of the denuded zone, 514 KHN. The denuded zone is mainly βNiAl and is free from carbides or refractory metal-rich precipitates.

Beneath the denuded zone was the diffusion zone, consisting of βNiAl matrix, $\gamma'Ni_3Al$, carbides and finger-like sigma phase. The hardness of this zone was of the order of 670 to 735 KHN (Fig. 31).

At the diffusion zone/substrate interface, a continuous dark band of γ solid solution had developed during the coating process, indicative of Co, Cr and Mo enrichment.

Coating A After 1650°F Testing

Hot corrosion rig (HCR) testing at 1650°F of the A coated specimen resulted in localized failure after 60 hours. The thickness of the coating was increased from

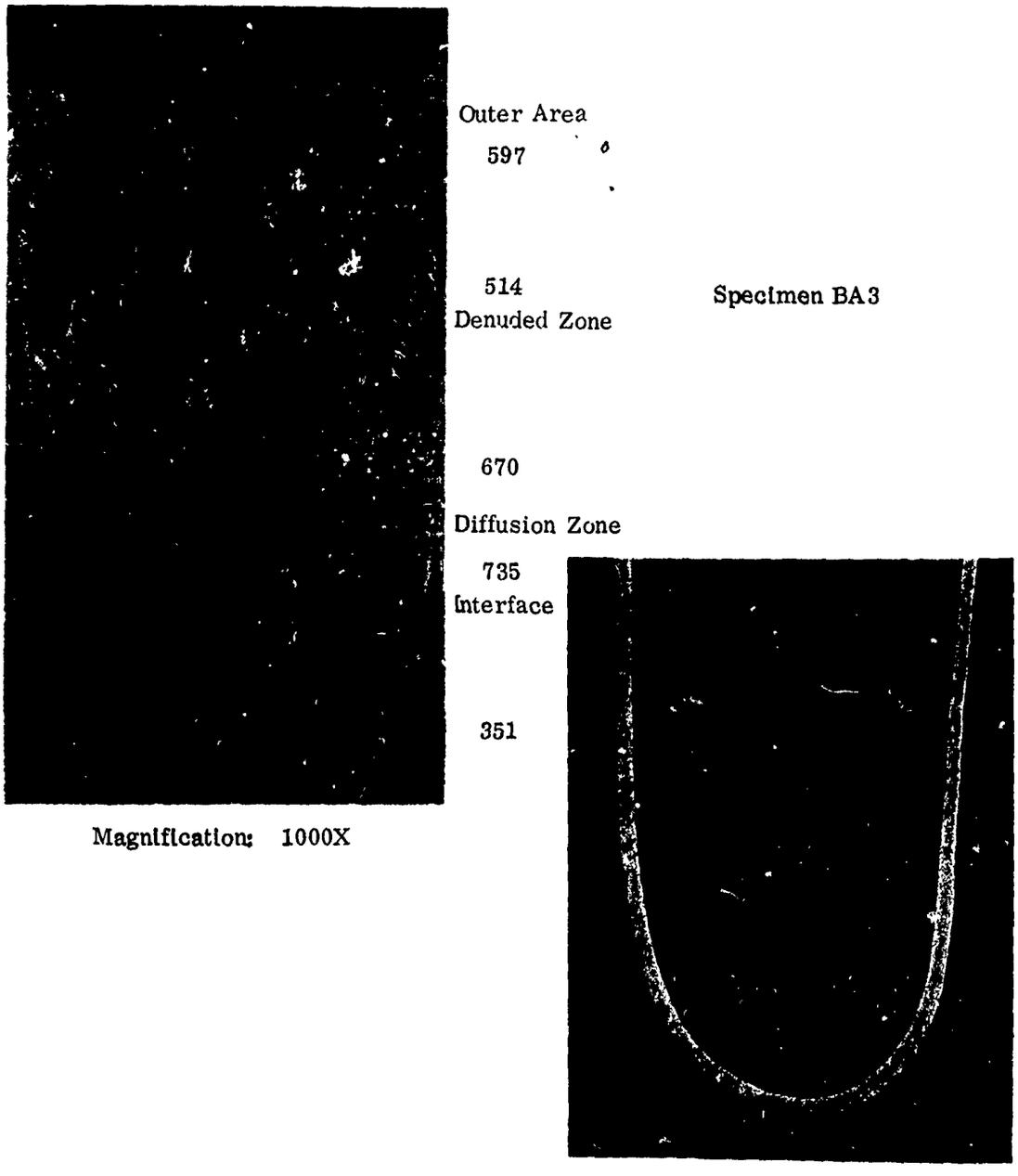

FIGURE 31. MICROSTRUCTURE OF AS-RECEIVED COATINGS; Coating A on B1900 Alloy

0.0034 inch to 0.0045 inch due to diffusion of Al into the substrate (Fig. 32). The diffusion instability is a significant weakness of this coating system.

The coating, after 1650°F and 60 hours HCR testing, was found to consist of an outer area (476 KHN), a denuded layer (521 KHN) and a diffusion zone (573 KHN). The hardness of the denuded zone (mainly βNiAl) was not changed after the HCR testing. The hardness values of the outer area and the diffusion zone were found to decrease because of rig testing. This could be due to loss of Al by oxidation or diffusion into the substrate.

The outer zone, most likely, consisted of βNiAl, carbides, chromium or refractory metal-rich precipitates and $\gamma'Ni_3Al$ (Fig. 32). The diffusion zone was βNiAl matrix, $\gamma'Ni_3Al$ phase, carbides and finger-like sigma phase. The finger-like sigma phase observed in the as-coated condition appears to have partially transformed into the carbides.

At the diffusion zone/substrate interface, the continuous dark band of γ (in the as-coated condition) was transformed into $\gamma'Ni_3Al$ with detectable sigma phase platelets. The B1900 substrate was not hardened by the exposure.

Coating A After 1800°F Testing

The A coating was found to withstand the test duration of 150 hours of HCR testing at 1800°F (compared to 60 hours at 1650°F). The increased protection afforded by the coating after 1800°F exposure, compared to 1650°F exposure, may be due to the decrease in the amount of salt present. The salt is more fluid at the 1800°F temperature and, consequently, both the centrifugal forces of blade rotation and erosion from the gas stream tend to decrease the amount of retained salt. The thickness of the coating was 0.0028 inch compared to 0.0034 inch in the as-coated condition or to 0.0045 inch after 1650°F and 60 hours exposure (Fig. 33).

General attack, based on decrease in coating thickness, was more severe at 1800°F even though localized failure required removal of the 1650°F test specimen at 60 hours.

Considerable carbide dissolution occurred in the outer area of the coating after 1800°F and 150 hours exposure. The outer layer was composed of βNiAl plus partially dissolved carbides and some chromium-rich precipitates. Beneath the outer layer was the denuded zone followed by the complex diffusion zone which consisted of βNiAl matrix, γ' phase and carbides. At the interface, sigma phase platelets in γ' matrix developed.

The A coating on the B1900 alloy, because of diffusion instability and only 60 hours protection at 1650°F, was not selected for further testing and evaluation.

Knoop Hardness Number (50-gram load)

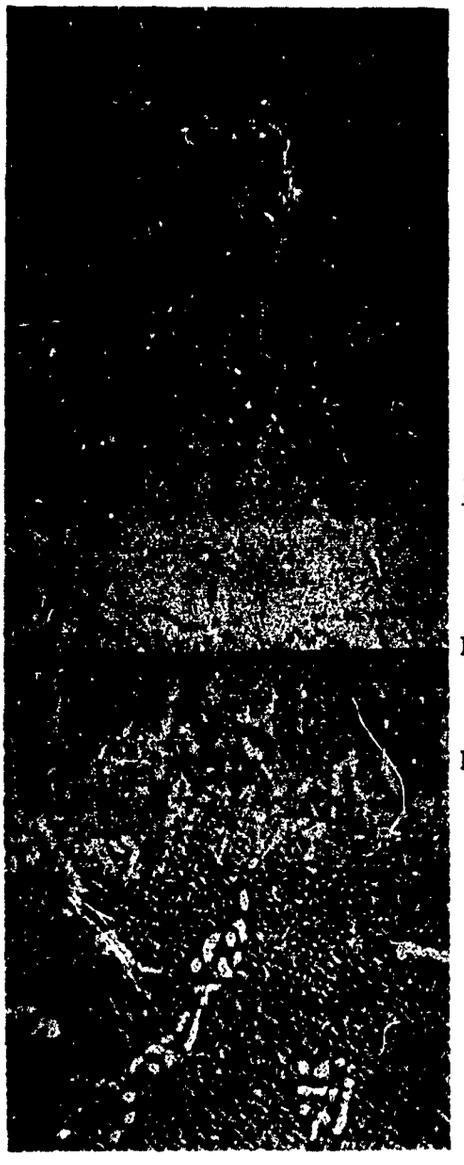

476

Outer Area

464

Denuded Zone

521

Diffusion Zone

573

Interface

285

285

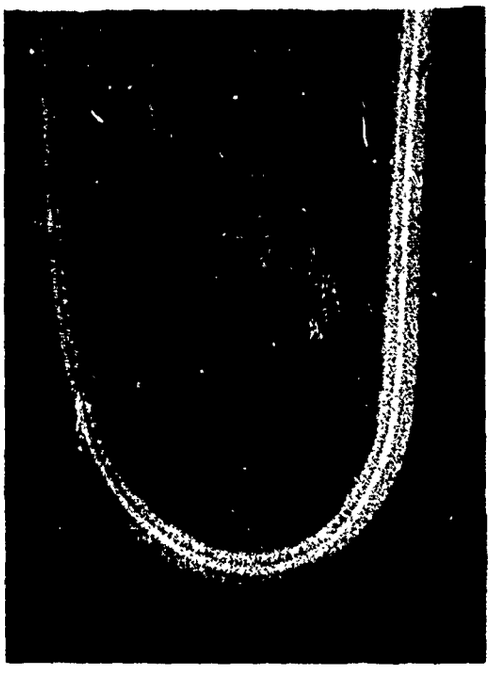

Magnification: 40X

Specimen BA2

Magnification: 1000X

FIGURE 32. MICROSTRUCTURE OF A COATING ON B1900 ALLOY AFTER HOT CORROSION TESTS FOR 60 HOURS AT 1650°F

Magnification: 1000X

Specimen BA6

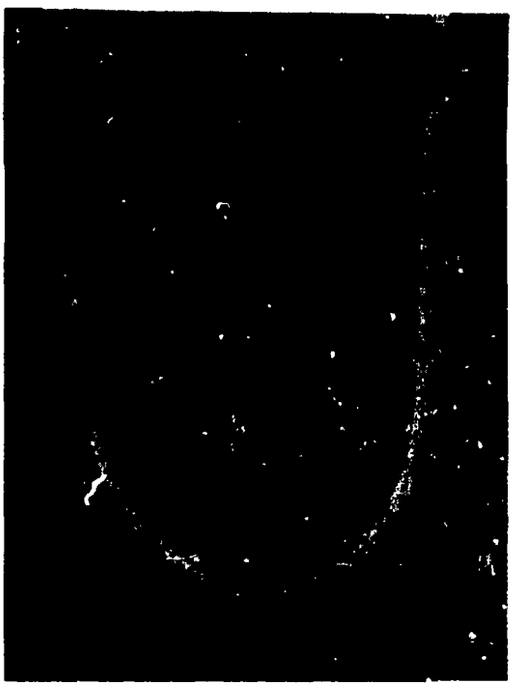

Magnification: 40X

FIGURE 33. MICROSTRUCTURE OF COATING A ON B1900 ALLOY AFTER HOT CORROSION TESTS FOR 150 HOURS AT 1800°F

The C Coating

The C coating showed a higher apparent density than the A coating, which could be an indication of codeposition of heavier elements than Al (e.g., Cr) during the coating process. The major coating phase was βNiAl with a very fine dispersion throughout. Carbides were only present in the lower part of the coating and the formation of a fine acicular precipitate of sigma was evident at the interface.

The B1900/C coating specimen was found to fail after 20 hours at 1650°F HCR testing and was therefore not extensively analyzed.

The F Coating

The F coating was one of the thinner coatings on B1900. The outer layer was identified by comparison to the X-ray diffraction of the F coating on SEL-15 alloy to be βNiAl plus large α-Al_2O_3 inclusions plus α-Cr (Table VI). The original pack-metal interface was delineated by a line of precipitates near the center of the coating. These precipitates have been shown to be titanium-rich (Ref. 3). The diffusion zone included carbide phases, a lamellar σ phase oriented perpendicular to the base metal interface, and βNiAl. The major interface phase was Ni_3Al.

The F coating on B1900 had poor corrosion resistance, failing in localized areas after only 30 hours. The outer area remained essentially unchanged (except probable loss of Al by conversion to Al_2O_3 or Al diffusion into the substrate), and most likely consisted of βNiAl + α-Al_2O_3. In the diffusion zone, partial transformation of sigma phase to carbides occurred. Also, sigma phase platelets in $\gamma'Ni_3Al$ matrix were observed just beneath the diffusion zone.

The F coating, because of its poor resistance to corrosion on B1900 alloy at 1650°F, was not selected for further testing and evaluation.

The I Coating

The I coating was the thinnest on B1900 averaging only 0.0017 inch. This thickness was below the range specified for nickel-base superalloys. The coating, most likely, consisted of a βNiAl matrix plus refractory metal-rich precipitates e.g., α-Cr, Cr_3Al_2 or Cr_2Al and some partially dissolved carbides.

The I coated specimens were found to fail completely after 30 hours at 1650°F HCR testing and was therefore not extensively evaluated.

Coating J As-Coated

The J coating on B1900 was almost as thick as the A coating. Remnants of grain boundary carbides ($M_{23}C_6$) from the original substrate were observed in the βMAl matrix all the way out to the surface of the coating. The white phase precipitates near the coating surface were identified by X-ray diffraction analyses to be Cr_3Al_2 and α-Cr (Table VII). The interface layers contained sigma and M_3Al phases (Fig. 34).

Coating J After 1650°F Testing

HCR testing of the J coating at 1650°F resulted in the specimen failure after 120 hours (i.e., twice the life attainable with the A coating). The thickness of the coating decreased from 0.0030 inch to 0.0028 inch (Fig. 35) and is due to the loss of Al by conversion to and/or spalling of Al_2O_3. The surface of the coating after rig testing consisted of βNiAl matrix plus chromium-rich precipitates (e.g., α-Cr and Cr_3Al_2) and Al_2O_3 particles. Oxidation extended selectively inward from the surface to about 0.0007 inch.

The denuded zone was present, as in the as-coated condition (Fig. 34 and 35). The hardness of this zone was low (447 KHN).

Below the denuded zone, a complex layer consisting of βNiAl matrix, $\gamma'Ni_3Al$, refractory metal carbides and finger-like sigma phase was formed. The hardness of this layer, 606 KHN, was less than in the as-coated condition (825 KHN). Decreased hardness is most likely due to decreased Al (or increased Ni) content of the coating or because of carbide precipitation. Carbide precipitation depletes Cr and/or Mo from the diffusion zone matrix and thereby decreases the σ-forming tendencies of this area.

Beneath the diffusion zone, sigma phase platelets in $\gamma'(Ni_3Al)$ matrix developed. This precipitation of sigma phase platelets did not appear to influence coating life or result in signification growth of the coating or diffusion zone.

Coating J After 1800°F Testing

The B1900/J coated specimens (as with the A coating) withstood the test duration of 150 hours of HCR testing at 1800°F (compared to 120 hours at 1650°F). The thickness of the coating was 0.0028 inch as compared to 0.0030 inch in the as-coated condition. The coating surface was essentially free from internal Al_2O_3 spots and showed less attack than after the 1650°F corrosion test (Fig. 36).

The coating surface consisted primarily of βNiAl matrix with lesser amounts of carbides and white $\gamma'(Ni_3Al)$ precipitates. Just beneath the surface oxide was a

Knoop Hardness Number (50-gram load)

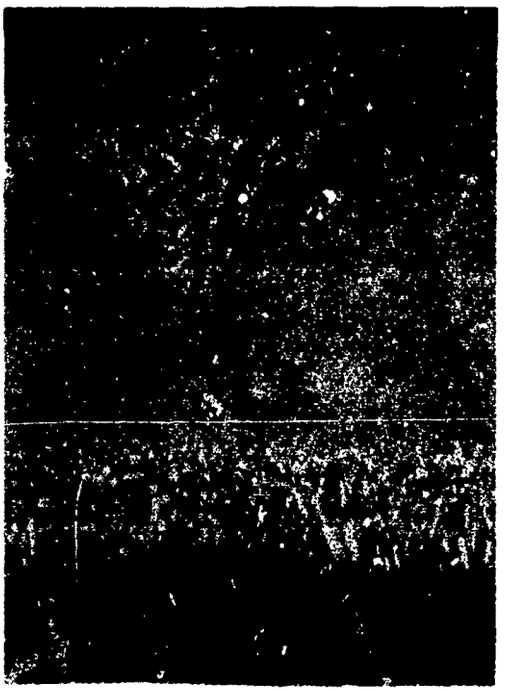

379 βNiAl + Cr_2Al_2 + α-Cr + carbides

482 βNiAl

825 βNiAl + $\gamma'Ni_3Al$ + carbides + sigma

← 274 (Substrate)

Magnification: 1000X

Specimen BJ6

Magnification: 40X

FIGURE 34. MICROSTRUCTURE OF AS-RECEIVED COATINGS; Coating J on B1900 Alloy

Knoop Hardness Number (50-gram load)

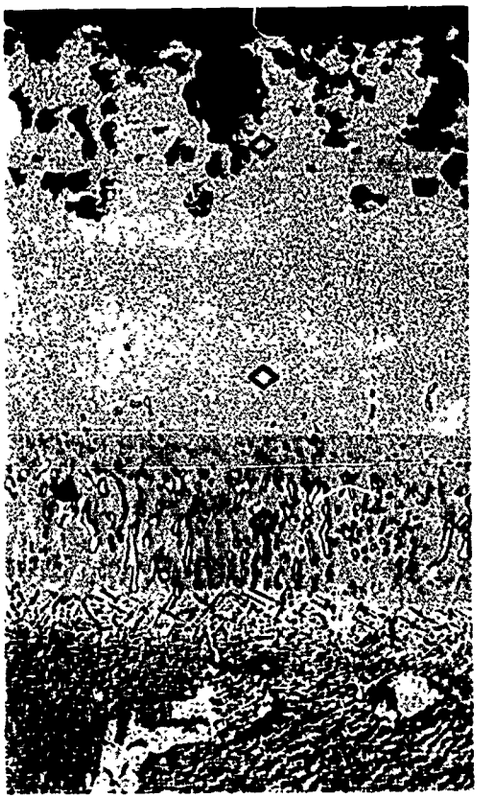

Magnification: 1000X

447 βNiAl + Refractory Metal Rich Precipitates

Denuded zone βNiAl (carbide free)

447

606 βNiAl + $\gamma'Ni_3Al$ + carbides + finger-like σ phase

Sigma phase platelets in γ phase matrix

235 (Substrate)

Specimen BJ1

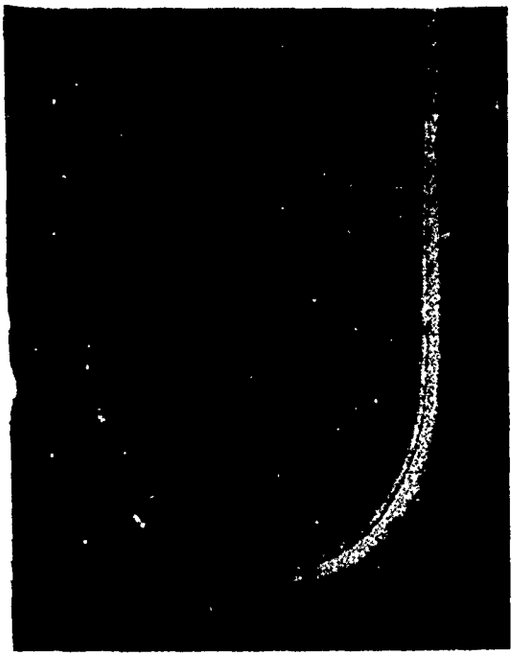

Magnification: 40X

FIGURE 35. MICROSTRUCTURE OF J COATING ON B1900 ALLOY AFTER HOT CORROSION TEST FOR 120 HOURS AT 1650°F

$\gamma'(Ni_3Al)$

$\beta NiAl + \gamma'(Ni_3Al)$ + Refractory Metal Carbides

Denuded zone

$\beta NiAl + \gamma'(Ni_3Al)$ + carbides

Sigma phase platelets in $\gamma'(Ni_3Al)$ matrix

Magnification: 1000X

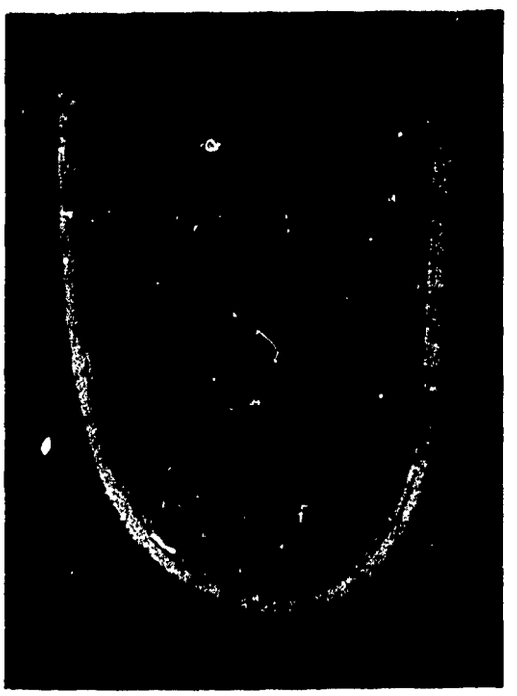

Specimen BJ4

Magnification: 40X

FIGURE 36. MICROSTRUCTURE OF J COATING ON B1900 ALLOY AFTER HOT CORROSION TEST AT 1800°F FOR 160 HOURS

thin discontinuous layer of $\gamma'(Ni_3Al)$ (Fig. 36). This shows the mechanism of degradation was loss by Al by oxidation to Al_2O_3 and transformation of β(NiAl) to $\gamma'(Ni_3Al)$. The denuded zone and the diffusion zone were similar to the respective zones in B1900/J coating after the 1650°F corrosion testing. The main difference was that the finger-like sigma phase could not be observed in the diffusion zone. This indicates that the transformation of sigma phase to carbides was essentially complete after 1800°F and the 150-hour exposure. Beneath the diffusion zone sigma phase platelets were observed in the $\gamma'(Ni_3Al)$ matrix. The zone of sigma phase platelets in γ' was slightly thicker than after the 1650°F exposure (Figs. 35 and 36).

The J coating was found to be the best coating for protection of B1900 alloy and the coating was the most diffusionally stable. The J coating for B1900 alloy was therefore evaluated in Phase II tests.

The K Coating

The microstructure of the K coating on B1900 alloy in the as-coated condition and after HCR testing for 120 hours at 1650°F and for 150 hours at 1800°F are shown in Figures 37, 38 and 39, respectively. The K coating was the thickest (0.0039 inch) of the coatings on B1900. The outer zone of the coating (Fig. 37) was found to consist of βNiAl matrix and fine dispersions of Cr_3Si and Cr_3Al_2, based on X-ray diffraction results (Table VIII) but EMP results are in conflict and indicate a $NiSi_x$ matrix (Fig. 124 and 125). This explains the high hardness of the outer zone (1020 KHN to 1315 KHN). The diffusion zone (1075 KHN) consisted most likely of $\gamma'Ni_3Al$, carbides, silicides and chromium-rich phases (Fig. 37). The high hardness values of the K coating appear to be due to the presence of relatively large amounts of silicon. The silicon content and a high chromium content were confirmed by EMP, X-ray diffraction, and fluorescence analyses.

After the HCR testing at 1650°F for 120 hours, Al and Si diffusion into the substrate occurred resulting in an increase in the thickness of the coating to 0.0054 inch (Fig. 38). The outermost layer (about 0.0008 inch thick) decreased in hardness to 760 KHN and consisted of a $NiSi_x$ matrix plus some very fine dispersion of chromium-rich phase. The zone beneath the outer layer, about 0.0030 inch thick, contained a major second phase (Cr_3Al_2 and/or Cr_3Si) in a matrix of $NiSi_x$ and βNiAl (Fig. 38, 125 and Table IX). This zone was higher in hardness (838-945 KHN) than the outer zone. The diffusion zone consisted of $NiSi_x$, $\gamma'Ni_3Al$ and chromium-rich phases. Electron microprobe analyses was conducted to identify more completely the structure of this coating (See Section 3.13.2).

After the HCR testing at 1800°F for 150 hours, the thickness of the coating varied from 0.0035 inch to 0.0050 inch (Fig. 39). Some coating at the edges and other places spalled off during metallographic mounting. The increase in thickness of the coating indicated a high interdiffusion rate. The outermost zone was oxidized

Knoop Hardness Number (50-gram load)

1165

1020

1315

1075

269

288

Magnification: 40X

Specimen E41

Magnification: 1000X

FIGURE 37. MICROSTRUCTURE OF AS-RECEIVED COATING; Coating K on B1900 Alloy

Knoop Hardness Number (50-gram load)

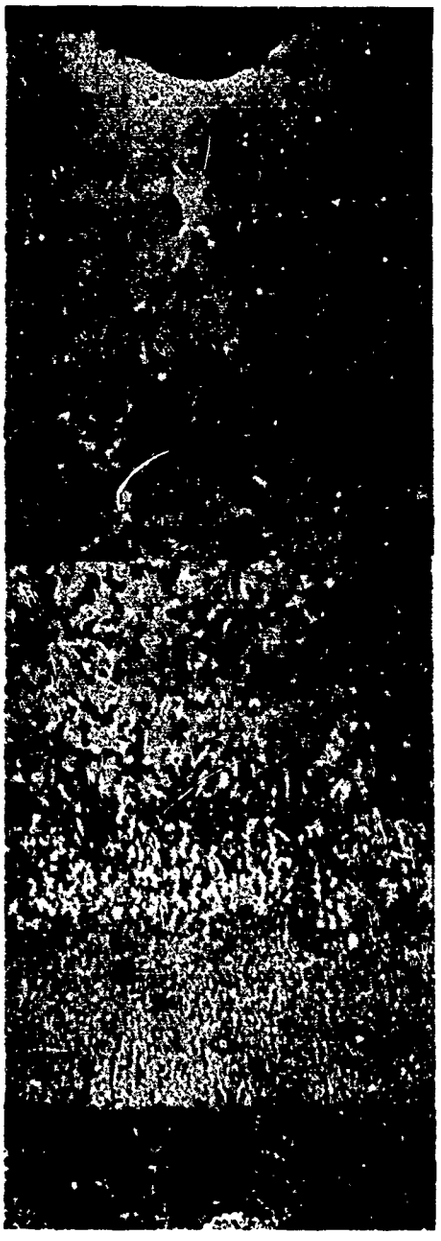

760

838

945

945

703

297

Magnification: 1000X

Magnification: 40X

Specimen BK39

FIGURE 38. MICROSTRUCTURE OF K COATING ON B1900 ALLOY AFTER HOT CORROSION TEST AT 1650°F FOR 120 HOURS

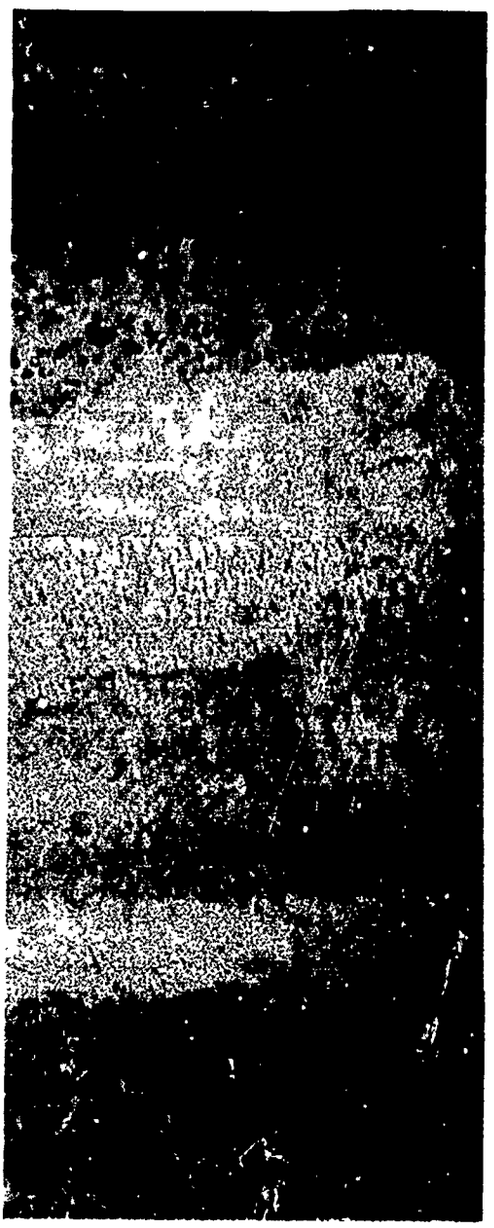

Magnification: 1000X

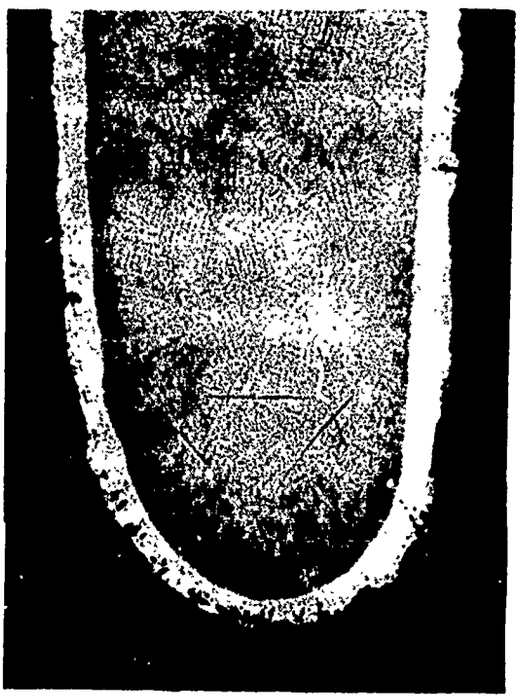

Magnification: 40X

Specimen E53

FIGURE 39. MICROSTRUCTURE OF K COATING ON B1900 ALLOY AFTER HOT CORROSION TEST AT 1800°F FOR 150 HOURS

indicating loss of Al and Si. The remaining coating was very complex and not readily identified (See Section 3.13.2).

This coating had only fair diffusional stability and high hardness, probably due to the high silicon content. The K coating did, however, provide protection for 150 hours at 1800°F and 120 hours at 1650°F in hot corrosion testing. The performance of this coating was therefore comparable to that of J coating on B1900 and was selected for additional analysis and inclusion in Phase II.

3.4 HOT CORROSION TEST RESULTS OF COATED Inco 713C

3.4.1 Weight Change and Appearance

Figures 40, 41 and 42 show the results of the tests performed on coated Inco 713C alloy at 1650°F and 1800°F. The J coated specimens showed excellent performance at both temperature levels. None of these coated specimens showed visual evidence of substrate oxidation or coating deterioration at the conclusion of the testing. The tubercles or coating nodules shown on the specimen after test at 1650°F were also apparent on this specimen prior to the hot corrosion tests. The G coating showed second best performance at both 1650°F and 1800°F. Specimens removed from the 1650°F test after 150 hours exposure showed minor pitting of the coating on the concave surfaces. The G coated specimens after test at 1800°F for 150 hours exhibited slight spalling of the coating on the convex surface towards the tips of the blades. No substrate oxidation, however, was apparent.

The A coating exhibited third best performance at both temperature levels. Failures were of the pinhole type, occurring on the concave surfaces of the specimens.

The C and F coatings did not show good performance at either temperature level. The C coating was removed from test after 120 hours at 1650°F and 60 hours exposure at 1800°F. The coating exhibited a considerable amount of spalling on both the concave and convex surfaces. The F coating primarily exhibited pinhole type failures. At 1650°F, specimens were removed from test after a total of 90 hours exposure, and specimens were removed from the 1800°F test after 60 hours exposure.

3.4.2 Metallographic Analyses of Coatings on Inco 713C

The Inco 713C alloy contains higher carbon and Cr additions than B1900 and also contains 2 percent Cb, which would favor formation of MC carbide in addition to $M_{23}C_6$ carbides.

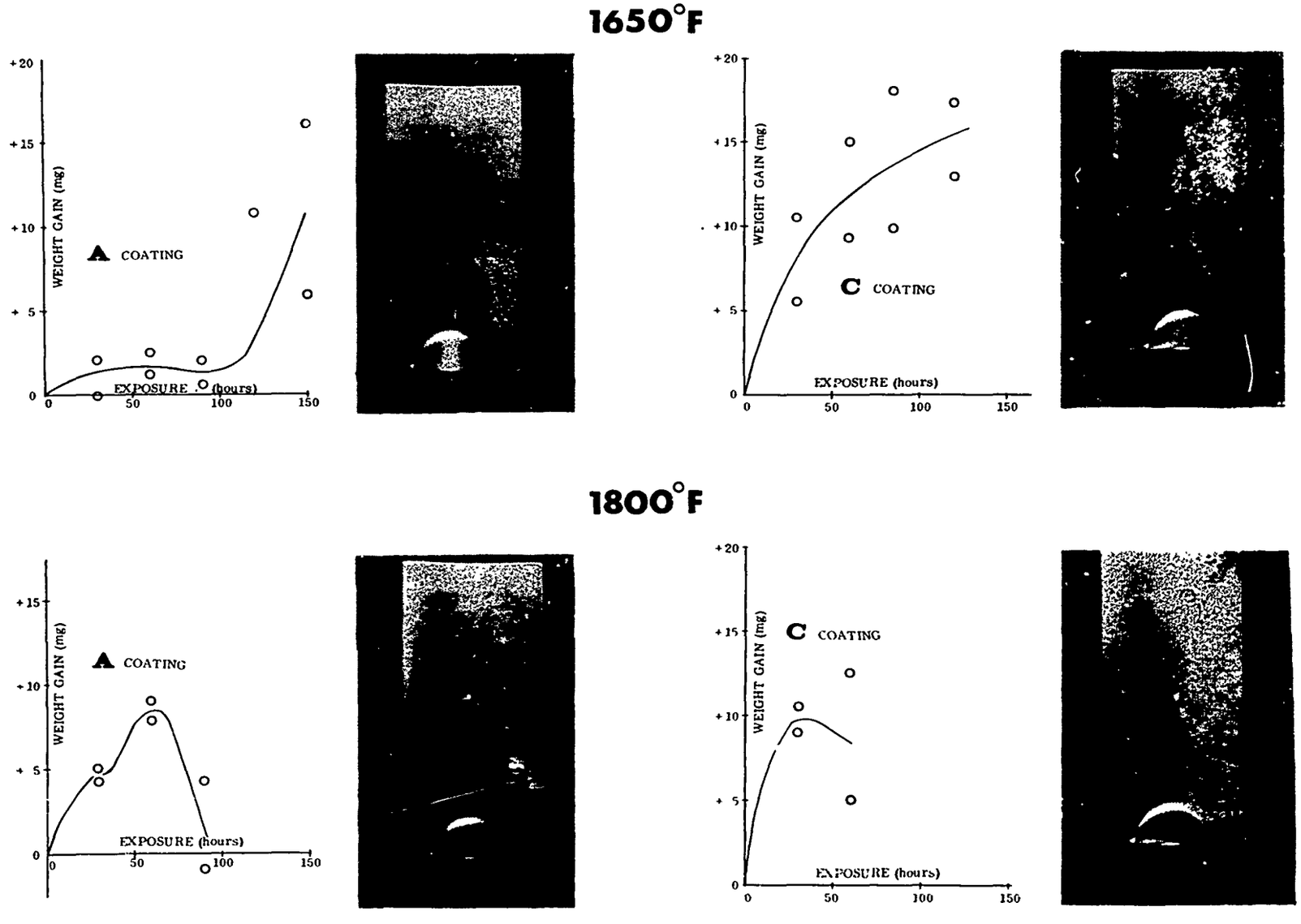

FIGURE 40. WEIGHT CHANGE AND APPEARANCE OF COATINGS A AND C ON INCO 713C ALLOY TESTED AT 1650°F AND 1800°F

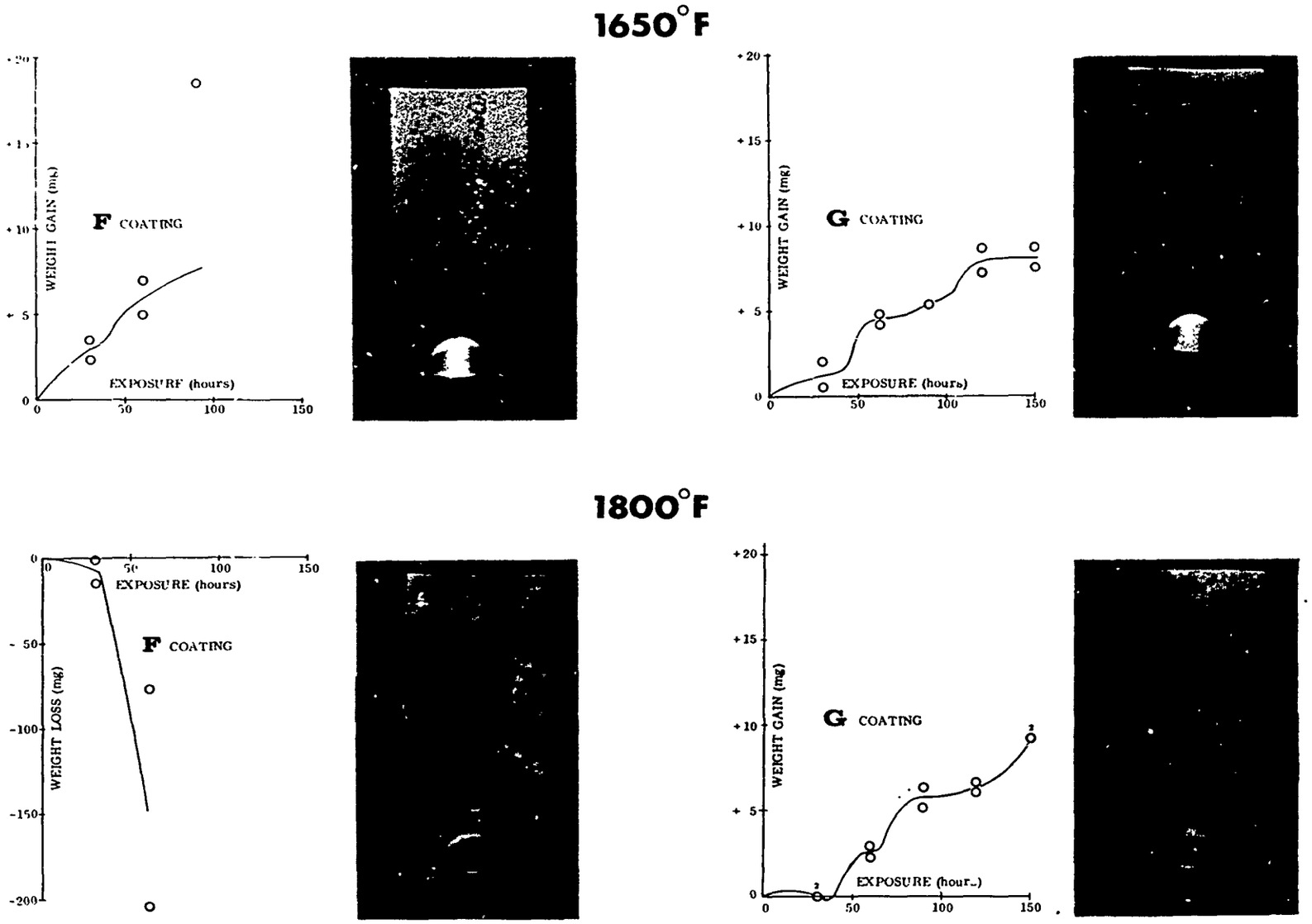

FIGURE 41. WEIGHT CHANGE AND APPEARANCE OF COATINGS F AND G ON INCO 713C ALLOY TESTED AT 1650° F AND 1800° F

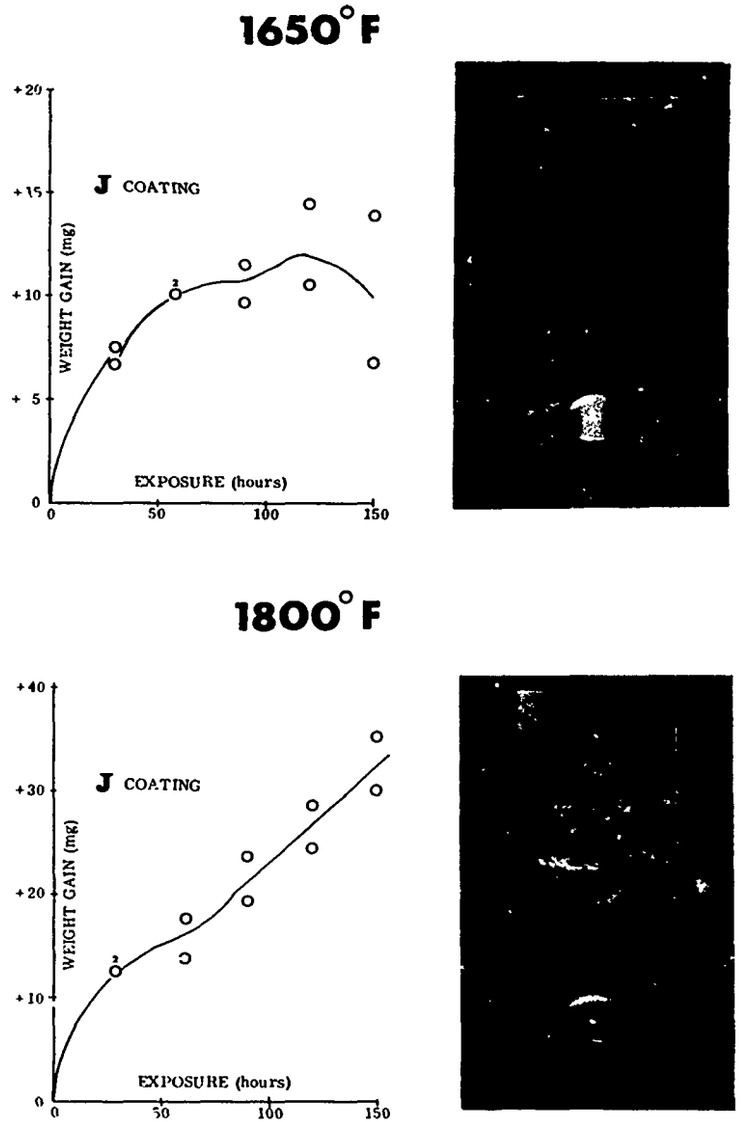

FIGURE 42. WEIGHT CHANGE AND APPEARANCE OF COATING J ON INCO 713C ALLOY TESTED AT 1650° F AND 1800° F

The A Coating

The microstructure of Inco 713C/A coating is very similar to that of the B1900/A coating shown previously (Fig. 31). The only difference was the presence of an unidentified white phase (probably chromium-rich) near the coating metal interface.

The effects of hot corrosion testing were similar to those described for the B1900/A coating (Sec. 3.3.2). The thickness of the coating was increased from 0.0033 inch to 0.0054 inch and to 0.0040 inch after HCR testing at 1650°F for 150 hours and at 1800°F for 90 hours, respectively, showing a rapid diffusion rate. The sigma phase platelets in γ' matrix at the interface could be detected only after the hot corrosion exposure at 1800°F for 90 hours and not after the exposure at 1650°F for 150 hours.

The A coating, because of diffusion instability and only 90 hours protection at 1800°F for Inco 713C, was not recommended for further evaluation.

The C Coating

The microstructures of the C coating on Inco 713C in the as-coated condition and after hot corrosion tests at 1650°F for 120 hours are shown in Figures 43 and 44, respectively.

Coating C As-Coated

The major coating phase was βNiAl with dispersion of a chromium-rich white phase at the surface of the coating. The microstructure of the C coating on Inco 713C was similar to that on B1900 in terms of structural details, coating thickness and weight gain (Sec. 3.3.2). A slightly higher population of carbide phases was present in the diffusion zone of the coating.

After HCR testing at 1650°F for 120 hours, the βNiAl phase was converted to $\gamma'Ni_3Al$ phase at the coating surface (Fig. 44). Internal oxide spots can be seen in the microstructure (Fig. 44). The diffusion zone consisted mostly of $\gamma'Ni_3Al$ (matrix) with beta, carbide precipitates and oxides. Finger-like sigma phase could not be detected in the diffusion zone. The sigma phase platelets in γ' matrix (second phase being γ) were present at the interface.

On the concave edge, the coating was over 50 percent consumed. The coating at the concave edge consisted of γ' matrix with remnants of beta phase, carbides and platelets of sigma phase at the interface.

Magnification: 1000X Magnification: 40X

FIGURE 43. MICROSTRUCTURE OF AS-RECEIVED COATINGS; Coating C on Inco 713C Alloy

The C coating after HCR testing at 1800°F for 60 hours was found to consist of γ' matrix, βNiAl, carbides and some internal oxide spots. Most of the β(NiAl phase) transformed to $\gamma'Ni_3Al$. The coating-substrate interface was found to consist of γ' matrix, sigma phase platelets and γ.

The C coating, because of short life (120 hours at 1650°F and 60 hours at 1800°F), was not further evaluated for protection of Inco 713C.

The F Coating

The microstructure of F coating on Incc 713C was similar to that of B1900/F coating, and is shown in Figure 45. The presence of a hard, white phase was noted at the surface of the F coating, which resembled the Ni_2Al_3 phase identified in the other coatings and therefore indicated a high Al content at the surface. The outer layer was found to consist of βNiAl + large α-Al_2O_3 inclusions + αCr by comparison to microstructure and X-ray diffraction pattern of SEL-15/F coating (Table VI). Other microstructural details were as described for the B1900/F coating.

Magnification: 40X

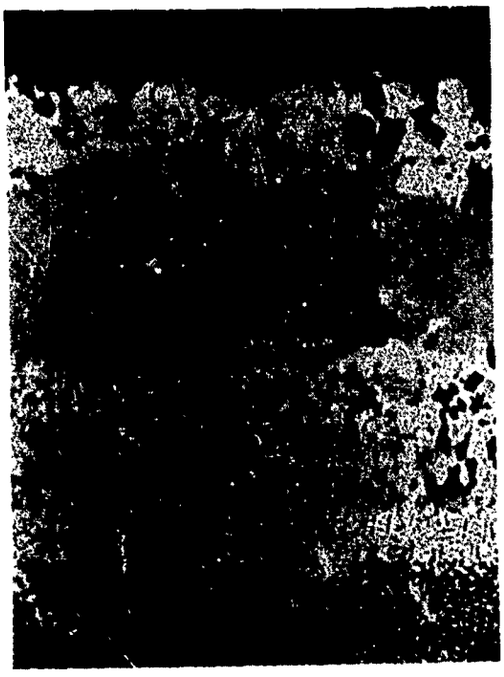

Magnification: 1000X

FIGURE 44. MICROSTRUCTURE OF C COATING ON INCO 713C AFTER HOT CORROSION TESTS AT 1650° F FOR 120 HOURS

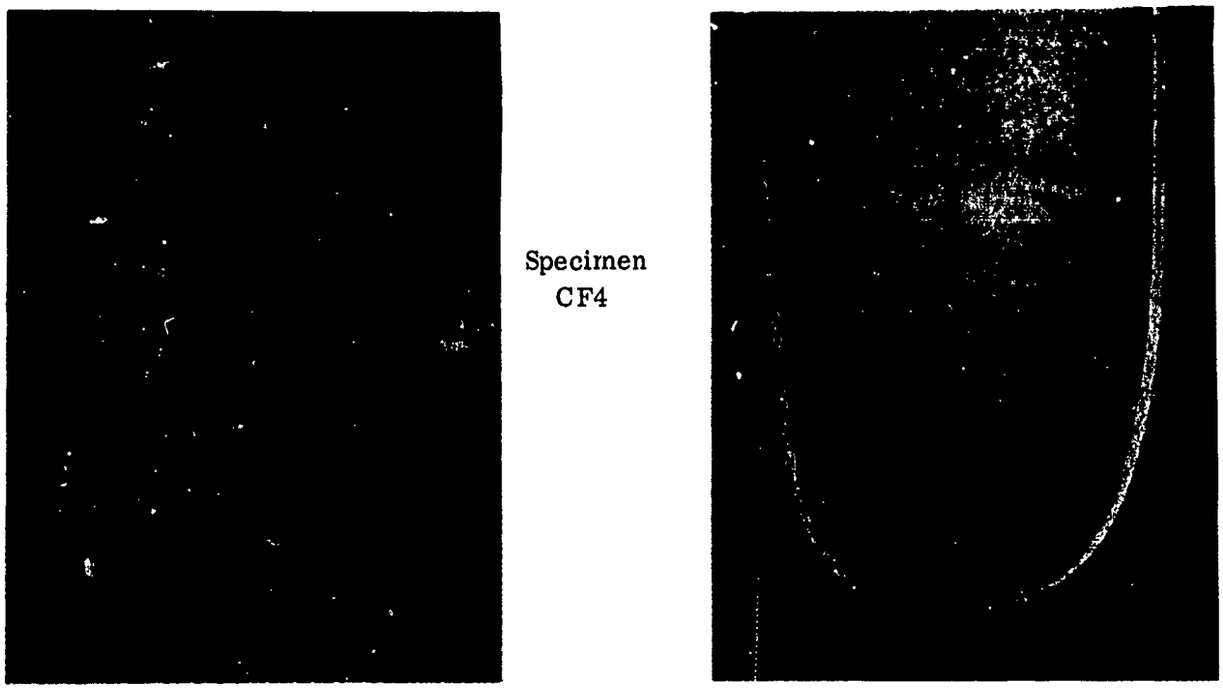

Specimen
CF4

Magnification: 1000X

Magnification: 40X

FIGURE 45. MICROSTRUCTURE OF AS-RECEIVED COATINGS; Coating F on Inco 713C Alloy

The microstructure of Inco 713C/F coated specimens after HCR testing at 1650°F for 90 hours is shown in Figure 46. The initial outer area, consisting mostly of βNiAl, large α-Al_2O_3 inclusions, and α-Cr, appeared to have oxidized and spalled off. The outer zone appeared to be free from carbides, oxides, or chromium-rich precipitates. There were no other significant changes.

After the test at 1800°F for 60 hours, the Inco 713C/F coating was over 60 percent consumed. The remaining coating appeared to consist of γ' matrix, β phase, carbides and sigma phase platelets.

Poor performance of the Inco 713C/F coating eliminated it from further evaluation in the program.

The G Coating

The microstructures of Inco 713C/G coating in the as-coated condition and after hot corrosion tests at 1650°F for 150 hours and at 1800°F for 150 hours are shown in Figures 47, 48 and 49, respectively.

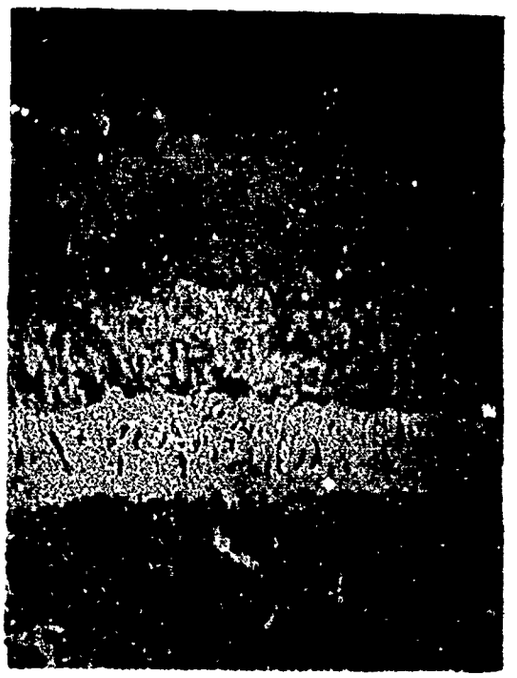

Specimen
CF6

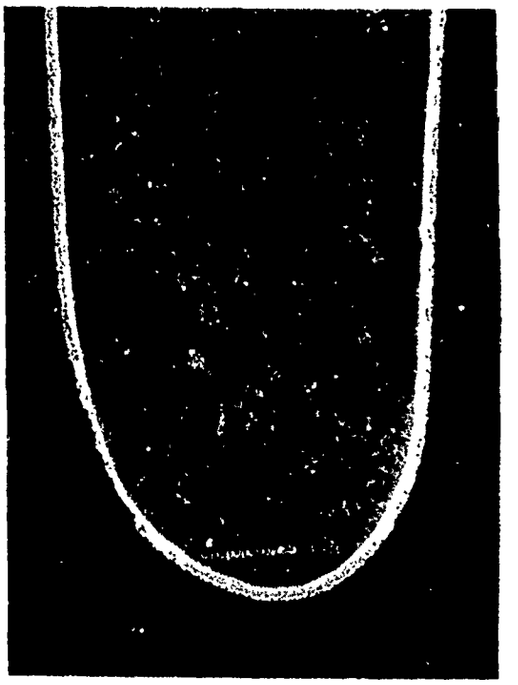

Magnification: 1000X

Magnification: 40X

FIGURE 46. MICROSTRUCTURE OF F COATING ON INCO 713C ALLOY AFTER HOT CORROSION TESTS AT 1650°F FOR 90 HOURS

Knoop Hardness
(50-gram load)

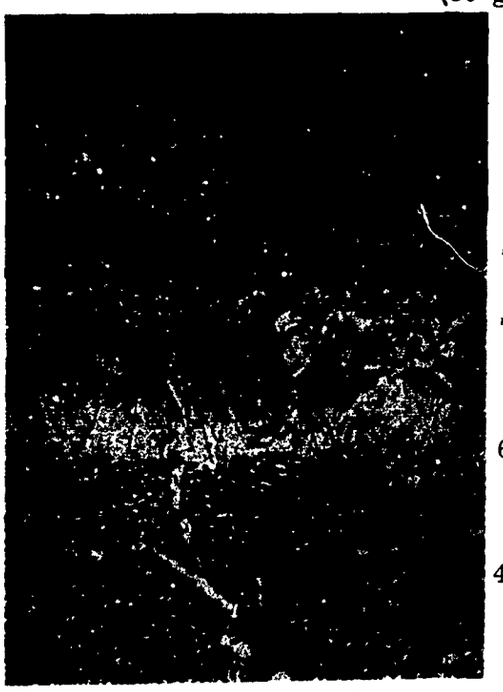

606

713

748

Specimen
CG6

643

401

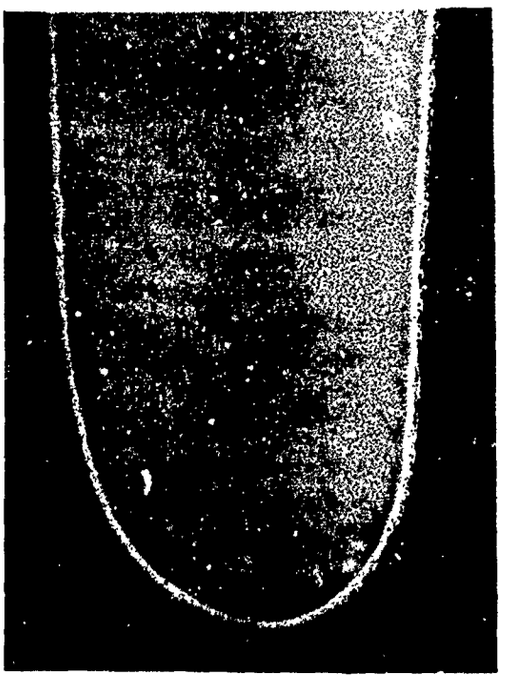

Magnification: 1000X

Magnification: 40X

FIGURE 47. MICROSTRUCTURE OF AS-RECEIVED COATINGS; Coating G on Inco 713C Alloy

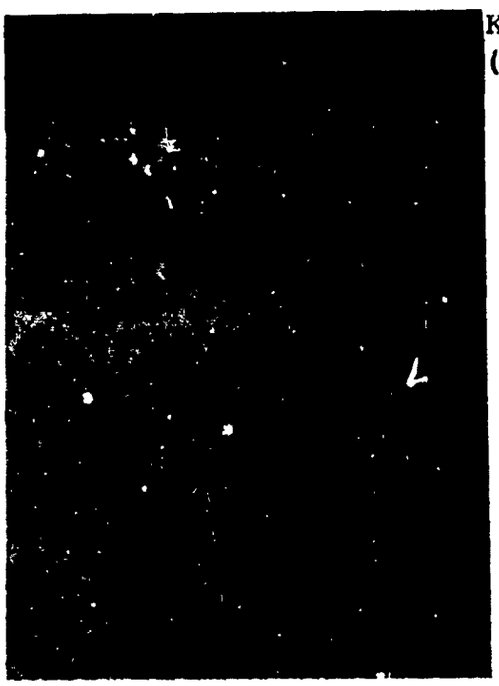

Knoop Hardness
(50-gram load)

488

465

Specimen
CG4

825

521

351

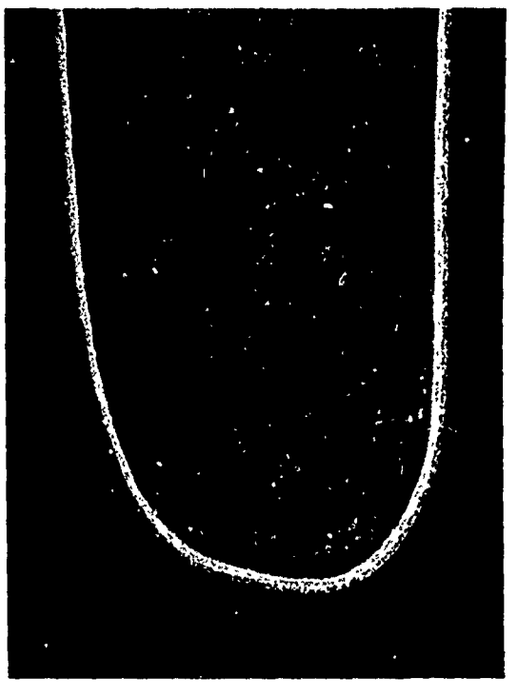

Magnification: 1000X

Magnification: 40X

FIGURE 48. MICROSTRUCTURE OF G COATING ON INCO 713C AFTER HOT CORROSION TESTS AT 1650° F FOR 150 HOURS

Specimen
CG3

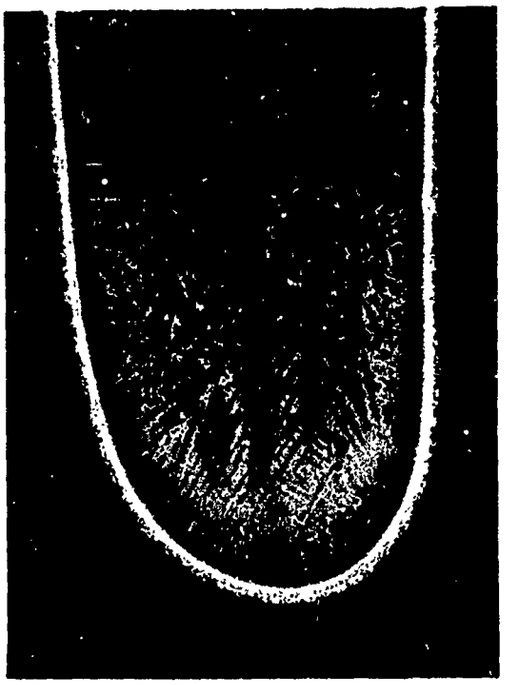

Magnification: 1000X

Magnification: 40X

FIGURE 49. MICROSTRUCTURE OF G COATING ON INCO 713C AFTER HOT CORROSION TESTS AT 1800° F FOR 150 HOURS

The outer area as-coated was found to consist of βNiAl matrix, large α-Al_2O_3 inclusions and α-Cr based on X-ray diffraction data (Table X). The diffusion zone consists of βNiAl matrix, γ' phase, carbides and sigma phase. At the interface, the predominant phase was γ' with sigma platelets.

There were no significant changes in the microstructure after 150 hours exposure at 1650°F in HCR testing on Inco 713C/G coated specimens (Fig. 48), but there was a decrease in hardness of the coating. The decrease in hardness is due to a loss of Al by Al diffusion or Al oxidation to Al_2O_3. The thickness of the coating remained about the same after this or after the exposure at 1800°F for 150 hours. After the test at 1800°F for 150 hours, the outer area of the coating appeared to consist of βNiAl (matrix), γ' phase, α-Al_2O_3 and possibly α-Cr (Fig. 49). The diffusion zone was substantially changed in microstructure and consisted most likely of βNiAl, γ'(Ni_3Al) and carbide precipitates. The sigma phase, present in the diffusion zone in the as-coated condition, transformed into the carbide precipitates. At the interface, the matrix was γ'(Ni_3Al) and the other phases were γ, sigma phase platelets and carbides.

The G coating, because of more than 150 hours of protection at both 1650°F and 1800°F for Inco 713C, was selected for Phase II evaluation.

The J Coating

The microstructures of Inco 713C/J coating in the as-coated condition and after 150 hours test at 1650°F were similar to those of the B1900/J coating. The outer layer of the J coating in the as-coated condition on Inco 713C was found to consist of βNiAl + Cr_3Al_2 + α-Cr (based on X-ray diffraction data, Table VII). Partially dissolved carbides were apparent at the coating surface (Fig. 50). The microstructural changes, as a result of the test at 1650°F for 150 hours, were similar to those for B1900/J coating specimen (Sec. 3.3.2). The major difference was a wider γ' matrix zone (at the interface) in which no sigma phase platelets could be detected (Fig. 51). Sigma phase platelets developed at the interface for B1900/J coating after tests at 1650°F for 150 hours.

The microstructure of Inco 713C/J coating after exposure at 1800°F for 150 hours is shown in Figure 52. The thickness of the coating increased from 0.0030 inch to 0.0032 inch, showing evidence of slight coating growth due to diffusion. The outer layer and denuded zone were similar to the microstructure in the as-coated condition. The diffusion zone appeared to consist of βNiAl matrix, carbide precipitates, and a chromium-rich phase. No sigma phase could be detected, indicating that sigma phase had transformed into the carbides. Sigma phase platelets were found to develop in γ' matrix (the other phase being γ) at the interface.

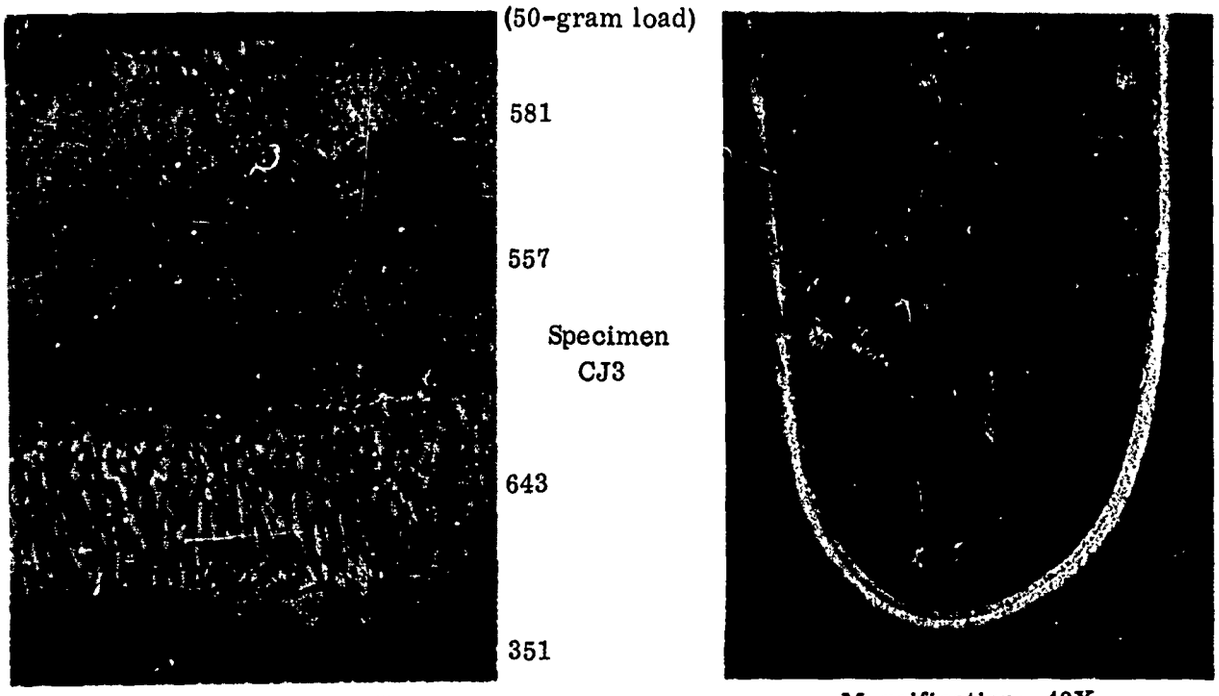

FIGURE 50. MICROSTRUCTURE OF AS-RECEIVED COATINGS;
Coating J on Inco 713C Alloy

The J coating for Inco 713C, because of satisfactory performance during HCR tests at 1650°F and 1800°F, was selected for further evaluation.

It should be noted that coatings A, C, F and J provided longer lives on Inco 713C alloy than on the B1900 alloy in the hot corrosion tests at 1650°F and 1800°F. This is most likely due to the higher chromium content in the Inco 713C (13.8% Cr) than in the B1900 alloy (8.5% Cr), and perhaps to the superior hot corrosion resistance of the uncoated alloys.

3.5 HOT CORROSION TEST RESULTS OF COATED IN-100 ALLOY

3.5.1 Weight Change and Appearance

Test results for the IN-100 alloy at 1650°F and 1800°F are shown in Figures 53, 54 and 55. The A and J coating systems showed excellent performance in the 1650°F tests. These two coatings were the only ones capable of providing protection in excess of 150 hours to this alloy. The surfaces of the J and A coated specimens

Text Continued on Page 75.

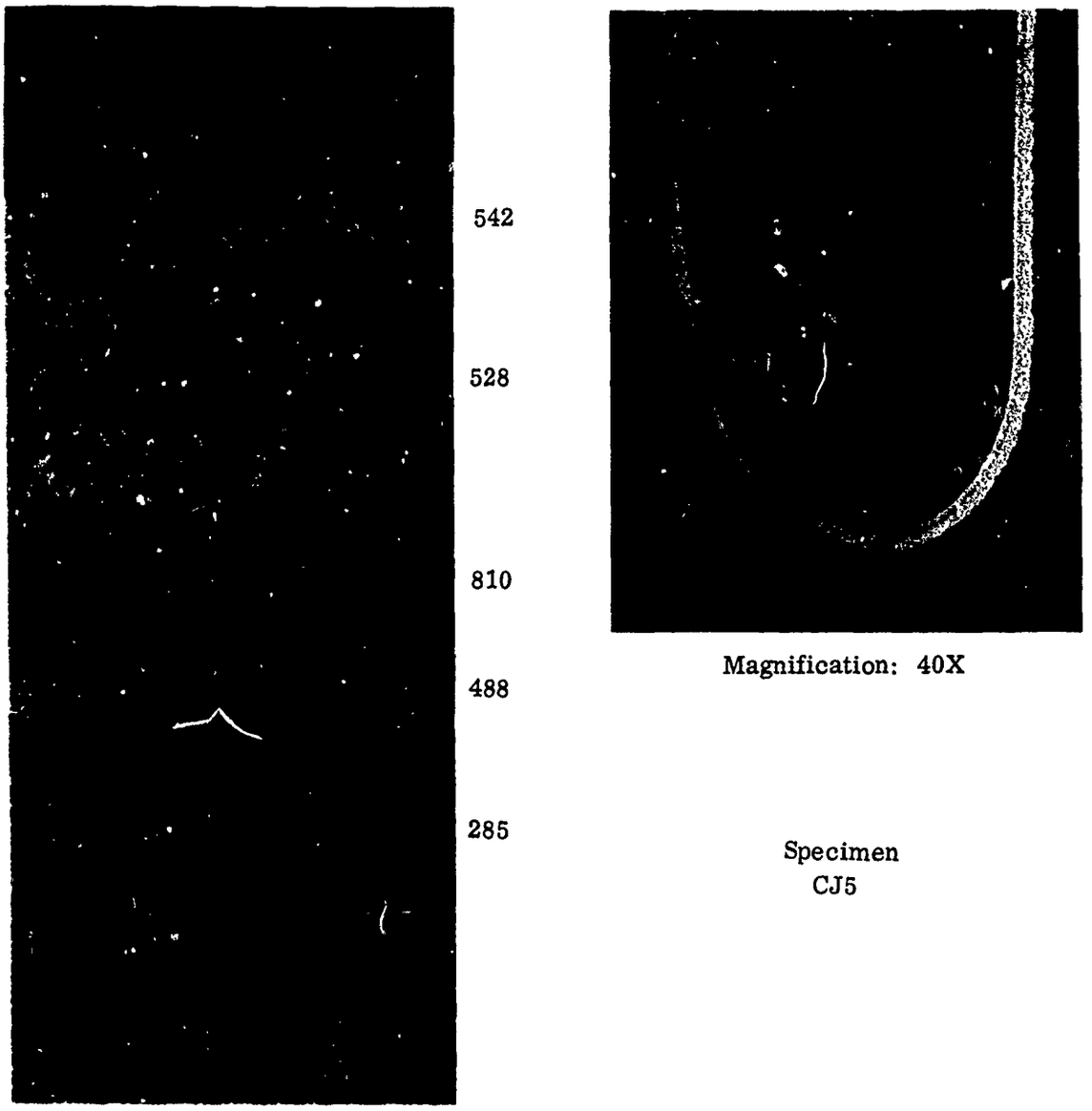

FIGURE 51. MICROSTRUCTURE OF J COATING ON INCO 713C AFTER HOT CORROSION TESTS AT 1650° F FOR 150 HOURS

Specimen
CJ2

Magnification: 40X

Magnification: 1000X

FIGURE 52. MICROSTRUCTURE OF J COATING ON INCO 713C AFTER HOT CORROSION TESTS AT 1800° F FOR 150 HOURS

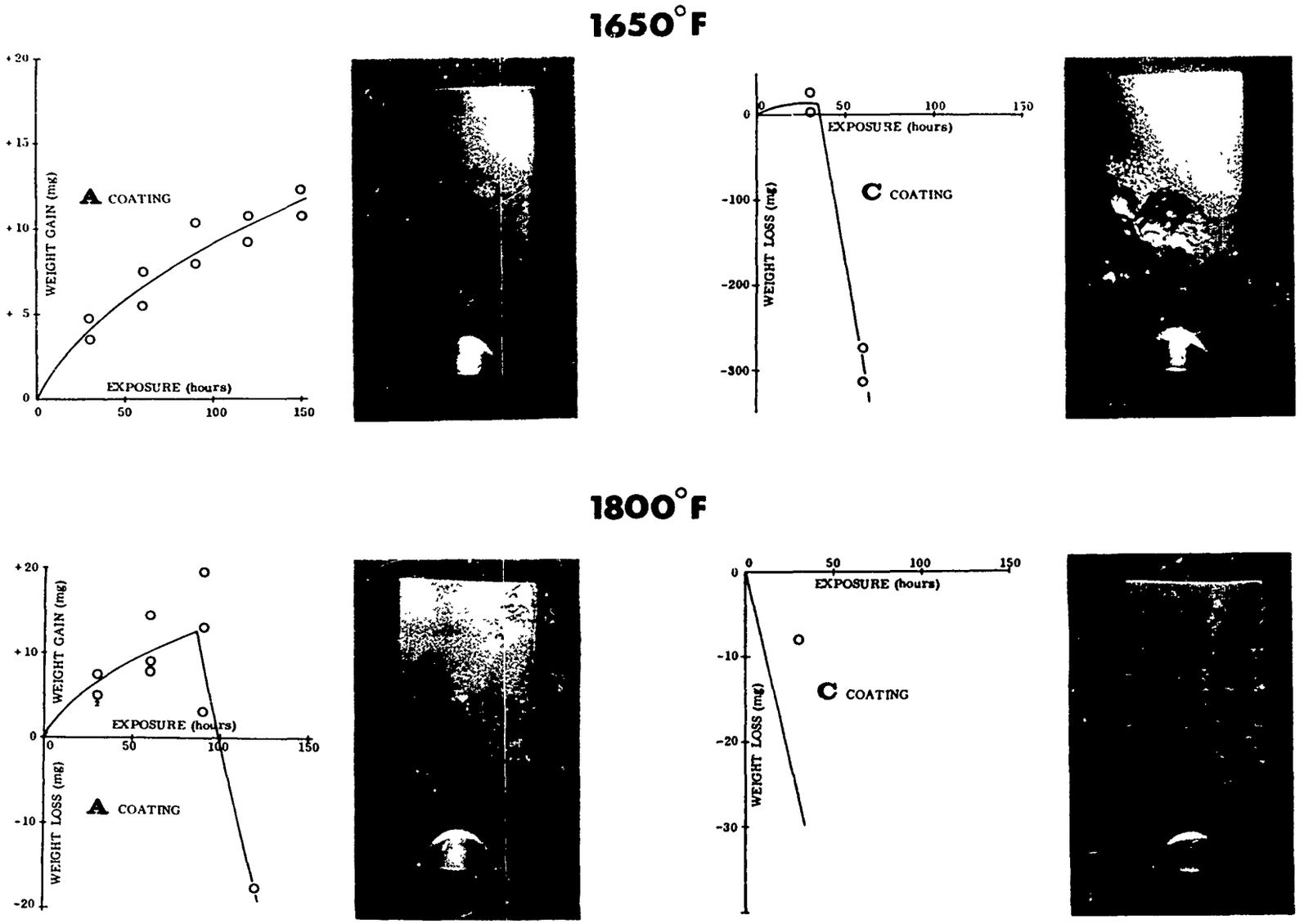

FIGURE 53. WEIGHT CHANGE AND APPEARANCE OF COATINGS A AND C ON IN-100 ALLOY TESTED AT 1650°F AND 1800°F

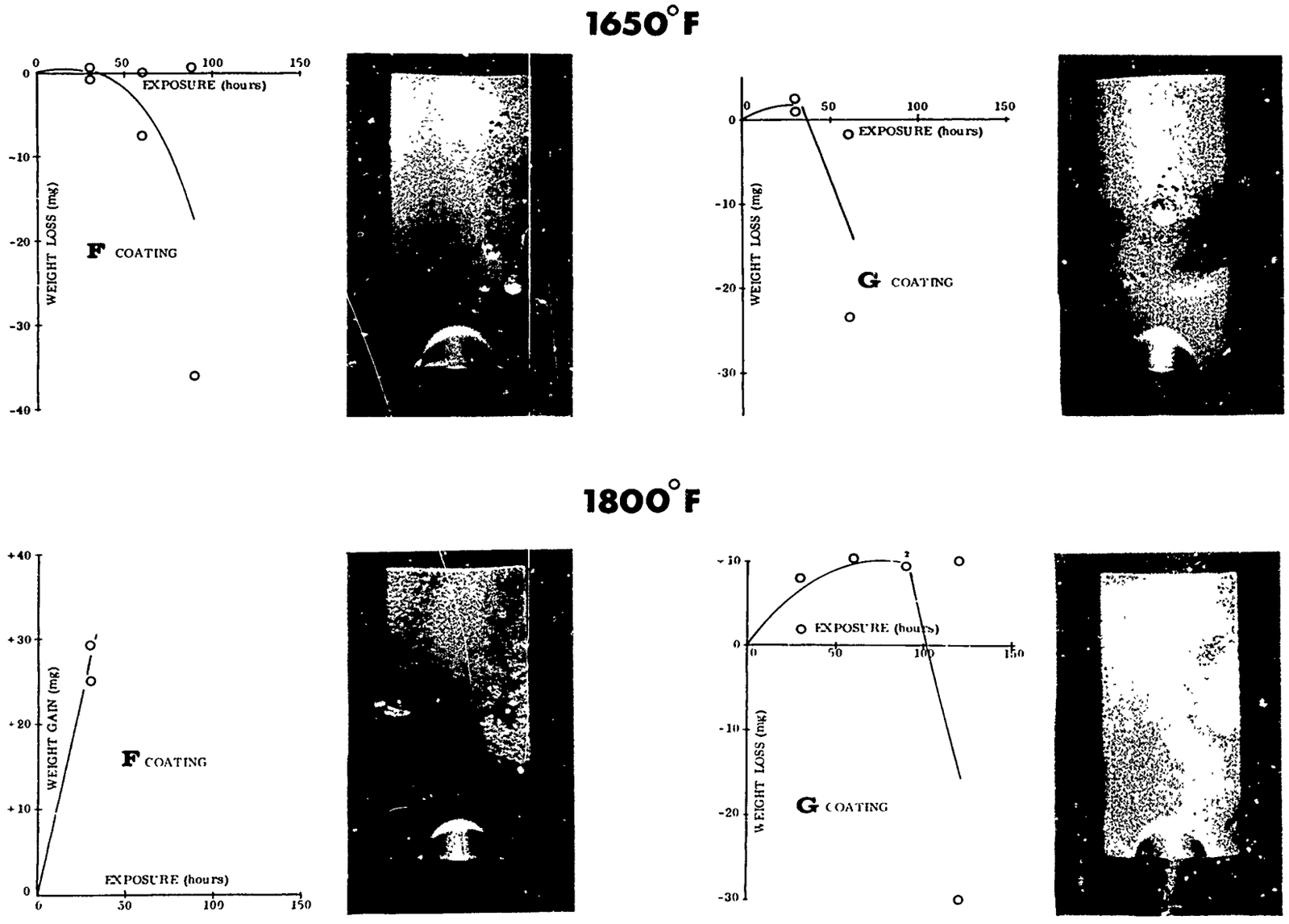

FIGURE 54. WEIGHT CHANGE AND APPEARANCE OF COATINGS F AND G ON IN-100 ALLOY TESTED AT 1650°F AND 1800°F

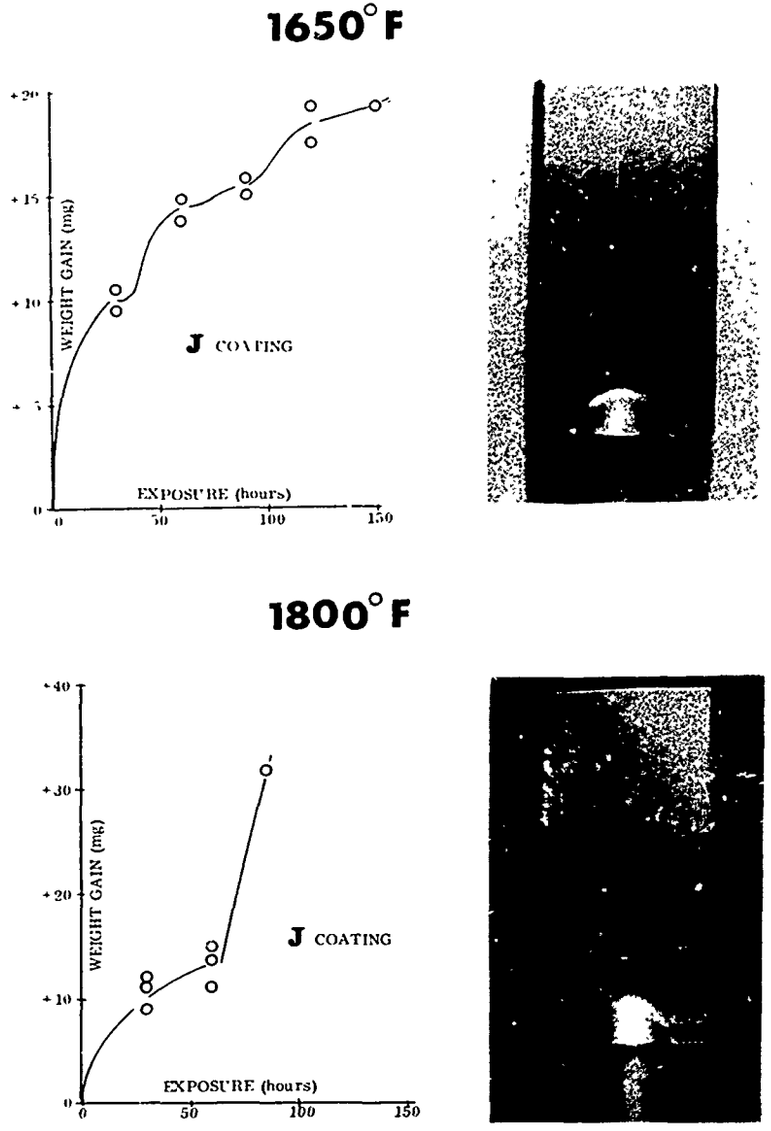

FIGURE 55. WEIGHT CHANGE AND APPEARANCE OF COATING J ON IN-100 ALLOY TESTED AT 1650° F AND 1800° F

were essentially unchanged as a result of the test. Coating system C, F and G all showed evidence of pinhole type coating failures and were removed from test with less than 100 hours exposure.

At 1800°F, none of the coatings provided protection for 150 hours exposure. Best performance was exhibited by the A, G and J coatings for approximately 90 hours total exposure. The C and F coatings failed within the first 30-hour exposure period. Failures were located on the concave surfaces of the specimens.

3.5.2 Metallographic Analyses of Coatings on IN-100 Alloy

The A Coating

The microstructures of IN-100/A coated specimens before and after hot corrosion exposures at 1650°F for 150 hours duration and at 1800°F for 120 hours duration were very similar to those of the B1900/A coating. The thickness of the coating increased from 0.0030 inch in as-coated condition (Fig. 56) to 0.0035 inch after exposure for 150 hours at 1650°F (Fig. 57) and to 0.0038 inch after exposure for 120 hours at 1800°F (Fig. 58). The coating substrate interdiffusion was less

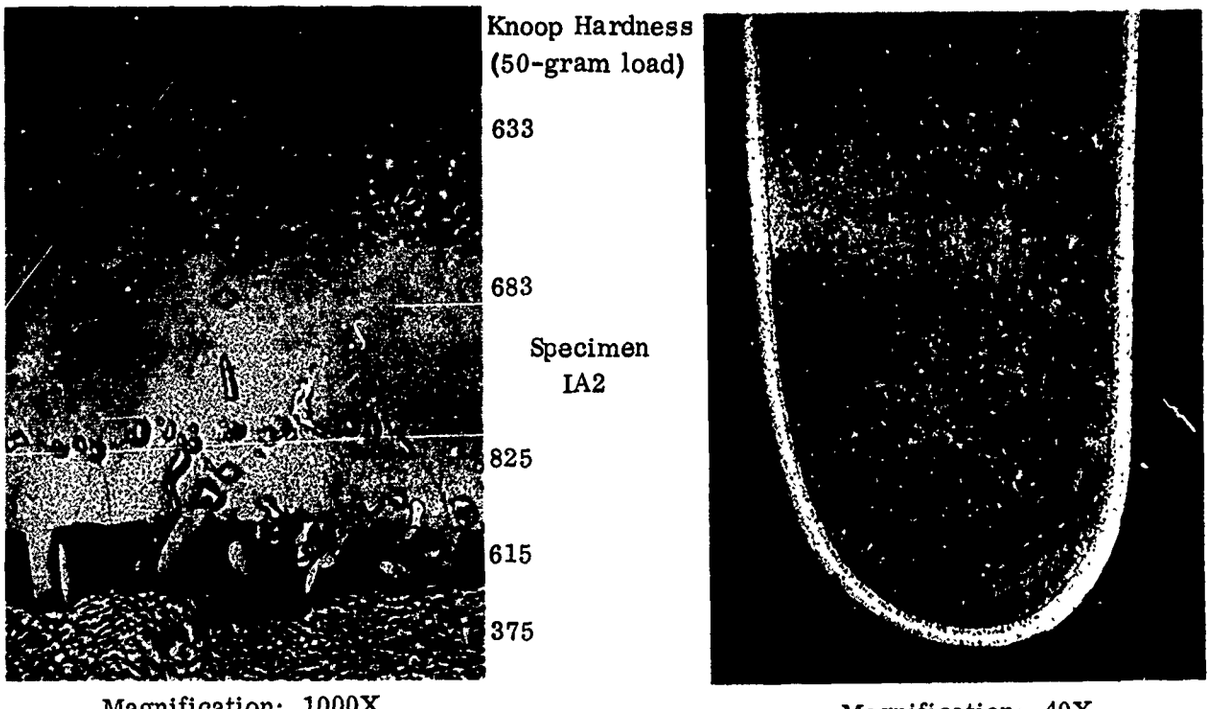

Magnification: 1000X

Magnification: 40X

FIGURE 56. MICROSTRUCTURE OF AS-RECEIVED COATINGS; Coating A on IN-100 Alloy

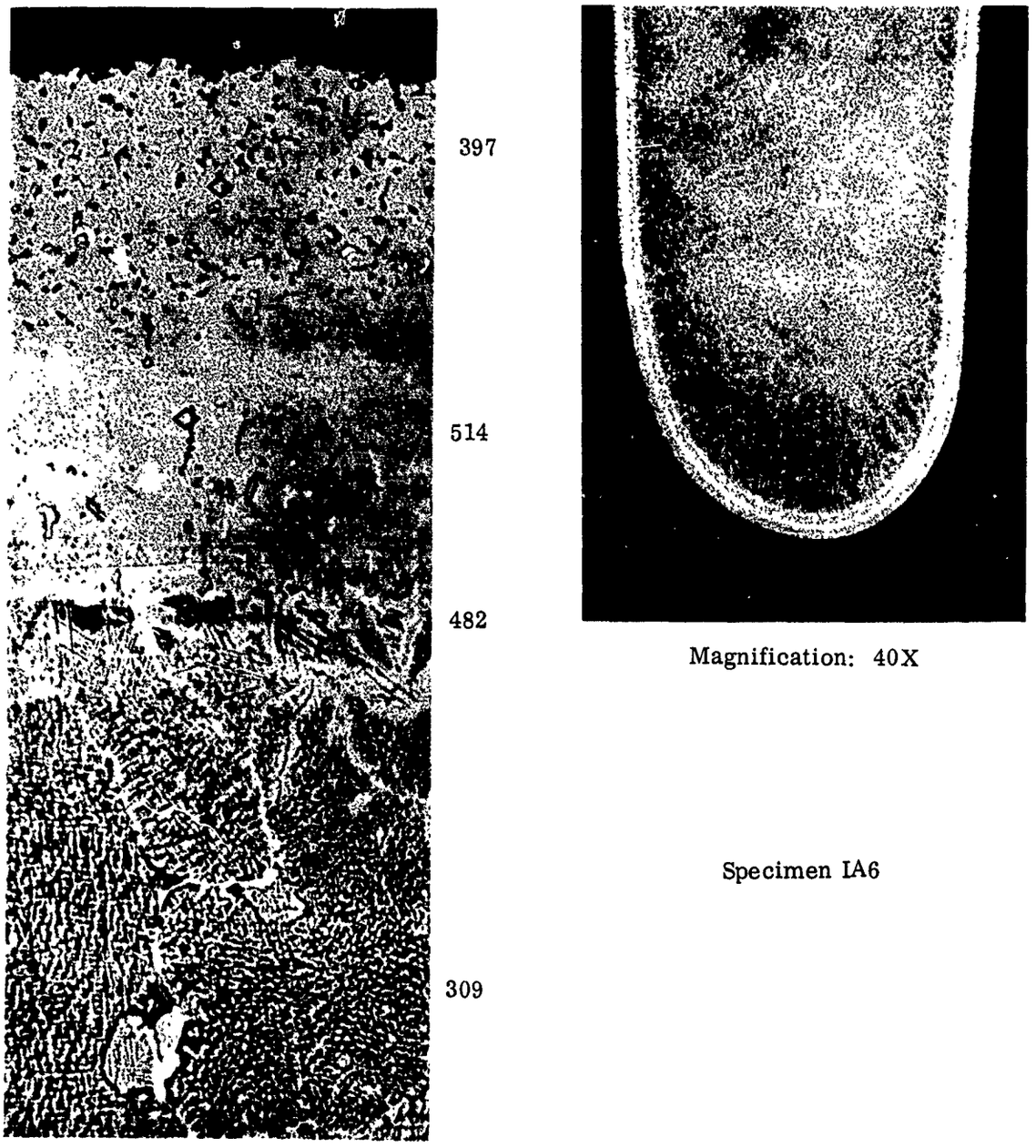

FIGURE 57. MICROSTRUCTURE OF COATING A ON IN-100 AFTER HOT CORROSION TESTS AT 1650° F FOR 150 HOURS

Magnification: 1000X

Magnification: 40X

Specimen IA5

FIGURE 58. MICROSTRUCTURE OF COATING A ON IN-100 AFTER HOT CORROSION TESTS AT 1800° F FOR 120 HOURS

severe with the A coating on IN-100 than on B1900 or Inco 713C alloys. The essential difference was in the interface structure of IN-100/A coating after exposure for 150 hours at 1650°F. The wide γ interface layer in the as-coated condition had transformed to a complex layer consisting of γ' matrix with sigma phase platelets, beta phase and some untransformed or retained gamma phase.

The A coating was selected for inclusion in Phase II and for EMP analysis (see Section 3.13) since it provided protection to the IN-100 alloy for more than 150 hours at 1650°F and for 120 hours at 1800°F. Interdiffusion was relatively slow compared to the A coating on B1900 or Inco 713C alloys.

The C Coating

The microstructure of IN-100/C coating was similar to that of the B1900/C coating. The main difference was the presence of an unidentified chromium-rich, white phase in the diffusion zone. Other phases present in the diffusion zone were βNiAl matrix, finger-like sigma phase and carbides. From the carbide "markers" it may be assumed that this coating was formed by outward diffusion of nickel (and cobalt). The relatively high aluminum phase M_3Al (higher Al than γ) tends to form at the interface under these conditions.

The IN-100/C coating failed after HCR testing at 1650°F for 60 hours and was therefore not extensively evaluated.

The F Coating

The microstructure of the F coating on IN-100 alloy before and after hot corrosion testing was very similar to that on the B1900 alloy (Sec. 3.3.2).

The F coated IN-100 specimens failed after 90 hours exposure at 1650°F. The IN-100 alloy contains a high amount of Ti (4.34%) compared to that of Inco 713C (Ti = 0.79%). Therefore, the probability of TiO_2 being present in the surface oxide is greater with the IN-100/F coated specimen than with the Inco 713C/F coated specimens. The TiO_2 in the surface oxides was reported to result in poorer oxidation resistance and coating stability (Ref. 4). Because of this and the slightly lower chromium content in IN-100 (Cr = 10.5%) than in Inco 713C (Cr = 13.8%), the F coating provided less corrosion protection to IN-100 than to Inco 713C. The 1800°F hot corrosion test caused the failure of the IN-100/F coated specimens after 30 hours compared to that of the Inco 713C/F coated specimens which survived 60 hours exposure.

The F coating on IN-100 alloy because of the relatively poor hot corrosion resistance was not included for further detailed evaluation.

The G Coating

The as-coated thickness (0.0016 inch) of the G coating on IN-100 was less than that on Inco 713C (0.0022 inch) and was lower than the minimum specified limit (Fig. 59). The outer area of the coating consisted of βNiAl matrix, α-Al_2O_3 inclusions and probably α-Cr based on comparison to the microstructure and X-ray diffraction data of Inco 713/G coated specimens (Table X).

The diffusion zone of the In-100/F coating consisted of βNiAl matrix, carbides and a chromium-rich white phase. This was quite different from the structure of the diffusion zone of Inco 713C/G coating, which contained finger-like sigma phase and γ' in addition to βNiAl matrix, carbides and chromium-rich phase. The interface was a thin layer of γ compared to a complex wide layer (γ' matrix and sigma phase platelets) for the F coating on Inco 713C.

After hot corrosion exposure for 60 hours at 1650°F the thickness of the coating was 0.0012 inch compared to 0.0016 inch in the as-coated condition. The outer layer appeared to consist of βNiAl matrix, large α-Al_2O_3 inclusions and internal oxide spots (Fig. 60). The significant change in the structure of the diffusion zone was the presence of γ' phase, finger-like sigma phase and large carbides in βNiAl matrix. The thin γ layer at the interface has transformed to a thin γ' layer after the exposure (Fig. 60).

The 1800°F exposure of the G coated specimen resulted in complete failure after 120 hours.

The G coating, because of its relatively poor corrosion resistance on IN-100 alloy was not selected for further evaluation.

The J Coating

The structural details of the J coating on IN-100 alloy in the as-coated condition and after exposure at 1650°F for 150 hours were similar to those for the B1900/J coating (Fig. 34) and to Inco 713C/J coating (Sec. 3.4.2). Carbide phases, either completely or partially dissolved, can be seen all the way out to the coating surface (Fig. 61). The outer coating consisted of βNiAl matrix, Cr_3Al_2 and α-Cr phases. The white dispersed phase, which resembled Cr_2Al, in the diffusion zone may have been formed as a result of carbide dissolution in the βNiAl matrix. A narrow band of γ' solid solution had formed at the coating substrate interface.

The higher hardness of the outer area and the denuded zone of the J coating on IN-100 alloy as compared to the J coating on B1900 alloy is most likely because of higher Co or Ti content in βMAl phase. The IN-100 alloy contains 15.4 percent Co

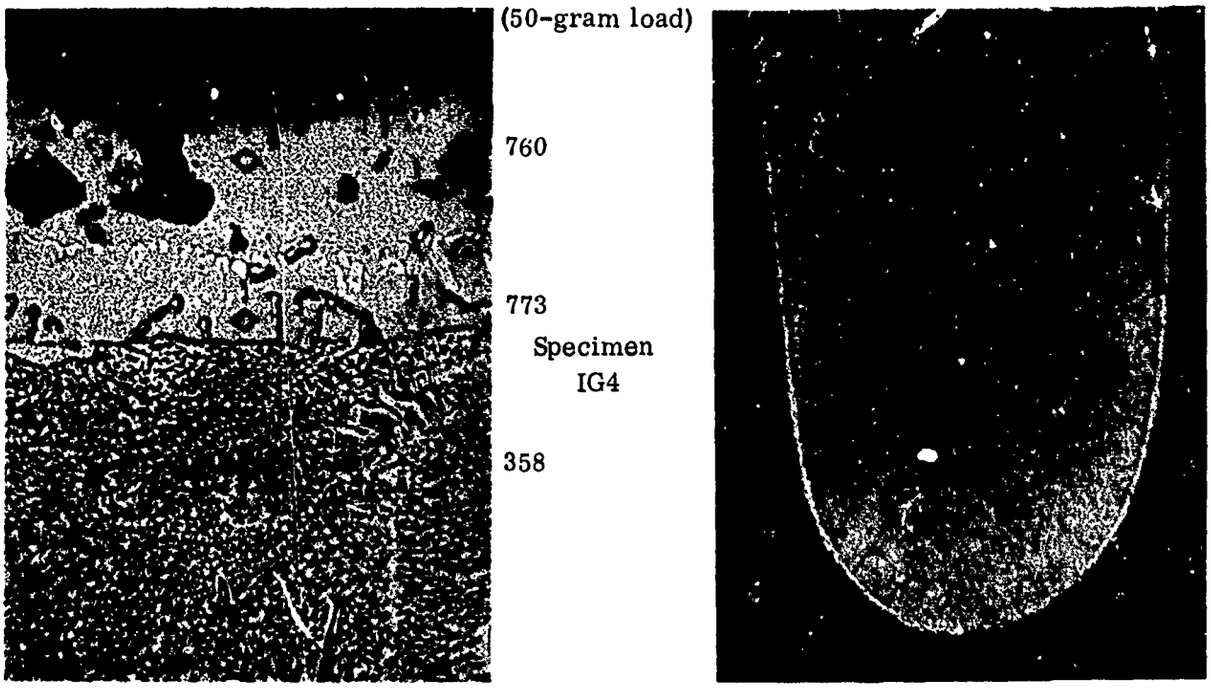

Magnification: 1000X

Magnification: 40X

FIGURE 59. MICROSTRUCTURE OF AS-RECEIVED COATINGS;
Coating G on IN-100 Alloy

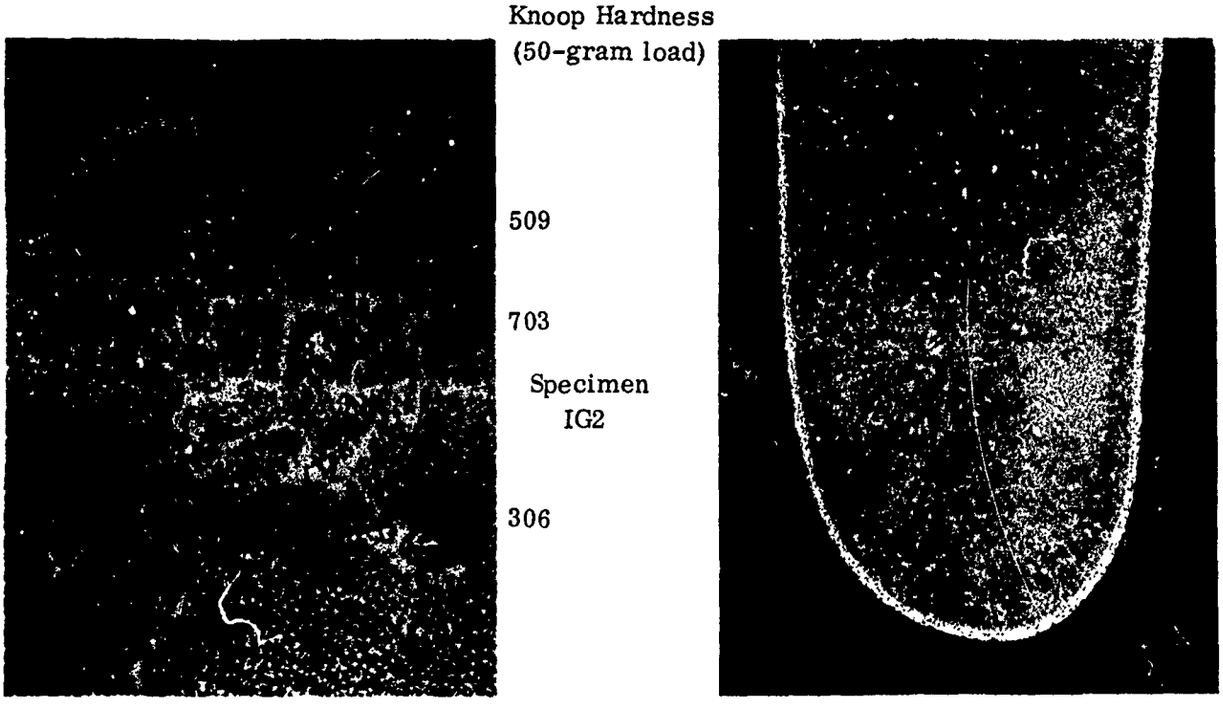

Magnification: 1000X

Magnification: 40X

FIGURE 60. MICROSTRUCTURE OF G COATING ON IN-100 ALLOY AFTER HOT CORROSION TESTING FOR 60 HOURS AT 1650° F

Magnification: 1000X

Magnification: 40X

FIGURE 61. MICROSTRUCTURE OF AS-RECEIVED COATINGS;
Coating J on IN-100 Alloy

and 4.3 percent Ti as compared to 10 percent Co and 1.0 percent Ti in B1900. The hardness values of the outer layer and the denuded zone were about the same for the J coating on IN-100 or on Inco 713C alloy.

The microstructural changes for the J coating on IN-100 after the 1650°F exposures (Fig. 62) were similar to those for the J coating on B1900. The longer life (150 hours) provided by the J coating on IN-100 alloy, compared to 120 hours on B1900 alloy, is because of the higher Cr in IN-100.

The microstructure of the IN-100/J coating after 90 hours exposure at 1800°F is shown in Figure 63. Most of the beta phase has been converted to γ'. Internal oxide spots and carbides were present throughout the coating. At the interface, detectable sigma phase platelets developed in the γ' matrix.

The failure after 90 hours at 1800°F exposure of this specimen (compared to 150 hours for B1900 or Inco 713C at 1800°F) could be due to the presence of TiO_2 in the surface oxides. The heterogeneous Al_2O_3-TiO_2 scale is reported to permit more rapid inward diffusion of oxygen and outward diffusion of nickel, cobalt and other base metal alloying elements to create an even less homogeneous oxide layer (Ref. 4). Both of these events contributed to more rapid oxidation, oxide spalling and eventual coating failure. The higher Co content in βMAl phase for the IN-100/J coating could also increase the oxidation rate.

3.6 HOT CORROSION TEST RESULTS OF COATED RENE' 41 ALLOY

3.6.1 Weight Change and Appearance

The results of the hot corrosion tests at 1650°F and 1800°F for coatings A, C, F and G on Rene' 41 alloy are shown in Figures 64 and 65. At the conclusion of 150 hours exposure at 1650°F only the A coating appeared to have survived the test without evidence of coating spalling or pitting. The coated specimens appeared to be essentially unchanged as a result of the exposure. Both concave and convex surfaces remain smooth with no evidence of coating degradation. The G coating exhibited several pinhole type failures on the convex surfaces and a small amount of coating spalling was apparent near the tips on the convex surfaces of the blades. The F coating showed a large number of pinhole type failures only on the concave surfaces of the blades which appear to be concentrated along a 1600°F metal temperature isotherm. The C coating exhibited considerable coating spalling on both the concave and convex surfaces of the blades.

At 1800°F, the A coating again appears to provide the best protection to the Rene' 41 alloy. At the conclusion of the tests only two small coating defects were observed on one of the specimens subjected to the test. The G coating showed failure

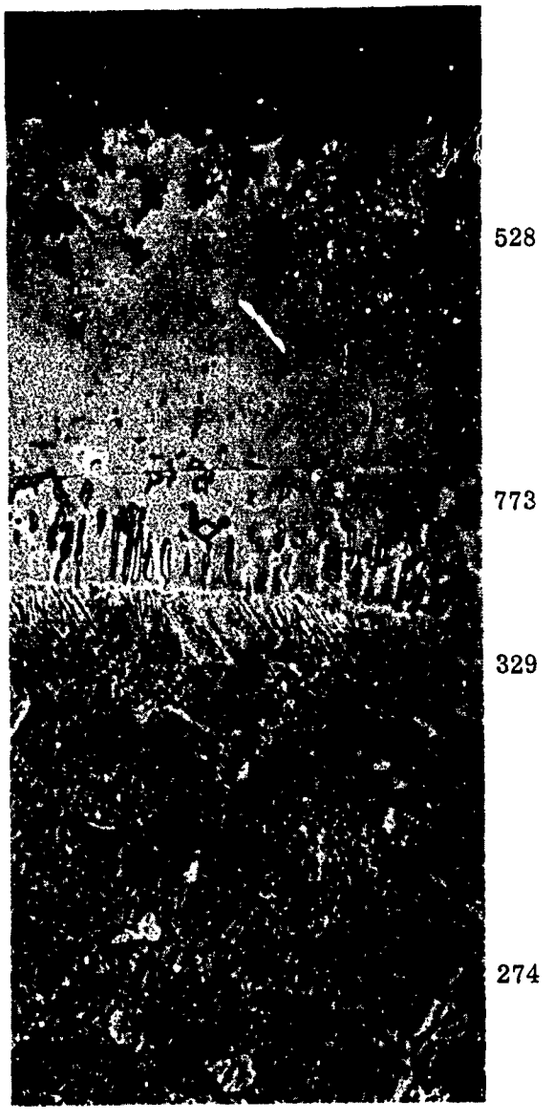

Magnification: 1000X

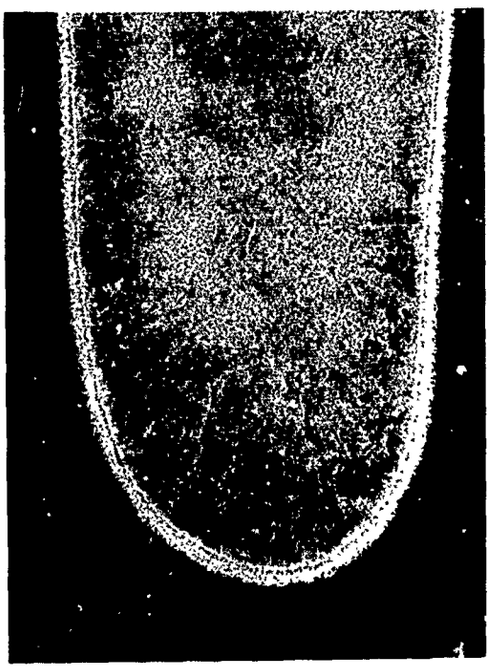

Magnification: 40X

Specimen LJ3

FIGURE 62. MICROSTRUCTURE OF J COATING ON IN-100 AFTER HOT CORROSION TESTS AT 1650° F FOR 150 HOURS

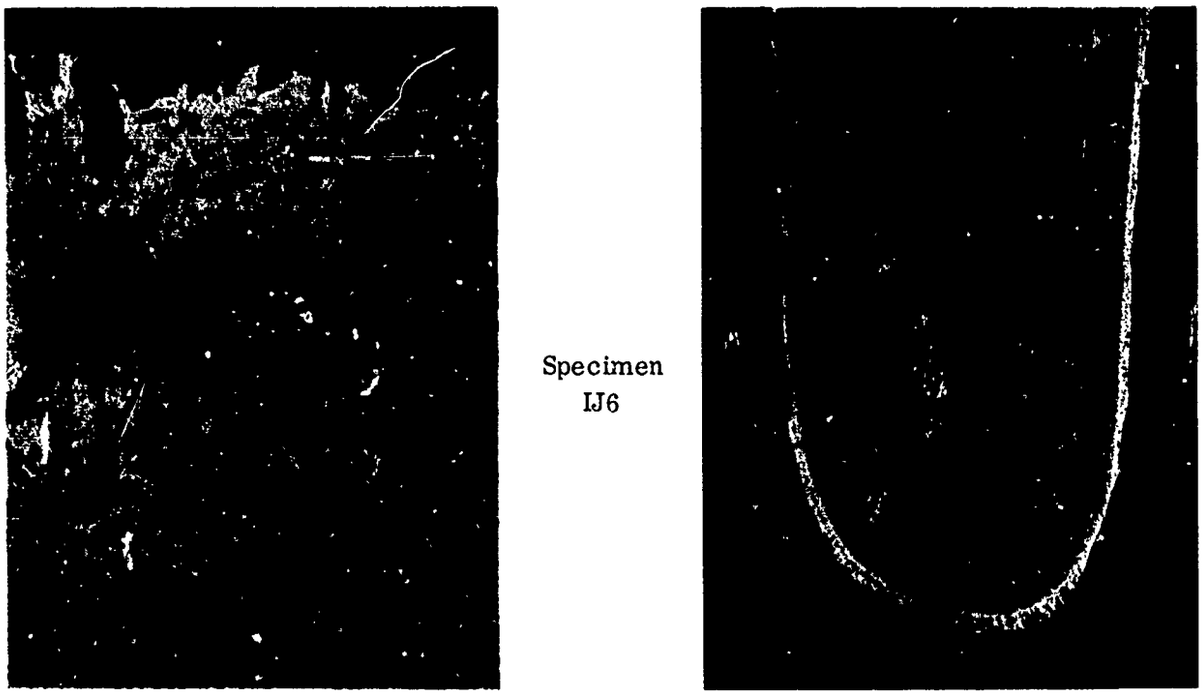

Specimen
IJ6

Magnification: 1000X

Magnification: 40X

FIGURE 63. MICROSTRUCTURE OF J COATING ON IN-100 AFTER HOT CORROSION TESTS AT 1800°F FOR 90 HOURS

along the trailing edge on the concave surface of the blades at the conclusion of the test. Failure appears to have been initiated after the final 30-hour exposure interval. The specimen exhibited a weight loss at the 60-hour inspection interval, and then showed a rapid increase in weight as the oxide built up on the specimen surfaces. Performance of the C coating was considerably better at the 1800°F test temperature. The coating spalling was not as severe at this temperature level and failures appeared to be primarily of the pinhole type failures occurring in the lower temperature region of the blade, i.e., in the 1550°F temperature range. The F coating exhibited a large amount of coating spalling and subsequent oxidation of the substrate. Failure was concentrated on the concave surface along the trailing edges of the blades in the hot test area.

3.6.2 Metallographic Analyses of Coatings on Rene' 41 Alloy

The A Coating

The A coating was the thinnest and was below the required thickness range; whereas on all the other alloys it was the thickest coating. Structurally, the coating was similar to the A coating on B1900 or Inco 713C except for some large geometrically

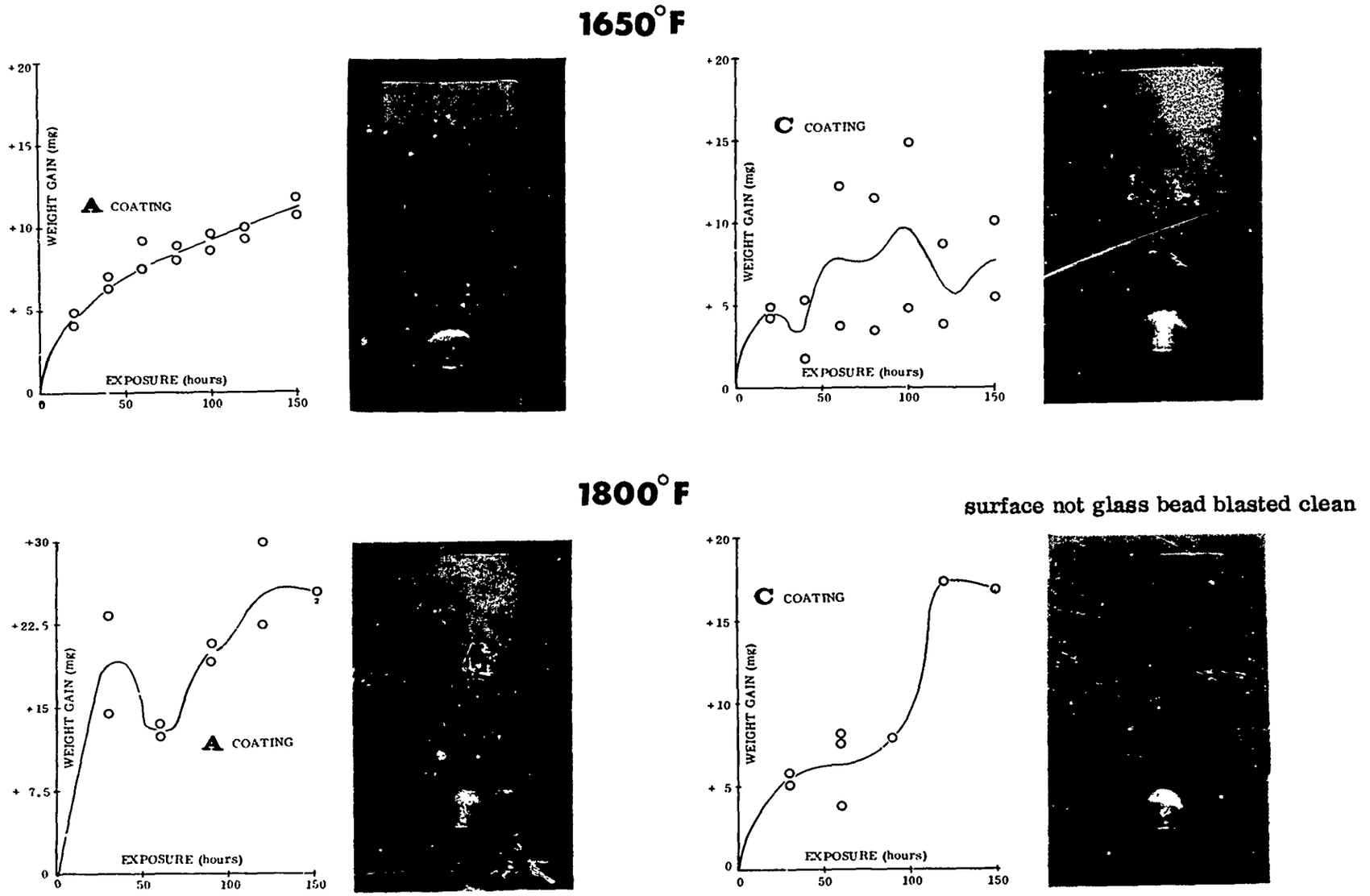

FIGURE 64. WEIGHT CHANGE AND APPEARANCE OF COATINGS A AND C ON RENE' 41 ALLOY TESTED AT 1650°F AND 1800°F

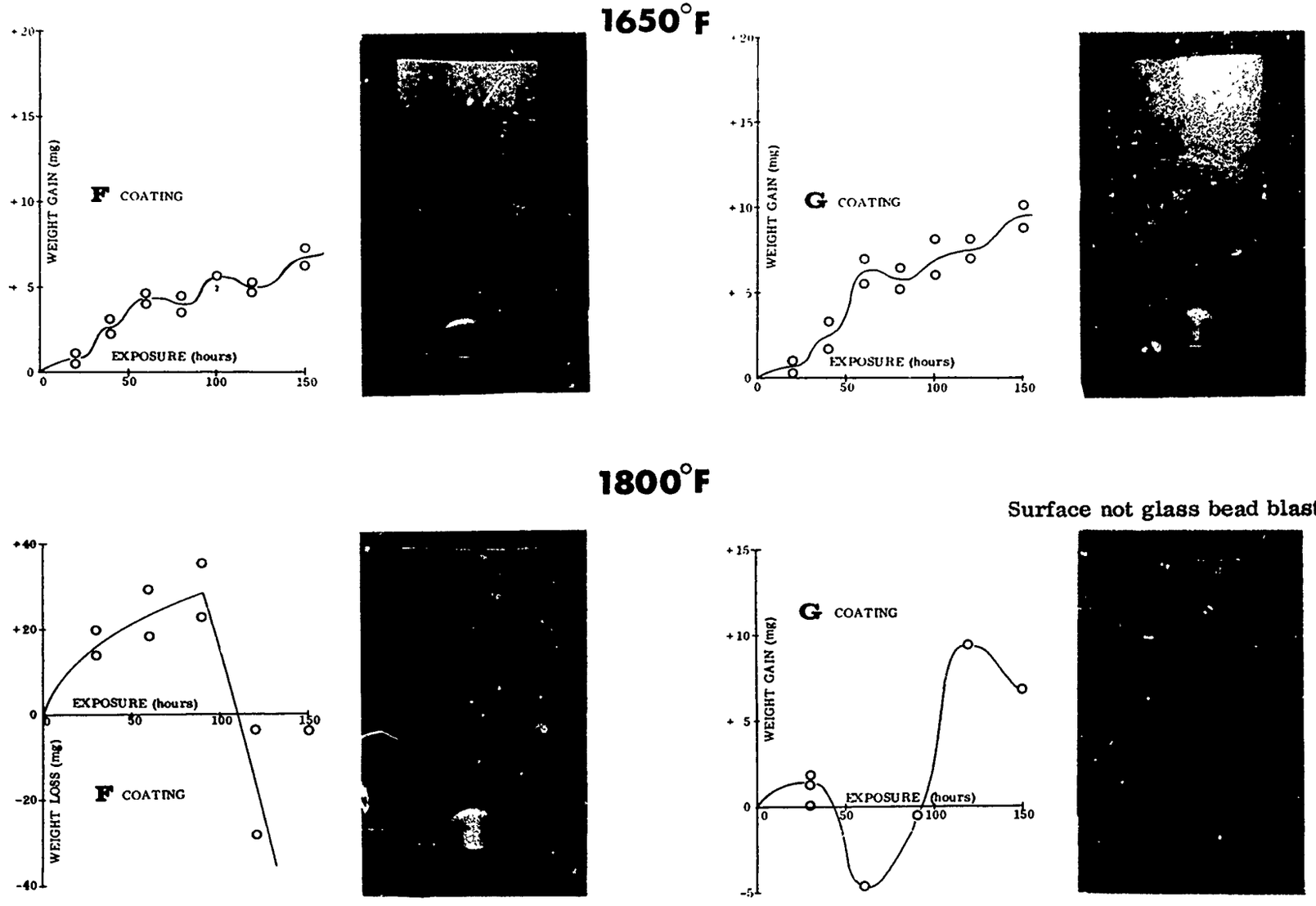

FIGURE 65. WEIGHT CHANGE AND APPEARANCE OF COATINGS F AND G ON RENE' 41 ALLOY TESTED AT 1650°F AND 1800°F

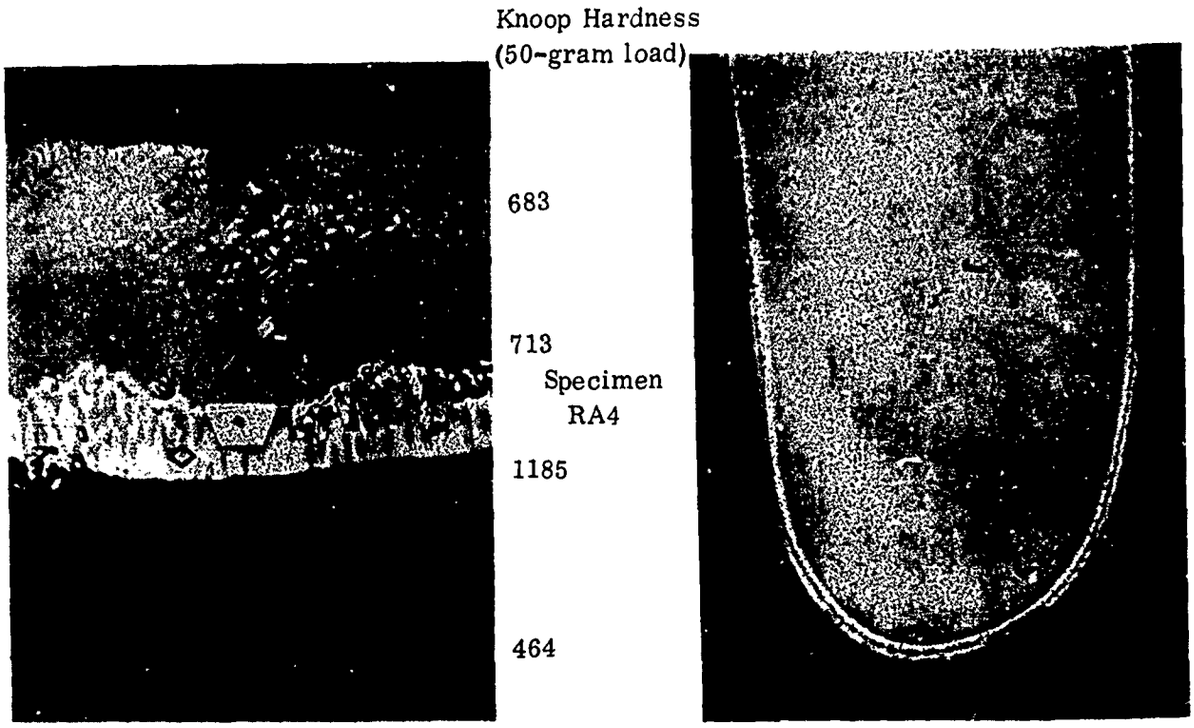

Magnification: 1000X Magnification: 40X

FIGURE 66. MICROSTRUCTURE OF AS-RECEIVED COATINGS; Coating A on Rene' 41 Alloy

shaped particles of a light etching phase which has formed in the intermediate layer. This phase could be Cr or Mo rich. An increased amount of dark etching γ solid solution was observed in the matrix at the coating interface (Fig. 66). X-ray diffraction analysis of the coating is contained in Table XI.

The microstructural changes after 150 hours exposure at 1650°F were similar to those of the A coating on B1900 or Inco 713C. The thickness of the A coating on Rene' 41 increased from 0.0010 inch in the as-coated condition to 0.0023 inch after 150 hours exposure at 1650°F (Fig. 67). This is much less increase in thickness than observed for the A coating on B1900 or Inco 713C. Thus the problem of diffusion instability is much less severe with the A coating on Rene' 41 than on B1900 or Inco 713C.

After 150 hours exposure at 1800°F most of the β phase in the outer area of the diffusion zone of the coating was converted to γ' (Fig. 68). The outer area of the coating had spalled off. The denuded zone consisted of β and γ' phases. The diffusion zone appeared to consist of γ' matrix, carbides and sigma phase. The sigma phase platelets in the γ' matrix, present at the interface after 150 hours exposure at 1650°F, were not present after the exposure for 150 hours at 1800°F.

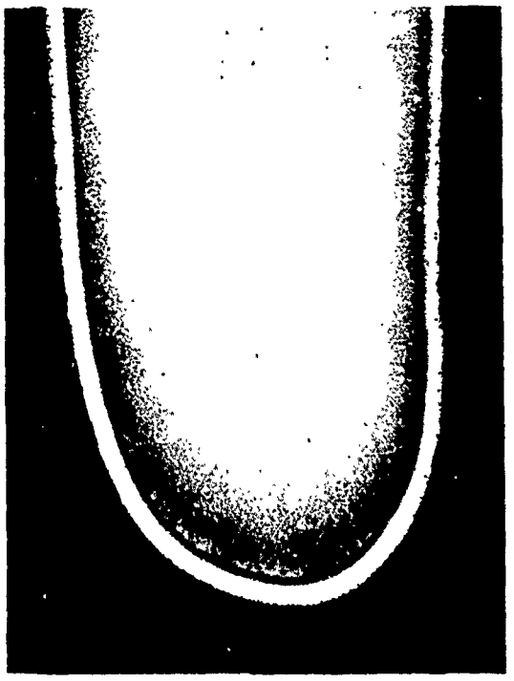

Magnification: 1000X

Magnification: 40X

FIGURE 67. MICROSTRUCTURE OF COATING A ON RENE' 41 AFTER HOT CORROSION TESTS AT 1650° F FOR 150 HOURS

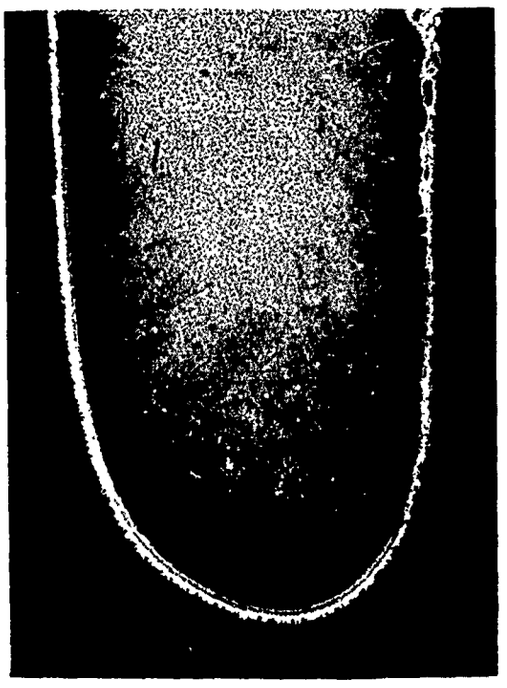

Magnification: 1000X

Magnification: 40X

FIGURE 68. MICROSTRUCTURE OF COATING A ON RENE' 41 AFTER HOT CORROSION TESTS AT 1800° F FOR 150 HOURS

The A coating provided longer protection (more than 150 hours in hot corrosion testing at 1650°F and 1800°F)to Rene' 41 than to B1900, Inco 713C, or IN-100 alloys. This is most likely because the Rene' 41 alloy has the highest chromium content of the eight nickel-base alloys in the program.

The A coating was selected for further evaluation because of its satisfactory performance in HCR testing and good diffusion stability.

The C Coating

The outer layer of the C coating on Rene' 41 in the as-coated condition was similar in microstructure to the C coating on the other nickel-base superalloys. The intermediate or diffusion layer, however, had a more strongly defined columnar structure (compared to the other alloys) composed of alternating bands of sigma and γ' phases. After 150 hours hot corrosion exposure at 1650°F the coating showed considerable spalling. The coating, after the exposure, appeared to consist of γ' matrix, retained β phase, oxide spots, etc. The diffusion zone still had a columnar structure composed of alternate bands of sigma and γ' phases.

The C coating on Rene' 41, because of spalling and localized failures, was not selected for further evaluation.

The F Coating

The F coating on Rene' 41 alloy in the as-coated condition and after 150 hours of hot corrosion exposure at 1650°F and 1800°F are shown in Figures 69, 70, and 71, respectively.

The main structural details as-coated were similar to the F coating on other nickel-base superalloys. The diffusion zone had a more strongly defined columnar structure composed of alternate bands of sigma and γ' phases. Rene' 41, being a high Cr alloy, is more sigma prone. This results in the columnar structure at the diffusion zone.

The thickness of the coating decreased from 0.0022 inch to 0.0020 inch after 150 hours exposure at 1650°F because of oxidation of Al to Al_2O_3 and spalling off of the oxide (Fig. 70). The outer layer consisted most likely of βNiAl + αAl_2O_3 + α-Cr. Beneath the outer zone was a narrow layer of oxide inclusion, β phase and γ' phase. The diffusion zone was the columnar structure of sigma and γ' phases similar to that found in the as-coated condition.

The thickness of the coating after 150 hours testing at 1800°F was 0.0016 inch compared to 0.0022 inch in the as-coated condition. Most of the coating was

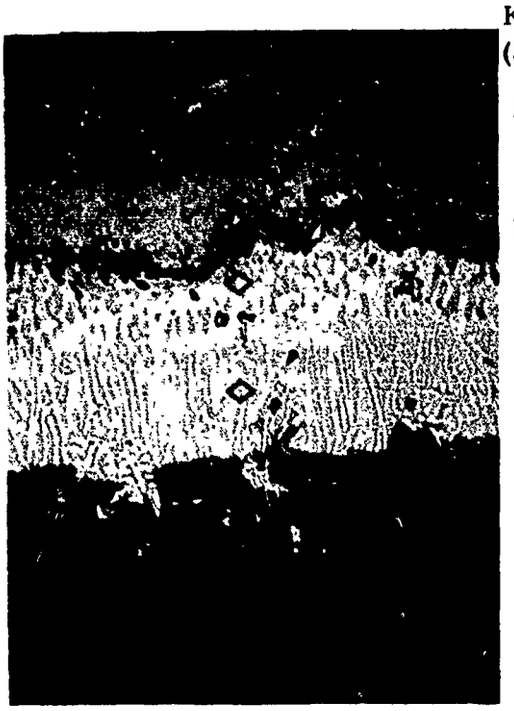

Magnification: 1000X

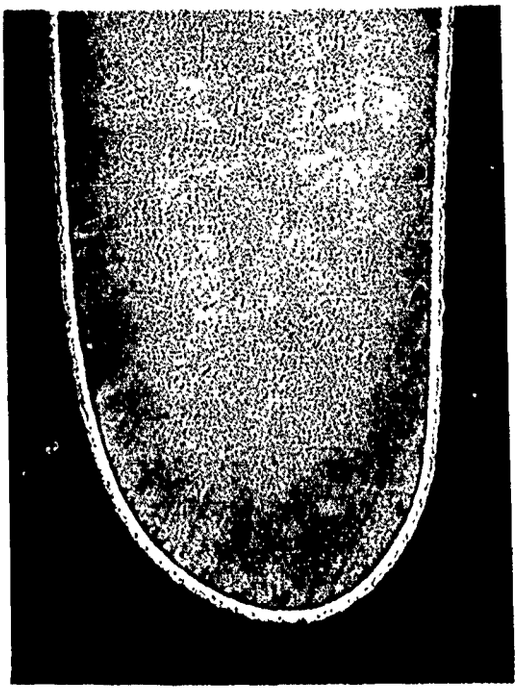

Magnification: 40X

FIGURE 69. MICROSTRUCTURE OF AS-RECEIVED COATINGS;
Coating F on Rene' 41 Alloy

Magnification: 1000X

Magnification: 40X

FIGURE 70. MICROSTRUCTURE OF F COATING ON RENE' 41 AFTER HOT CORROSION TESTS AT 1650° F FOR 150 HOURS

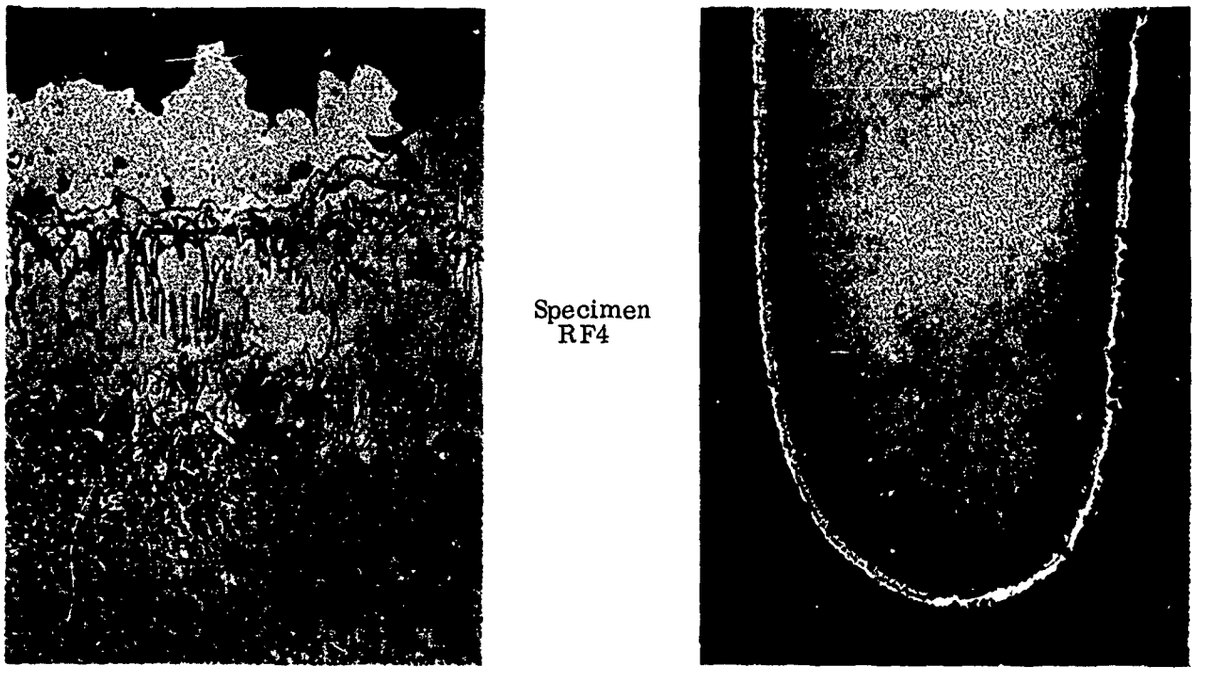

Magnification: 1000X Magnification: 40X

FIGURE 71. MICROSTRUCTURE OF F COATING ON RENE' 41 AFTER HOT CORROSION TESTS AT 1800° F FOR 150 HOURS

converted to γ'; however some untransformed β phase was present. Finger-like sigma phase was present in the diffusion zone. Some sigma phase dissolution in γ' matrix occurred, resulting in a considerably reduced columnar structure (Fig. 71). The F coating at the center section of the trailing edge had failed after 150 hours of testing at 1800°F (Fig. 65).

The F coating, because of a large number of pinhole type failures and failure at the trailing edge of the specimen, was not selected for further evaluation. However, performance of the F coating was good and comparable to that of the G coating, as described in the following paragraphs.

The G Coating

The G coating on Rene' 41 alloy was very similar to that of the G coating on Inco 713C. The outer area of the coating was found to consist of βNiAl matrix, large α-Al_2O_3 inclusions and α-Cr. The diffusion zone consisted most likely of βNiAl matrix, γ' phase, carbides and sigma phase. At the interface, the predominant phase was γ' with sigma platelets.

After 150 hours hot corrosion testing at 1650°F usual microstructural effects were observed, viz., oxidation of Al to Al_2O_3, conversion of β to γ', internal oxide spots in the coating, etc. (Fig. 72). A carbide layer in the γ' matrix could be observed in the diffusion zone. Finger-like sigma phase had developed at the interface.

After 150 hours hot corrosion testing at 1800°F the G coating on Rene' 41 alloy had failed at the trailing edge (Fig. 56 and Fig. 73) as was the case with the F coating on Rene' 41 alloy.

The G coating, which provided 150 hours protection in hot corrosion testing at 1650°F or 1800°F to Rene' 41 alloy, was selected for further evaluation in the program. The performance of the G coating was slightly better than that of the F coating, based on weight change data and surface appearance.

3.7 HOT CORROSION TEST RESULTS OF COATED SEL-15 ALLOY

3.7.1 Weight Change and Appearance

Curves of cumulative weight change versus exposure time at 1650°F and 1800°F are shown in Figures 74 and 75 for the SEL-15 alloy. Also included are photographs of the surfaces of typical specimens of each coating system after test.

At 1650°F, only the A coating provided protection to the SEL-15 alloy. This coating successfully withstood 150 hours exposure without any evidence of coating failure. The surfaces of the specimens were smooth and unchanged after testing.

The C, F and G coatings all exhibited coating failures and were removed from the test after only 30 hours total exposure. The C coating failed by spalling along the trailing edge on both the concave and convex surfaces. The F coating exhibited numerous pinhole type failures only on the concave surfaces and were concentrated on the trailing edge and along a 1575°F metal temperature isotherm. The G coating failed on the convex surfaces of the specimens. Both specimens showed considerable substrate corrosion when removed from test after 30 hours exposure.

At 1800°F the A coating again exhibited the best performance in the test. Both specimens, however, did contain failed areas in the coating at the completion of 150 hours exposure. The C coating again failed catastrophically during the 30-hour exposure interval. Failures in this test were concentrated on the concave surface towards the leading edges of the blades. The F coating exhibited coating spalling on the concave surfaces along the trailing edges and, from subsequent analysis, appeared to have been prematurely removed from test at the 60-hour inspection interval because substrate corrosion had just been initiated on one of the two test specimens. The G

Specimen
RG3

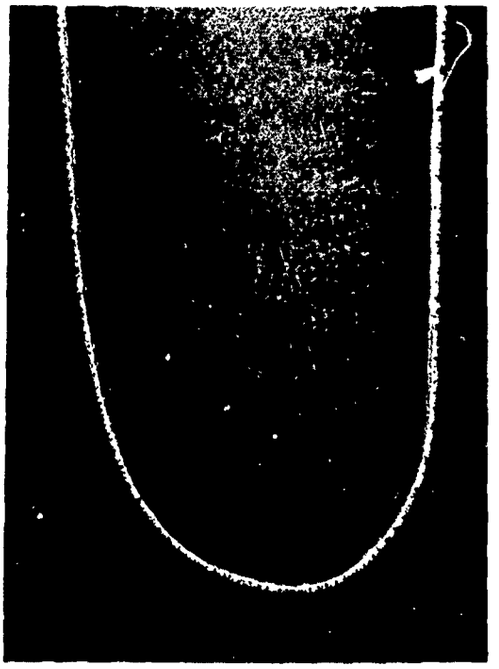

Magnification: 1000X

Magnification: 40X

FIGURE 72. MICROSTRUCTURE OF G COATING ON RENE' 41 ALLOY AFTER HOT CORROSION TESTS AT 1650°F FOR 150 HOURS

Specimen
RG6

FIGURE 73. MICROSTRUCTURE OF G COATING ON RENE' 41 ALLOY AFTER HOT CORROSION TESTS AT 1800°F FOR 150 HOURS

Magnification: 40X

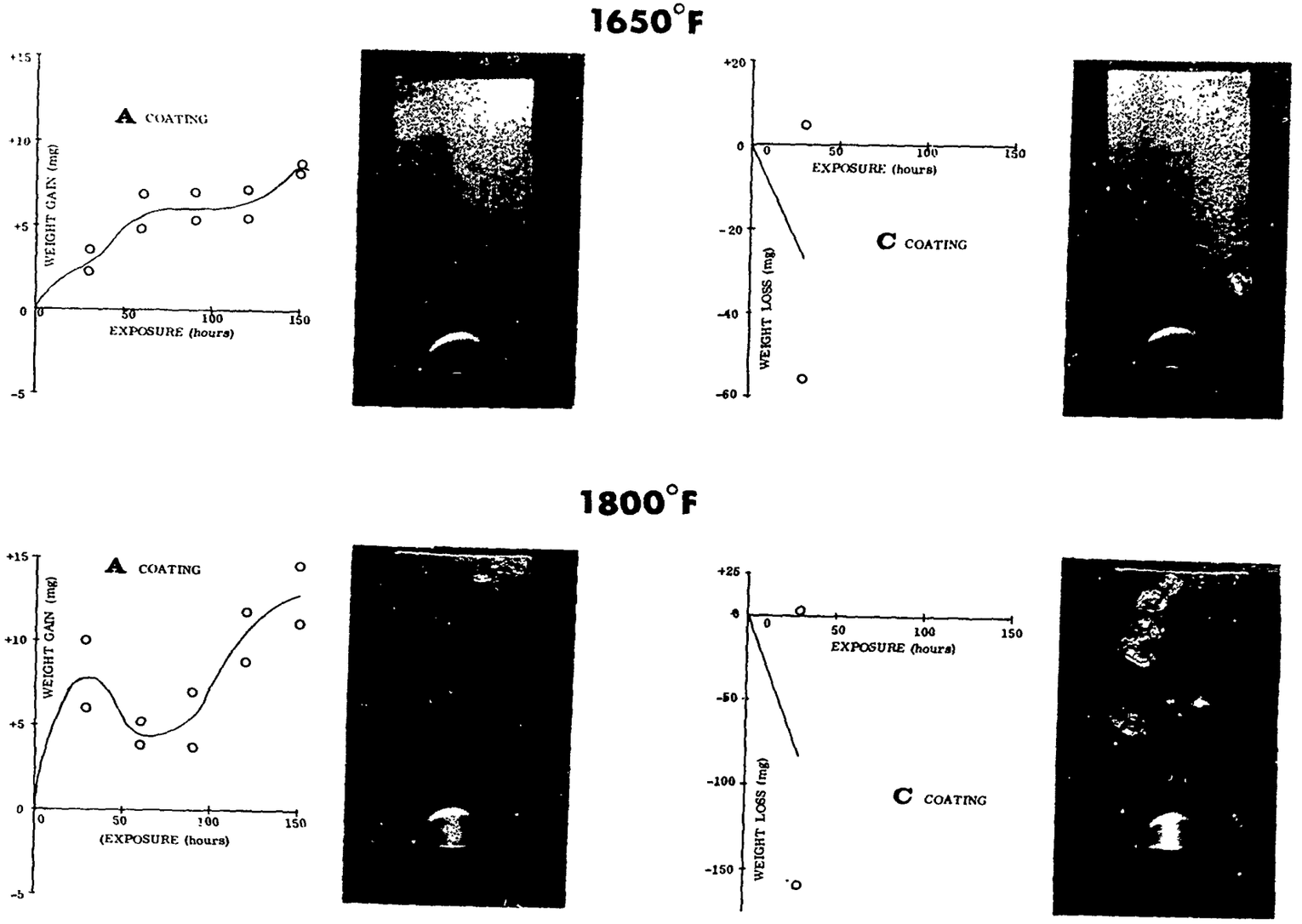

FIGURE 74. WEIGHT CHANGE AND APPEARANCE OF COATINGS A AND C ON SEL-15 ALLOY TESTED AT 1650° F AND 1800° F

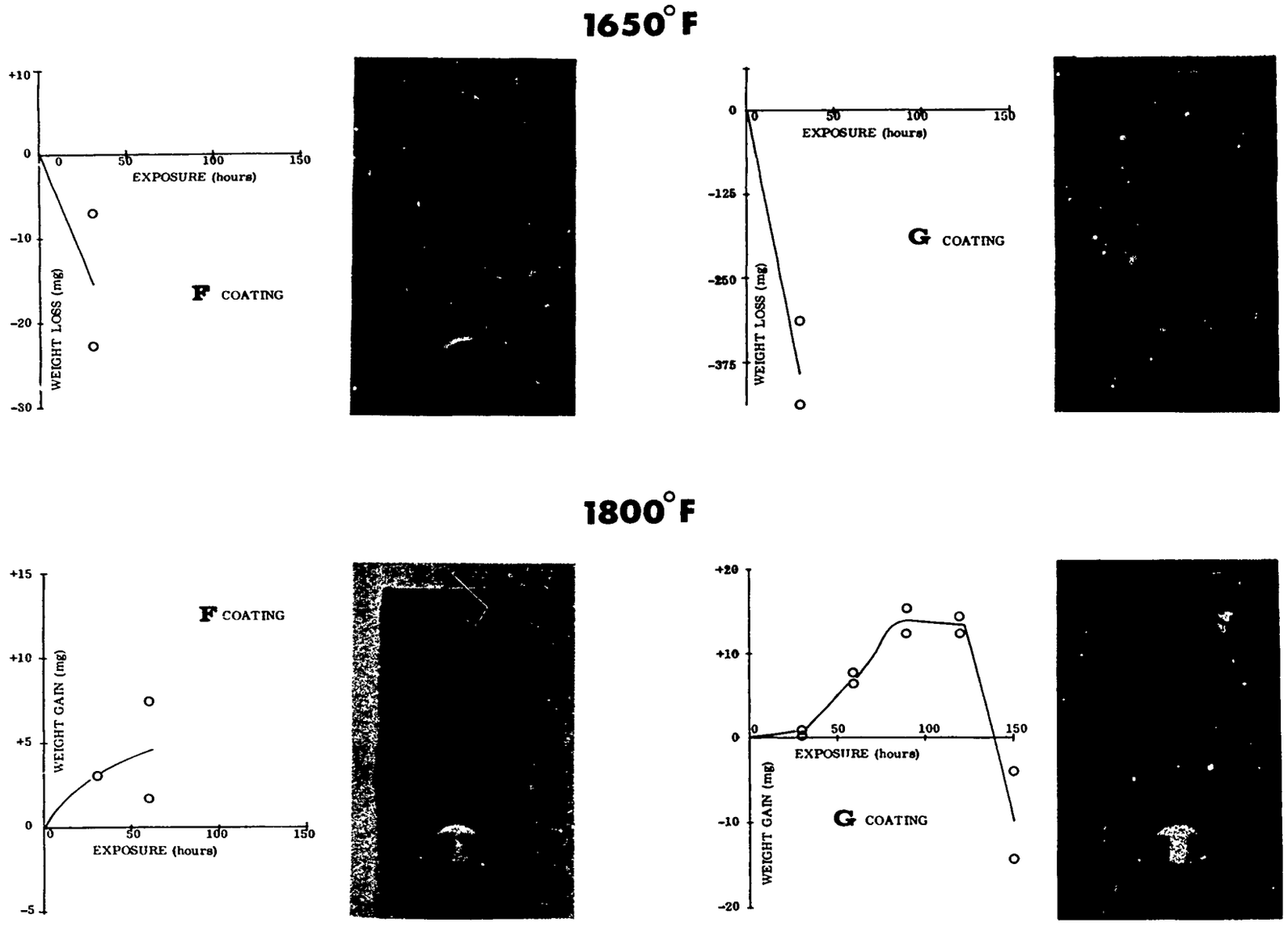

FIGURE 75. WEIGHT CHANGE AND APPEARANCE OF COATINGS F AND G ON SEL-15 ALLOY TESTED AT 1650°F AND 1800°F

coating exhibited better performance in the 1800°F test than in the 1650°F test. Both specimens remained in the test for the scheduled 150-hour duration without severe substrate corrosion. Failure occurred mainly along the trailing edge in the hot test area, although corrosion was also observed on the convex surfaces near the shank of the blades.

3.7.2 Metallographic Analyses of Coatings on SEL-15 Alloy

The A Coating

The A coating was the thickest on SEL-15 and had the typical structure on nickel-base alloys. The structure was similar to that of the A coating on Inco 713C before and after 150 hours of hot corrosion testing at 1650°F or 1800°F (Sec. 3.4.2). In the as-coated condition, a continuous solid solution layer had formed at the interface and was in "equilibrium" with the βMAl (Fig. 76). The thickness of the coating increased from 0.0033 inch to 0.0044 inch after 150 hours exposure at 1650°F (Fig. 77) and to 0.0038 inch after 150 hours exposure at 1800°F (Fig. 78). This diffusion instability with the A coating on SEL-15 was intermediate between that with the A coating on Inco 713C and with the A coating on IN-100 or Rene' 41. Other microstructural changes were similar to those described for B1900 and Inco 713C alloys in Section 3.3.2 and 3.4.2, respectively.

The A coating provided the longest protection to SEL-15 compared to any other coating, and was selected for additional evaluation.

The C Coating

A very homogeneous structure was displayed by the C coating with the outer two-thirds being essentially single phase, βMAl. Carbides were present in the intermediate zone and the light etching phase was present as irregularly shaped dispersions rather than as the columnar particles as in the C coating on Rene' 41. There was a tendency for γ' to form at the interface.

The C coating on SEL-15 after 30 hours exposure at 1650°F was found to spall off and was therefore not extensively evaluated.

The F Coating

The F coating on SEL-15 was similar in microstructure to that of the F coating on Inco 713C. The outer area of the coating consisted of βNiAl, large α-Al_2O_3 inclusions and α-Cr phases based on X-ray diffraction data (Table VI). The microstructural changes after 1650°F or 1800°F exposure were similar to those described for the F coating on Inco 713C or other nickel-base superalloys and are therefore not presented again. The F coating on SEL-15 failed after 30 hours exposure at 1650°F

Knoop Hardness Number (50 gram load)

735

653

925

606

426

Magnification: 1000X

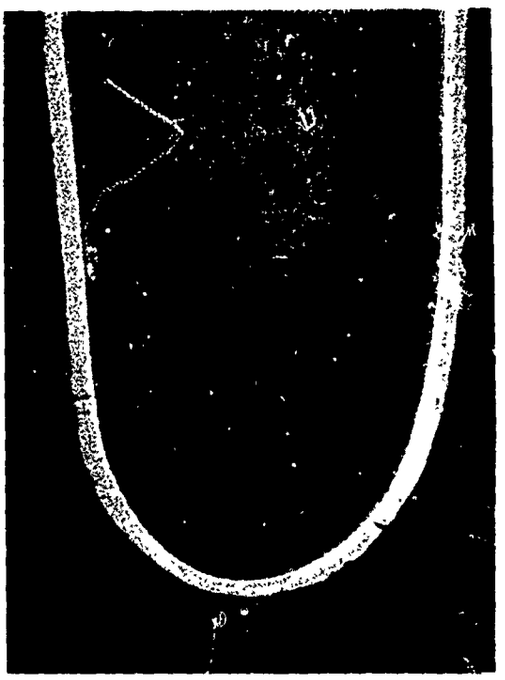

Magnification: 40X

Specimen SA3

FIGURE 76. MICROSTRUCTURE OF AS-RECEIVED COATINGS;
Coating A on SEL-15 Alloy

Knoop Hardness Number (50 gram load)

606

499

683

319

Magnification: 1000X

Magnification: 40X

Specimen SA2

FIGURE 77. MICROSTRUCTURE OF COATING A ON SEL-15 ALLOY AFTER HOT CORROSION TEST AT 1650° F FOR 150 HOURS

Magnification: 1000X

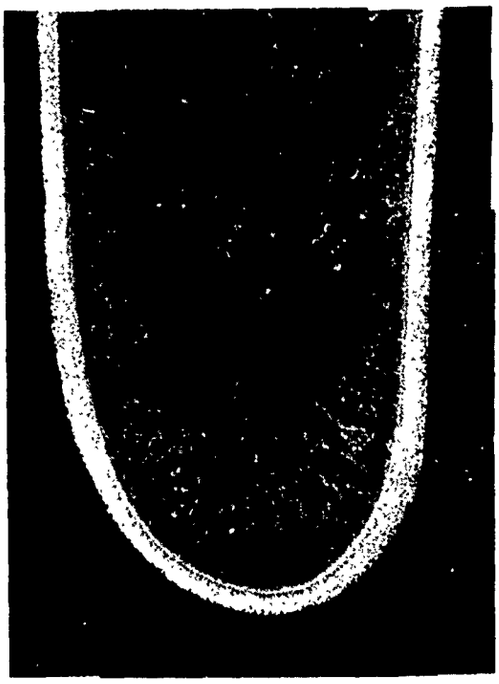

Magnification: 40X

Specimen SA5

FIGURE 78. MICROSTRUCTURE OF COATING A ON SEL-15 ALLOY AFTER HOT CORROSION TEST AT 1800° F FOR 150 HOURS

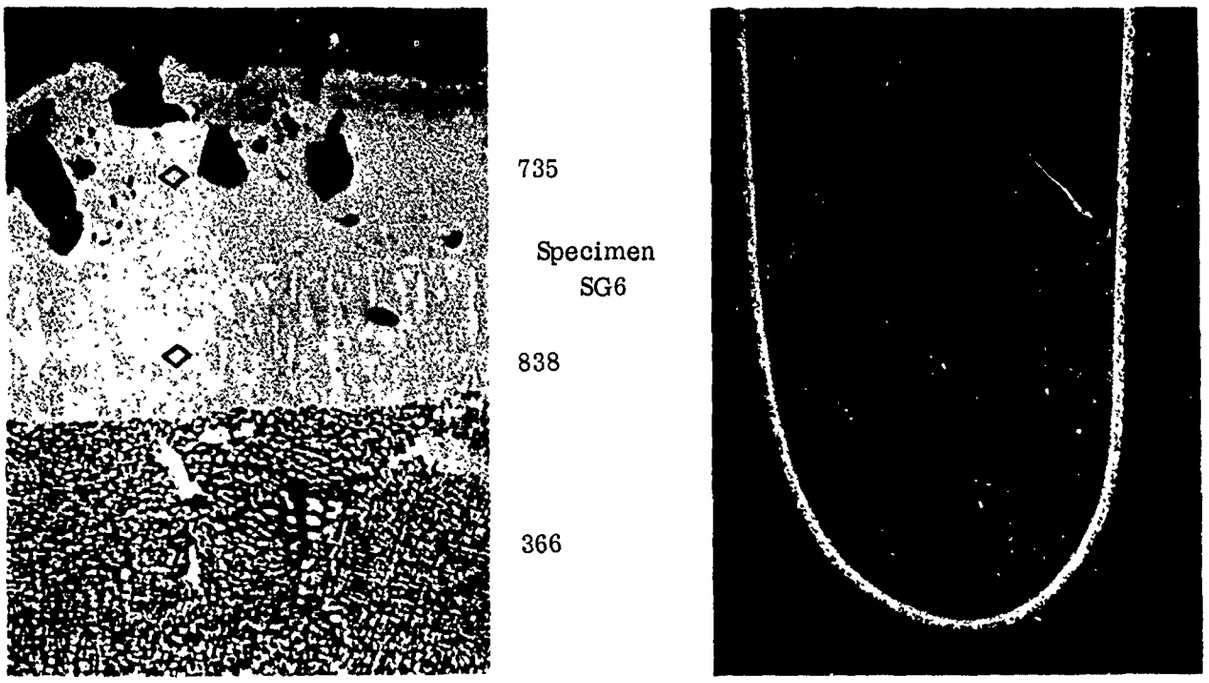

FIGURE 79. MICROSTRUCTURE OF AS-RECEIVED COATINGS;
Coating G on SEL-15 Alloy

and after 60 hours exposure at 1800°F. The F coating was selected for further evaluation in Phase II mechanical property tests rather than the G coating, primarily because of lower weight losses at 1650°F.

The G Coating

The microstructure of the G coating on SEL-15 consisted of βNiAl, large α-Al_2O_3 inclusions, and α-Cr. The diffusion zone appeared to consist of a βNiAl matrix with carbides and sigma phase (Fig. 79).

After the 30 hours exposure at 1650°F, finger-like sigma phase has developed in the diffusion zone (Fig. 80). The diffusion zone appeared to consist of βNiAl, γ' carbides or internal oxide spots and sigma phase. The outer layer was comprised of β matrix, large α-Al_2O_3 inclusions, internal oxide spots and α-Cr.

After 150 hours exposure at 1800°F, the coating was reduced in thickness from 0.0020 inch to 0.0015 inch. Most of the β phase was converted to γ' as a

Knoop Hardness Number (50 gram load)

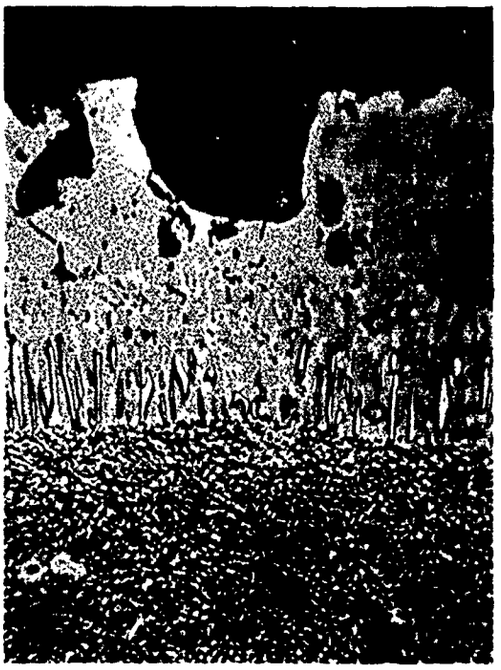

371

606

683

241

Magnification: 1000X

Specimen SG2

Magnification: 40X

FIGURE 80. MICROSTRUCTURE OF COATING G ON SEL-15 ALLOY AFTER HOT CORROSION TEST AT 1650°F FOR 30 HOURS

Specimen SG5

Magnification: 1000X

Magnification: 40X

FIGURE 81. MICROSTRUCTURE OF COATING G ON SEL-15 ALLOY AFTER HOT CORROSION TEST AT 1800°F FOR 150 HOURS

result of loss of Al by oxidation and spalling of the oxides (Fig. 81). Carbides were present. The finger-like sigma phase appeared to be dissolved in the γ' matrix.

3.8 HOT CORROSION TEST RESULTS OF COATED U-700 ALLOY

3.8.1 Weight Change and Appearance

Results of the hot corrosion tests at 1650°F and 1800°F on the coated U-700 alloy are shown in Figures 82, 83 and 84.

Best performance at both temperature levels was exhibited by the A and J coating systems. After test at 1650°F for 150 hours the surfaces of the A and J coated specimens were smooth and essentially unchanged.

At 1650°F, the C and F coatings failed and were removed from the test after 120 hours exposure. The C coating exhibited spalling and severe substrate corrosion on both the concave and convex surfaces, and showed a weight loss after only 60 hours

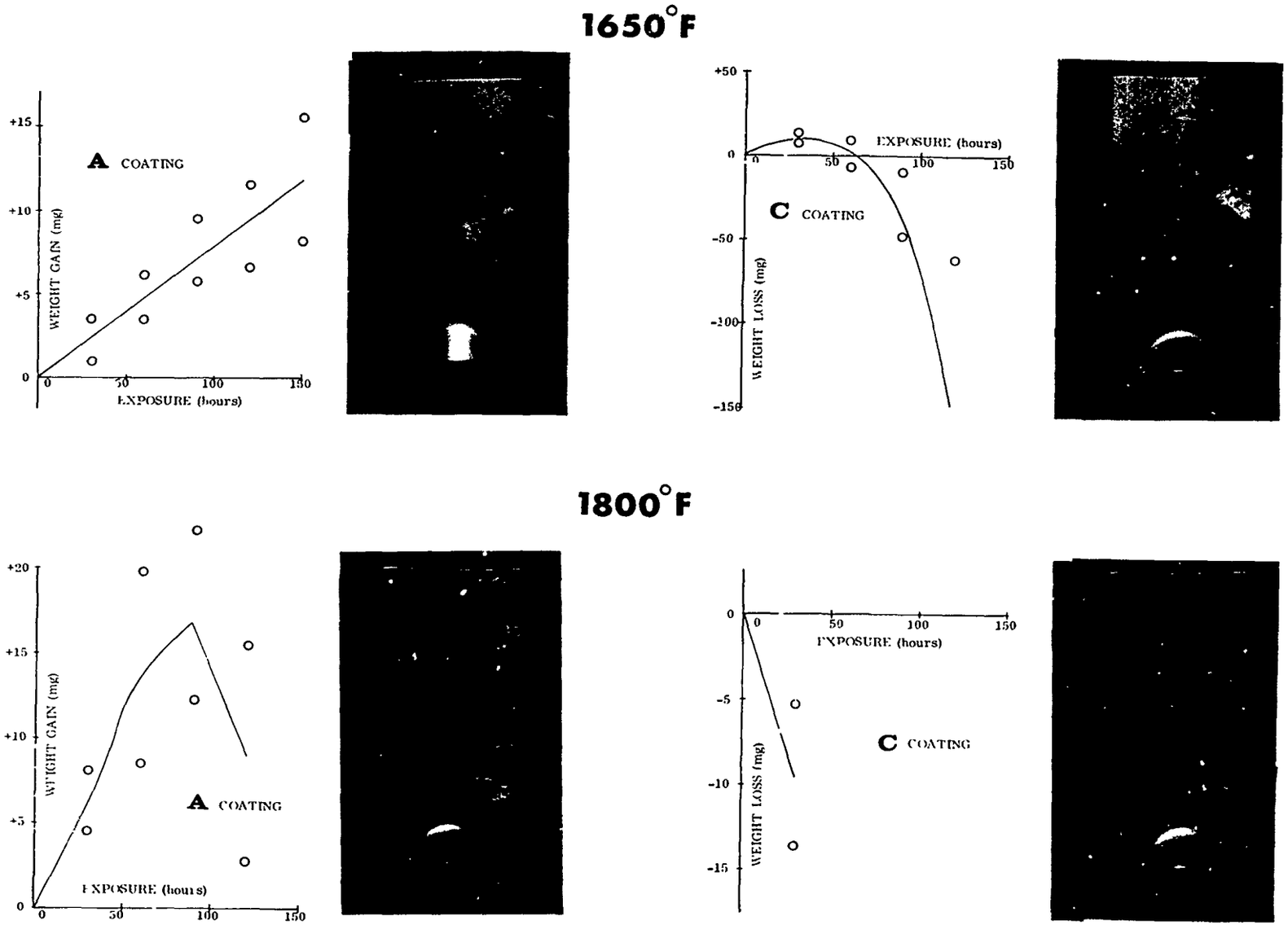

FIGURE 82. WEIGHT CHANGE AND APPEARANCE OF COATINGS A AND C ON U-700 ALLOY TESTED AT 1650°F AND 1800°F

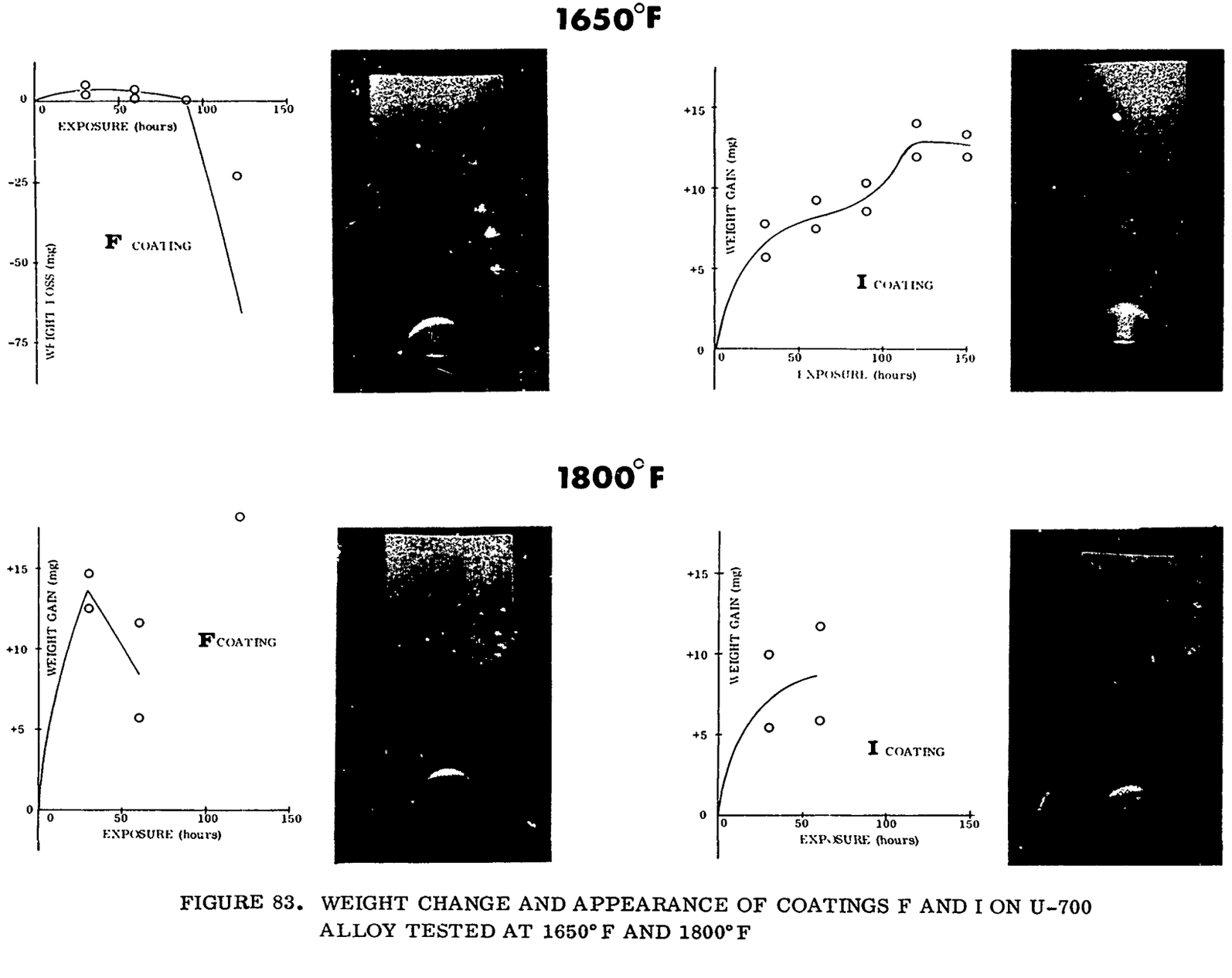

FIGURE 83. WEIGHT CHANGE AND APPEARANCE OF COATINGS F AND I ON U-700 ALLOY TESTED AT 1650° F AND 1800° F

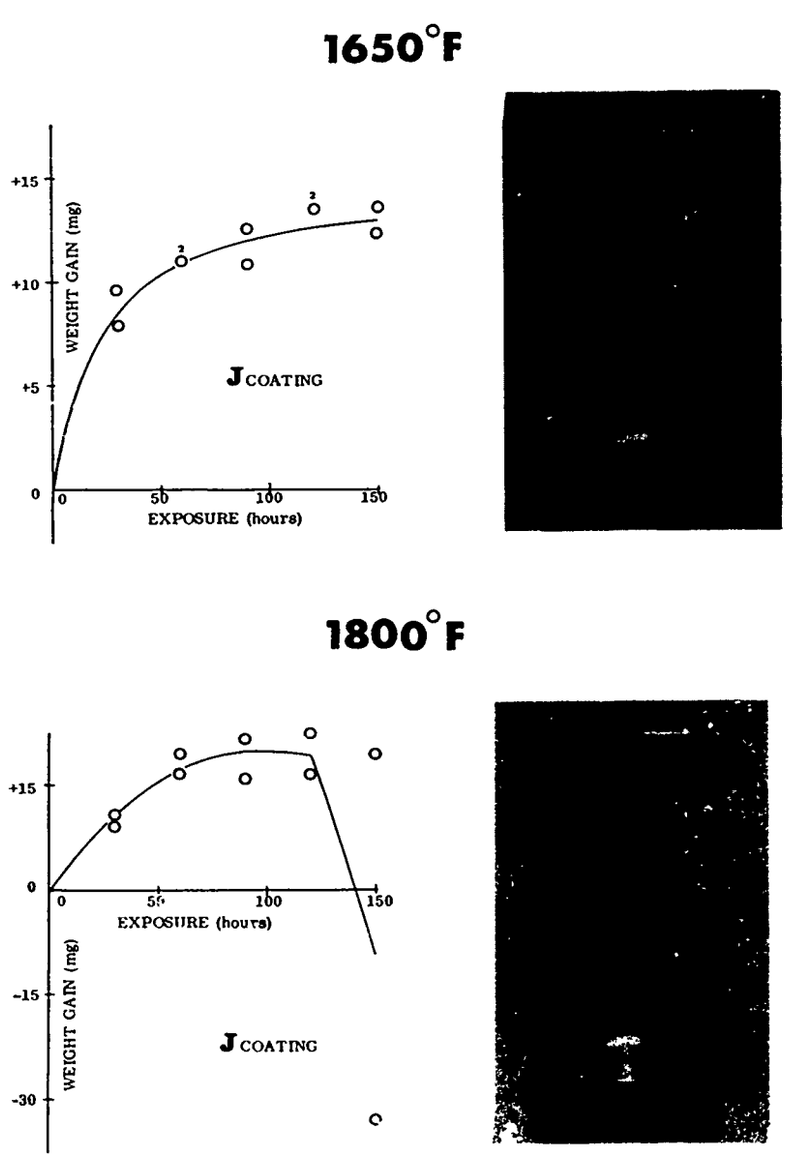

FIGURE 84. WEIGHT CHANGE AND APPEARANCE OF COATING J ON U-700 ALLOY TESTED AT 1650° F AND 1800° F

total exposure. The F coating again exhibited pinhole type coating failures on the concave surfaces similar to that exhibited by this coating system on Inco 713C, IN-100, Rene' 41 and SEL-15 alloys. Specimens were removed from the test after 120 hours exposure. The I coating system was rated the third best in this test. Both specimens remained in test for 150 hours total exposure, but slight coating spalling was apparent on the convex surfaces after test.

At 1800°F the A and J coatings again exhibited best performance on U-700 alloy. The J coating was exposed for a total of 150 hours; however the coating failed on one specimen between 120 and 150 hours exposure. The A coating was removed from test after 120 hours. Coating failure was observed on the concave surface towards the cooler base section of the blade. Coating C again spalled quite badly and was removed from test after 30 hours exposure. Coating F and I both exhibited pinhole type failures and were removed from test after 60 hours.

3.8.2 Metallographic Analyses of Coatings on U-700 Alloy

The A Coating

The A coating on U-700 alloy was unusually thick (0.0045 inch), being almost one and one-half times the thickness of the A coating on the other nickel-base alloys (Fig. 85). Structurally, the A coating was "typical" with $M_{23}C_6$ carbides throughout the MAl matrix and coarse, finger-like sigma phase in the diffusion zone. There was a continuous layer of γ solid solution developed at the interface contiguous with βMAl.

The thickness of the A coating on U-700 decreased from 0.0045 inch to 0.0034 inch after 150 hours exposure at 1650°F (Fig. 86) in contrast to the A coating on the other superalloys. (The thickness of the A coating on B1900, Inco 713C, etc., increased after exposure at 1650°F, exhibiting diffusion instability.) The decrease in thickness or hardness values is due to loss of Al by oxidation and spalling of the oxide. Other microstructural changes were similar to those of the A coating on other superalloys as described in prior sections. At the diffusion zone/substrate interface sigma phase platelets developed.

The thickness of the coating was 0.0038 inch after 120 hours exposure at 1800°F as compared to 0.0045 inch as the as-coated condition (Fig. 87). The outer area of the coating consisted most likely of βNiAl + oxides + Cr_2Al and some carbides. From the microstructure it appears that the Cr_2Al phase was oxidized. Other microstructural changes for the A coating were as described in previous sections.

The A coating was selected for further evaluation in Phase II - Mechanical Property Tests.

Magnification: 1000X

Specimen
UA1

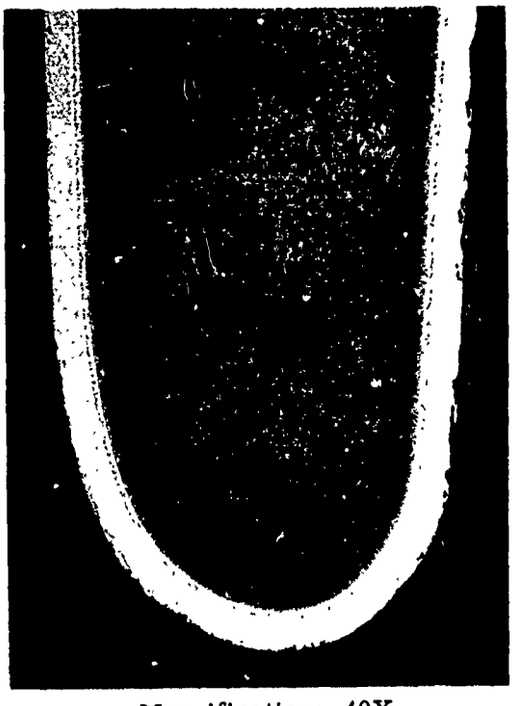

Magnification: 40X

FIGURE 85. MICROSTRUCTURE OF AS-RECEIVED COATINGS;
Coating A on U-700 Alloy

Knoop Hardness Number (50 gram load)

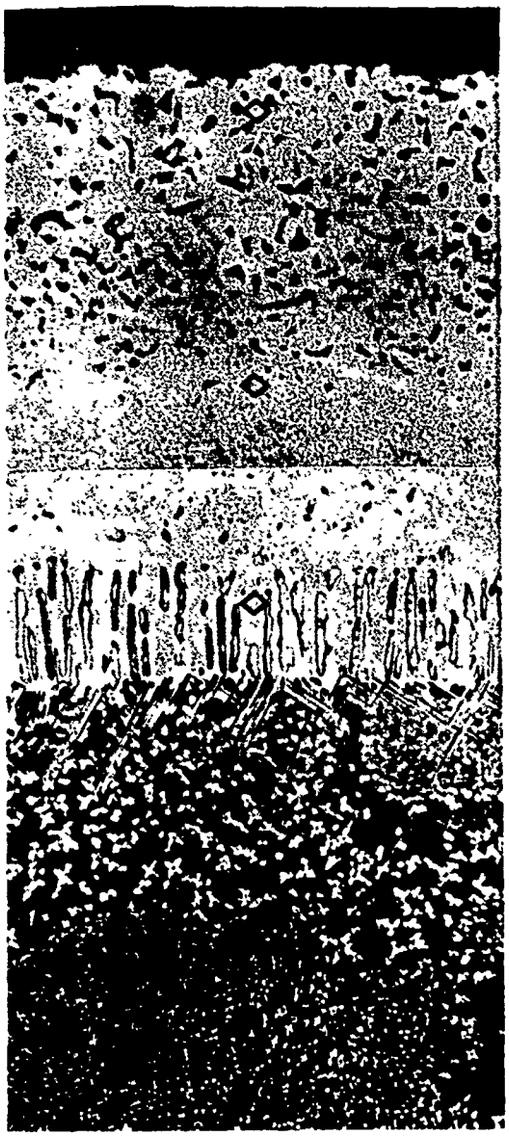

436

528

565

421

411

Magnification: 1000X

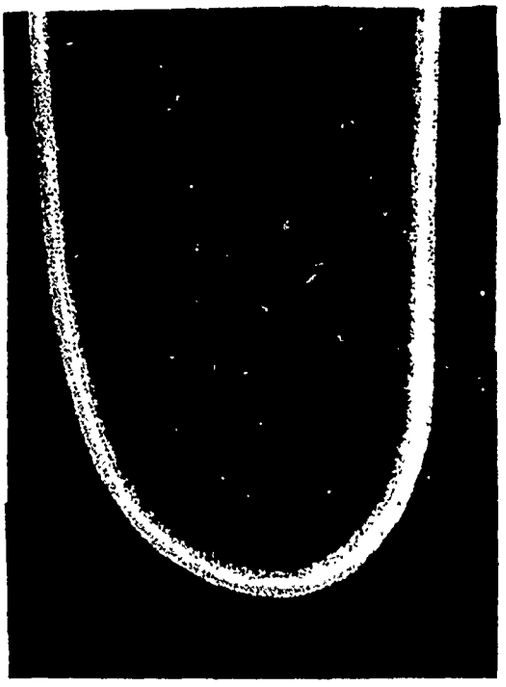

Magnification: 40X

Specimen UA2

FIGURE 86. MICROSTRUCTURE OF COATING A ON U-700 ALLOY AFTER HOT CORROSION TEST AT 1650° F FOR 150 HOURS

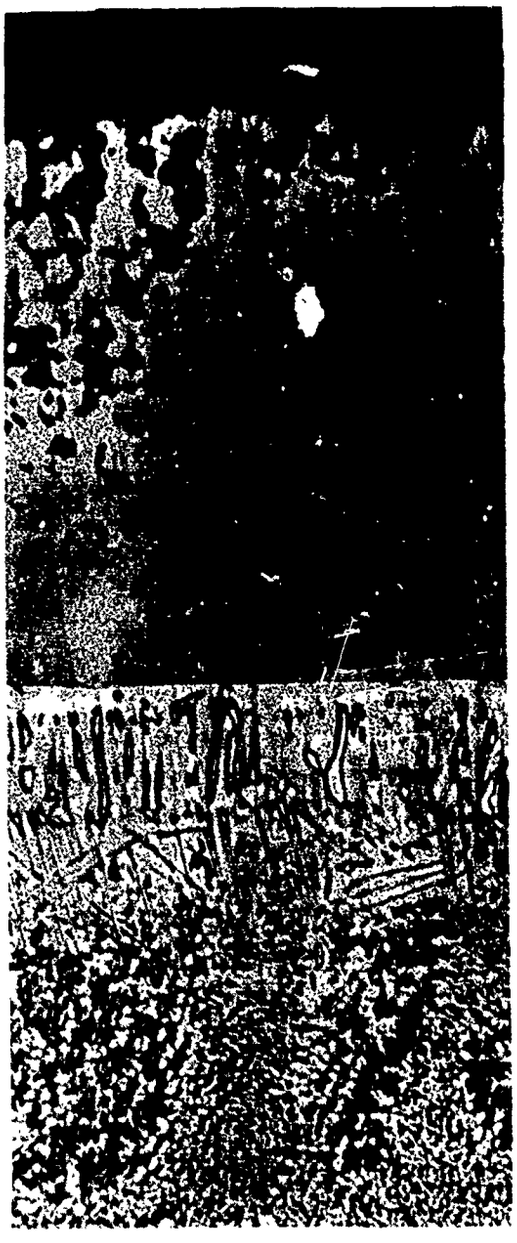

Magnification: 1000X

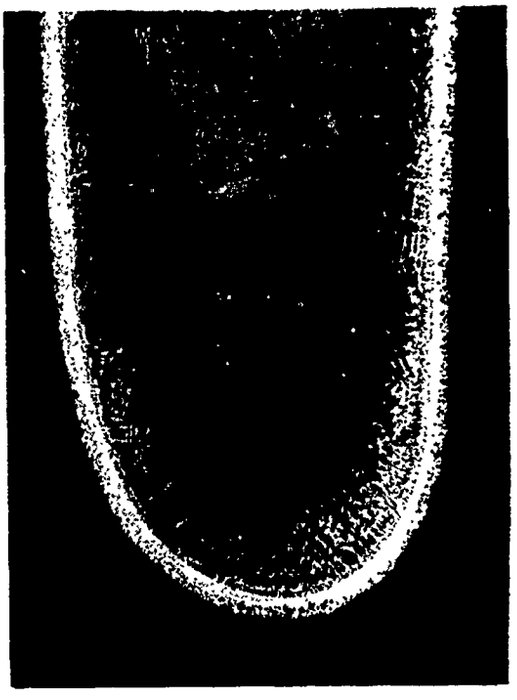

Magnification: 40X

Specimen UA4

FIGURE 87. MICROSTRUCTURE OF COATING A ON U-700 ALLOY AFTER HOT CORROSION TEST AT 1800° F FOR 120 HOURS

The C Coating

The microstructure of the C coating on U-700 was very similar to that of the C coating on SEL-15, but had formed a slightly more columnar structure in the diffusion zone. Comparison with the compositions of SEL-15 and Rene' 41 and with the structures of coatings on these alloys, indicate that the chromium content of the substrate was largely responsible for the observed variations in phase morphology in the diffusion zone.

The C coating on U-700 failed after 120 hours at 1650°F. The coating had spalled off all along the specimen except at the trailing edge and the substrate was corroded. Oxidation attack proceeded along grain boundaries.

The C coating provided only 30 hours of protection to the U-700 alloy in the 1800°F exposure. The C coating, because of poor corrosion resistance and spalling, was not further analyzed.

The F Coating

The microstructure of the F coating on U-700 was similar to that of the F coating on SEL-15 or IN-100 or other alloys, as previously described. The F coating on U-700 had a slightly more columnar structure in the diffusion zone than that of the F coating on SEL-15.

The F coating provided 120 hours of protection at 1650°F and 60 hours at 1800°F. The life of the F coating on U-700 was greater than that of the F coating on SEL-15, B1900, Inco 713C or IN-100, but less than that of the F coating on Rene' 41 alloy. This is most likely because the Cr content of the alloy U-700 is lower than that of the Rene' 41, but greater than the other program alloys. The 3.4 percent Ti in U-700 alloy probably resulted in some TiO_2 in the surface oxide (Ref. 4).

This coating, because of shorter life than the A and J coatings on U-700 was not included in Phase II.

The I Coating

The I coating was only applied to B1900 and U-700 and was practically identical in thickness and structure on both of the alloys. The measured thickness was below the required range in both cases. This coating had a very homogeneous appearance with a relatively small amount of second phase. There was a tendency to form γ' at the interface (Fig. 88).

Specimen UI5

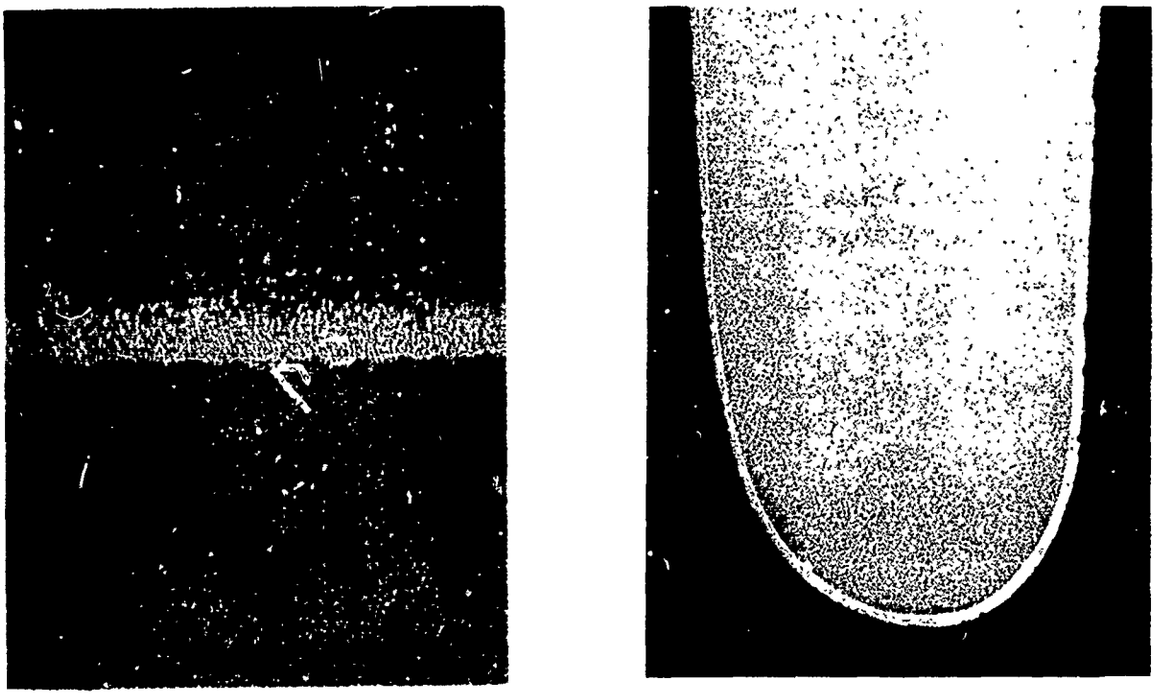

Magnification: 1000X

Magnification: 40X

FIGURE 88. MICROSTRUCTURE OF AS-RECEIVED COATINGS; Coating I on U-700 Alloy

The thickness of the coating decreased from 0.0018 inch to 0.0016 inch after 150 hours exposure at 1650°F (Fig. 89). The outer coating was found to consist of βNiAl, γ' matrix, chromium-rich phase and internal oxides. There was considerable loss of Al inasmuch as the matrix phase in the coating was γ'. The diffusion zone consisted of γ' matrix, carbide layer, chromium-rich phase and sigma phase. Sigma phase platelets developed in the γ' matrix at the interface.

The thickness of the coating increased from 0.0018 inch to 0.0023 inch after 60 hours exposure at 1800°F (Fig. 90). The outer coating consisted mainly of βNiAl phase and appeared free from oxides or carbides. The carbides were concentrated in the diffusion zone. The diffusion zone appeared to consist of β, γ', carbides and sigma phase. Sigma phase platelets developed in the γ' matrix at the interface.

The performance of the I coating on U-700 was much better than that on B1900, most likely because of the higher Cr in U-700. This coating, however, was not selected for further evaluation due to the poor performance at 1800°F.

Knoop Hardness Number (50 gram load)

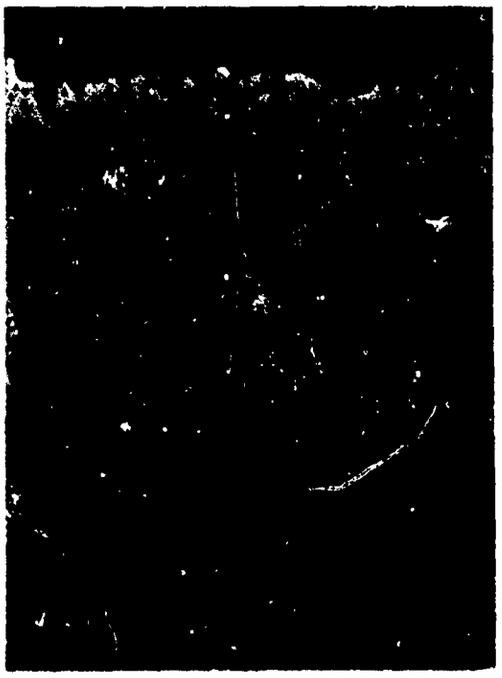

452

703

388

Specimen
UI2

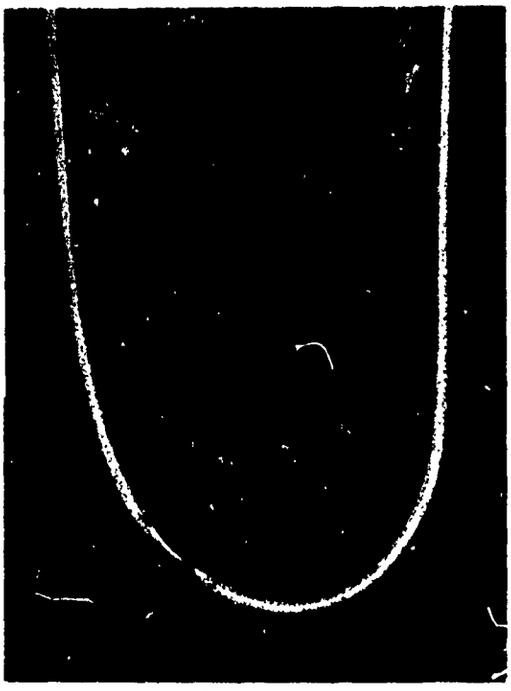

Magnification: 1000X

Magnification: 40X

FIGURE 89. MICROSTRUCTURE OF COATING I ON U-700 ALLOY AFTER HOT CORROSION TEST AT 1650° F FOR 150 HOURS

Specimen
UI4

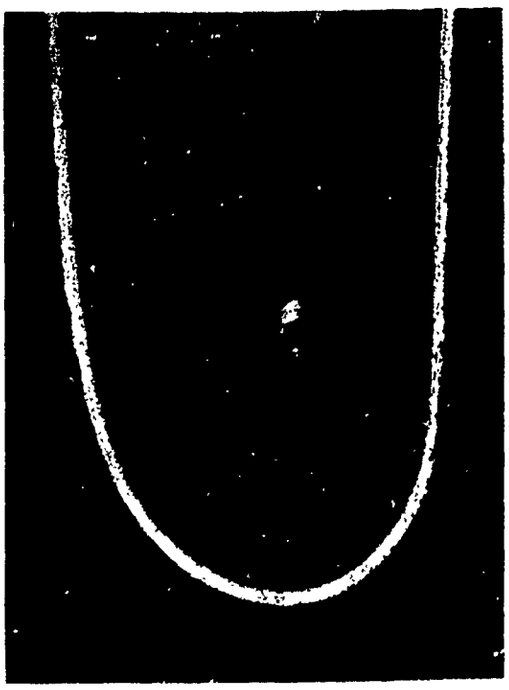

Magnification: 1000X

Magnification: 40X

FIGURE 90. MICROSTRUCTURE OF COATING I ON U-700 ALLOY AFTER HOT CORROSION TEST AT 1800° F FOR 60 HOURS

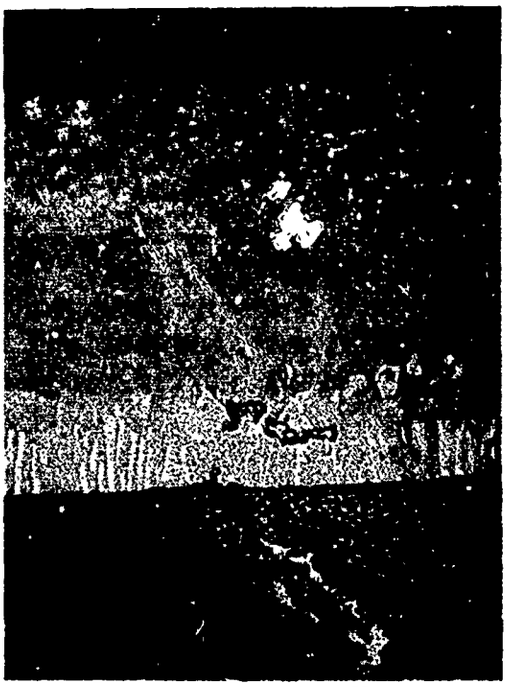

Specimen
UJ2

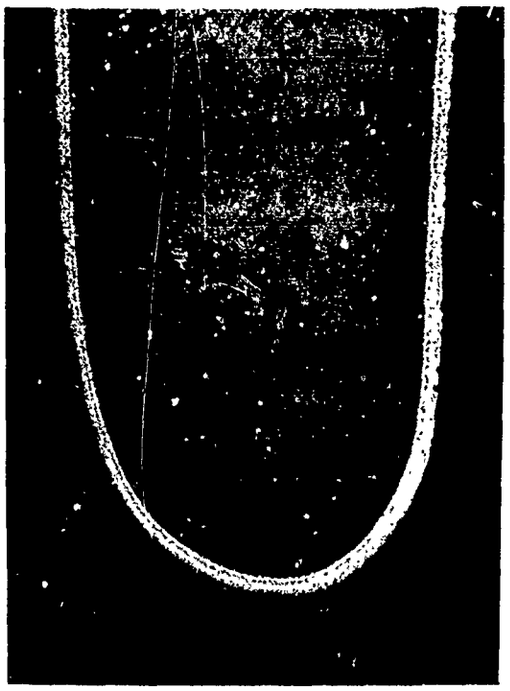

Magnification: 1000X

Magnification: 40X

FIGURE 91. MICROSTRUCTURE OF AS-RECEIVED COATINGS;
Coating J on U-700 Alloy

The J Coating

The J coating had a homogeneous structure containing small amounts of secondary phases, e.g., Cr_3Al_2 and α-Cr. Beneath the outer layer was the denuded βNiAl matrix. There was a continuous γ solid solution layer at the interface in contact with the βMAl, indicating a moderately high concentration of Cr, Co or Mo (Fig. 91).

The changes in microstructure after 150 hours exposure at 1650°F (Fig. 92) were similar to those described for the J coating on B1900 alloy.

The microstructure of U-700/J coating after 150 hours exposure at 1800°F is shown in Figure 93. In the outer zone just beneath the oxide, a thin layer of γ' phase is formed as a result of Al loss by oxidation from the βMAl phase. The outer zone consisted primarily of β phase, but transformation to γ' was evident. The diffusion zone consisted of γ' matrix with β phase, carbides and finger-like sigma phase. Some sigma phase dissolution was apparent. At the diffusion zone/substrate interface sigma phase platelets had developed in γ' matrix.

Knoop Hardness Number (50 gram load)

530

550

355

Specimen UJ1

Magnification: 1000X

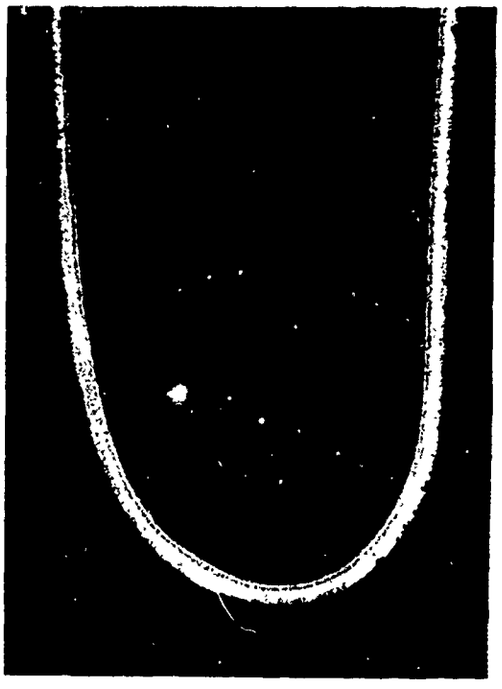

Magnification: 40X

FIGURE 92. MICROSTRUCTURE OF COATING J ON U-700 ALLOY AFTER HOT CORROSION TEST AT 1650° F FOR 150 HOURS

Specimen UJ3

Magnification: 1000X

Magnification: 40X

FIGURE 93. MICROSTRUCTURE OF COATING J ON U-700 ALLOY AFTER HOT CORROSION TEST AT 1800° F FOR 150 HOURS

The J coating was found to be the best coating for the protection of the U-700 alloy and was therefore selected for further evaluation in Phase II.

3.9 HOT CORROSION TEST RESULTS OF COATED U-710 ALLOY

3.9.1 Weight Change and Appearance

Results of the hot corrosion tests at 1650°F and 1800°F on the coated U-710 alloy are shown in Figures 94 and 95.

Best performance at both temperature levels was exhibited by the A and J coating systems. After test at 1650°F for 150 hours, the surfaces of the A and J coated specimens were smooth and essentially unchanged. The G coating, however, showed considerably coating spalling, particularly on the concave surfaces.

At 1800°F the A and J coatings again exhibited best performance on the U-710 alloy. The J coated specimens showed slight loss of coating on the concave surface but substrate oxidation was not apparent. The A coating was smooth and essentially unchanged as a result of the test. Coating G again exhibited spalling and pinhole type substrate oxidation failures at the conclusion of the test.

3.9.2 Metallographic Analyses of Coatings on U-710 Alloy

The A Coating

Assuming the A coating on U-710 was applied under identical conditions as the A coating on U-700, the small changes in Mo, Cr and Ti contents had a relatively pronounced effect on "as-applied" coating thickness. The A coating on U-710 (Fig. 96) was only 66 percent of the coating thickness on U-700. Other as-applied features of the A coated U-710 alloy were similar to coated U-700 (see Sec. 3.8.2).

After exposure to 150 hours of HC testing at 1650°F, the retained thicknesses of the A coating on U-700 (Fig. 86) and U-710 (Fig. 97) were approximately the same, i.e., 0.0035 inch, indicating either an excessively thick coating was selected for "as-coated" thickness measurements on U-700, or rapid interdiffusion in U-710. The former appears more likely. Gamma prime and sigma phase were in evidence at the interface, as is typical for the coated nickel-base alloys; however little observable β-NiAl depletion in aluminum could be seen indicating excellent resistance to attack by the coating at 1650°F. One undesirable feature of the A coating on U-710 after 1650°F exposure is the extreme hardness of the diffusion zone layer, up to 1020 KHN (Fig. 97). This hardness may indicate a significantly higher amount of sigma phase than for the A coating on U-700. This high hardness may promote coating shear under service conditions.

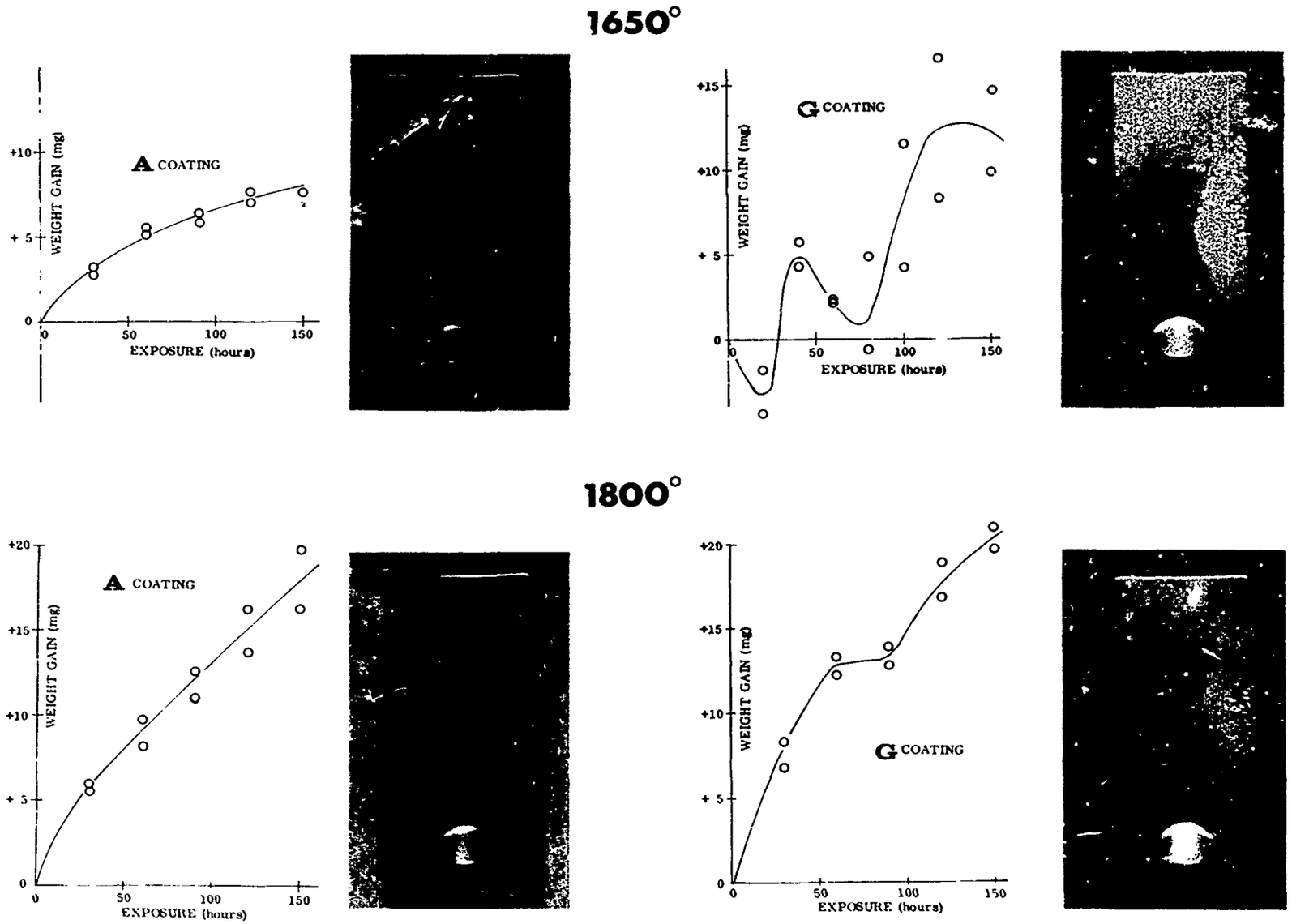

FIGURE 94. WEIGHT CHANGE AND APPEARANCE OF COATINGS A AND G ON U-710 ALLOY TESTED AT 1650°F AND 1800°F

1650°

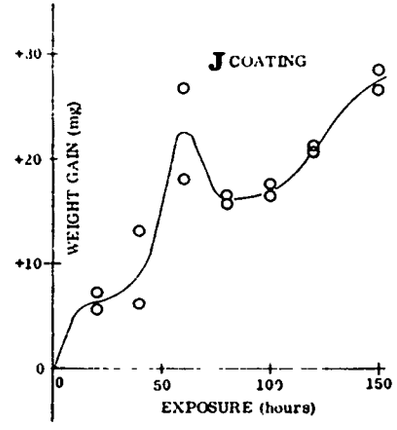

1800°

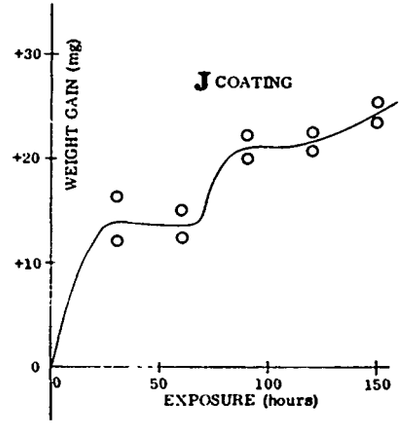

FIGURE 95. WEIGHT CHANGE AND APPEARANCE OF COATING J ON U-710 ALLOY TESTED AT 1650°F AND 1800°F

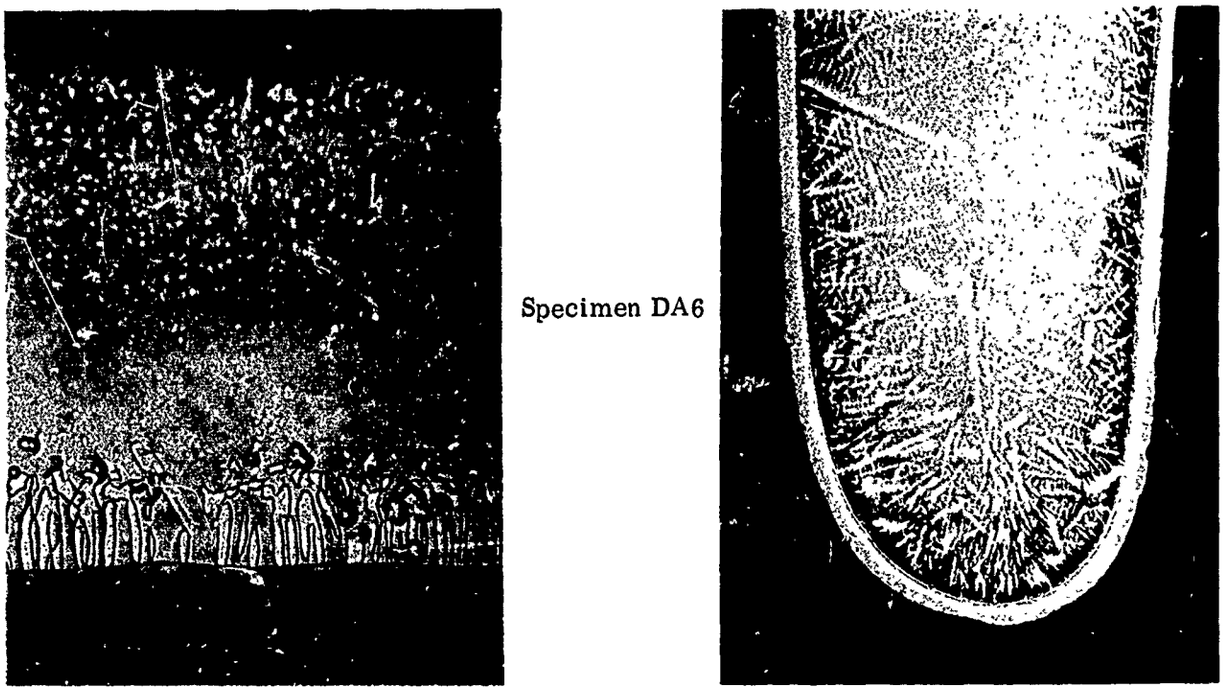

Specimen DA6

Magnification: 1000X

Magnification: 40X

FIGURE 96. MICROSTRUCTURE OF AS-RECEIVED COATINGS; Coating A On U-710 Alloy

The microstructure of specimens exposed at 1800°F, Figure 98, exhibited essentially the same structure as the 1650°F specimens. Retained coating thickness was slightly less with the surface showing evidence of selected attack.

Because of the coating's excellent resistance to hot corrosion, the A coating on U-710 was selected for further evaluation in Phase II - Mechanical Property Tests.

The J Coating

Microstructure of the U-710 alloy "as-coated", after exposure for 150 hours at 1650°F and 1850°F are shown in Figures 99, 100 and 101. The overall appearance as-coated is very similar to the J coating on U-700, Figure 91, with the exception that the higher chromium content of the U-710 alloy appeared to promote a significant increase in sigma phase formation at the interface. As with the A coating on U-710 alloy, this increase in sigma phase produced significant hardening after the 150-hour, 1650°F exposure (Fig. 100).

606

530

1020

825

670

573

℄ 470

Magnification: 1000X

Magnification: 40X

Specimen DA1

FIGURE 97. MICROSTRUCTURE OF COATING A ON U-710 AFTER HOT CORROSION TESTS AT 1650°F FOR 150 HOURS

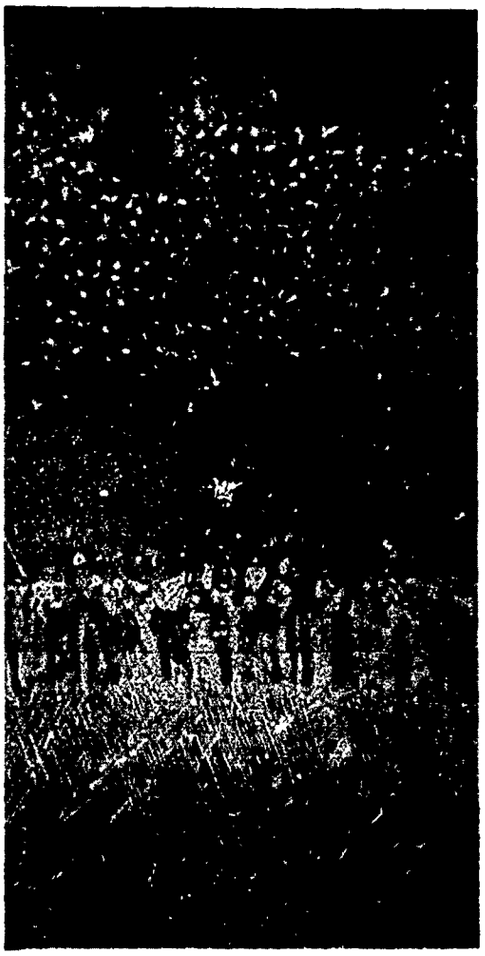

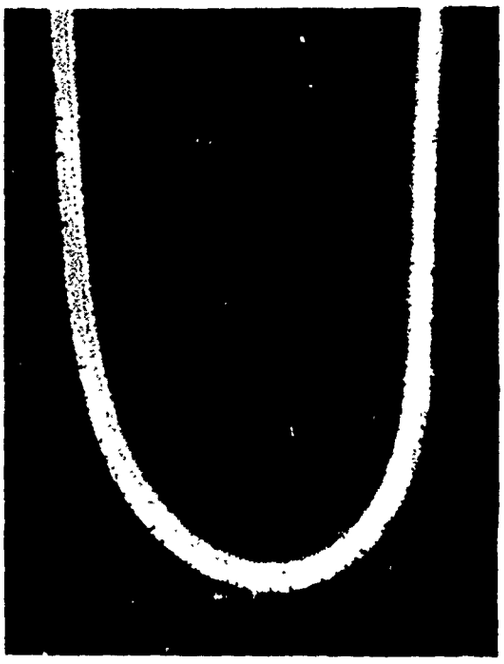

Magnification: 40X

Specimen DA3

Magnification: 1000X

FIGURE 98. MICROSTRUCTURE OF COATING A ON U-710 AFTER HOT CORROSION TESTS AT 1800° F FOR 150 HOURS

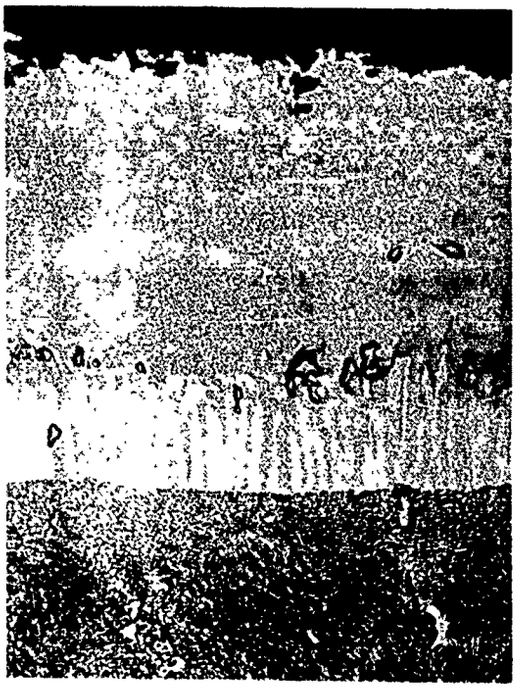

Specimen
DJ6

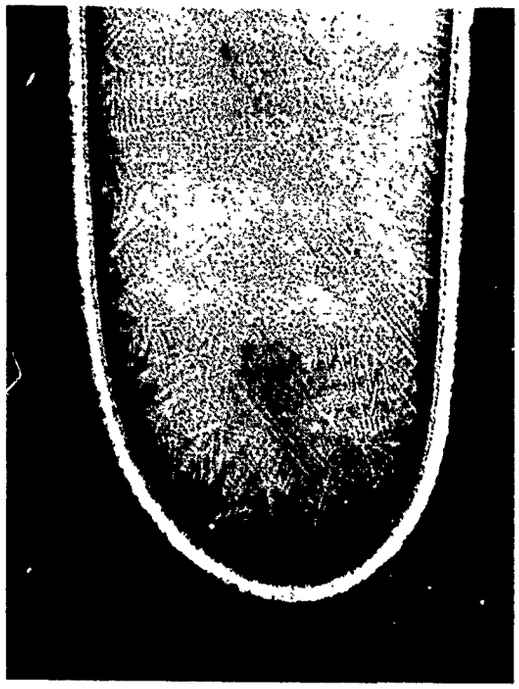

Magnification: 1000X

Magnification: 40X

FIGURE 99. MICROSCTRUCTURE OF AS-RECEIVED COATINGS; Coating J on U-710 Alloy

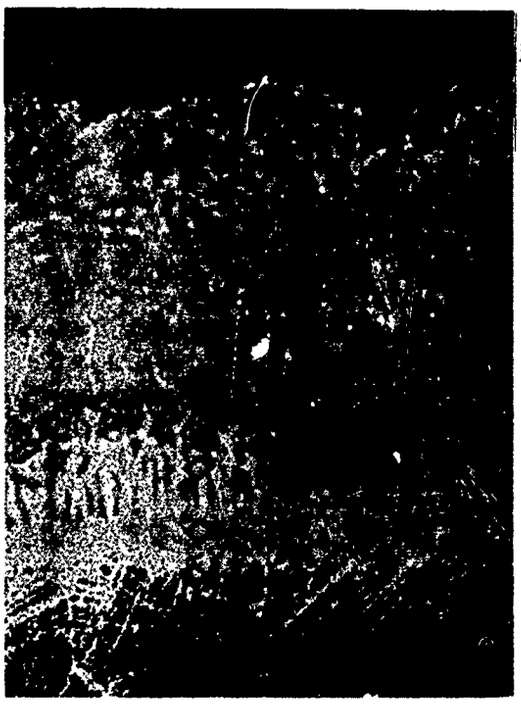

Knoop Hardness
(50-gram load)

810

660

Specimen
DJ2

960

860

615

488

℄ 542

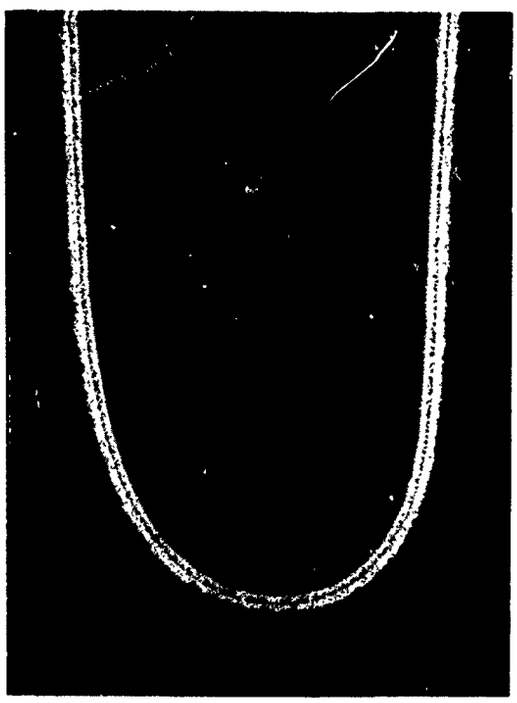

Magnification: 1000X

Magnification: 40X

FIGURE 100. MICROSTRUCTURE OF J COATING ON U-710 AFTER HOT CORROSION TESTS AT 1650°F FOR 150 HOURS

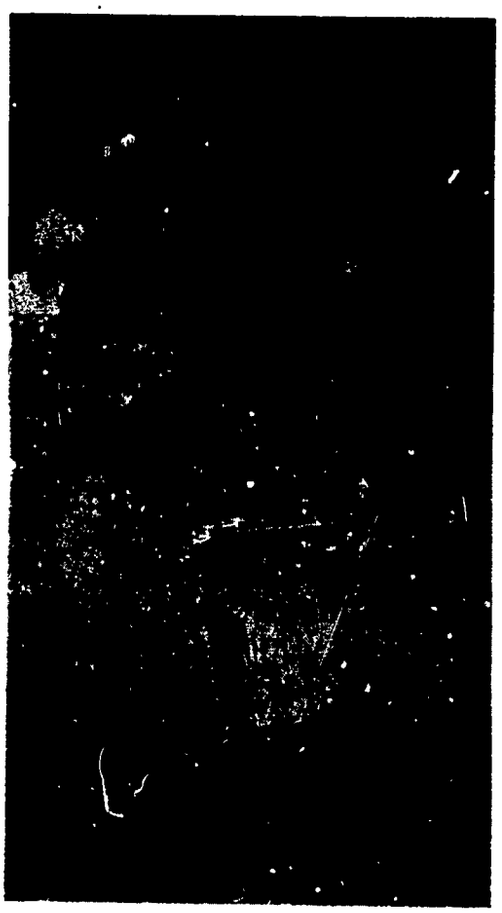

Magnification: 1000X

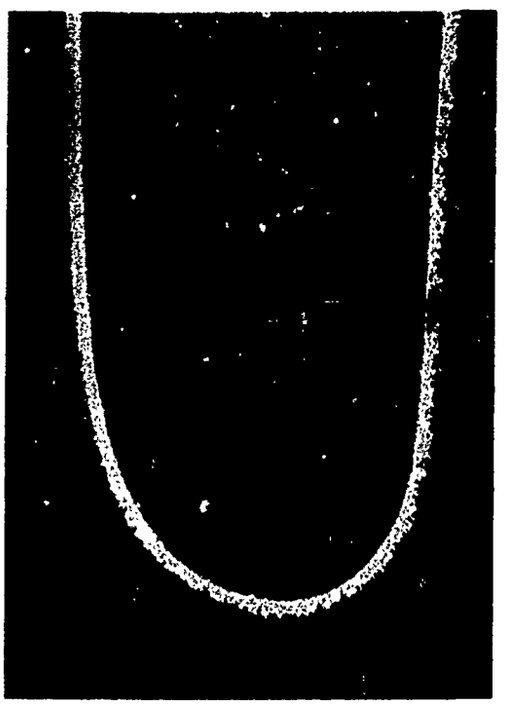

Magnification: 40X

Specimen DJ4

FIGURE 101. MICROSTRUCTURE OF J COATING ON U-710 ALLOY AFTER HOT CORROSION TESTS AT 1800°F FOR 150 HOURS

Although the J coating on U-710 withstood the 150-hour HCR test at both 1650°F and 1800°F, the coating was definitely inferior to the A coating. As can be noted in Figure 101, the coating was essentially consumed after the 1800°F HCR test; also surface attack had been initiated by the end of the 1650°F HCR test. The J coating was, however, the second best system tested on U-710 and was, therefore, selected for testing in Phase II.

3.10 HOT CORROSION TEST RESULTS OF COATED MAR-M-246 ALLOY

3.10.1 Weight Change and Appearance

The results of the hot corrosion tests at 1650°F and 1800°F for coatings A, G, and J on MAR-M-246 alloy are shown in Figures 102 and 103. At the conclusion of 40 hours exposure at 1650°F, the G coated specimens exhibited severe substrate

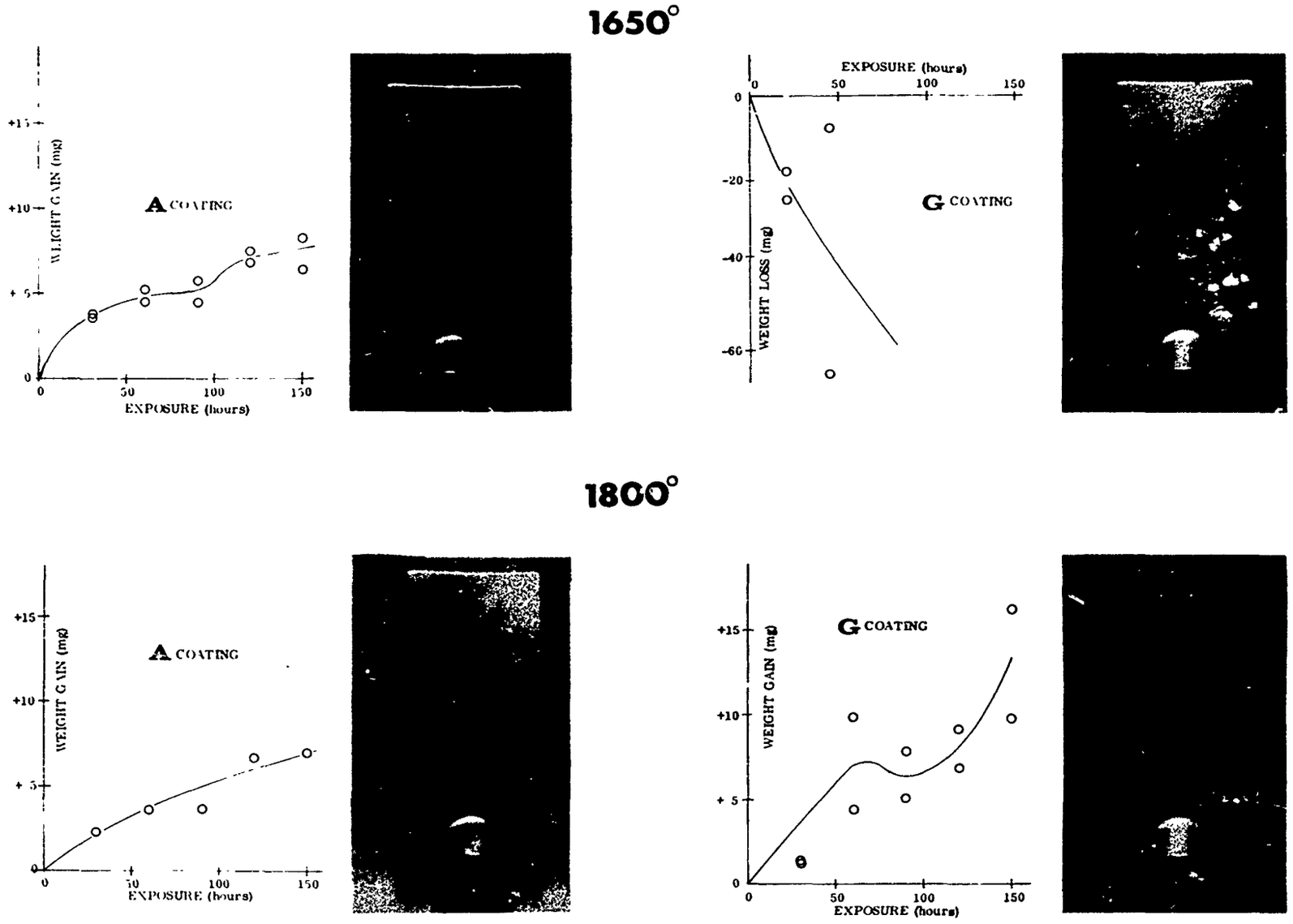

FIGURE 102. WEIGHT CHANGE AND APPEARANCE OF COATINGS A AND G ON MAR-M-246 ALLOY TESTED AT 1650°F AND 1800°F

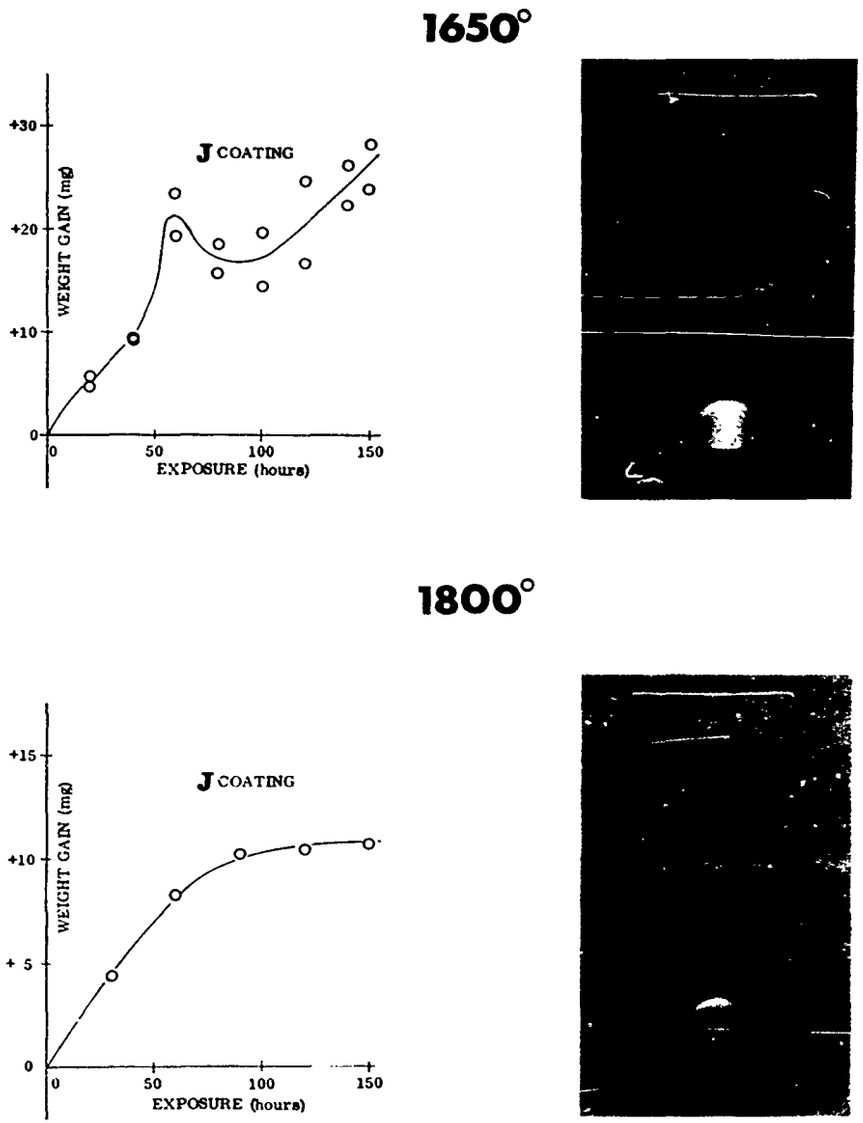

FIGURE 103. WEIGHT CHANGE AND APPEARANCE OF COATING J ON MAR-M-246 ALLOY TESTED AT 1650°F AND 1800°F

corrosion and were removed from test. The A and J coatings were continued in test to 150 hours total exposure without any evidence of coating failure or substrate attack.

At 1800°F, all three of the coatings were capable of providing protection for 150 hours exposure without catastrophic substrate oxidation. However, at the conclusion of the test, the G coated specimens showed extensive coating spalling and pitting type coating failures were observed on the concave surfaces. The A and J coatings exhibited slight roughening of the surfaces of the specimens but substrate oxidation was not apparent.

3.10.2 Metallographic Analyses of Coatings on MAR-M-246 Alloy

Metallographic analyses were performed on the two coatings showing the better hot corrosion resistance on MAR-M-246 alloy, i.e., A and J.

The A Coating

The A coating on MAR-M-246 (Fig. 104) appeared to be formed predominantly by the inward diffusion of aluminum. Carbides, possibly of tungsten, are present to the outermost regions of the coating. The high concentration of Cr_2Al present, e.g., in A coated U-710, is absent from this A coated MAR-M-246; however the interface concentration of secondary phases and the presence of gamma phase between the diffusion zone and substrate are nearly similar to the A coating on U-710. The MAR-M-246 alloy has a markedly more stable γ-γ' structure than the majority of alloys coated with the A process. The low chromium and titanium and high tungsten and aluminum are probably responsible for greater phase stability.

The microstructure after testing for 150 hours at 1650°F is quite interesting (Fig. 105). No acicular sigma phase has developed. The diffusion and interface zones appear to be primarily γ'. There was almost no change in coating thickness after the 1650°F exposure, but there was evidence that selective surface attack had occurred. It is possible that the presence of carbides to the outermost regions of the coating may accelerate this type of attack.

Diffusion zone hardness after 1650°F exposure was high (Fig. 105) being comparable with the A coated U-710 alloy and much higher than A coated alloys such as U-700, SEL-15, and IN-100. Tungsten, chromium and tantalum carbides, as well as γ and γ' solution of these elements, are probably responsible for the hardness.

The A coating was selected for tests in Phase II because of its excellent resistance to HCR testing on this low-chromium alloy.

Magnification: 1000X

Specimen MA6

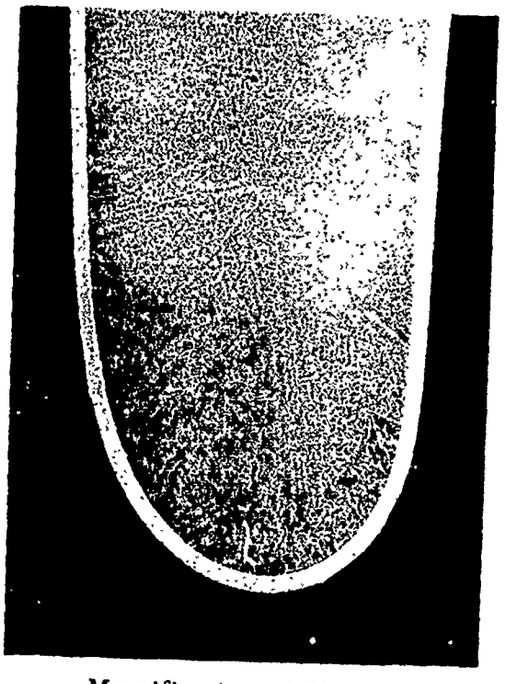

Magnification: 40X

FIGURE 104. MICROSTRUCTURE OF AS-RECEIVED COATINGS; Coating A on MAR-M-246 Alloy

Magnification: 1000X

Knoop Hardness (50-gram load)

565

Specimen MA2

597

898

735

358

℄ 501

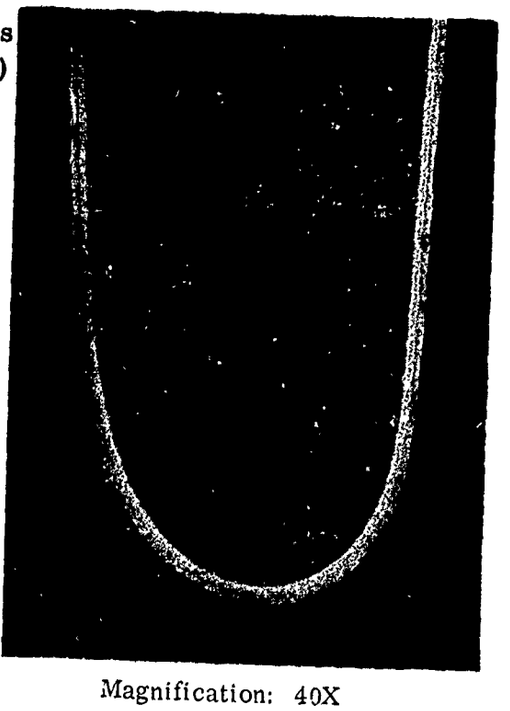

Magnification: 40X

FIGURE 105. MICROSTRUCTURE OF A COATING ON MAR-M-246 AFTER HOT CORROSION TESTS AT 1650°F FOR 150 HOURS

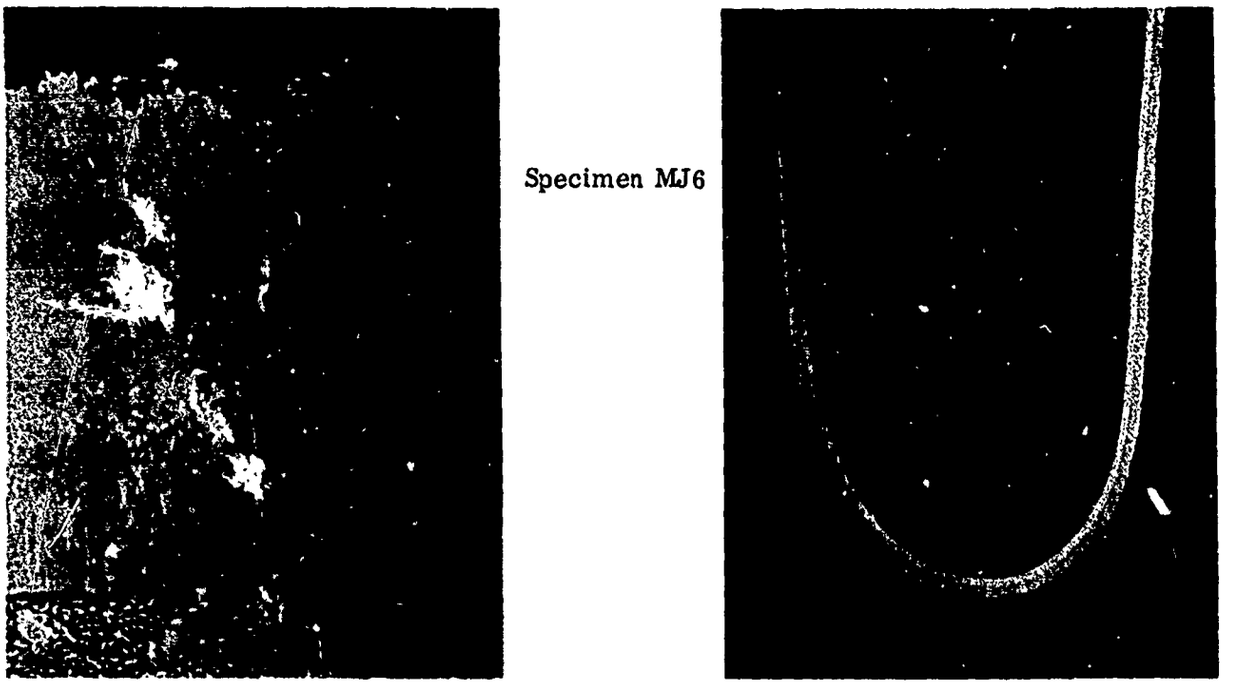

Magnification: 1000X Magnification: 40X

FIGURE 106. MICROSTRUCTURE OF AS-RECEIVED COATINGS: Coating J on MAR-M-246 Alloy

The J Coating

The microstructure of the J coating on MAR-M-246 is almost identical to the as-coated (Fig. 106) and as-tested at 1650°F (Fig. 107) as the A coating on the same alloy (Fig. 104 and 105). A notable exception is the absence of carbides in the outermost region of the βNiAl.

The J coating showed minimal gross coating consumption in the 1650°F test (Fig. 107), but the microstructure showed evidence of deep selective attack that may result in a relatively short life for the coating. The microstructure of specimens exposed at 1800°F (Fig. 108) exhibited essentially the same structure as the 1650°F specimens. Retained coating thickness was approximately the same with the coating again exhibiting evidence of deep selective attack.

Favorable characteristics over the A coating were a softer diffusion zone and a thinner interface γ' layer.

As a result of the HCR tests and examination of the microstructure, this coating was selected for testing in Phase II.

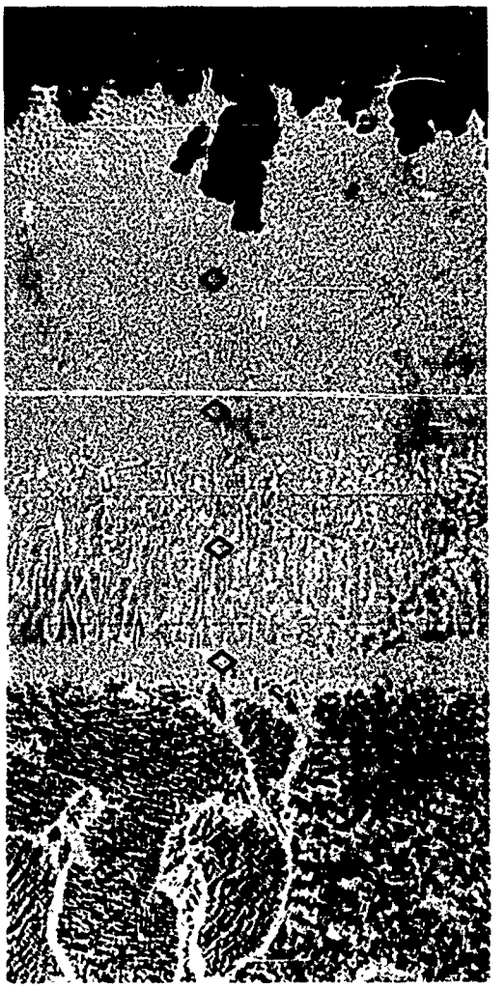

Magnification: 40X

Knoop Hardness (50-gram load)

Specimen MJ1

FIGURE 107. MICROSTRUCTURE OF J COATING ON MAR-M-246 AFTER HOT CORROSION TESTS AT 1650°F FOR 150 HOURS

Magnification: 1000X

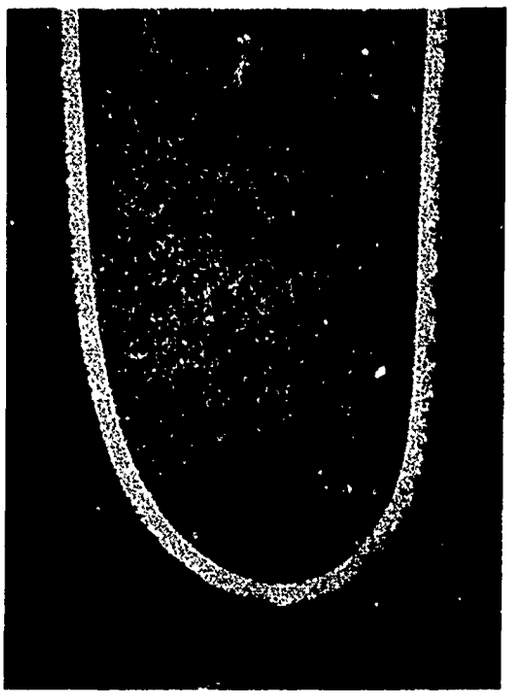

Magnification: 40X

Specimen MJ4

FIGURE 108. MICROSTRUCTURE OF J COATING ON MAR-M-246 AFTER HOT CORROSION TESTS AT 1800°F FOR 150 HOURS

3.11 HOT CORROSION TEST RESULTS OF COATED WI-52 ALLOY

3.11.1 Weight Change and Appearance

A summary of the weight change during testing at 1800°F and 2000°F for the A, B, C, D and H coatings on WI-52 alloy is shown in Figures 109, 110 and 111. At 1800°F, best performance was exhibited by the C coating. At the completion of 150 hours exposure, both specimens exhibited a steady weight gain. The surfaces of the two specimens were very smooth and essentially unchanged as a result of the test. Coatings A, B, D and H all exhibited failure of the coatings, generally on the convex surfaces. For coatings A, B, and D failure appeared to be initiated after approximately 120 hours exposure. These specimens lost weight at approximately the same

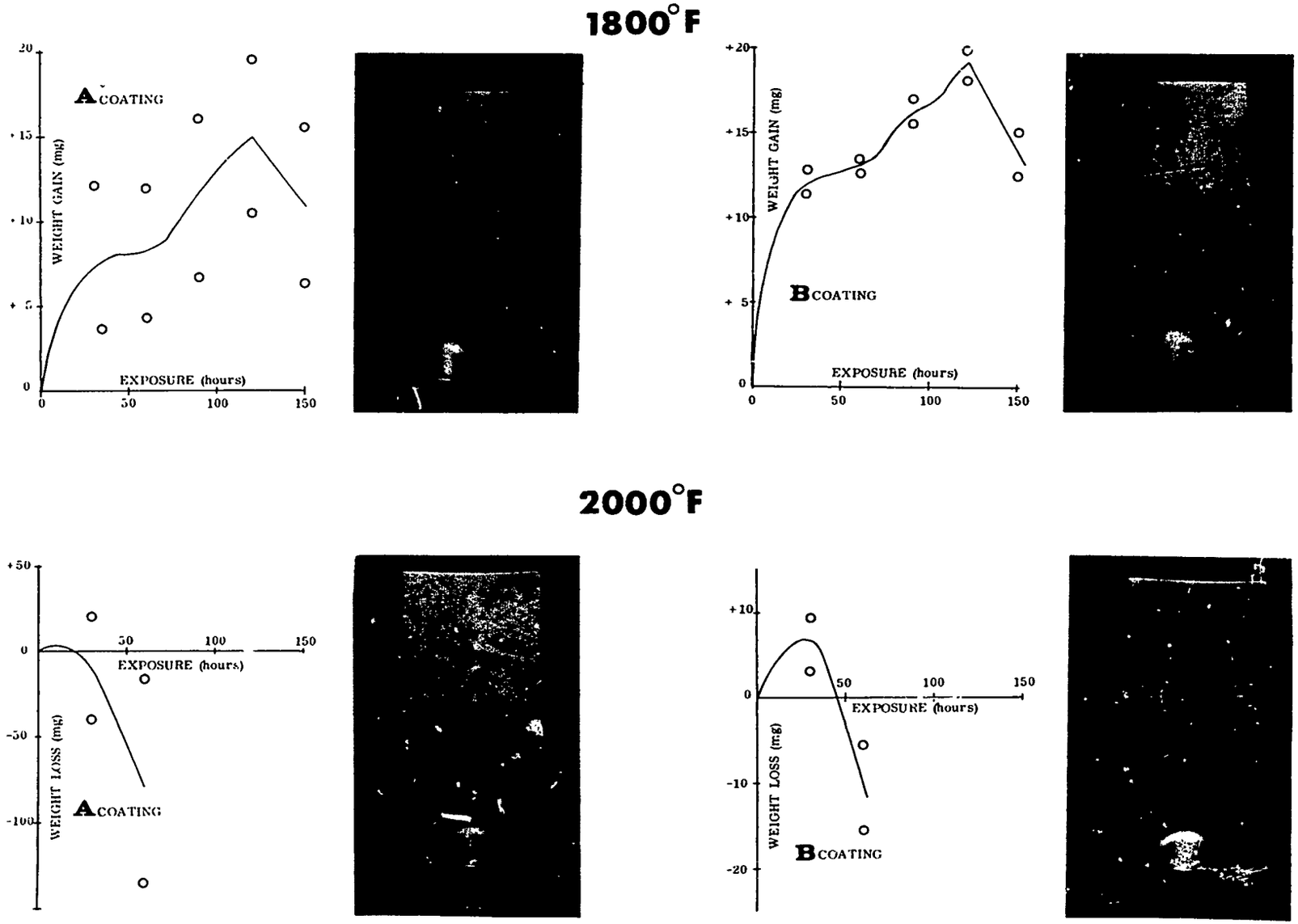

FIGURE 109. WEIGHT CHANGES AND APPEARANCE OF COATINGS A AND B ON WI-52 ALLOY TESTED AT 1800° F AND 2000° F

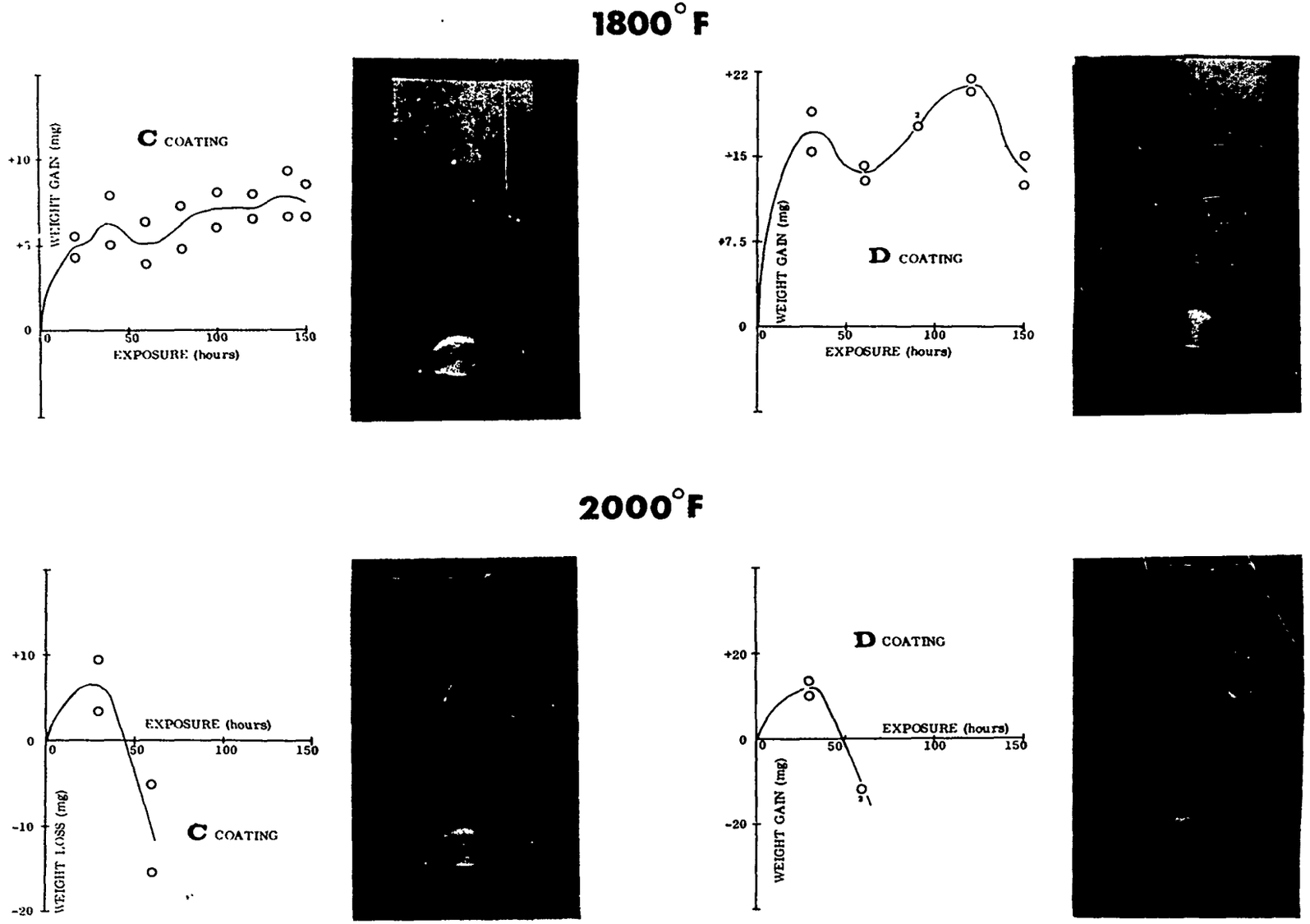

FIGURE 110. WEIGHT CHANGES AND APPEARANCE OF COATINGS C AND D ON WI-52 ALLOY TESTED AT 1800° F AND 2000° F

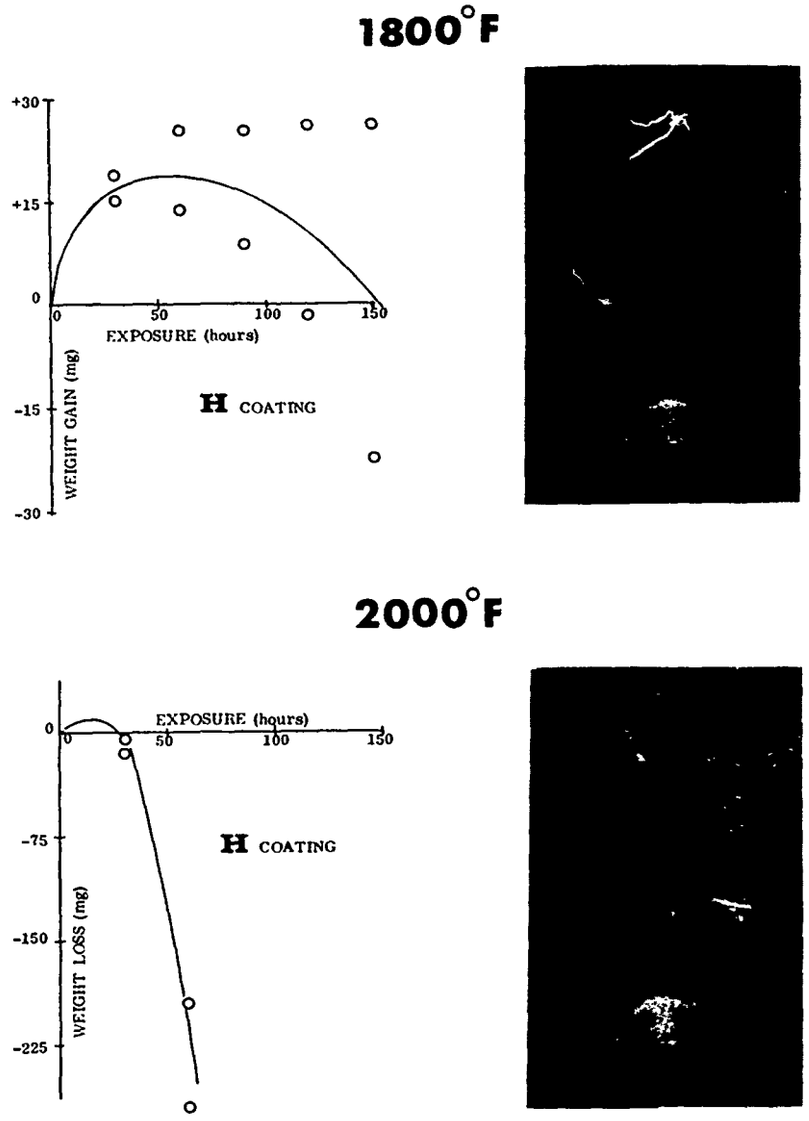

FIGURE 111. WEIGHT CHANGES AND APPEARANCE OF COATING H ON WI-52 ALLOY TESTED AT 1800° F AND 2000° F

rate, i.e., 0.2 mg per hour from 120 to 150 hours total exposure. One H coated specimen exhibited good performance in the test; whereas the other specimen was badly corroded along the trailing edge and the concave surface.

Results of the tests at 2000°F show that the selected test conditions (temperature and sea salt concentration) were too severe. All coatings failed and were removed from test after 60 hours of exposure. Failure ranged from slight coating spalling and substrate oxidation (the B and D coatings) to severe loss of substrate (225 mg loss for the H coating).

3.11.2 Metallographic Analyses of Coatings on WI-52 Alloy

The A Coating

The A coating on WI-52 was the thickest coating on this alloy (0.0022 inch). Carbides from the substrate were present throughout the coating as the major secondary coating phase. A hard white phase had formed at the βCoAl/WI-52 interface and was continuous with some of the carbide phase in the substrate.

The A coating after 150 hours exposure at 1800°F was found to spall off at the trailing edge. The substrate was not damaged. After exposure, the A coating consisted of β-CoAl phase, internal oxide spots, carbides and γ-Co solid solution.

The A coating, because of failure at the trailing edge was not selected for additional evaluation.

The B Coating

The B coating was 0.0018 inch thick and consisted of white etching dispersed phase in β-CoAl matrix (Fig. 112). MC carbides were visible in the intermediate layer. The white etching phase at the interface was continuous and therefore isomorphous with γ solid solution. Interface voids and dark etching geometric-alloy shaped particles identified as internal oxidation products were also present.

After exposure for 150 hours at 1800°F, the β-CoAl was transformed partially to γ-Co because of loss of Al as Al_2O_3 (Fig. 113). Internal oxidation of the coating was apparent. Slight Al diffusion into the substrate may also have occurred. This coating-alloy combination was selected for inclusion in Phase II.

The C Coating

The C coating was about the same thickness (0.0019 inch) as the B coating (Fig. 114). The outer zone consisted most likely of β-CoAl matrix with small amounts

Specimen
WB5

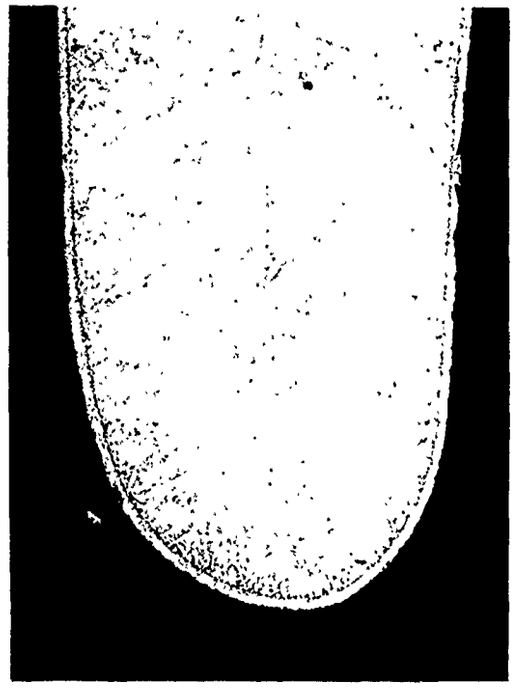

Magnification: 1000X

Magnification: 40X

FIGURE 112. MICROSTRUCTURE OF AS-RECEIVED COATINGS;
Coating B on WI-52 Alloy

Knoop Hardness Number (50-gram load)

514

910

565

470

Magnification: 1000X

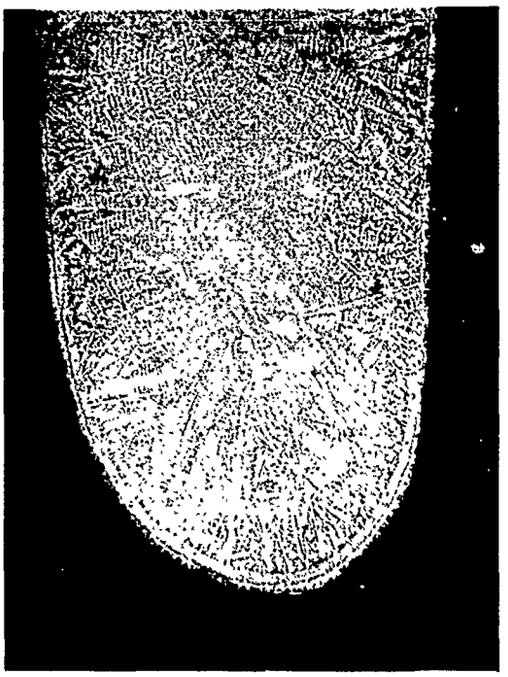

Magnification: 40X

Specimen WB1

FIGURE 113. MICROSTRUCTURE OF COATING B ON WI-52 ALLOY AFTER HOT CORROSION TEST AT 1800° F FOR 150 HOURS

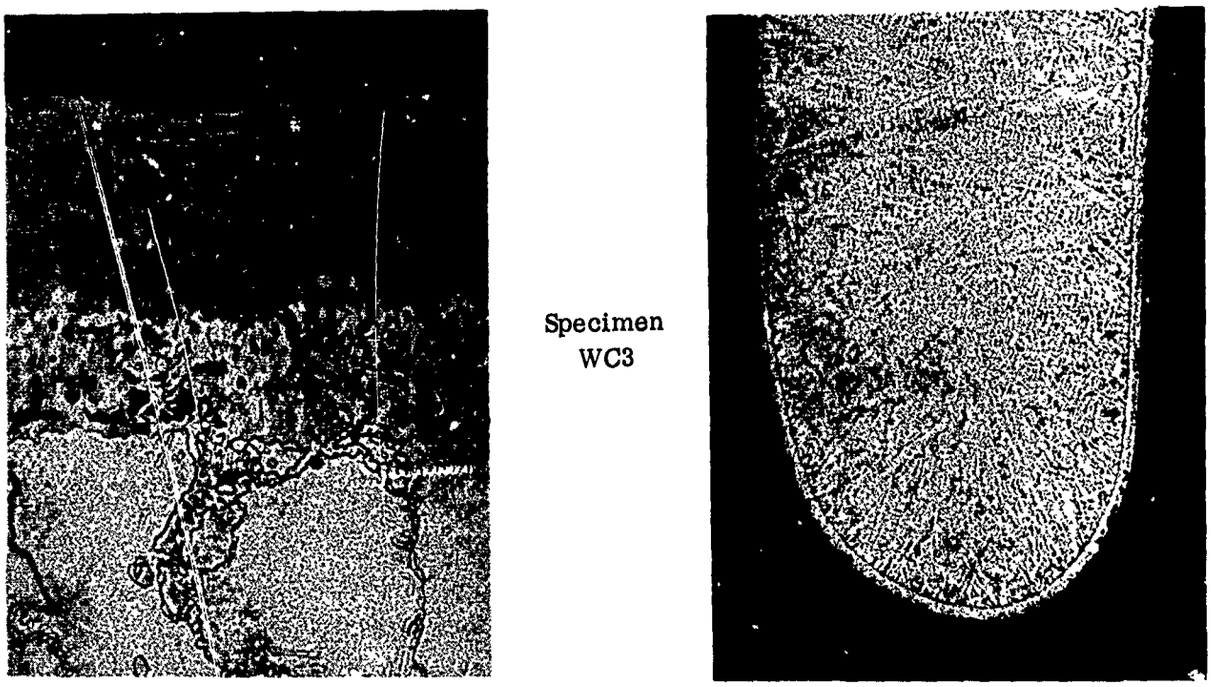

Magnification: 1000X

Magnification: 40X

FIGURE 114. MICROSTRUCTURE OF AS-RECEIVED COATINGS;
Coating C on WI-52 Alloy

of dispersed white phase. The diffusion zone appeared to consist of γ-Co matrix, β phase carbides and internal oxide spots.

After the HCR testing for 150 hours at 1800°F the coating structure was essentially the same except for the formation of an unidentified phase in the outer layer and for some Al diffusion into the substrate (Fig. 115). The 60-hour exposure at 2000°F resulted in loss of some Al as Al_2O_3 and transformation of β-CoAl to γCo at the outer-layer (Fig. 116). Beneath the outer γCo layer was the β-CoAl matrix with carbides and internal oxide spots distributed in the matrix. Limited Al diffusion into the matrix also occurred.

The C coating was found to be the best coating for the protection of WI-52 alloy and was evaluated for its effects on the mechanical properties of the alloy in Phase II.

The D Coating

The D coating (thickness 0.0014 inch) consisted mainly of β-CoAl phase with fine dispersion of carbides in the outer layer and white etching phase in the intermediate

Knoop Hardness Number (50-gram load)

550

Specimen WC1

810

436

528

Magnification: 1000X

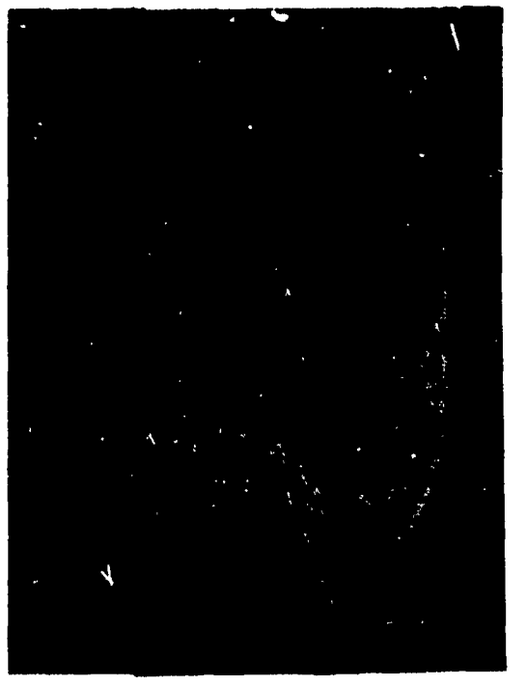

Magnification: 40X

FIGURE 115. MICROSTRUCTURE OF COATING C ON WI-52 ALLOY AFTER HOT CORROSION TEST AT 1800° F FOR 150 HOURS

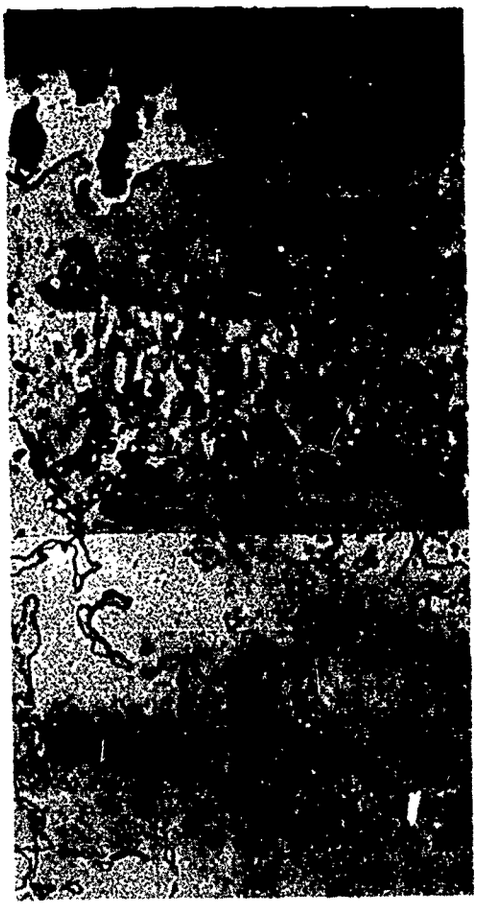

Specimen WC4

Magnification: 1000X

Magnification: 40X

FIGURE 116. MICROSTRUCTURE OF COATING C ON WI-52 ALLOY AFTER HOT CORROSION TEST AT 2000° F FOR 60 HOURS

layer. Interface oxides or voids, characteristic of coatings on cobalt-base alloys, were present.

After 150 hours corrosion testing at 1800°F most of the coating at the trailing edge was consumed. The β-CoAl phase was transformed into γCo which had been extensively oxidized. This coating therefore was not selected for evaluation in Phase II.

The H Coating

The H coating on WI-52 alloy contained a relatively large amount of white etching phase throughout the coating indicating significant deposition of chromium during the coating process. The H coating (0.0014 inch thick) was below the required thickness range.

The coating, after 150 hours hot corrosion exposure at 1800°F, was about 80 percent consumed. The effects of the exposure were similar to other coatings on WI-52 alloy, viz., loss of Al by oxidation to Al_2O_3, transformation of β-CoAl to γCo and internal oxidation. This coating was not further evaluated.

3.12 HOT CORROSION TEST RESULTS OF COATED X-40 ALLOY

3.12.1 Weight Change and Appearance

Figure 117, 118 and 119 show the weight change curves and surfaces of coatings A, B, C, D and H on X-40 alloy after testing at a peak metal temperature of 1800°F and 2000°F. The best performance as judged by visual inspection and weight change was exhibited by the A and D coatings. The surfaces of these two coatings were very smooth and unchanged as a result of the test. Coatings B, C and H all showed evidence of coating failure at the completion of the test. The B coating exhibited slight loss of coating generally along the trailing edges on the concave surface in the hottest area of the blades. Only one specimen, however, had lost enough coating at 120- and 150-hour inspection intervals to show an indication of cumulative weight loss in the test. The C coating exhibited a weight loss (after 120 hours exposure), which indicated spalling and loss of the oxidized coating. Visual evidence of the coating loss is shown in the photograph accompanying the weight change curve. With the C coating, failure was initiated on the convex surface of the air foil and extended towards the cooler region near the shank of the blade. The H coating exhibited poorest performance in the hot corrosion test. At the completion of the 1800°F test, both H coated specimens exhibited a considerable amount of corrosion on the concave surfaces of the blade. The H coating exhibited poorest performance in the hot corrosion test. At the completion of the 1800°F test, both H coated specimens exhibited a considerable amount of corrosion on the concave surfaces of the blades. At 2000°F the H coating apparently failed immediately after initiation of the test. Both

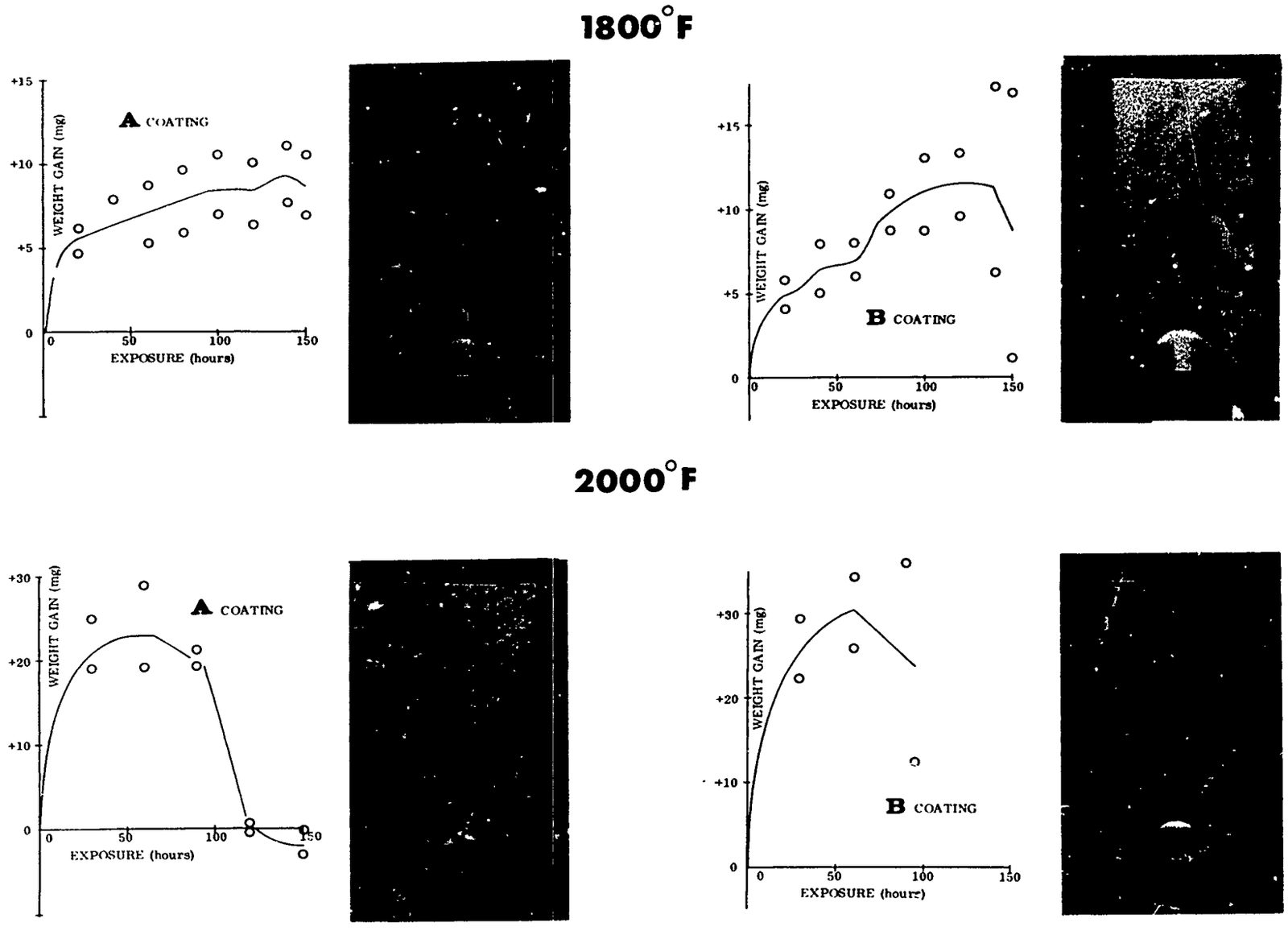

FIGURE 117. WEIGHT CHANGES AND APPEARANCE OF COATINGS A AND B ON X-40 ALLOY TESTED AT 1800° F AND 2000° F

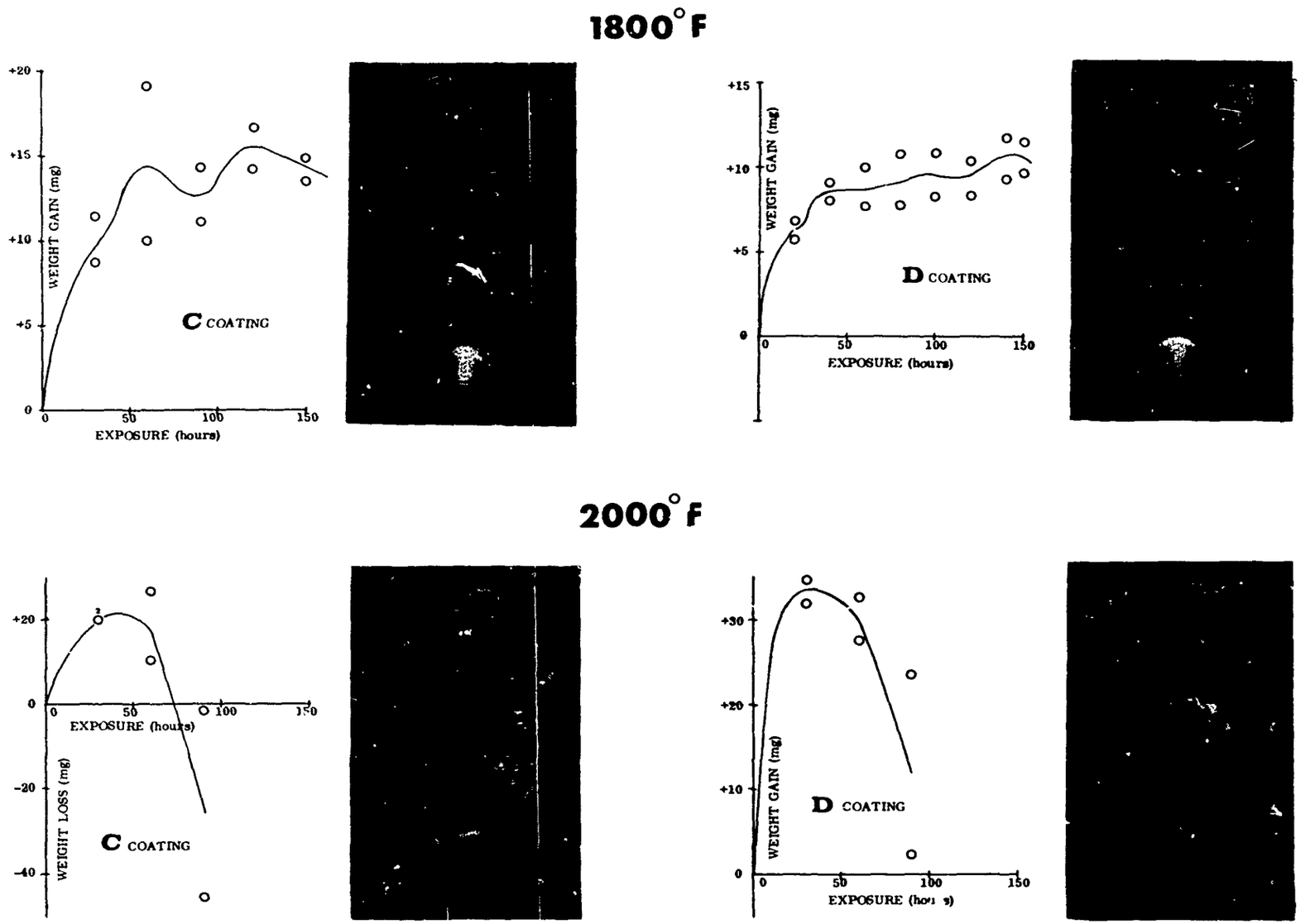

FIGURE 118. WEIGHT CHANGES AND APPEARANCE OF COATINGS C AND D ON X-40 ALLOY TESTED AT 1800°F AND 2000°F

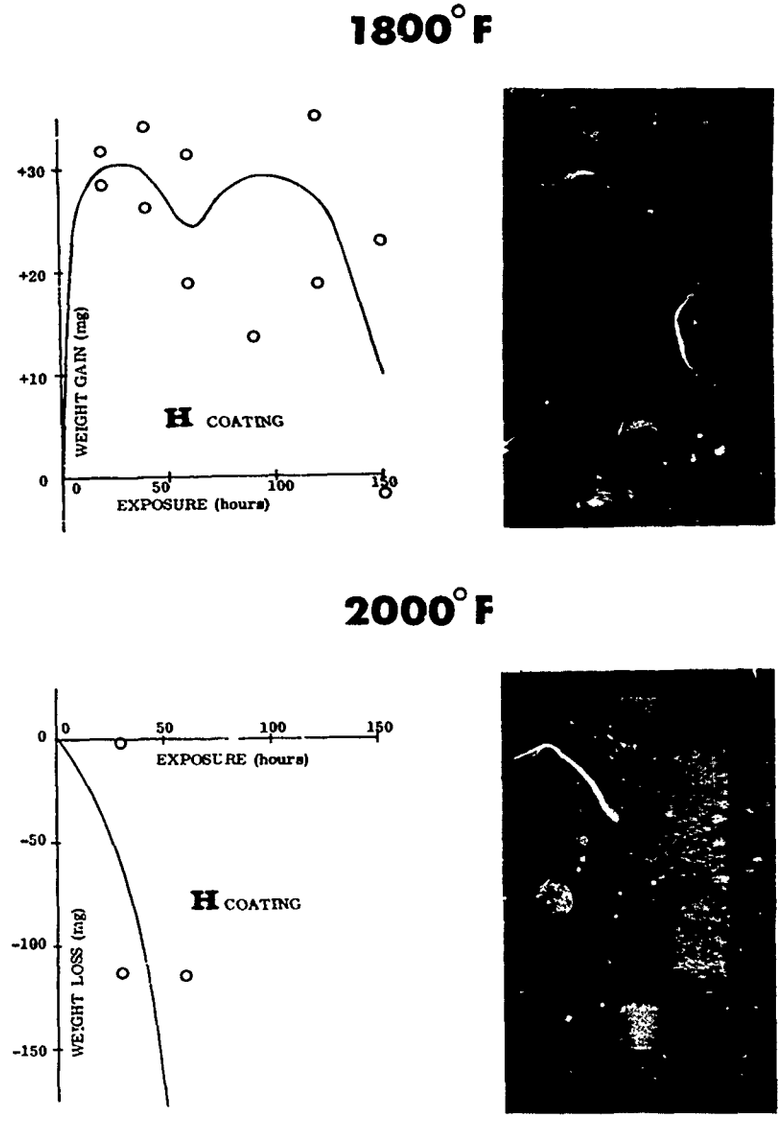

FIGURE 119. WEIGHT CHANGES AND APPEARANCE OF COATING H ON X-40 ALLOY TESTED AT 1800° F AND 2000° F

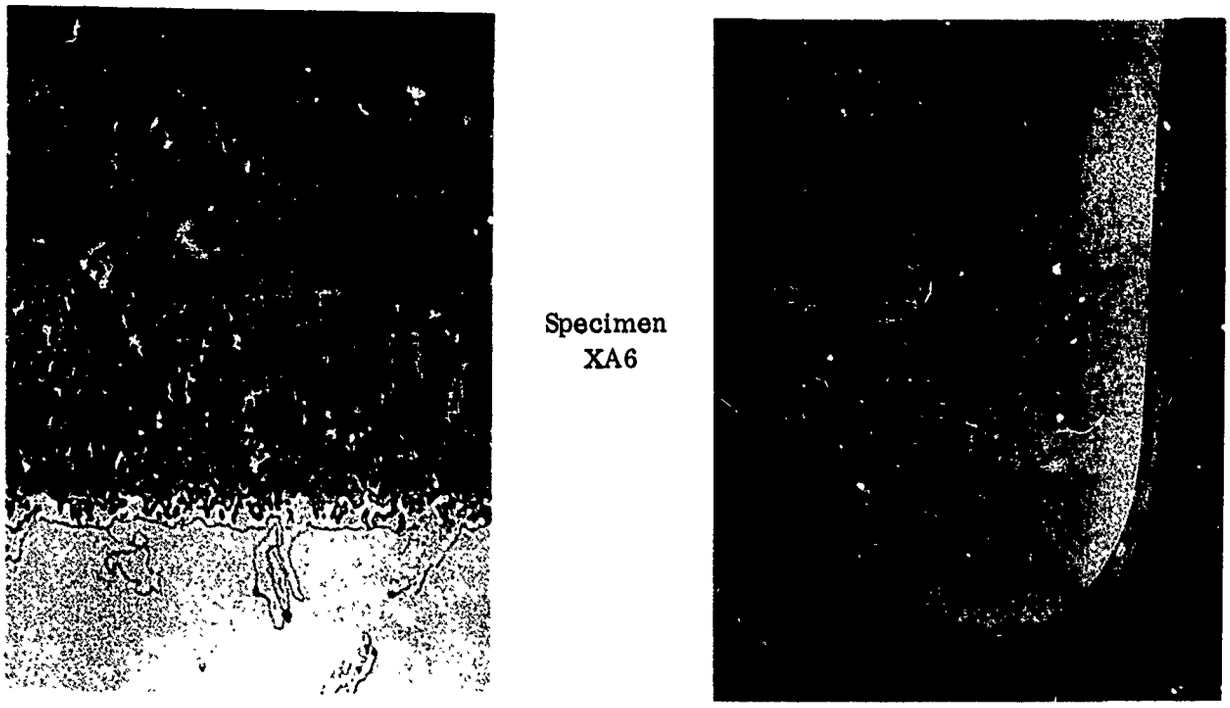

Magnification: 1000X

Magnification: 40X

FIGURE 120. MICROSTRUCTURE OF AS-RECEIVED COATINGS;
Coating A on X-40 Alloy

specimens exhibited coating spalling and substrate corrosion at the first 30-hour inspection interval. Specimens were removed from test after a total of 60 hours exposure.

3.12.2 Metallographic Analyses of Coatings on X-40 Alloy

The A Coating

The A coating was the thickest (0.0026 inch) coating applied to X-40 and was, in fact, slightly in excess of the required thickness range. The structure was very uniform with white etching, irregularly shaped particles dispersed throughout the β-CoAl matrix (Fig. 120).

After 150 hours exposure at 1800°F, loss of Al by oxidation, conversion of β to γ, and internal oxidation effects were observed (Fig. 121). Some diffusion of the Al into the substrate occured. This coating was found satisfactory for the protection of X-40 substrate and was selected for further evaluation.

Knoop Hardness Number (50-gram load)

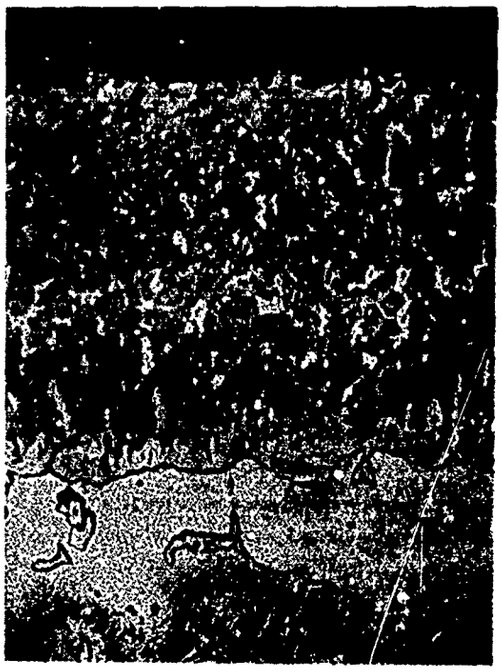

773

Specimen XA2

653

421

392

Magnification: 1000X

Magnification: 40X

FIGURE 121. MICROSTRUCTURE OF COATING A ON X-40 ALLOY AFTER HOT CORROSION TEST AT 1800° F FOR 150 HOURS

The B Coating

The B coating on X-40 consisted of β-CoAl phase with dispersed white phase (Cr-rich) and carbides. The thickness of the coating was 0.0015 inch. After 150 hours hot corrosion testing at 1800°F the coating was over 80 percent consumed and was therefore not further evaluated in detail.

The C Coating

The C coating was structurally similar to the B coating, but was only 0.0013 inch thick. After the 150-hour exposure at 1800°F Al diffusion into the substrate resulted in an increase in thickness to 0.0016 inch. There were no other significant microstructural changes. This coating, because of excessive pinholes, was not selected for further evaluation in Phase II.

The D Coating

The D coating on X-40 was below the specified minimum thickness on X-40, i.e., only 0.0011 inch. It consisted of β-CoAl matrix with carbides and chromium-rich phase (white phase) (Fig. 122). After the 150-hour exposure at 1800°F the coating was about 50 percent consumed. The remaining coating consisted mainly of β-CoAl phases with internal oxides at the interface (Fig. 123). This coating was selected for the Phase II - Mechanical Property Tests.

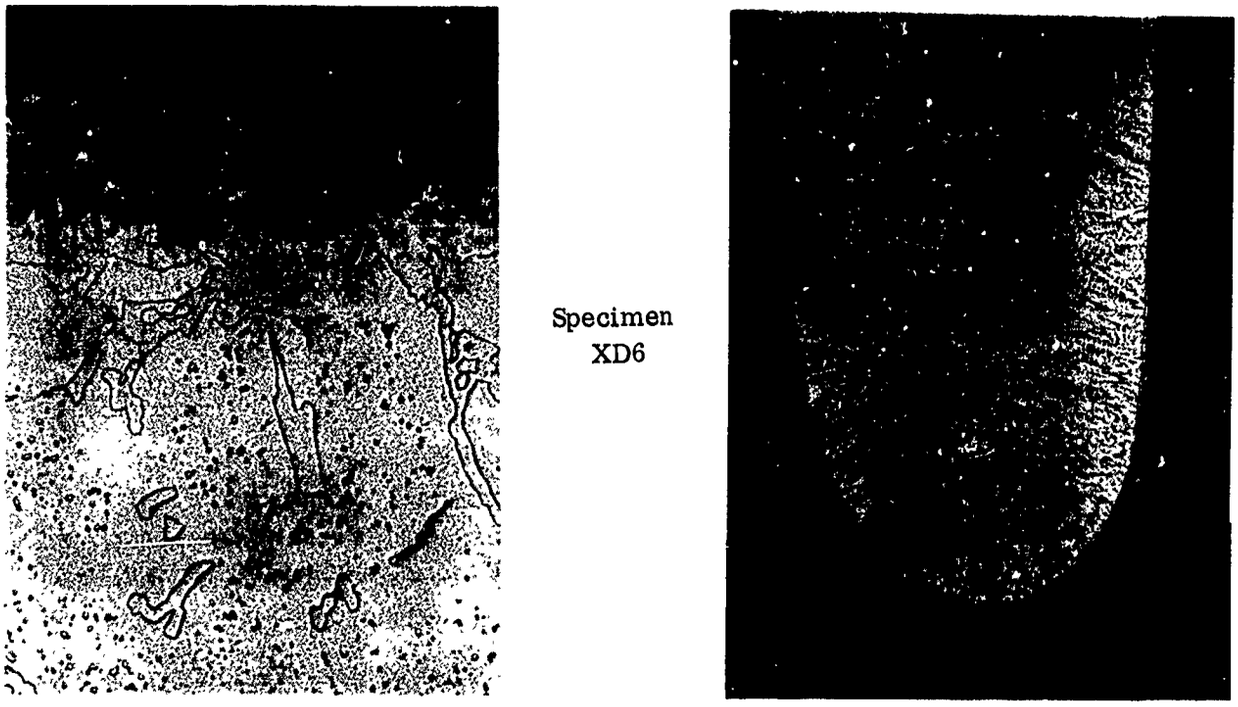

Specimen XD6

Magnification: 1000X

Magnification: 40X

FIGURE 122. MICROSTRUCTURE OF AS-RECEIVED COATINGS; Coating D on X-40 Alloy

Knoop Hardness Number (50-gram load)

499

366

375

Specimen XD2

Magnification: 1000X

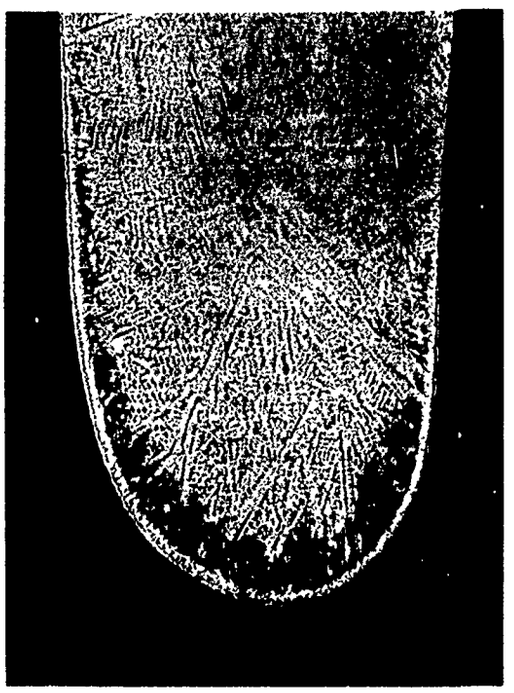

Magnification: 40X

FIGURE 123. MICROSTRUCTURE OF COATING D ON X-40 ALLOY AFTER HOT CORROSION TEST AT 1800° F FOR 150 HOURS

The H Coating

The H coating on X-40 contained a large amount of a second phase in the outer layer, which indicated codeposition or addition of elements such as Cr. Coating H was below the required thickness range and was only 0.0011 inch thick. The coating was almost entirely consumed after 150 hours exposure at 1800°F and therefore was not further evaluated.

3.13 DIAGNOSTIC EVALUATION

3.13.1 X-Ray Diffraction Analyses

X-ray diffraction analyses on coated superalloys in the as-coated and/or after hot corrosion testing were conducted to identify the type of aluminides formed and other coating phases. The X-ray diffraction analyses were conducted only for the selected coatings on nickel-base alloys.

X-ray diffraction patterns were obtained using a Norelco X-ray Diffractometer. A copper target with a nickel filter and a power level of 50 kv and 20 ma resulted in CuKα radiation ($\lambda = 1.5418$Å). The values of the Bragg angle (θ) and the relative intensity (I/Io) were obtained from the X-ray diffraction charts. Using Bragg's law ($2d \sin\theta = \lambda$), "d" values (lattice spacings) were calculated. For the identification of aluminides, the X-ray patterns of the coated superalloys were compared with the standard patterns of NiAl, Ni_3Al, $NiAl_3$, α-Al_2O_3, Cr_3Al_2, Cr_2Al, αCr, etc.

The X-ray diffraction patterns as described by Bragg angle (2θ), lattice spacings ("d" values) intensity values and the indexed phases for the different phases identified for the various alloy-coating combinations are given in Tables V through XI.

The different phases identified for the various alloy-coating combinations are:

• Coating A on Rene' 41	As-coated	βNiAl + Cr_2Al (Table XI)
• Coating A on B1900	As-coated	βNiAl + Cr_2Al (Table V)
• Coating F on SEL-15	As-coated	βNiAl + α-Al_2O_3 + αCr (Table VI)
• Coating G on Inco 713C	As-coated	βNiAl + α-Al_2O_3 + αCr (Table X)
• Coating J on Inco 713C	As-coated	βNiAl + Cr_3Al_2 + αCr (Table VII)
• Coating K on B1900	As-coated	βNiAl + Cr_3Si + Cr_3Al_2 (Table VIII)
• Coating K on B1900	After HCR testing 1650°F-120 hours	βNiAl* + α-Al_2O_3 + Cr_3Al_2 + Cr_3Si (Table IX)

All the coated specimens showed the presence of βNiAl.

* The formation of NiAl is not supported by EMP analysis.

TABLE V

X-RAY DIFFRACTION ANALYSIS OF COATING A ON B1900 ALLOYS; As-Coated Condition

2θ, degrees	"d", Å	Relative Intensity I/I_o	Indexed Phase
31.00	2.8823	10	βNiAl
42.30	2.1348	13	Cr_2Al
44.50	2.0342	100	βNiAl
55.20	1.6626	10	βNiAl
81.80	1.1764	25	βNiAl
98.30	1.0183	5	βNiAl
135.60	0.8319	10	Cr_2Al
136.00	0.8307	7	?
136.50	0.8292	5	?
Phases identified are βNiAl + Cr_2Al			

TABLE VI

X-RAY DIFFRACTION ANALYSIS OF COATING F ON SEL-15 ALLOY; As-Coated Condition

2θ, degrees	"d", Å	Relative Intensity I/I_o	Indexed Phase
25.62	3.4740	5	α-Al_2O_3
30.90	2.8914	13	βNiAl
35.20	2.5474	6	α-Al_2O_3
43.42	2.0823	6	α-Al_2O_3
44.30	2.0429	100	βNiAl + αCr
52.50	1.7415	3	α-Al_2O_3
54.90	1.6709	4	βNiAl
57.72	1.5958	3	α-Al_2O_3
64.30	1.4475	9	βNiAl + αCr
73.10	1.2934	5	βNiAl
81.40	1.1812	60	βNiAl + αCr
97.80	1.0221	20	βNiAl + αCr
114.40	0.9153	20	αCr
135.00	0.8337	5	αCr
Phases identified are βNiAl + α-Al_2O_3 + αCr			

TABLE VII

X-RAY DIFFRACTION ANALYSIS OF COATING J ON 713C ALLOY; As-Coated Condition

2θ, degrees	"d", Å	Relative Intensity I/I_o	Indexed Phases
31.02	2.8805	48	βNiAl + Cr_3Al_2
43.50	2.0786	30	Cr_3Al_2
44.50	2.0342	100	βNiAl + Cr_3Al_2 + αCr
55.40	1.6570	16	βNiAl
61.12	1.5149	8	Cr_3Al_2
64.80	1.4375	48	βNiAl + Cr_3Al + αCr
73.50	1.2874	27	βNiAl
77.30	1.2333	16	Cr_3Al_2
82.06	1.1734	88	βNiAl + Cr_3Al_2 + αCr
98.60	1.0160	20	βNiAl + αCr
115.52	0.9106	20	αCr
136.60	0.8290	12	αCr
Phases identified are βNiAl + Cr_3Al_2 + αCr			

TABLE VIII

X-RAY DIFFRACTION ANALYSIS OF COATING K
B1900 ALLOY; As-Coated Condition

2θ, degrees	"d", Å	Relative Intensity I/I_o	Indexed Phase
28.00	3.1839	17	Cr_3Si
34.46	2.6004	11	?
39.84	2.2607	11	Cr_3Si
43.60	2.0741	2	Cr_3Al_2
44.90	2.0170	100	Cr_3Si + βNiAl
49.40	1.8790	45	Cr_3Si + Cr_3Al_2
61.50	1.5065	8	Cr_3Al_2
65.10	1.4316	4	Cr_3Si + βNiAl
68.74	1.3644	6	?
72.36	1.3048	2	Cr_3Si + βNiAl
75.64	1.2562	2	Cr_3Si
79.10	1.2097	37	Cr_3Si + βNiAl
85.72	1.1324	2	Cr_3Si
89.00	1.0989	6	?
89.20	1.0970	4	?
92.30	1.0681	2	?
92.50	1.0663	4	?
95.70	1.0389	4	?
96.00	1.0365	4	?
98.98	1.0131	2	Cr_3Si + βNiAl
102.40	0.9883	17	Cr_3Si
102.60	0.9869	11	βNiAl
105.70	0.9664	1	Cr_3Si
120.20	0.8885	6	?
120.60	0.8867	4	?
124.00	0.8724	2	?
124.50	0.8704	2	?
132.50	0.8415	6	Cr_3Si
137.00	0.8278	2	?
147.80	0.8017	4	Cr_3Si
154.80	0.7893	2	?
Phases present are βNiAl, Cr_3Si and probably Cr_3Al_2			

TABLE IX

X-RAY DIFFRACTION ANALYSIS OF COATING K ON B1900 ALLOY;
After Hot Corrosion Test at 1650°F for 120 Hours

2θ, degrees	"d", Å	Relative Intensity I/I_0	Indexed Phase
25.50	3.4901	15	α-Al_2O_3
32.50	2.7526	25	βNiAl
35.10	2.5544	30	α-Al_2O_3
37.70	2.3840	5	α-Al_2O_3
39.44	2.2828	25	Cr_3Si
42.32	2.1338	75	Cr_3Al_2
43.42	2.0823	70	α-Al_2O_3 + Cr_3Al_2
44.30	2.0429	70	Cr_3Si + Cr_3Al_2
45.50	1.9918	100+	βNiAl
48.82	1.8638	75	Cr_3Si + Cr_3Al_2
53.32	1.7167	20	α-Al_2O_3
57.50	1.6014	15	α-Al_2O_3 + NiAl
61.30	1.5109	10	Cr_3Al_2
64.90	1.4355	10	βNiAl
66.50	1.4048	20	α-Al_2O_3
68.10	1.3757	20	α-Al_2O_3
75.20	1.2624	55	βNiAl + Cr_3Al_2
76.30	1.2469	20	βNiAl + Cr_3Al_2
78.54	1.2169	55	Cr_3Si + Cr_3Al_2
82.00	1.1741	55	Cr_3Al_2
86.50	1.1242	30	Cr_3Al_2
88.82	1.1007	85	βNiAl
95.20	1.0431	20	α-Al_2O_3
97.12	1.0275	30	α-Al_2O_3
98.50	1.0168	20	α-Al_2O_3
101.82	0.9924	20	βNiAl
116.00	0.9083	20	α-Al_2O_3
Phases identified are βNiAl + α-Al_2O_3 + Cr_3Al_2 + Cr_3Si			

TABLE X

X-RAY DIFFRACTION ANALYSIS OF COATING G ON 713C ALLOY; As-Coated Condition

2θ, degrees	"d", Å	Relative Intensity I/I_o	Indexed Phase
25.60	3.4767	5	α-Al_2O_3
30.92	2.8896	13	βNiAl
35.10	2.5544	3	α-Al_2O_3
36.90	2.4338	3	?
37.80	2.3779	1	α-Al_2O_3
43.32	2.0869	4	?
44.44	2.0368	100	βNiAl + αCr
52.60	1.7384	3	α-Al_2O_3
55.26	1.6609	3	βNiAl
57.52	1.6009	4	α-Al_2O_3
59.32	1.5565	1	?
61.30	1.5109	1	?
64.50	1.4435	9	βNiAl + αCr
66.50	1.4048	1	α-Al_2O_3
68.32	1.3718	3	α-Al_2O_3
73.30	1.2904	4	βNiAl
77.10	1.2360	1	α-Al_2O_3
81.80	1.1764	60	βNiAl + αCr
98.20	1.0191	11	βNiAl + αCr
115.20	0.9123	11	αCr
136.20	0.8302	7	αCr
Phases identified are βNiAl + α-Al_2O_3 + αCr			

TABLE XI

X-RAY DIFFRACTION ANALYSIS OF COATING A ON RENE' 41 ALLOY; As-Coated Condition

2θ, degrees	"d", Å	Relative Intensity I/I_o	Indexed Phases
31.00	2.8823	10	βNiAl
43.10	2.0970	20	Cr_2Al
44.38	2.0394	100	βNiAl
55.10	1.6653	10	βNiAl
64.60	1.4415	6	βNiAl
79.00	1.2109	15	Cr_2Al
81.70	1.1776	75	βNiAl
98.20	1.0191	15	βNiAl
135.50	0.8322	15	Cr_2Al
Phases identified are βNiAl + Cr_2Al			

3.13.2 Electron Microprobe Analyses of Selected Coatings

The number of combination of coatings, substrate alloys and test conditions was so great that comprehensive EMP analyses of all systems were impractical. Rather, four coating-alloy systems of significantly different microstructures were EMP analyzed in the "as-coated" and "as-tested" conditions at 1650°F. The systems selected for analysis and the basis for this selection are noted below.

- K coating on B1900 - Showed a microstructure that was not typical of β-NiAl coatings and also exhibited a hardness as-coated significantly higher than all other coatings. Hot corrosion resistance was also good.

- J coating on Inco 713C - The J coating was one of the more consistently performing coatings on nickel-base alloys, and appeared to be primarily β-NiAl, but had sufficient modification to distinguish it from the majority of the other coatings in hot corrosion resistance.

- F Coating on SEL-15 - This coating had an unusual microstructure containing an extremely stable phase near the mid-point of the β-NiAl phase. Hot corrosion resistance on this alloy was fair, only, and exhibited extreme temperature sensitivity, i.e., performance was poorer at selective low temperatures than at temperatures of 1650°F or above.

- A Coating on U-700 - The A coating similarly to the J coating performed well in HCR testing on the majority of alloys. Its structure was relatively simple, but it appeared to be applied at a high temperature from a relatively high aluminum activity source.

The electron microprobe analyses were determined using pure element standards and the Colby computer program (Ref. 5) to provide semi-quantitative results. Without alloy standards it is not possible to estimate the percentage that the electron microprobe analyses vary from absolute values. Microprobe analyses were conducted at the same location on all specimens, viz., the blade center, concave side. As shown in previous work (Ref. 3), phase compositions may be related (to a first approximation) to the binary Ni-Al equilibrium phase diagram by assuming that Co can substitute for Ni up to about 15 weight percent. Some knowledge of ternary and quaternary phase equilibria helps in understanding many of the phase separations, but, obviously, some extremely complicated diffusional processes may occur where ten or more major coating and substrate elements are present.

EMP Analysis on the K Coating on B1900 Alloy

In the as-coated condition, the single phase outer layer "A" (Fig. 124) is definitely not β-NiAl. The layer has almost twice the atomic percent silicon as aluminum. The aluminum concentration is only 6.7 percent. XRD data and EMP analyses discloses very little about the composition of the outer layer. Optically, the layer appears single-phased, but XRD indicated multiple phases (Table VIII). The presence of Cr_3Si and possibly β-NiAl are indicated; however the high concentration of silicon and nickel indicates the predominance of a silicide of nickel with substitution of Cr, Co, etc. in the $NiSi_x$ lattice. Centerline comparison of the as-coated EMP analysis with the vendor furnished analysis indicate an accuracy of ±10 percent for the majority of elements. Tantalum, chromium and molybdenum are outside these limits, however, which may be due to the location or segregation of elements or to basic errors that can be expected from the EMP results in this complex alloy system. The coating process should not have had an influence on the centerline composition of the alloy.

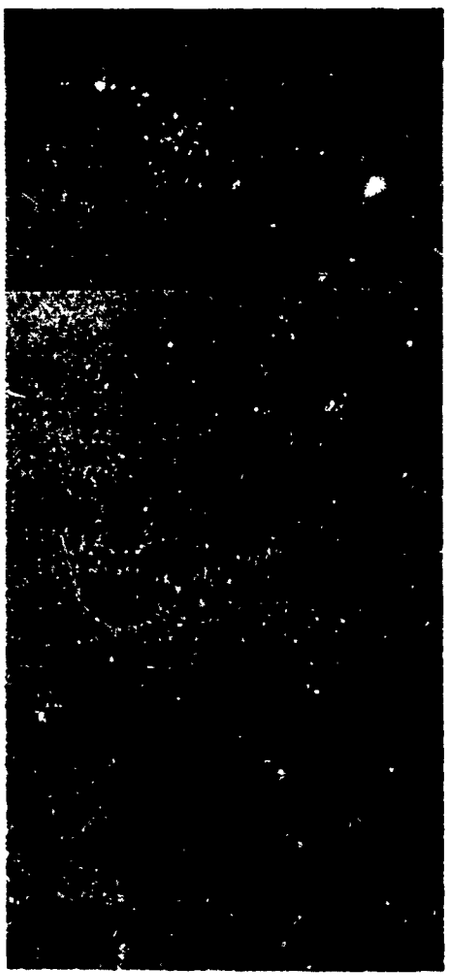

Specimen E-41

Magnification: 1000X

COMPOSITION (WT%)

	Al	Co	Cr	Si	Ti	Ni	Mo	Ta
A	6.7	4.4	2.7	12	0.2	61	0.0	0.0
B	8.0	9.3	3.0	15	0.7	43	1.9	1.2
C	12	8.2	7.6	5.1	1.4	64	7.8	4.7
℄D	6.6	8.9	6.2	0.0	1.0	62	3.8	1.0
S*	6.07	9.99	8.26	---	1.00	63.75	6.00	4.48

C = 0.081, Zr = 0.09, B = 0.010, Fe = 0.18

*S - SUBSTRATE COMPOSITION

FIGURE 124. ELECTRON MICROPROBE ANALYSES OF "K" COATING ON B1900 ALLOY IN AS-COATED CONDITION

The microstructure of EMP analysis of the K coating after 120 hours of hot corrosion rig testing at 1650°F is shown in Figure 125. The outer region of the coating retained its high silicon composition, i.e., above 11 percent, with a notable increase in nickel content indicating a high thermodynamic driving force for Ni. The aluminum concentration tended to decrease indicating an insolubility for this element in the $NiSi_x$ surface layer. Tantalum and molybdenum are present in significant quantities at point C indicating that the combination of coating application and exposure has resulted in an 0.002 inch loss per side in the original substrate cross section. The substrate centerline showed no presence of silicon.

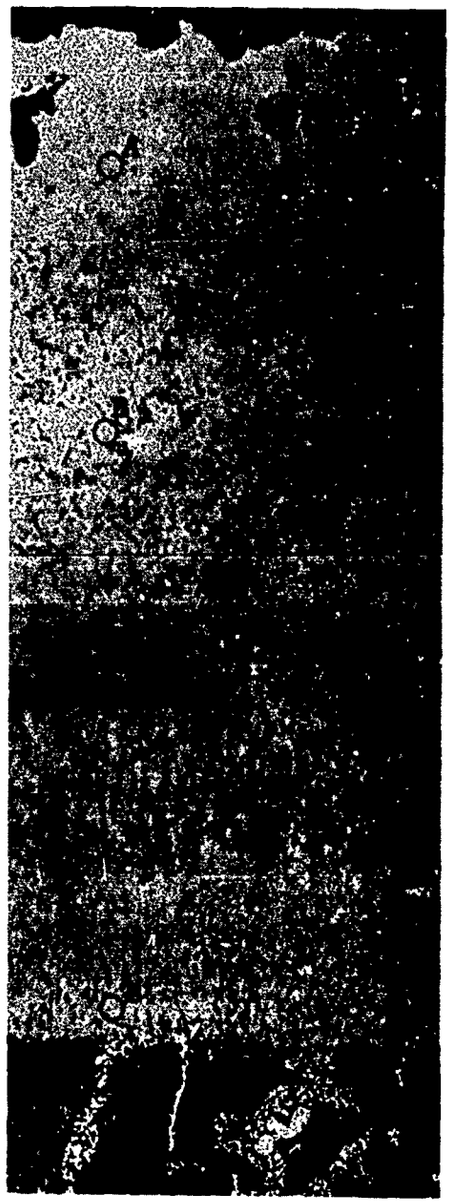

Specimen E-39

Magnification: 1000X

COMPOSITION (WT %)

	Al	Co	Cr	Si	Ti	Ni	Mo	Ta
A	1.0	8.5	1.1	13	3.0	70	0.0	0.0
B	5.8	7.5	2.3	11	0.2	67	0.5	0.0
C	3.0	8.4	9.5	6.8	0.5	43	3.6	1.6
D	7.8	8.1	13	6.4	1.3	34	6.4	4.7
E	8.7	8.3	7.5	2.6	1.3	33	6.6	6.8
F	6.1	9.6	5.4	0.0	0.8	61	4.4	0.9
S*	6.07	9.99	8.26	--	1.00	63.75	6.00	4.48
	C = 0.081, Zr = 0.09, B = 0.010, Fe = 0.18							

*S = SUBSTRATE COMPOSITION

FIGURE 125. ELECTRON MICROPROBE ANALYSES OF "K" COATING ON B1900 ALLOY AFTER HOT CORROSION TEST FOR 120 HOURS AT 1650°F

EMP Analysis on the J Coating on Inco 713C Alloy

The EMP analyses of that coating on the Inco 713C are shown in Figure 126 "as coated". EMP and microstructural appearance indicate a predominantly two-phased appearance in the A-B area. Based on the relatively high chromium concentration in these areas and the XRD results (Table VII), three phases could be present - β-NiAl, β-Ni_3Al and Cr_3Al_2; however the XRD results do not support the presence of Ni_3Al, although the microstructural appearance, particularly the surface, indicates the presence of γ'. The concentration of this phase may, however, be in a range insensitive to XRD analysis.

The microstructural appearance presents strong evidence for the predominant formation of the coating by the inward diffusion of aluminum. The linear porosity near B (Fig. 126) is undoubtedly the Kirkendall interface. Outward diffusion of nickel, as evidence by the increased concentration of Cr, Mo and sigma phase in the C-D area, is also very evident. The microstructural and EMP data indicate that the coating was probably applied in a two-step process. Initially, a high activity, thin layer of Al with perhaps a small additive of Si was applied. The coating was then diffused under low aluminum activity conditions to reduce the Al concentration below that of the single phase β-NiAl region.

After exposure for 150 hours in hot corrosion rig testing, the microstructure and EMP analysis (Fig. 127) shows that the outer layer (A in Figure 126) was probably completely consumed, but the denuded zone B to C (same figure) was very resistant to attack. The excellent performance of this coating would indicate that a trace of silicon and a relatively low aluminum content were more significant in resisting hot corrosion than a high aluminum single phase β-NiAl coating. The high chromium content in the coating may also be significant since XRD data (Table VII) indicates the coating to be above the saturation limit in this element. The area A-B after test, formerly believed to be the denuded zone, shows a finely dispersed phase, rich in chromium, which must have precipitated upon the cyclic exposure.

The interface zone, after testing. point D, showed a large drop in aluminum content and a major γ' formation in addition to significant carbide and sigma phase precipitate. Growth of sigma phase platelets are in evidence at the substrate, adjacent to the coating-substrate interface.

EMP Analysis on the F Coating on SEL-15

The distinctive feature of the F coating is the irregular but relatively continuous line running through the center of the coating. This line is too thin in width for an accurace analysis, but EMP analysis at point C indicates that it is high in titanium. The location of this line of inclusions, believed to be deposited before

Specimen CJ3

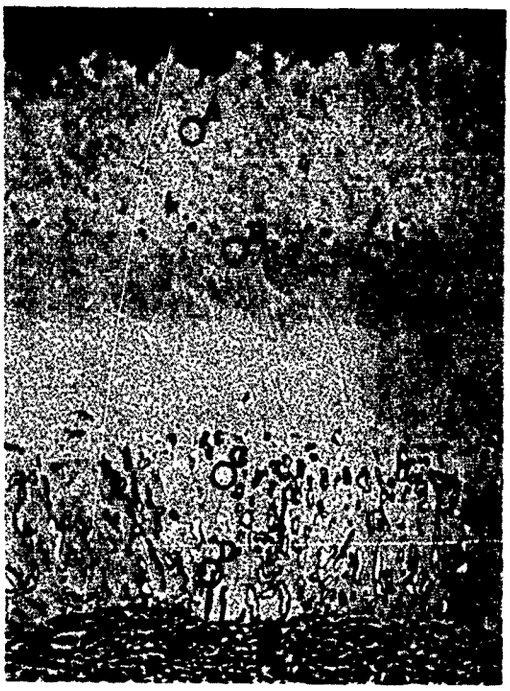

Magnification: 1000X

Composition (wt %)

	Al	Si	Ti	Cr	Co	Ni	Mo
A	20	0.5	0.2	6.9	0.3	63	0.8
B	18	0.4	0.3	6.3	0.1	67	1.4
C	15	0.1	0.5	26	0.1	57	6.3
D	12	0.1	0.9	17	0.1	60	4.5
E	5.0	0.1	0.1	14	0.3	74	3.7
S*	5.85	--	0.78	13.80	0.22	---	4.55
	Cb = 2.27, C = 0.135, Zr = 0.10, B = 0.007						

*S - Substrate Composition

FIGURE 126. MICROPROBE ANALYSES OF AS-RECEIVED COATING - COATING J ON INCO 713C ALLOY

Specimen CJ5

Magnification: 1000X

Composition (wt %)

	Al	Si	Ti	Cr	Co	Ni	Mo
A	15	0.3	0.5	5.6	0.2	74	0.2
B	11	0.1	0.3	5.6	0.2	51	12
C	10	0.2	0.8	16	0.2	60	4.0
D	6.6	0.1	1.4	14	0.2	72	2.8
E	5.3	0.1	0.8	15	0.2	73	2.4
S*	5.85	--	0.78	13.80	0.22	--	4.55
	Cb = 2.27, C = 0.135, Zr = 0.10, B = 0.007						

*S - Substrate Composition

FIGURE 127. ELECTRON MICROPROBE ANALYSES OF J COATING ON INCO 713C AFTER HOT CORROSION RIG TESTING AT 1650°F FOR 150 HOURS

aluminizing, is probably the Kirkendall interface. The high titanium content throughout the coating, without a proportional drop in the Ti content of the substrate indicates some codeposition of Ti with the aluminum. Basically, the outer layer of this coating is predominantly β-NiAl with the concentration of Al well within the β range. Between points C and F, the composition appears to be primarily γ' but with significant quantities of sigma fingers and carbides. The light-colored phase (points E and F) is not believed to be different in composition or structure than the adjacent gray layer.

The tested specimens, Figure 129, show no significant chemical changes from the as-coated specimen, which is due to the short time of exposure at 1650°F. The surface does, however, show roughening and apparent penetration at the inclusions. These inclusions can also be seen in the as-coated specimen, Figure 128.

EMP Analysis of the A Coating on Udimet 700

The EMP analysis of the A coating on Udimet 700 (Fig. 130) supports very strongly the XRD analysis of the A coating on Rene' 41, i.e., that the coating is predominantly β-NiAl with small quantities of Cr_2Al. Large sigma fingers are present at the coating-substrate interface, undoubtedly due to the high initial chromium content of the substrate and to the increased concentration resulting from the outward diffusion of nickel and cobalt.

After exposure of the A coated U-700 alloy to the hot corrosion rig testing environment for 150 hours, the EMP analysis and microstructure are shown in Figure 131. The aluminum concentration dropped by a full 10 percent, and approximately 50 percent of the coating was consumed. A major unidentified phase precipitated in the outer layer of the coating, area A. Chromium was concentrated at the interface during test. Phase D, for example, contained 54 percent chromium. Also resulting from this high concentration of chromium was extensive formation of sigma phase within the substrate below the coating interface.

3.14 DISCUSSION OF TEST RESULTS

3.14.1 Coatings on Nickel-Base Alloys

Coating A was evaluated on all of the program nickel-base superalloys. The thickness of coating A was 0.0019 inch for Rene' 41 to 0.0045 inch for U-700 and about 0.0030 inch for the remaining nickel-base alloys. The weight gain for coating A was 3.3 mg/cm^2 for Rene' 41 and between 6.5 to 8 mg/cm^2 for the other nickel-base alloys. For all the program nickel-base alloys the coating was found to consist of βNiAl + Cr_2Al (white phase) in the outer area, mainly βNiAl in the denuded zone and βNiAl, γ' Ni_3Al, carbides and finger-like sigma phase in the diffusion zone. At the diffusion zone/substrate interface, a continuous dark band of γ solid solution had

Specimen SF6

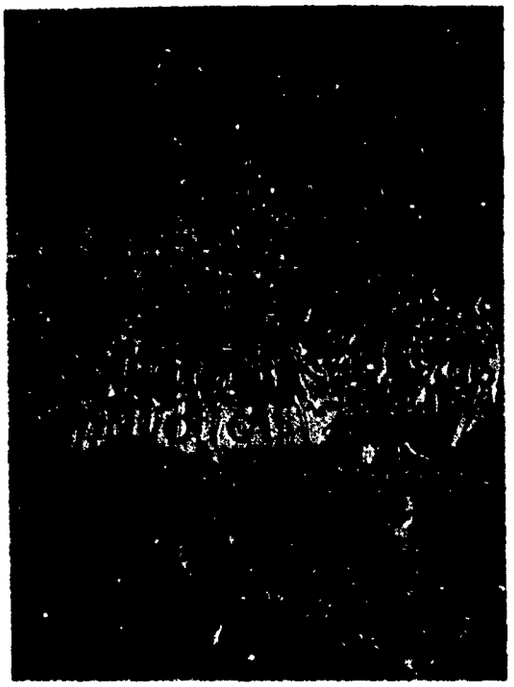

Magnification: 1000X

Composition (wt %)

	Al	Si	Ti	Cr	Co	Ni	W
A	31	0.1	2.4	1.1	4.3	39	0.1
B	24	0.1	3.7	0.9	13	56	0.1
C	12	0.2	7.5	3.8	11	46	1.7
D	10	0.3	3.3	17	13	48	2.3
E	5.5	0.1	4.9	10	12	58	1.5
F	6.5	0.4	5.1	10	13	56	1.4
G	4.9	0.3	2.1	11	14	60	1.4
S*	5.51	--	2.18	10.70	13.70	--	1.90
	Cb = 0.45, C = 0.057, Zr = 0.10, B = 0.014, Fe = 0.15, Mo = 6.18						

*S - Substrate Composition

FIGURE 128. ELECTRON MICROPROBE ANALYSES OF AS-RECEIVED COATING - COATING F ON SEL-15 ALLOY

Specimen SF2

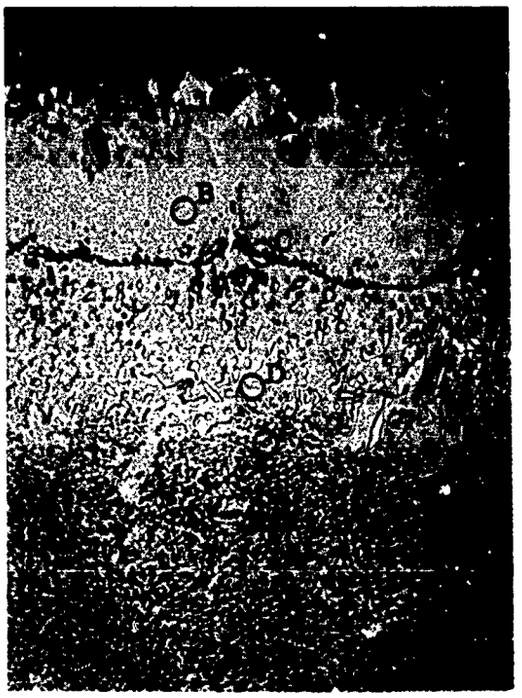

Magnification: 1000X

Composition (wt %)

	Al	Si	Ti	Cr	Co	Ni	W	Mo
A	32	0.2	3.6	0.5	5.4	53	0.0	0.0
B	18	0.2	5.3	2.7	11	50	0.0	0.1
C	18	0.2	11	4.2	9.2	43	0.3	1.3
D	14	0.1	3.3	7.2	11	48	1.4	8.3
E	5.5	0.1	4.4	9.3	13	55	0.8	3.7
℄ F	4.6	0.1	2.1	8.6	13	50	1.5	4.3
S*	5.51	--	2.18	10.70	13.70	--	1.90	6.18
	Cb = 0.45, C = 0.057, Zr = 0.10, B = 0.014, Fe = 0.15							

FIGURE 129. ELECTRON MICROPROBE ANALYSES OF F COATING ON SEL-15 AFTER HOT CORROSION TEST AT 1650°F FOR 30 HOURS

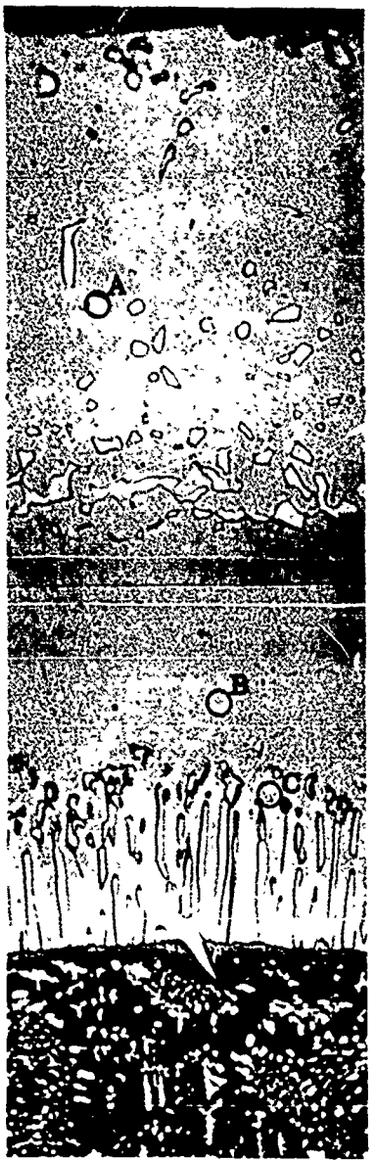

Specimen UA1

Magnification: 1000X

Composition (wt %)

	Al	Si	Ti	Cr	Cc	Ni	Mo
A	27	0.0	1.0	27.	8.8	41	4.0
B	27	0.0	1.3	2.4	12	54	0.0
C	14	0.1	5.4	16	13	47	0.7
GL D	3.8	0.1	4.6	15	14	59	2.2
S*	4.25	--	3.42	14.30	14.90	58.90	4.10
	C = 0.06, B = 0.020, Fe = 0.10						

*S - Substrate Composition

FIGURE 130. ELECTRON MICROPROBE ANALYSES OF AS-RECEIVED COATING - COATING A ON U-700 ALLOY

Specimen UA2

Magnification: 1000X

Composition (wt %)

	Al	Si	Ti	Cr	Co	Ni	Mo
A	20	0.2	0.2	9.2	13	56	0.5
B	17	0.1	0.6	7.1	13	60	0.5
C	12	0.1	1.1	14	15	54	1.7
D	0.2	0.1	0.6	54	4.6	21	13
E	7.2	0.1	1.7	10	12	59	1.8
℄ F	4.0	0.1	1.4	12	16	63	5.9
S*	4.25	--	3.42	14.30	14.90	58.90	4.10
	C = 0.060, B = 0.020, Fe = 0.10						

*S - Substrate Composition

FIGURE 131. ELECTRON MICROPROBE ANALYSES OF A COATING ON U-700 AFTER HOT CORROSION RIG TESTING AT 1650°F FOR 150 HOURS

developed for the different alloys. This γ band was quite pronounced for IN-100 and SEL-15 alloys. Coating A on Rene' 41 was found to contain some large geometrically shaped particles which were Cr or Mo rich.

Effective protection was provided by the A coating during HCR testing for the test duration of 150 hours on all program alloys except B1900 at 1650°F (60 hours), Inco 713C (90 hours), IN-100 (120 hours), and U-700 (120 hours) at 1800°F. After HCR testing, the thickness of A coating on various substrate alloys increased except for U-700 at 1650°F and at 1800°F for B1900, Rene' 41 and U-700, indicating diffusion instability (Fig. 132). The diffusion instability of the A coating was more severe than

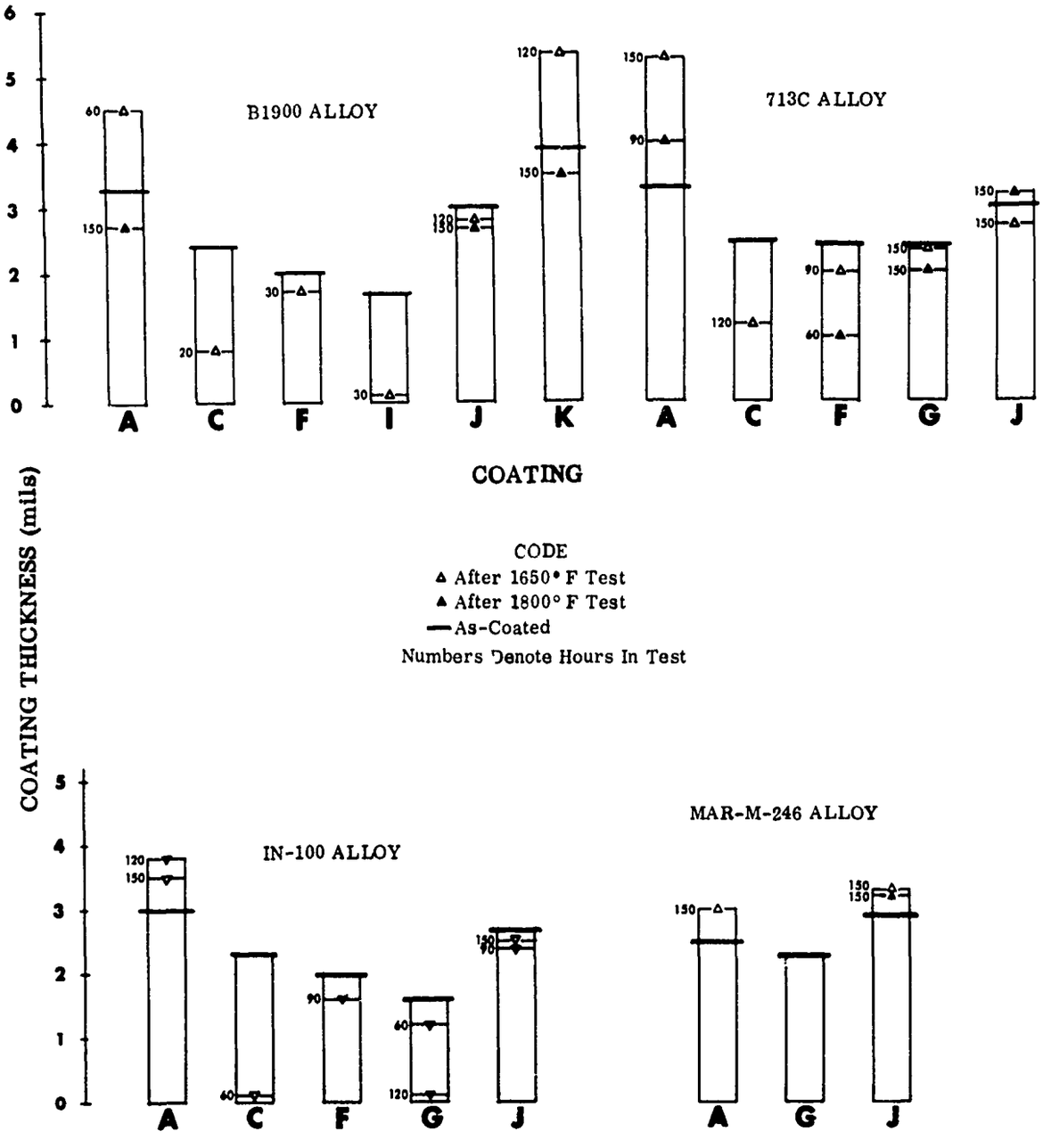

FIGURE 132. COMPARISON OF COATING THICKNESS BEFORE AND AFTER HOT CORROSION TESTING; Nickel-Base Alloys (Sheet 1 of 2)

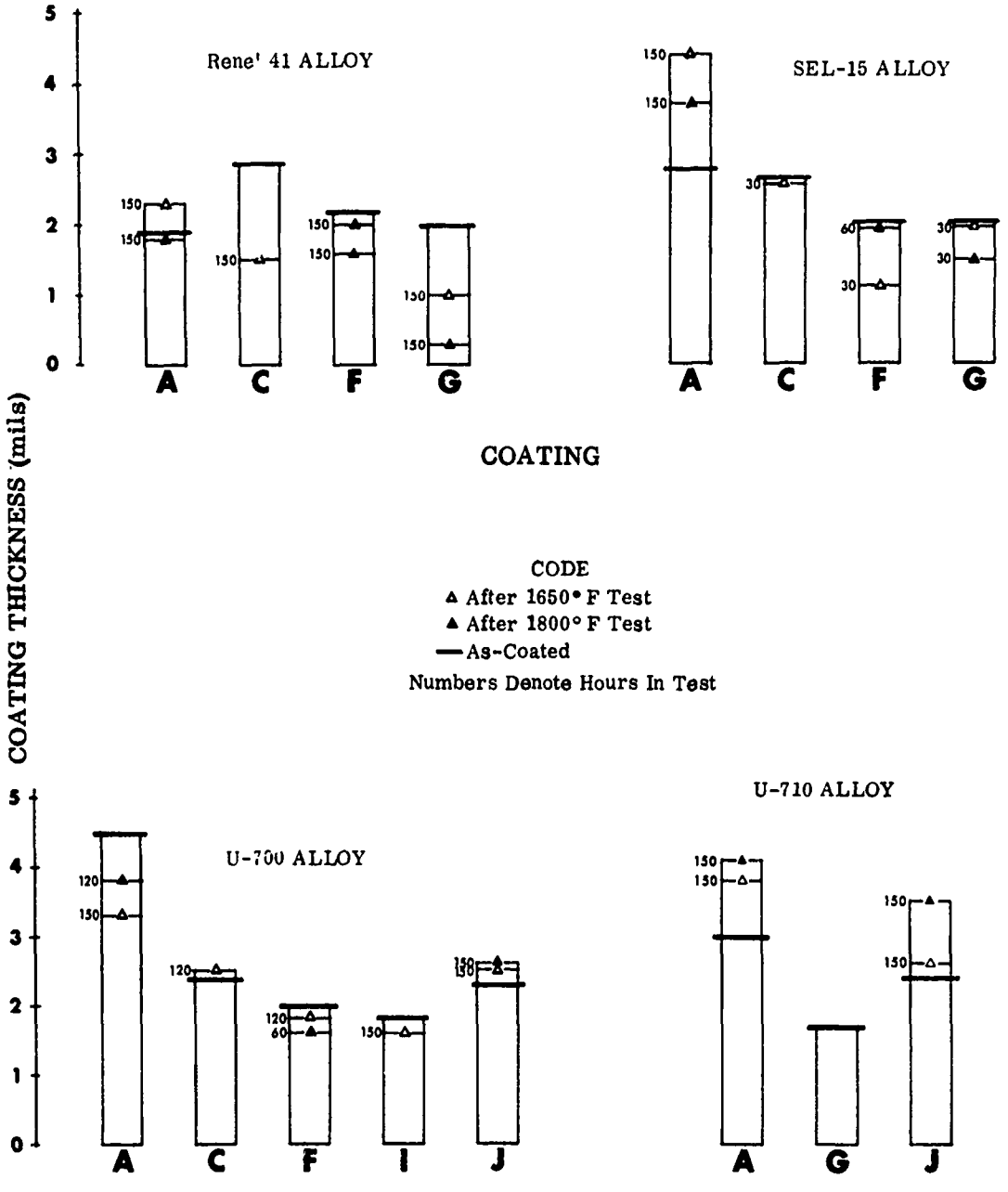

FIGURE 132. COMPARISON OF COATING THICKNESS BEFORE AND AFTER HOT CORROSION TESTING; Nickel-Base Alloys (Sheet 2 of 2)

with the other coatings evaluated in the program. The diffusion instability is the main drawback of this coating.

During HCR testing at 1650°F there was, in general, a weight gain -- the maximum weight gain being about 15 mg/specimen. During HCR testing at 1800°F there was weight gain up to 90 hours in the case of B1900, IN-100 and U-700, and up to 60 hours for Inco 713C. After this time there was a sudden decrease in weight gain indicating coating spalling or failure. The 1800°F HCR testing resulted in increasing weight gain for Rene' 41, SEL-15, U-710 and MAR-M-246, up to the test duration of 150 hours. With coating A on various substrates, numerous pinhole type failures occurred.

After 1650°F HCR testing there was a decrease in hardness of the coating due to loss of Al by oxidation or by Al diffusion into the substrate. In the outer zone and in the diffusion zone, βNiAl was partially transformed to $\gamma'Ni_3Al$. The finger-like sigma phase observed in the as-coated condition partially transformed into the carbides. At the interface, the continuous dark band of γ was transformed into $\gamma'Ni_3Al$ with detectable sigma phase platelets. At the higher exposure temperature of 1800°F, general attack on the coating was more severe based on decrease in coating thickness. Considerable carbide dissolution occurred in the outer area of the coating. Other microstructural changes were similar, but more pronounced than those after the 1650°F HCR exposure, e.g., the sigma phase platelets at the interface of A-coated Inco 713C specimen were observed only after the 90-hour exposure at 1800°F, but not after the 150-hour exposure at 1650°F.

The performance of the A coating in HCR testing at 1650°F and 1800°F, as evaluated by weight change, appearance and metallographic examination, was quite satisfactory. The A coating was selected for Phase II - Mechanical Properties Testing on seven of the ten substrate alloys, viz., Rene' 41, SEL-15, IN-100, U-700, U-710, MAR-M-246, and X-40. The performance of the A coating was surpassed mainly by the J coating on various substrate alloys and also by the K coating on B1900 and by the G coating on Inco 713C. Overall, the A coating was second only to the J coating.

The C coating was evaluated on all program nickel- and cobalt-base superalloys. The thickness of the C coating was between 0.0023 inch and 0.0029 inch and the weight gain was in the range of 7.2 to 8.1 mg/cm^2 for the six nickel-base alloys. Microstructure of the C coating consisted of βNiAl (major phase) with a very fine dispersion of chromium-rich phase. Carbides were present in the diffusion zone and fine acicular sigma phase precipitated at the interface. On Rene' 41 the diffusion zone had a more strongly defined columnar structure composed of alternating bands of sigma and γ' phases; whereas on SEL-15, light etching irregularly shaped dispersions, rather than the columnar structure, were observed in the diffusion zone. The

chromium content of the substrate alloy was largely responsible for observed variations in the phase morphology in the diffusion zone.

The performance of the C coating was best on Rene' 41 as compared to that on other program nickel-base alloys in the HCR testing at both 1650°F and 1800°F. This is most likely due to the higher Cr content (19.2%) of Rene' 41 and the greater thickness of the C coating on Rene' 41 (0.0029 inch). The C coating provided protection for the test duration of 150 hours for Rene' 41, only, at both 1650°F and 1800°F. The greater the Cr content of the substrate alloy the longer the life obtainable from the C coating.

The C coating on various substrates was found to spall off during HCR testing. Coating spalling or pinhole type failures were the main disadvantages of the C coating. The coating was consumed during HCR testing, as is evident from a decrease in coating thickness (Fig. 132) and from weight loss rather than weight gain, the only exception being the C coating on Rene' 41. With the C coating on Rene' 41 there was weight gain instead of weight loss after 150 hours of HCR testing at 1650°F and 1800°F.

After HCR testing at 1650°F most of the βNiAl phase was converted to $\gamma'$$Ni_3Al$. The diffusion zone consisted mostly of γ' with remnants of β, carbide precipitates and internal oxides. Platelets of sigma phase were present at the interface. After HCR testing at 1800°F the above microstructural changes were more pronounced. The performance of the C coating was poor and suffered from spalling, pinhole failures and short life. The C coating was not selected for the Phase II mechanical properties testing for any of the program nickel-base alloys. This coating, however, was found to be the best coating for protection of the cobalt-base alloy, WI-52, as will be discussed in Section 3.14.2.

The F coating was evaluated on six of the nickel-base alloys. The thickness of the F coating was in the range of 0.0020 inch to 0.0024 inch and the weight gain was between 4.8 and 5.8 mg/cm^2. The F coating was found to consist of βNiAl + large α-Al_2O_3 inclusions and α-Cr precipitates in the outer zone, a line of titanium-rich precipitates near the center of the coating and βNiAl, carbides and lamellar sigma phase oriented perpendicular to the base-metal interface in the diffusion zone. The interface phase was $\gamma'$$Ni_3Al$. In the case of Inco 713C the presence of a hard, white phase, most likely Ni_2Al_3, was present at the surface of the F coating, indicating a high Al activity during the application cycle. As was the case with the C coating on Rene' 41, the F coating on Rene' 41 and U-700 had a strongly defined columnar structure in the diffusion zone composed of alternating bands of sigma and γ' phases.

The performance of the F coating on various substrate alloys was slightly better than that of the C coating. In many respects the performance of the F coating was analogous to that of the C coating. The F coating, like the C coating, provided life of 150 hours (test duration) in the HCR tests at both 1650°F and 1800°F for Rene' 41 only (highest Cr content alloy - 19.2% Cr).

Numerous pinhole type failures occurred with the F coating on various substrate alloys. Coating spalling was also observed in some cases. The HCR testing resulted in loss of Al as Al_2O_3, decrease in thickness or consumption of the coating (Fig. 132), and weight loss in several cases. Weight gain occurred only with the F coating on Inco 713C and Rene' 41 during HCR test at 1650°F and with the coating on IN-100, Rene' 41 (loss after 110 hours), and on SEL-15 during HCR test at 1800°F.

After the HCR test at 1650°F the outer area of the coating was oxidized and spalled off. The addition of large α-Al_2O_3 inclusions did not appear to be beneficial and the heterogeneous TiO_2-Al_2O_3 oxide layer probably caused coating spalling. After HCR testing at 1650°F the outer zone appeared to consist mainly of βNiAl, free from carbide, oxide inclusions or chromium-rich precipitates. The HCR testing at 1800°F usually resulted in coating consumption of over 60 percent. The remaining coating consisted of γ' matrix, β phase, carbides and sigma phase platelets.

The F coating was recommended for inclusion in Phase II Mechanical Property Testing for SEL-15 alloy only. The hot corrosion resistance of the F coating, under the program test conditions, on other superalloys except Rene' 41 was poor and only slightly better than that of the C coating.

The G coating was evaluated on six nickel-base alloys, viz., Inco 713C, U-710, MAR-M-246, IN-100, Rene' 41 and SEL-15. The thickness of the G coating was in the range of 0.0016 inch to 0.0023 inch and was slightly less than the thickness of the F coating.

The outer area of the coating consisted of βNiAl + large α-Al_2O_3 inclusions and α-Cr precipitates. The diffusion zone consisted of βNiAl matrix, γ' phase, carbides and sigma phase. At the interface, the predominant phase was γ' with σ phase platelets. The structure of the G coating was similar to that of the F coating except that the line of titanium-rich precipitates in the F coating was not present in the G coating. The α-Al_2O_3 inclusions were larger in the G coating than in the F coating.

The G coating protected Inco 713C and Rene' 41 for the test duration of 150 hours in HCR testing at both 1650°F and 1800°F and also SEL-15 for 150 hours in the 1800°F HCR test. The performance of the G coating was comparable or slightly better than that of the F coating. Pitting or pinhole failure or coating spalling were observed in the specimens after HCR testing. There was, in general, a decrease in coating thickness after the HCR test exposure (Fig. 132). There was gain in weight with the G coating on Inco 713C, Rene' 41 and U-710 after 150 hours of HCR testing at both 1650°F and 1800°F. With the G coating on IN-100, SEL-15, and MAR-M-246 alloys there was weight loss during the HCR testing at 1650°F. The better performance of the G coating on the Inco 713C and Rene' 41 substrates than on IN-100 and SEL-15 is probably due to higher Cr content of these alloys.

There were no significant changes in microstructure of the G coating on Inco 713C after 150 hours of HCR testing at 1650°F. Loss of Al as Al_2O_3, or by diffusion, resulted in reduced hardness of the coating. After testing at 1800°F for 150 hours, partial transformation of βNiAl to $\gamma'Ni_3Al$ and precipitation of carbides from the σ phase in the diffusion zone occurred. After the 1650°F HCR testing on Rene' 41, IN-100 and SEL-15, conversion of βNiAl to γ' in the outer zone was quite pronounced. The coating thickness was decreased as shown in Figure 132. The 1800°F HCR testing of the G coating on IN-100, Rene' 41, U-710 and MAR-M-246 alloys resulted in complete failure at the T_{max} area.

The G coating was selected for Phase II Mechanical Property Testing for Inco 713C and Rene' 41 alloys only. It is interesting to note that on the Inco 713C alloy the thin (0.0022 inch) G coating performed better than the thick A coating (0.0033 inch).

The I coating was evaluated only on B1900 and U-700 alloys. The thickness of the I coating was 0.0018 inch and was below the specified range of coating thickness for the nickel-base superalloys. The weight gain for the I coating on B1900 and U-700 was 3.8 and 6.1 mg/cm^2, respectively. The coating most likely consisted of βNiAl matrix, refractory metal-rich precipitates and some partially dissolved carbides. There was a tendency to form γ' phase at the interface.

The I coating on B1900 failed after 30 hours of HCR testing at 1650°F. The performance of the I coating on U-700 was much better than that on B1900, providing 150 hours protection during 1650°F HCR testing and 60 hours during 1800°F HCR testing. The I coating was not selected for inclusion in mechanical property testing on U-700 or B1900 alloys in Phase II.

The J coating was evaluated on six of the eight nickel-base superalloys, viz., B1900, Inco 713C, IN-100, U-700. U-710 ard MAR-M-246 and was found to be the best coating for protecting five of these substrates in a hot corrosion environment at 1650°F and 1800°F. The thickness of the J coating for different substrates was in the range of 0.0023 inch to 0.0030 inch. The weight gain was 5.4 to 6.9 mg/cm^2. The coating was found to consist of βNiAl, Cr_3Al_2, α-Cr and carbides in the outer area, mainly βNiAl in the denuded zone and βNiAl, $\gamma'Ni_3Al$ carbides and sigma phase in the diffusion zone. Remnants of the grain boundary carbides from the original substrate were observed in the βMAl matrix all the way out to the surface of the coating.

The J coating was found to afford protection during the HCR testing for the test duration of 150 hours to the different substrates except to B1900 at 1650°F (120 hours) and to IN-100 at 1800°F (90 hours). There was weight gain with the J coating on the different substrates up to 150 hours of HCR testing except on B1900 at 1650°F for 120 hours and on IN-100 after 90 hours exposure at 1800°F. After hot corrosion testing there were no major changes in the thickness of the J coating indicating diffusion stability.

After the 1650°F HCR testing, there was loss of Al as Al_2O_3 resulting in decreased hardness of the coating. The coating consisted of βNiAl matrix, chromium-rich precipitates and α-Al_2O_3 particles in the outer zone, βNiAl mainly in the denuded zone and a complex layer consisting of βNiAl matrix, $\gamma'Ni_3Al$, carbides and finger-like sigma phase in the diffusion zone. Sigma phase platelets had formed in γ' matrix at the interface except for Inco 713C alloy. The microstructural changes after HCR testing at 1800°F were similar to those after the 1650°F test. The main difference was that the finger-like sigma phase in the diffusion zone had transformed to carbides after 150 hours exposure at 1800°F. Failures were of the pinhole type.

The J coating was selected for further evaluation in Phase II on six nickel-base alloys. The performance of the J coating was excellent. This coating was the most stable of those tested from the point of view of diffusion.

The J coating is considered the best coating for protecting nickel-base alloys in a hot corrosion environment. The overall order of preference for the different coatings for the nickel-base alloys is as follows:

- First Choice — J Coating
- Second Choice — A Coating
- Third Choice — G Coating
- Fourth Choice — F Coating
- Fifth Choice — I Coating
- Poorest — C Coating

Coating K was not included in the above overall rating because it was applied to the B1900 alloy only.

The order for nickel-base alloys for ease of protection is as follows:

- U-710
- U-700
- Rene' 41
- Inco 713C
- MAR-M-246
- IN-100
- SEL-15
- B1900

The B1900 alloy with the lowest Cr content (8.2%) proved to be the most difficult alloy to protect.

The K Coating was evaluated only on the B1900 alloy and was the thickest (0.0039 inch) of the six coatings on B1900 alloy. This coating was found to have a high silicon content. The phases Cr_3Si and Cr_3Al_2 in a $NiSi_x$ matrix were found to be present in the outer area of the coating. The silicides in the coating resulted in increased hardness of the outer zone (1020 to 1315 KHN) and of the diffusion zone (1075 KHN). The coating had the highest hardness of all coatings evaluated in the program. After 120 hours exposure at 1650°F the coating increased in thickness to 0.0054 inch, indicating diffusion instability (Figure 132). The coating, however, provided protection for the test duration of 150 hours in HCR testing at 1800°F. Coating spalling occurred in the coating after HCR testing. This coating was included for further evaluation in Phase II - Mechanical Property Tests on the B1900 alloy only.

3.14.2 Coating on Cobalt-Base Alloys

The aluminide coatings on the two cobalt-base alloys in the as-coated condition were found to consist of βCoAl, carbides from the substrate, and a chromium-rich, white phase. All five coatings on WI-52 alloy showed the presence of interface oxides or voids. The interface oxides or voids were not present in the coatings on X-40 alloy. The coatings were within the required range of coating thickness (0.0015 inch to 0.0025 inch) except for coating C on X-40 (0.0013 inch thick) and coatings D and H on WI-52 and X-40 (0.0011 inch thick) (Fig. 133). The thickness and average weight gain for the coatings on WI-52 alloy were greater than those for the coatings on X-40 alloy except for the thickness of coating A on WI-52 alloy (0.0022 inch), and on X-40 alloy (0.0025 inch), and for the weight gain for H coating on WI-52 alloy (3.1 mg/cm^2) and on X-40 alloy (3.6 mg/cm^2) (Fig. 133 and Table IV). The weight gain for the aluminide coatings on WI-52 and X-40 alloys varied in the range of 2 to 7 mg/cm^2. These weight gain and thickness values were somewhat lower than the coatings on the nickel-base alloys.

All coatings protected the WI-52 and X-40 alloys for the test duration of 150 hours during HCR testing at T_{max} of 1800°F. The effects of the 150-hour exposure at 1800°F consisted mainly in loss of Al by oxidation to Al_2O_3, limited Al diffusion into the substrate, partial conversion of βCoAl to γCo and internal oxidation and pinhole failures. Coatings C and B on WI-52 alloy and coatings A and D on X-40 alloy exhibited best overall performance. The coatings D and H on WI-52 alloy and coatings B and H on X-40 alloy were over 80 percent consumed as a result of the 150-hour HCR testing at 1800°F. Coating A on WI-52 alloy and coating C on X-40 alloy were found to spall off, especially at the trailing edge. Coatings B and C on WI-52 alloy and coatings A and C on X-40 alloy were found to be increased in

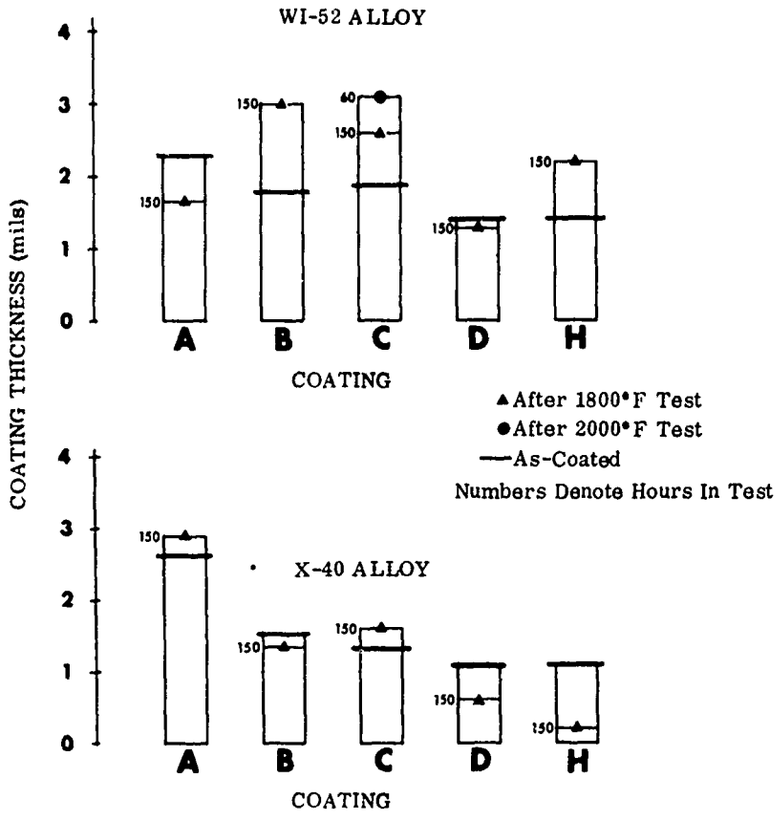

FIGURE 133. COMPARISON OF COATING THICKNESS BEFORE AND AFTER HOT CORROSION TESTING; Cobalt-Base Alloys

thickness after HCR testing at 1800°F for 150 hours (Fig. 133) because of Al diffusion into the substrate. The maximum weight gain was about 20 mg/specimen for the coated WI-52 and X-40 alloys after testing at 180°F for 150 hours. There was, in general, an increase in weight gain with increasing exposure time up to about 120-130 hours except for the H coating on WI-52 alloy. After this time there was a decrease in weight gain, indicating that the life of these coatings was about 150 hours under the program test conditions.

The HCR testing at T_{max} of 2000°F proved to be too severe on the coated cobalt-base alloys. Only coating A on X-40 alloy lasted about 100 hours. All of the other coatings failed in a relatively short period of 50 hours, or less. The increased severity of aluminide oxidation in the presence of sea salt is undoubtedly responsible for the short coating life at 2000°F. Even without sea salt ingestion, coated cobalt-base alloys have less than 200 hours life at 2050°F (Ref. 3).

3.15 SELECTION OF THE TWO BEST COATINGS PER ALLOY

Selection of the two best coatings for each substrate alloy was based on their performance in HCR testing. Weight change, appearance and metallographic examination were used as a base for selection. In order of preference, the coatings and the two best selected coatings for each program alloy are given in Table XII. In selecting the two coatings, more emphasis was placed on the performance of the coatings in HCR tests at 1650°F than at 1800°F for nickel-base alloys and on 1800°F tests rather than 2000°F for cobalt-base alloys.

TABLE XII

RANKING OF COATINGS IN HOT CORROSION TESTS

Alloy	Temp. (F)	Best	2nd	3rd	4th	5th	6th	Selection of Two Best Coatings For Phase II
B1900	1650	J	K	A	I	F	C	J and K
	1800	J	A	K	I	F	C	
713C	1650	J	G	A	C	F	-	J and G
	1800	J	G	A	C	F	-	
IN-100	1650	J	A	F	G	C	-	J and A
	1800	G	J	A	F	C	-	
Rene' 41	1650	A	G	F	C	-	-	A and G
	1800	A	C	G	F	-	-	
SEL-15	1650	A	F	C	G	-	-	A and F
	1800	A	G	F	C	-	-	
U-700	1650	J	A	I	F	C	-	J and A
	1800	J	A	I	F	C	-	
U-710	1650	A	J	G	-	-	-	A and J
	1800	A	J	G	-	-	-	
MAR-M-246	1650	J	A	G	-	-	-	J and A
	1800	J	A	G	-	-	-	
WI-52	1800	C	B	D	A	H	-	C and B
	2000	D	B	C	A	H	-	
X-40	1800	D	A	H	C	B	-	A and D
	2000	A	D	B	C	H	-	

Coating selection based on visual examination of specimens after test, weight change during test, and metallographic examination of tested specimens.

4

PHASE II - MECHANICAL PROPERTIES OF SELECTED COATINGS

The function of any protective coating is the preservation of the properties of the substrate. Retention of properties is particularly critical in a gas turbine engine, especially in the highly stressed blades. A coating completely inhibiting oxidation or sulfidation of the substrate is inadequate if it extensively interdiffuses with the substrate and changes the microstructure or mechanical properties. The importance of recoat or repair capability also cannot be overemphasized. High component cost or limited coating life under severe operating conditions makes recoating capability mandatory. Logistic problems also will require that this recoating be performed at facilities other than the engine manufacturers - perhaps at a Naval repair facility. It is an important area where progress is needed in the repair of turbine engines. However, recoating procedures have not yet been established for nickel-base alloy turbine blades. Also, the influence of long term service exposure on the metallurgical properties of coated turbine hardware has not been extensively evaluated.

This phase of the evaluation program was established to determine the ability of selected coating vendors to recoat exposed stress rupture bars and to evaluate the effect of exposure and recoating on the stress rupture properties.

The two coatings selected for each alloy were also subjected to fatigue testing to determine the effects of the coating and/or processing conditions and high temperature exposures on the low-cycle fatigue life of the alloys; specific details of the tests are discussed in subsequent paragraphs.

The Phase II test program was divided into four separate tasks. These tasks were:

- Task I - Mechanical Fatigue Tests
- Task II - Stress Rupture Tests
- Task III - Diagnostic Tests
- Task IV - Final Coating Selection and Characterization

4.1 TEST SPECIMENS

The standard R3 tensile (or stress rupture) bar with a 0.250 inch diameter reduced test section (per Federal Test Standard 151A, Method 211.1) was selected for the stress rupture tests. This bar was cast to size by Misco Division of Howmet Corporation for all alloys except the Rene' 41 and U-700.

The wrought Rene' 41 and Udimet 700 alloys for stress-rupture and fatigue test specimens were obtained from Allvac, Monroe, North Carolina, and Special Metals Corporation, New Hartford, New York, respectively. Specimens of Rene' 41 and U-700 alloys required for the stress-rupture and fatigue tests in this phase were machined from 1/2 inch and 5/8 inch diameter wrought bar stock (WBS).

The Rene' 41 WBS was received in the solution annealed condition (1975°F, 1 hour, water quenched). Machining and thread grinding operations required for making the test bars for stress-rupture and fatigue test specimens were performed at Solar in this metallurgical condition. Following machining, the Rene' 41 specimens were aged at 1650°F for 4 hours in argon and air cooled. The Udimet 700 WBS alloy was received in the as-produced condition, i.e., no heat treatment after extruding. The alloy was solution annealed (2150°F, 4 hours, air cooled) followed by preliminary aging (1975°F, 4 hours, air cooled) prior to machining at Solar. After machining and thread grinding to produce test bars for stress-rupture and fatigue testing, the Udimet 700 alloy specimens were subjected to the stabilization and final aging treatments, i.e., 1550°F, 24 hours, air cooled; and 1400°F, 16 hours, air cooled. All heat treatments were performed in an argon atmosphere.

Initially, all the cast and wrought bar stock fatigue test specimens had the standard 0.250 inch diameter test section. The ratio of the cross-sectional area of the thread root section to the test section was 2 to 1. This ratio consequently proved to be inadequate as many of the low-cycle fatigue test failures occurred at the root of the 1/2-13 threads rather than the 0.250 inch diameter test section. The effect of this sharp notch at the thread root was essentially eliminated by reducing the diameter of the test section of all fatigue specimens to 0.185 inch. The area ratio between thread root and specimen test section was thereby increased to over 4 to 1.

Prior to testing, the reduced section of all specimens was carefully polished to remove all scratches, machining marks, discontinuities, and surface oxidation products. The surface finish after polishing was less than 10 microinches (rms) for the uncoated specimens and less than 25 microinches (rms) for the coated specimens.

4.2 TASK I - LOW-CYCLE FATIGUE TESTS

There are numerous mechanical fatigue test methods currently being used to evaluate turbine materials. Considering the complex fatigue modes existing in a high-performance gas turbine engine, the wide variety of test methods is understandable. However, the conditions that result in the highest stresses are usually low cycle in nature. For turbine blades, excluding thermal stresses, the low cycle, alternating tensile stresses resulting from centrifugal forces due to turbine rotation are the most intense. Nozzle vanes are not as highly stressed as blades, but do see cyclical stresses caused by gas bending loads and thermal expansion under restraint during transient engine operation. The cyclic stresses, with the exception of blade vibrations, are low frequency in nature and depend to a large extent on the mission requirements of the engine. Extensive fatigue testing for all conditions was beyond the scope of the program; however, an evaluation of the 20 coating-alloy systems (two coatings per alloy) to withstand low cycle mechanical stresses appeared to be most meaningful to determine the influence of the coatings, coating processes, and high temperature exposures.

4.2.1 Test Procedures

The fatigue tests were performed using a tension-tension test. The MTS closed-loop electrohydraulic fatigue testing machine shown in Figure 134 was used. This unit has capabilities of producing test frequencies ranging from 0.001 to 100 cps with sine, square, triangular, and ramp wave load programs available. The sine wave load program was used throughout the program. All tests were run at a constant stress ratio of 0.15 ($R = \sigma_{min}/\sigma_{max}$) at a frequency of 20 cycles per second.

The flow chart of the fatigue test program is shown in Figure 135. As shown in Figure 135, the tests were performed in such a manner that the effects of exposure in an oxidizing environment were assessed, as well as the ability of the coatings to provide protection to the alloys for a minimum of 500 hours. Duplicate specimens of all uncoated alloys and the 20 coating-alloy combinations were tested as follows:

- The stress for failure in 5,000 to 50,000 cycles was established at 1400°F in an oxidizing environment.

- Coated and uncoated specimens of each alloy were subjected to furnace exposure for 500 hours at the following temperatures:

  Nickel-base alloys - 1800°F
  Cobalt-base alloys - 2000°F
  (Uncoated alloys were exposed in an inert environment and the coated alloys in air.)

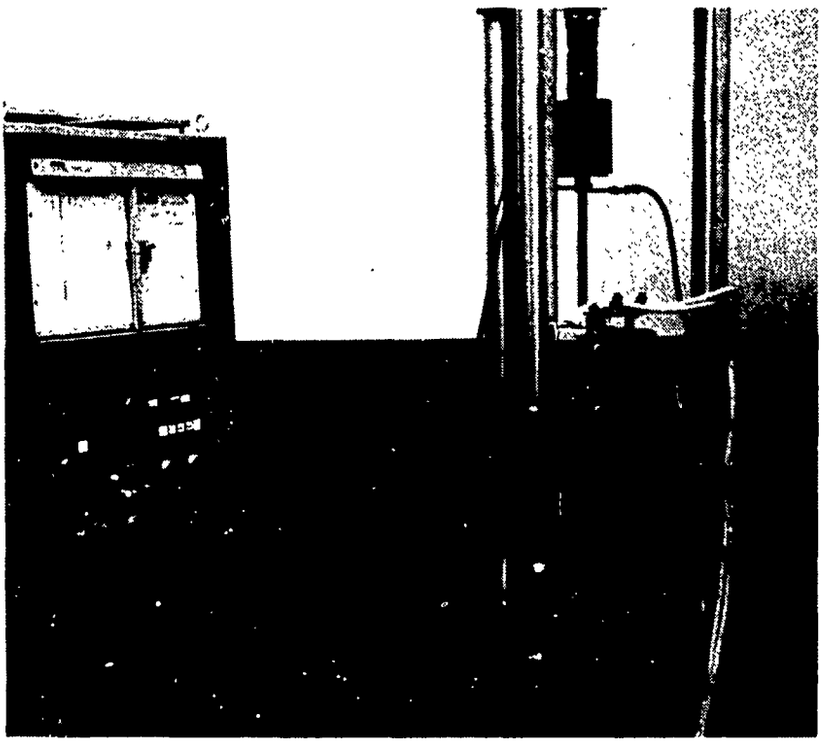

FIGURE 134. MECHANICAL FATIGUE TEST APPARATUS

- Following the furnace exposures, specimens were fatigue tested to failure at 1400°F.

- The test stresses were calculated based on original cross-sectional areas of the bars measured before coating, and also on the unaffected cross-sectional areas of the coated specimens after the high temperature exposures.

The 1400°F temperature was selected because many of the nickel-base alloys experienced a ductility minimum in the 1200 to 1600°F temperature range. Thus, the combination of a hard, brittle coating and a substrate of minimum ductility would be expected to exhibit the maximum interaction in this temperature range. Any notches formed by the craze cracking of the coating can be expected to markedly affect the low cycle fatigue life.

4.2.2 Test Results

Curves of stress versus cycles to failure are presented in Figures 136 through 145 for the uncoated and the coated alloys. The test data are summarized and contained in the tables in Appendix III.

Text Continued on Page 192.

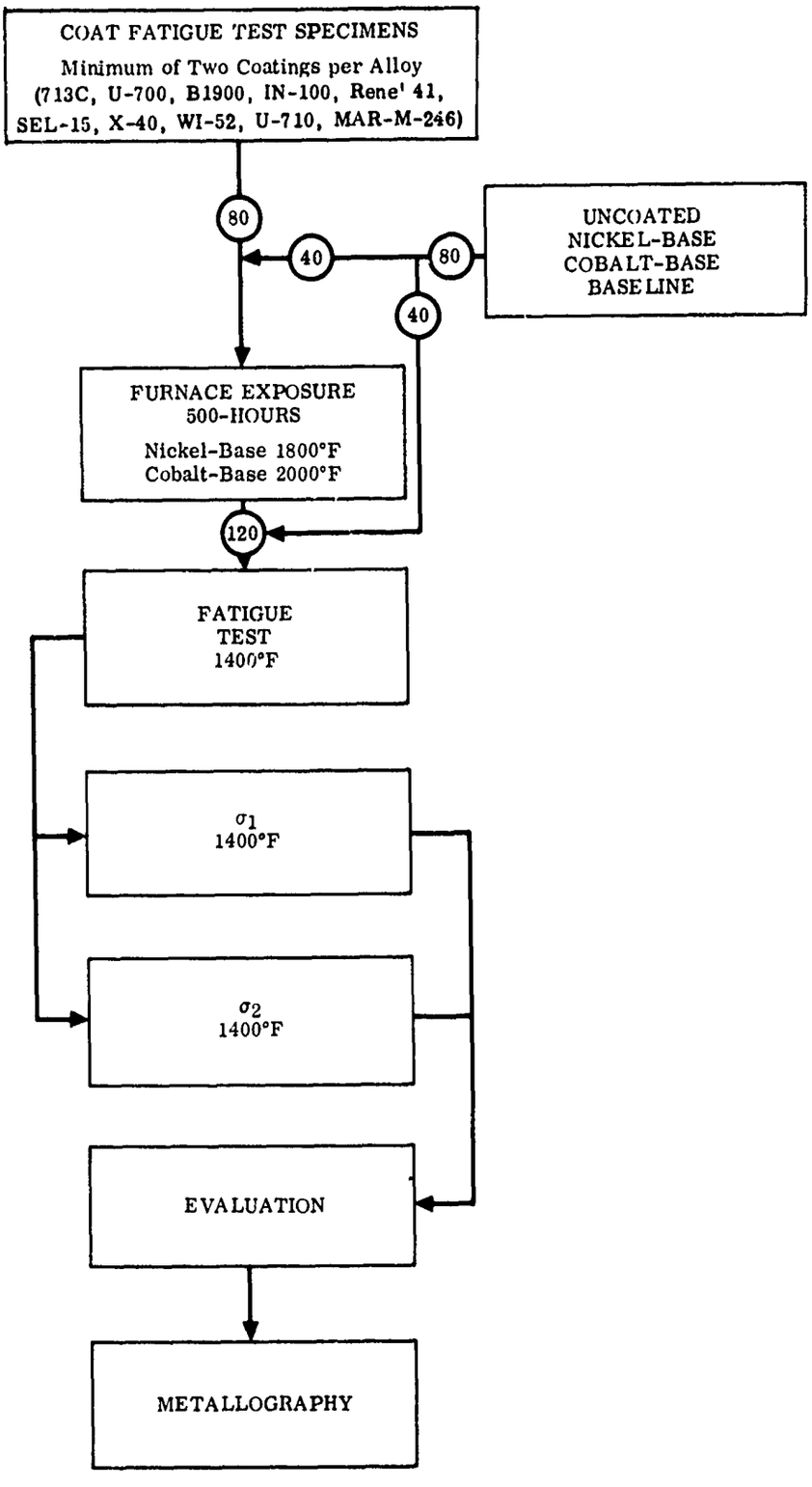

FIGURE 135. FLOW CHART OF PHASE II LOW-CYCLE FATIGUE TESTS

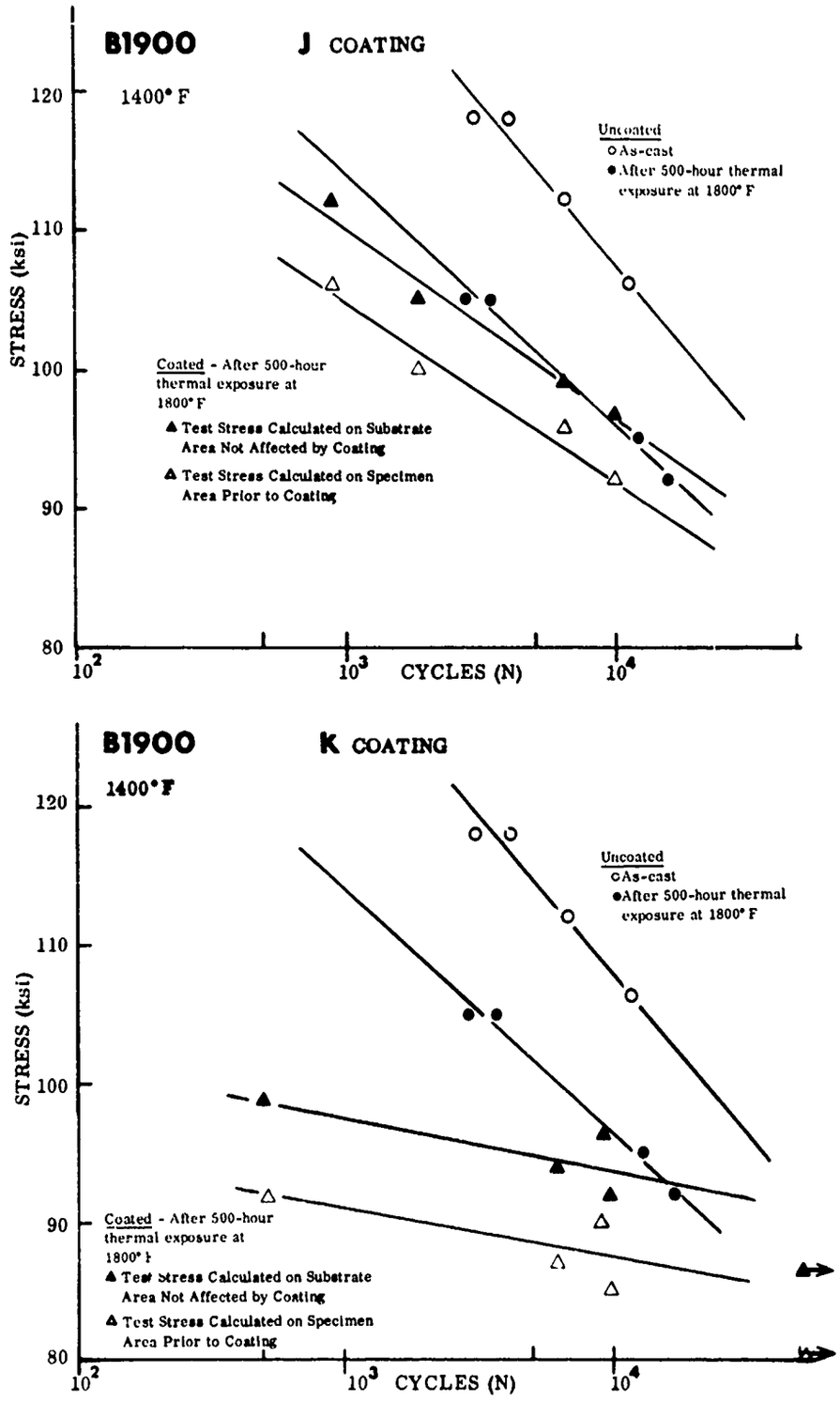

FIGURE 136. LOW-CYCLE FATIGUE LIFE OF B1900 ALLOY AT 1400°F

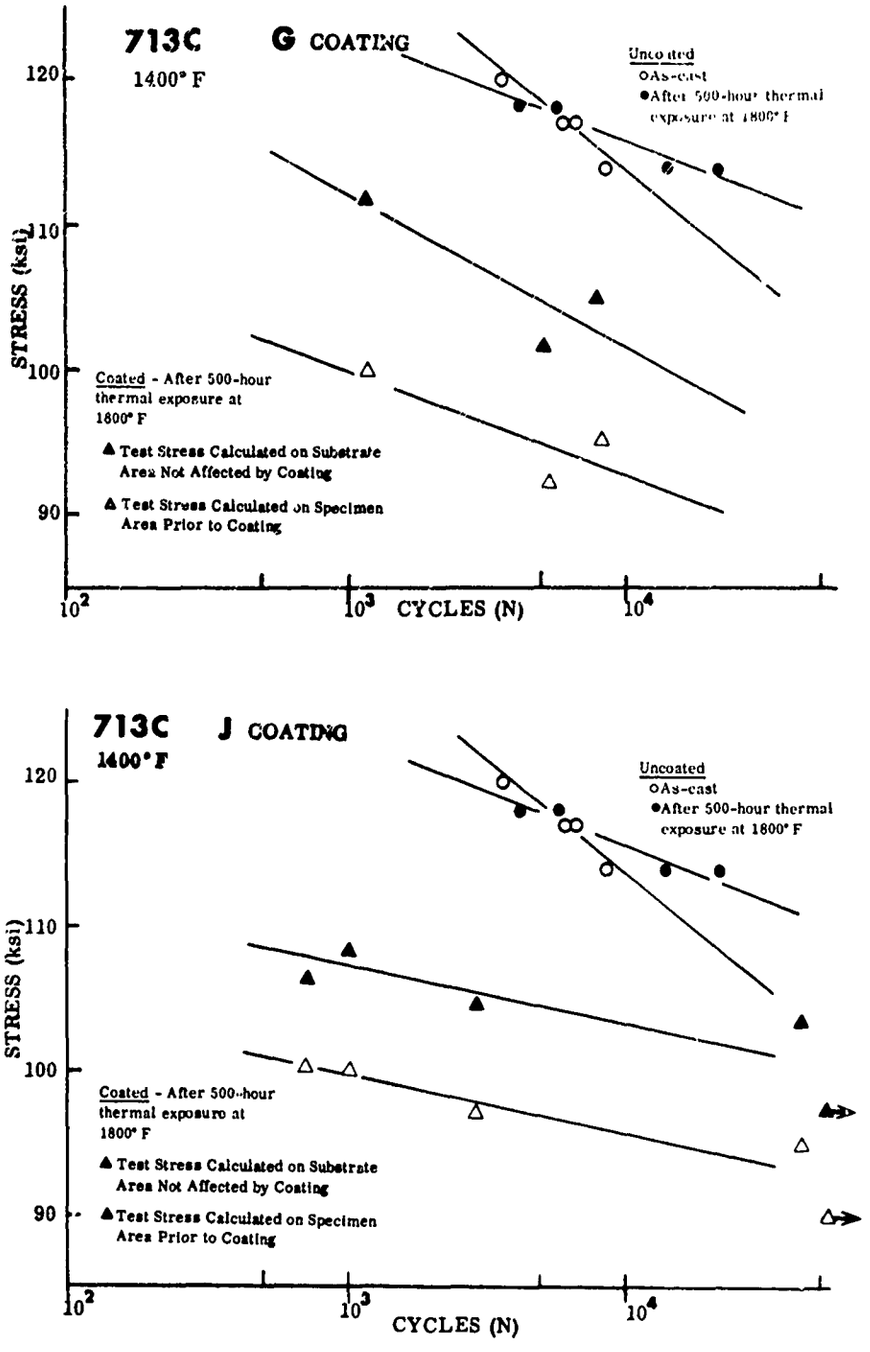

FIGURE 137. LOW-CYCLE FATIGUE LIFE OF 713C ALLOY AT 1400°F

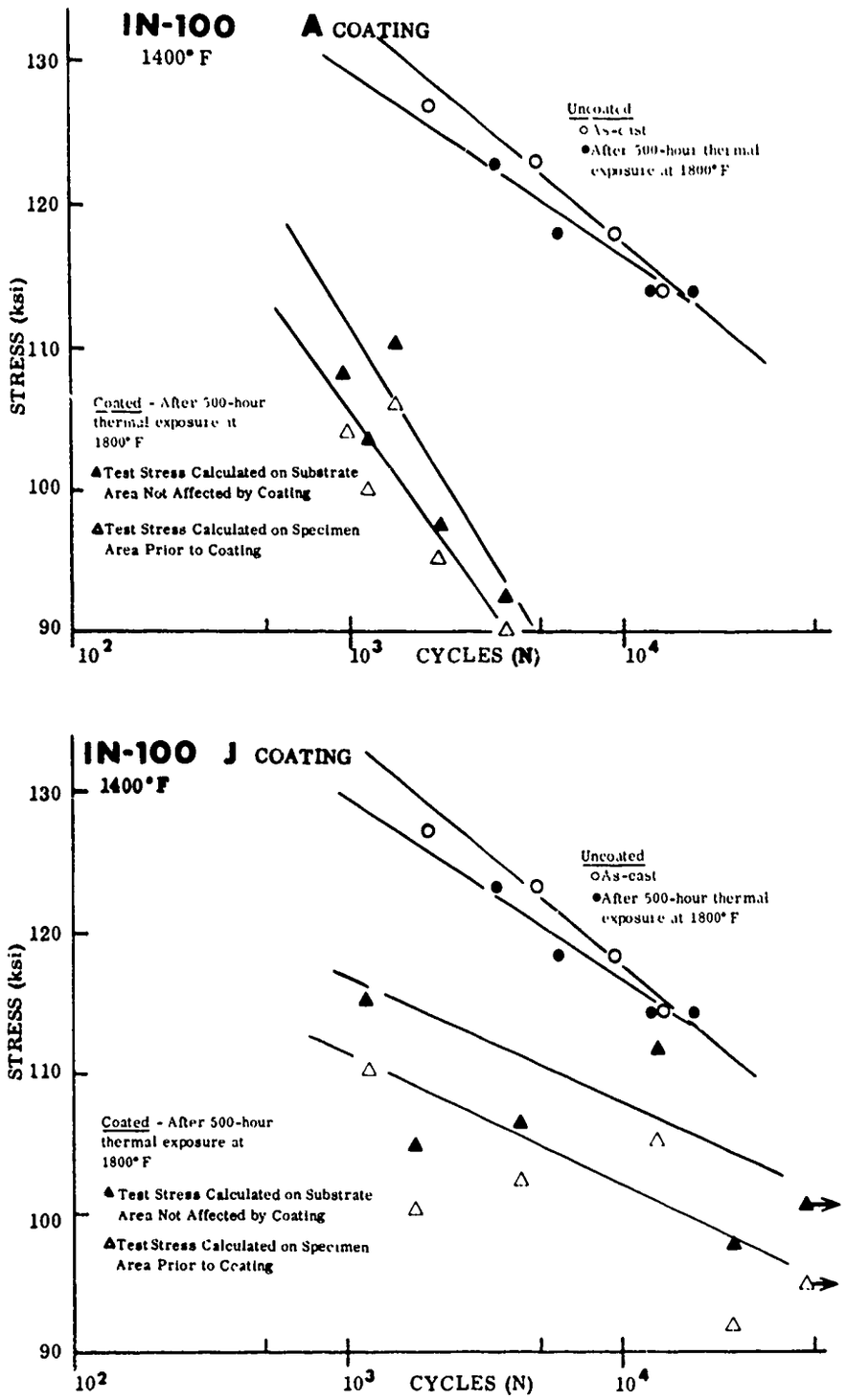

FIGURE 138. LOW-CYCLE FATIGUE LIFE OF IN-100 ALLOY AT 1400°F

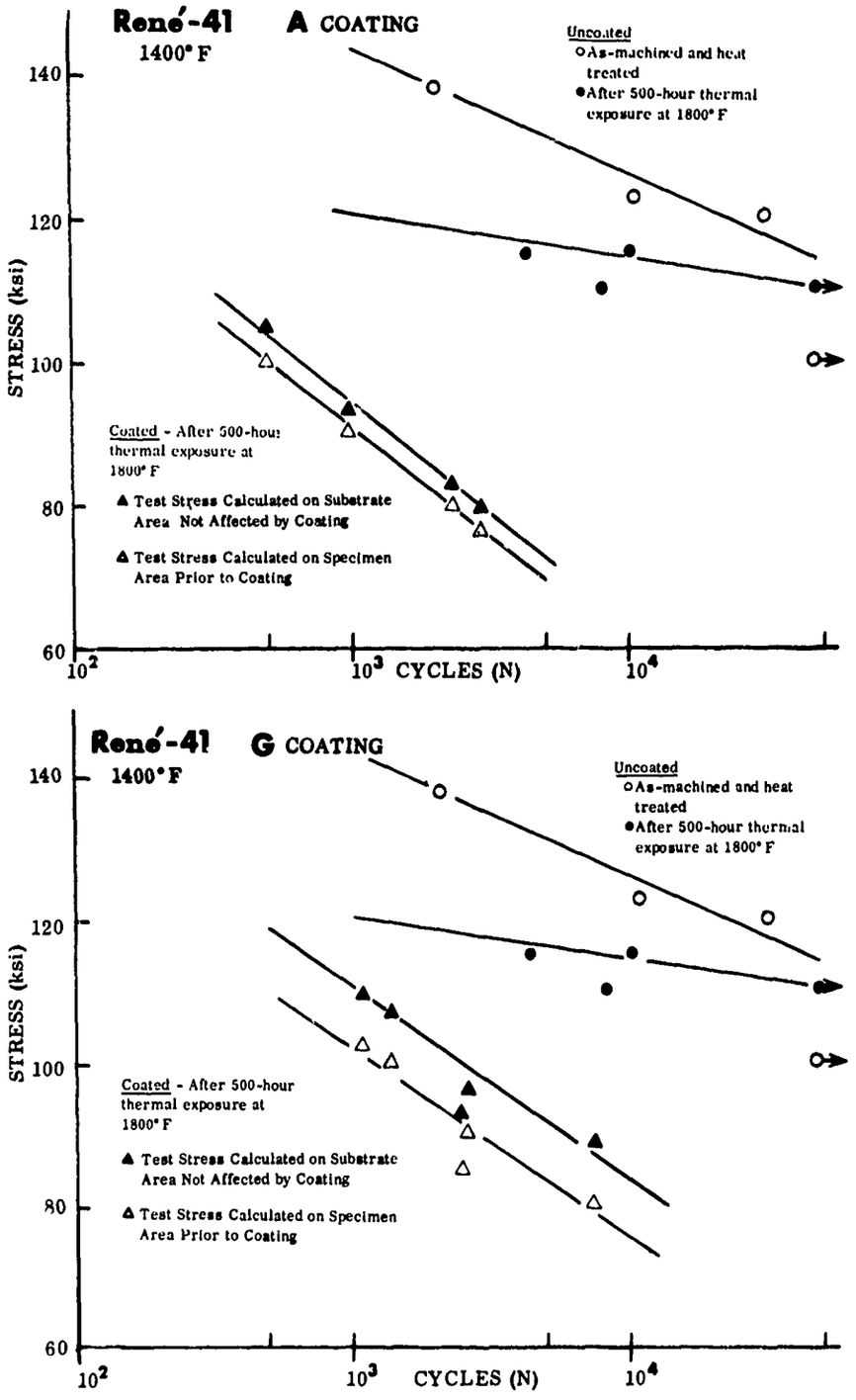

FIGURE 139. LOW-CYCLE FATIGUE LIFE OF RENE' 41 ALLOY AT 1400°F

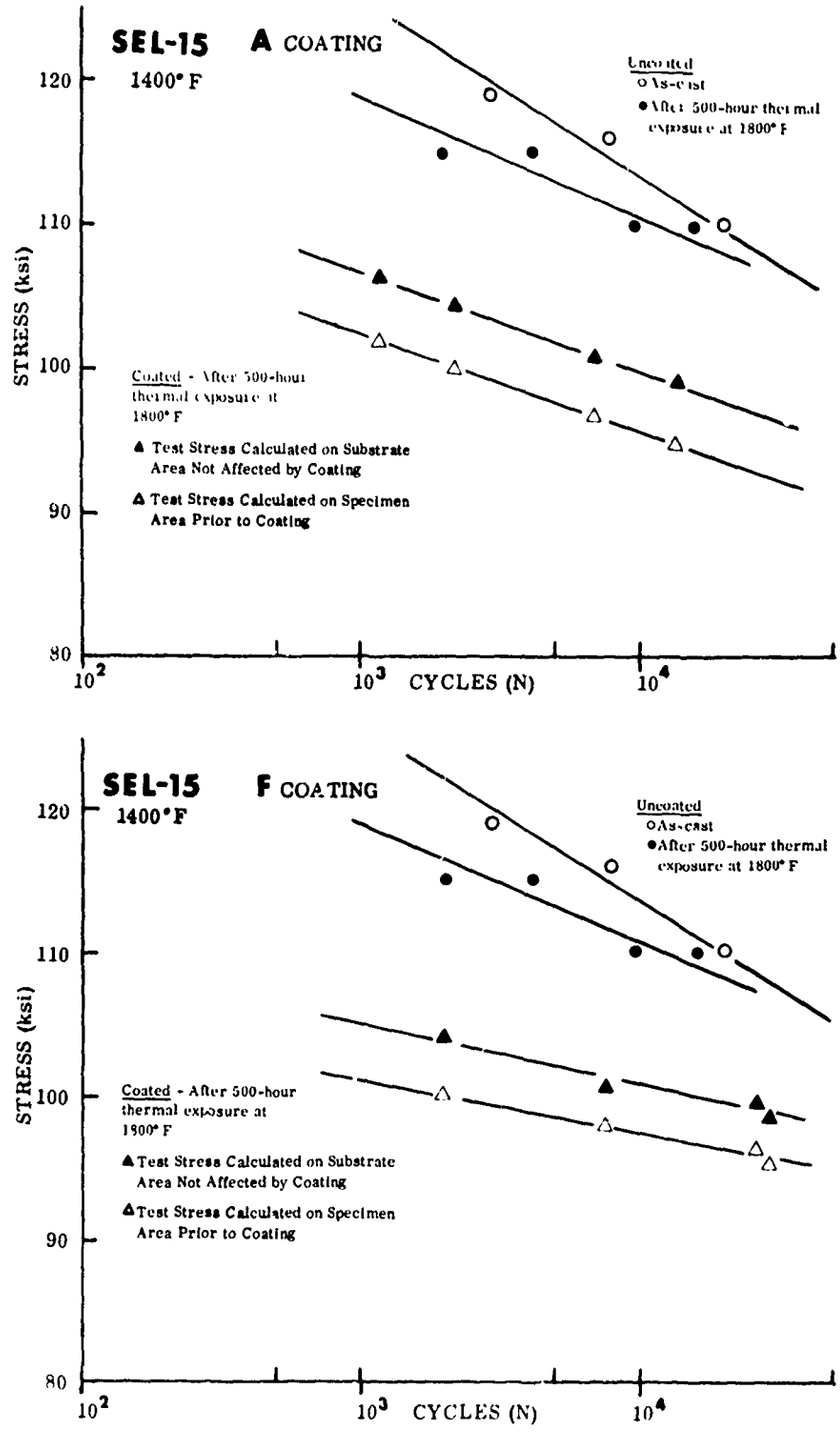

FIGURE 140. LOW-CYCLE FATIGUE LIFE OF SEL-15 ALLOY AT 1400°F

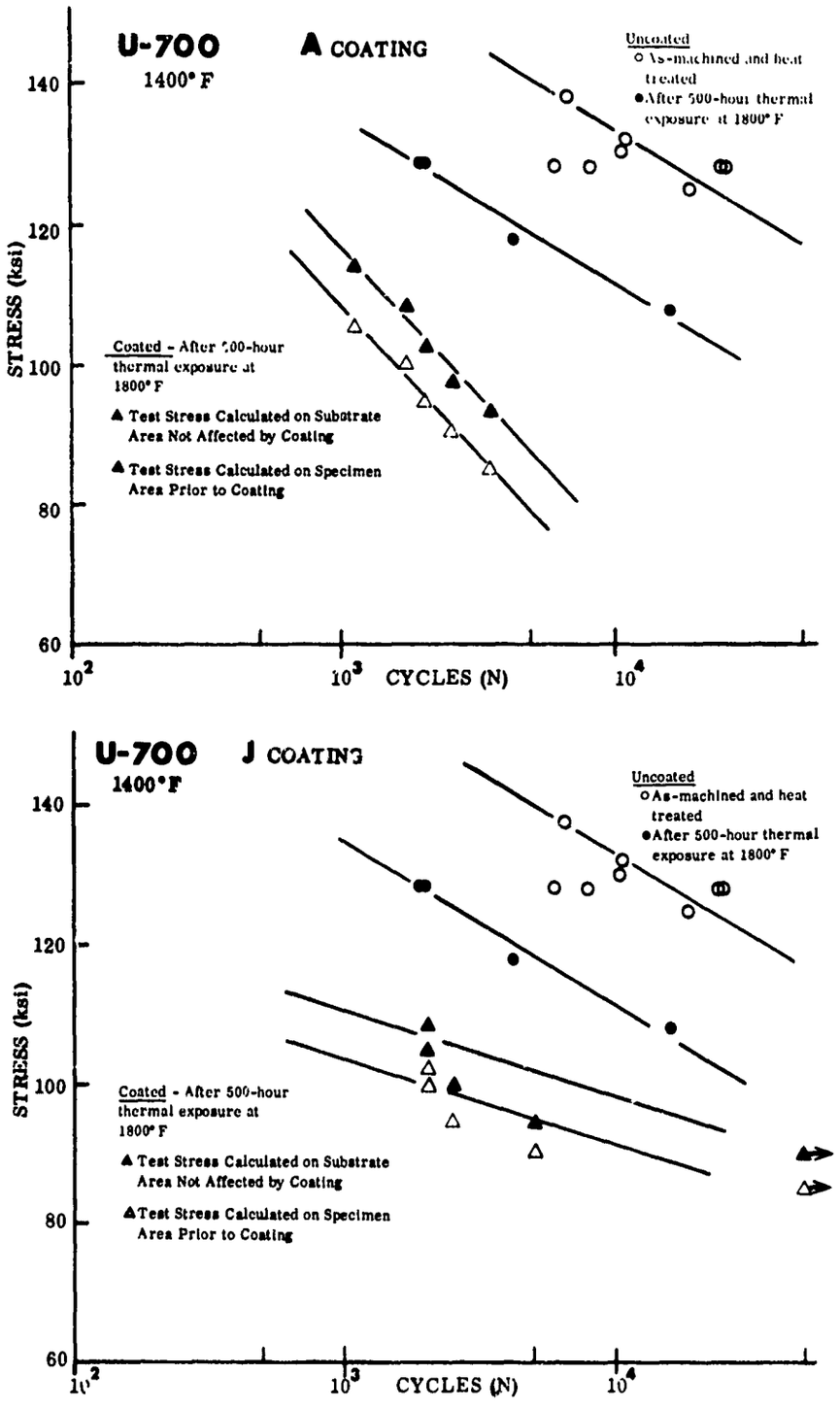

FIGURE 141. LOW-CYCLE FATIGUE LIFE OF U-700 ALLOY AT 1400°F

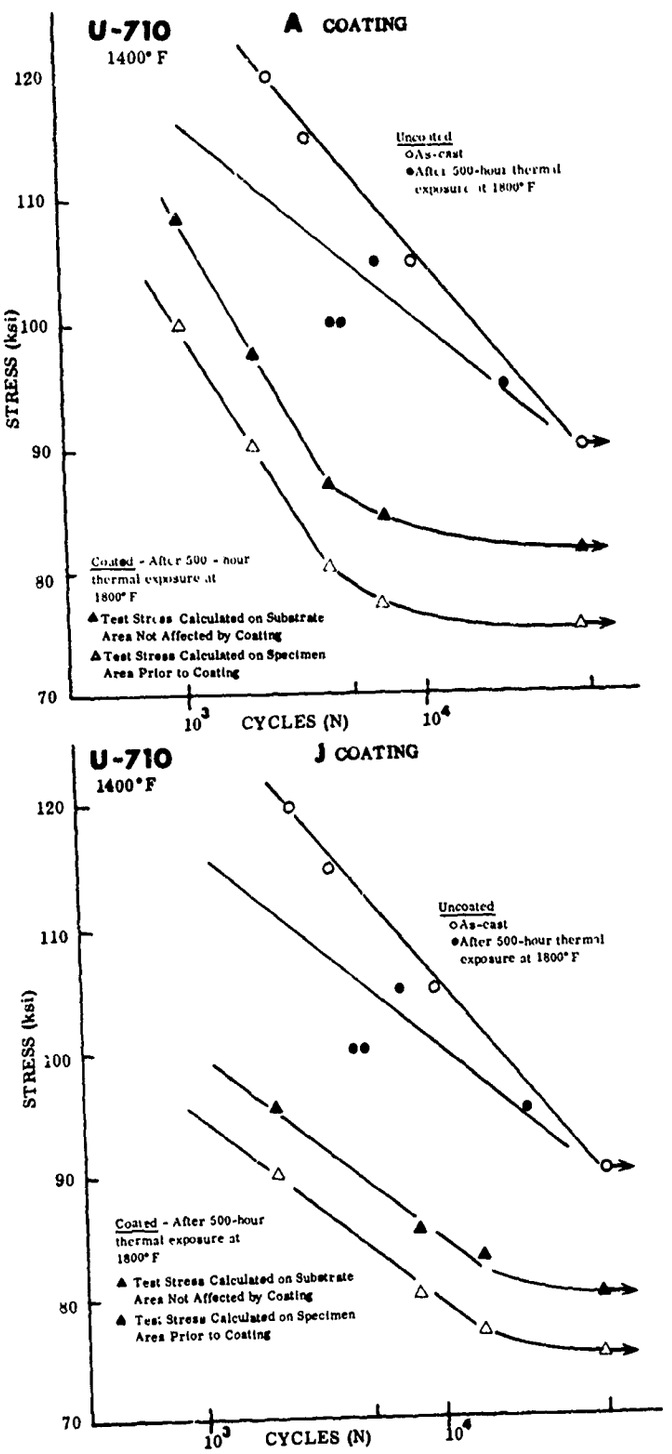

FIGURE 142. LOW-CYCLE FATIGUE LIFE OF U-710 ALLOY AT 1400°F

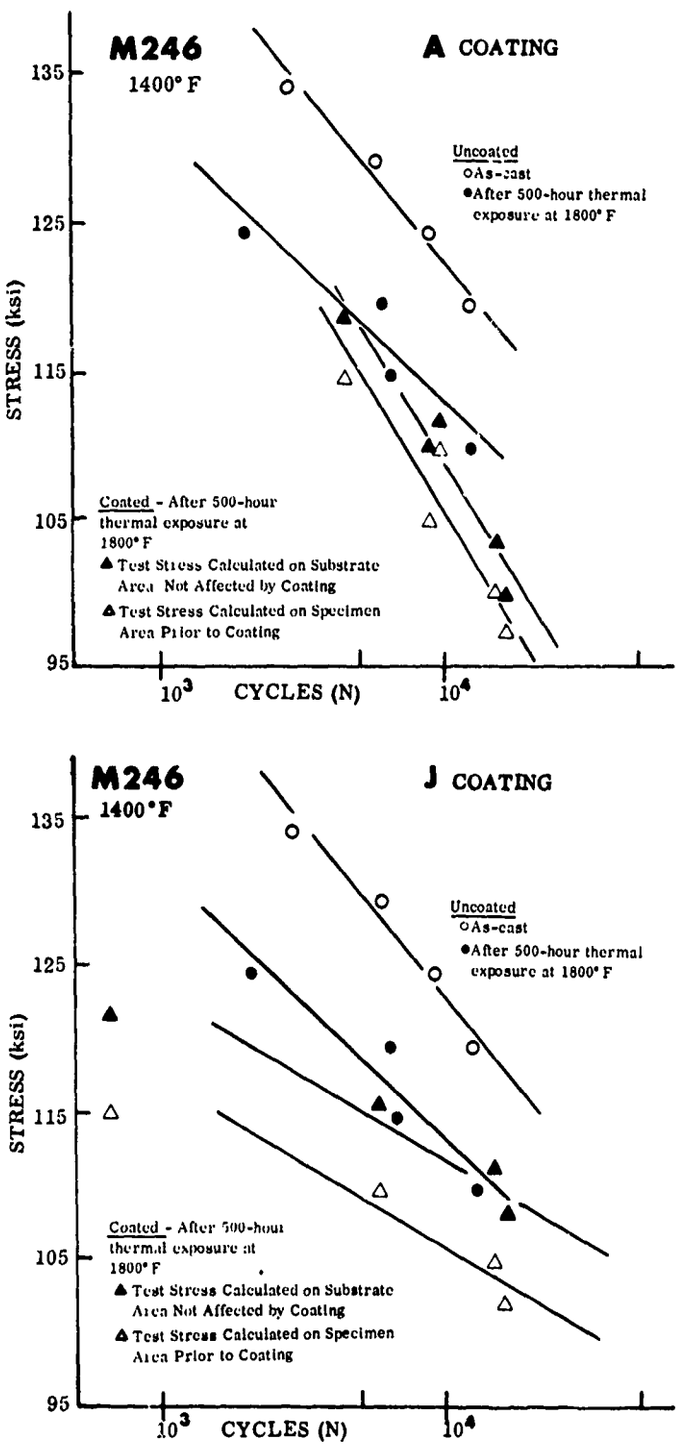

FIGURE 143. LOW-CYCLE FATIGUE LIFE OF MAR-M-246 ALLOY AT 1400°F

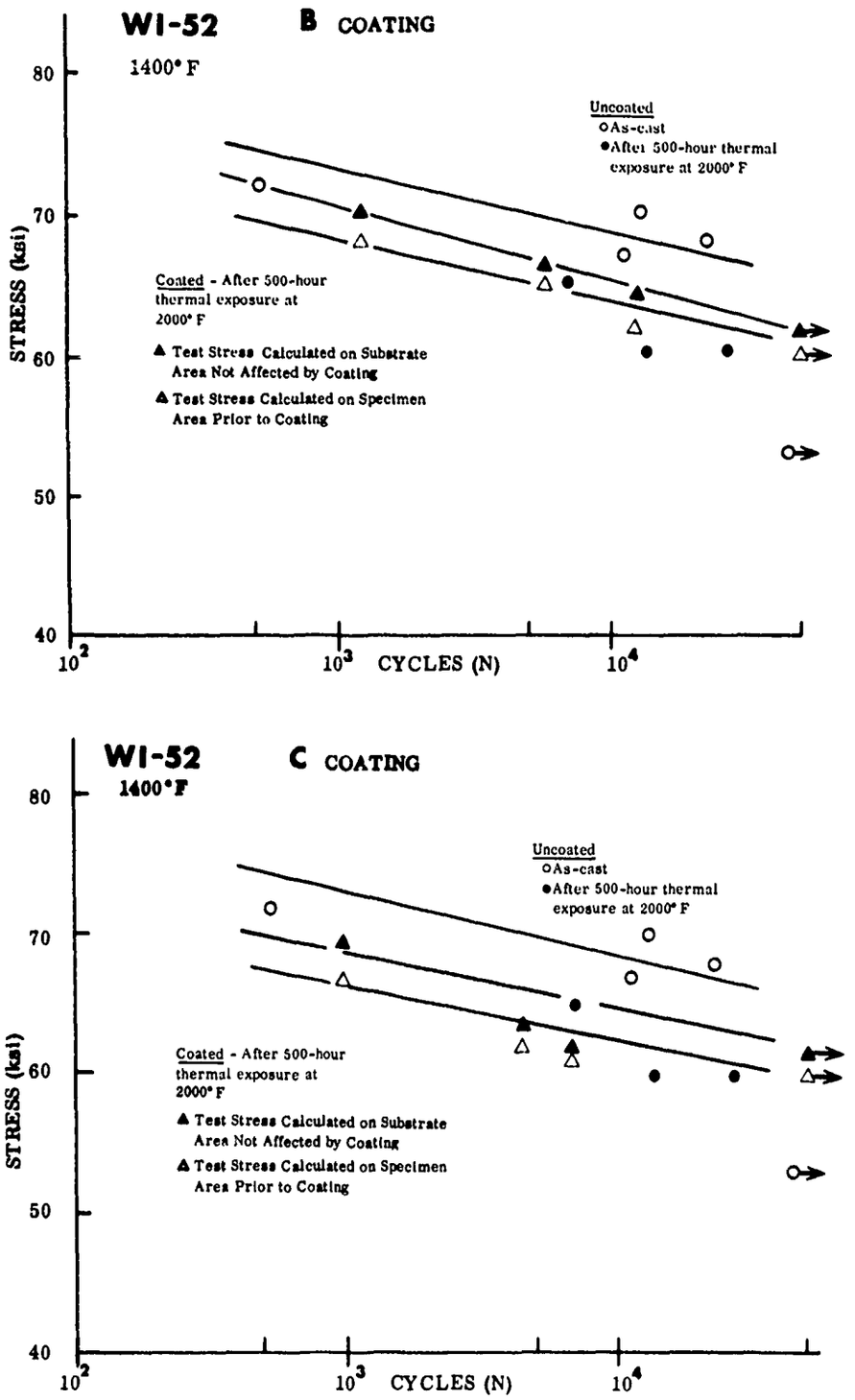

FIGURE 144. LOW-CYCLE FATIGUE LIFE OF WI-52 ALLOY AT 1400°F

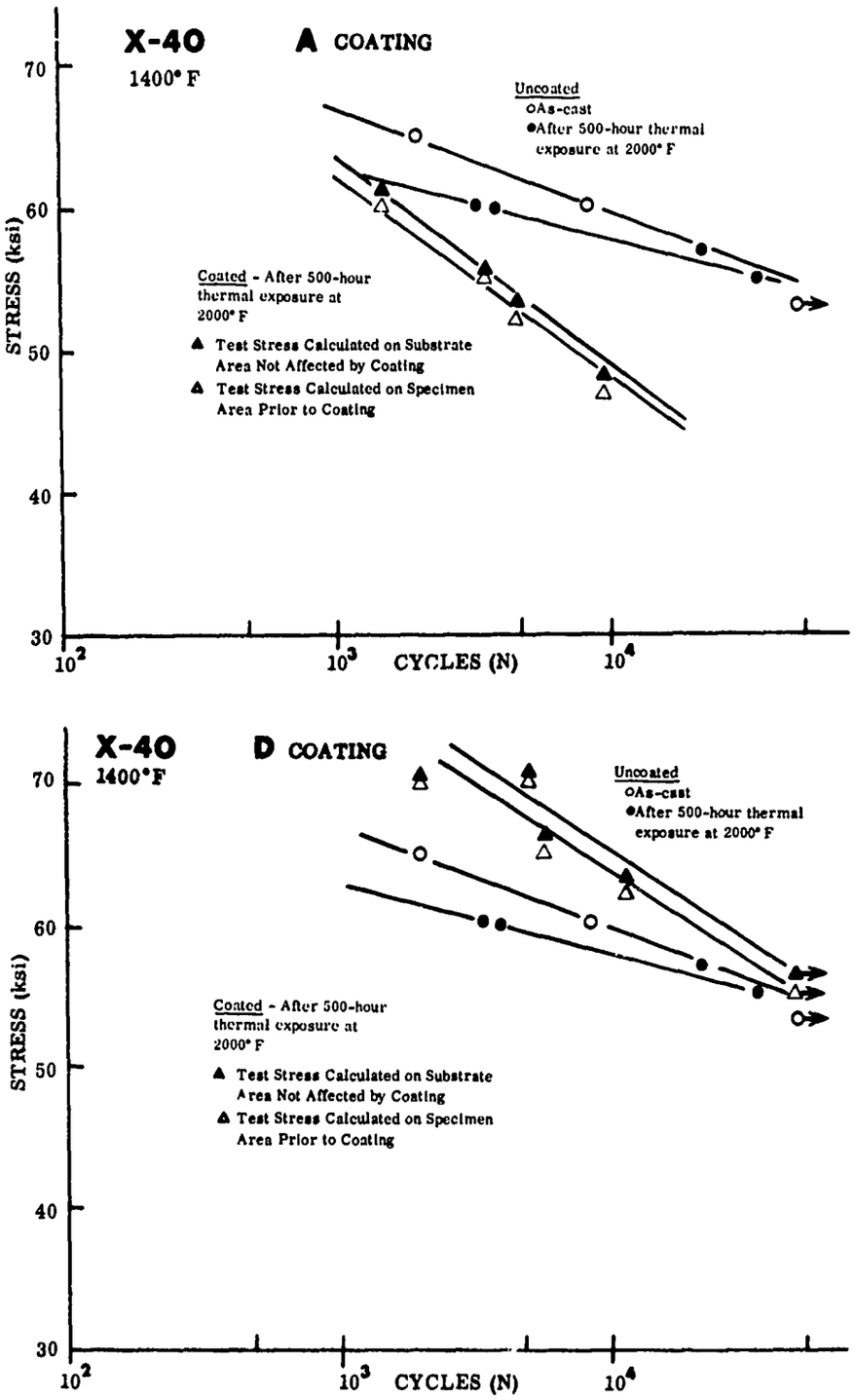

FIGURE 145. LOW-CYCLE FATIGUE LIFE OF X-40 ALLOY AT 1400°F

The curves contain data points for each tested specimen and are presented for the coated specimens with the test stress calculated based on (1) the specimen area prior to coating and (2) the unaffected substrate area after the 500-hour thermal exposure.

The low-cycle fatigue data are summarized and presented in Figure 146 and Table XIII for each coating-alloy combination to show the stress level that will produce failure in 10^4 cycles.

Baseline Tests

From the mechanical strength standpoint, the two wrought alloys, U-700 and Rene' 41, exhibited the highest fatigue strength for a 10^4 cycle life. The U-700 alloy in the as-machined and heat-treated condition (1975°F - 4 hours AC, + 1550°F - 24 hours AC, + 1400°F - 16 hours AC) was superior to the Rene' 41 alloy (133.0 ksi to 126.1 ksi). For the six as-cast nickel-base alloys, the MAR-M-246 alloy exhibited a fatigue strength of 123 ksi, approximately the same as the Rene' 41 alloy. All other cast alloys, however, were lower in strength, with the U-710 alloy showing a strength of 105.8 ksi or 21 percent less than the wrought U-700 alloy.

The fatigue strength of the two cobalt-base alloys was considerably lower than the nickel-base alloys. The maximum stress level for a 10^4 cycle life was 69.5 ksi for the WI-52 alloy and 59.5 ksi (15% less) for the X-40 alloy.

Uncoated Alloys - Thermally Exposed

All uncoated specimens were thermally exposed in an inert atmosphere (gettered flowing dry argon). After exposure, the nickel-base alloys exhibited a superficial gray film oxide on the surfaces; the cobalt-base alloys both appeared bright and shiny. The test sections of all fatigue specimens were then machined from the initial 0.250 inch diameter to the 0.185 inch diameter required for consistent failure in the gage section of the specimens. Therefore, the removal of 0.0325 inch of metal from the aged section of the specimens should have eliminated any effects of intergranular oxidation on the test results.

The test data indicate a reduction in fatigue life following the prolonged exposure for all of the uncoated alloys except Inco 713C. The 713C alloy showed good metallurgical stability with the fatigue strength slightly higher, 1.8 percent (based on only four specimens tested) after the extended exposure at 1800°F. Only a small decrease in strength was exhibited by the IN-100 (-1.1%), SEL-15 (-2.6%), and X-40 (-2.9%) alloys. All others showed a loss of strength in excess of 3 percent indicating a potential problem for long-term, high-temperature operation with these alloys.

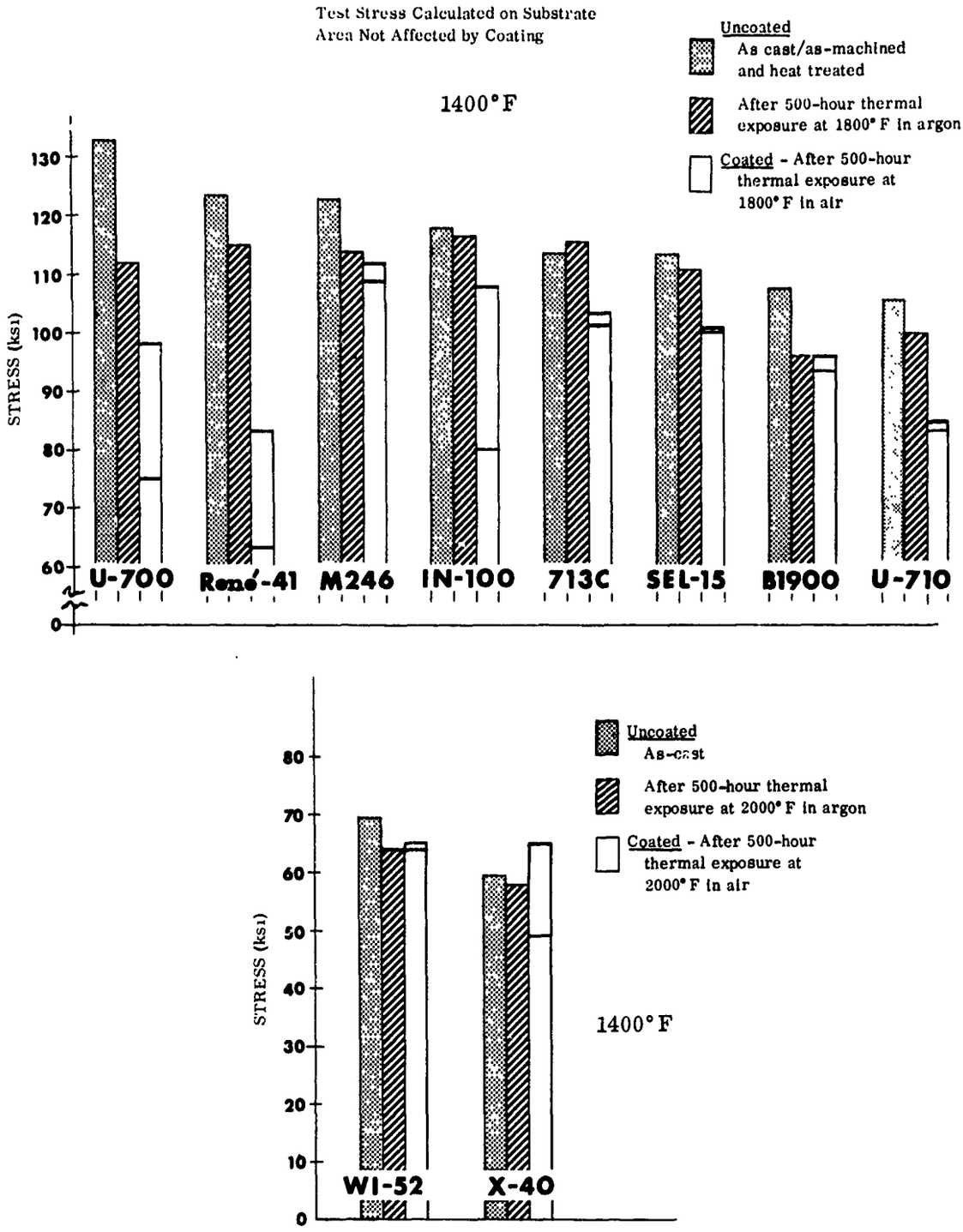

FIGURE 146. COMPARISON OF FAILURE STRESSES AT 10^4 CYCLES

TABLE XIII

STRESS TO PRODUCE FATIGUE FAILURE IN 10^4 CYCLES AT 1400°F

Alloy	As-Cast (ksi)	Uncoated Exposed in Argon for 500 Hours (ksi)	Coated and Exposed in Air for 500 Hours (ksi)			
U-700	133.0	111.5	J	98.0	A	75.0
Rene' 41	123.5	115.0	G	83.6	A	63.2
MAR-M-246	123.0	113.5	J	112.1	A	108.0
IN-100	117.8	116.5	J	107.9	A	80.0
SEL-15	113.5	110.5	F	100.8	A	100.0
713C	113.5	115.5	J	103.5	G	101.5
B1900	107.5	96.0	J	96.4	K	93.8
U-710	105.8	100.0	J	84.6	A	83.4
WI-52	69.5	64.0	B	64.8	C	65.1
X-40	59.5	57.8	D	65.0	A	49.0

The largest reduction in fatigue life, approximately 16 percent, occurred with the U-700 wrought bar stock alloy which had exhibited the highest "as-received", low-cycle fatigue strength.

Both the cobalt-base alloys showed a decrease in fatigue strength following the exposure at 2000°F for 500 hours duration. The X-40 alloy exhibited a small decrease in strength (-2.9%); whereas the WI-52 alloy showed a significant loss of 7.9 percent, dropping from 69.5 ksi to 64.0 ksi for a 10^4 cycle life.

Coated Alloys - Thermally Exposed

Another reduction in fatigue strength was apparent for most of the nickel-base alloys after coating, and then exposing the specimens in an air environment at high temperature for 500 hours (Fig. 146).

The J coating on B1900 and MAR-M-246 alloys did not cause any significant reduction in the low-cycle fatigue strength of these alloys. This coating, which was applied to six of the eight nickel-base alloys, appeared to have the best influence on the mechanical properties of any of the coatings evaluated. Loss in strength ranged from zero (on B1900) to a maximum of 15 percent on the U-710 alloy. Largest loss in strength was exhibited by the A coating on Rene' 41 (45%). This coating system was applied to seven of the alloys and caused the largest drop in fatigue strength of any of the coatings evaluated. This is undoubtedly due to the diffusional instability of this coating system. Rapid diffusion of aluminum into the substrate was noted for the A coating system as a result of the hot corrosion tests at 1650°F and 1800°F.

Best metallurgical stability was exhibited by the MAR-M-246 and B1900 alloys. The A and J coatings on these two alloys only reduced the 10^4 cycle fatigue strength by 3 percent of the MAR-M-246 alloy (average loss of both coatings) and ~2 percent of the B1900 alloy. However, the total loss in strength of these two alloys after the coating and prolonged exposures at 1800°F was generally in excess of 10 percent (Table XIII).

The two wrought alloys, Rene' 41 and U-700, showed the largest average loss in strength due to the coating and prolonged exposure. The two coatings on Rene' 41 dropped the strength 27 and 45 percent, whereas on U-700, the coatings reduced the strength by 12 and 33 percent.

The WI-52 alloy did not show any drop in fatigue strength due to the coating and prolonged exposure at 2000°F (Fig. 144). Both the B and C coated WI-52 alloy specimens exhibited a 10^4 cycle fatigue strength of 64 ksi, approximately the same strength as the uncoated exposed specimens. The X-40 alloy (Fig. 145) with the A coating showed a severe decrease of 15 percent in strength after coating and exposing at 2000°F. The strength dropped from 57.8 ksi (uncoated-exposed) to 49.0 (coated-exposed). The D coating on X-40 exhibited a 12 percent increase in strength due to the coating-exposure cycle. This strengthening mechanism is not readily apparent; however it is known that the D coating was developed by an engine manufacturer specifically for use on the X-40 alloy in one of their gas turbine engines.

Fracture Characteristics of Coated Specimens

Several of the coating-alloy combinations were examined. The large number of coating-alloy combinations however did not permit an investigation of all of the systems subjected to low cycle fatigue testing. Therefore, no comparisons were made between the different alloy-coating combinations. In general, as much variation in the fracture surface was observed within a given alloy-coating system as between different systems.

Figure 147 shows an example of a "classic" fatigue failure. Failure initiated from one point on the surface and the fatigue portion of the failure propagated slowly (a small increment during each cycle) in a radial direction. The arrow in Figure 147 indicates the origin, and the extent of the fatigue portion is indicated by the markers. This region is flat and featureless in appearance and the fracture propagated perpendicular to the applied stress. As the load bearing cross-section was reduced, the effective stress increased to a value which caused a tensile overload failure. This portion of the fracture surface (in this case ≃80% of the cross-section) was rough, coarse, and bounded by a narrow shear lip.

A MAR-M-246 Alloy

J Coating
Failure at 13,500 cycles, 108.6 ksi

The arrow indicates the origin of fatigue. The markers show the extent of the cyclic propagation.

Magnification: 13X

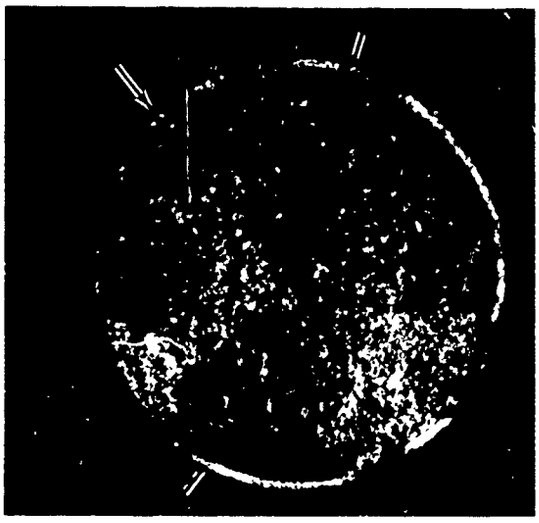

B MAR-M-246 Alloy

J Coating
Failure at 600 cycles, 122.5 ksi

The fatigue failure initiated around almost half of the circumference as indicated by the markers.

Magnification: 13X

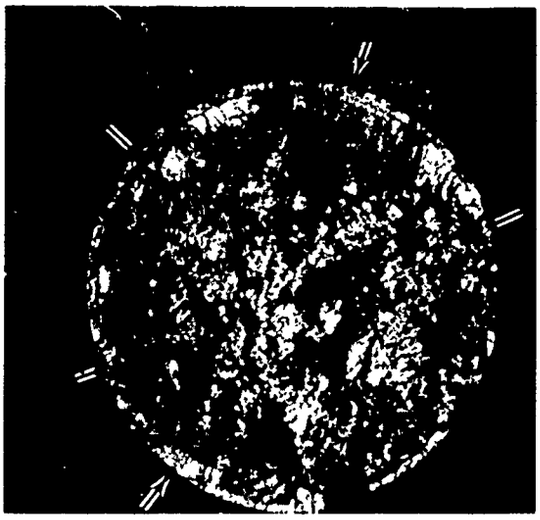

C IN-100 Alloy

A Coating
Failure at 1200 cycles, 104 ksi

Multiple fatigue origins as indicated by markers.

Magnification: 13X

FIGURE 147. SURFACES OF SPECIMENS AFTER LOW-CYCLE FATIGUE TESTS
(Sheet 1 of 3)

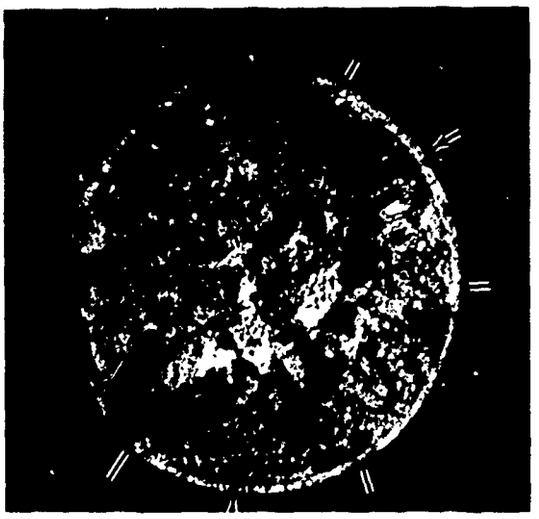

D U-710 Alloy

A Coating
Failure at 4200 cycles, 87 ksi

Multiple fatigue origins as indicated by markers.

Magnification: 13X

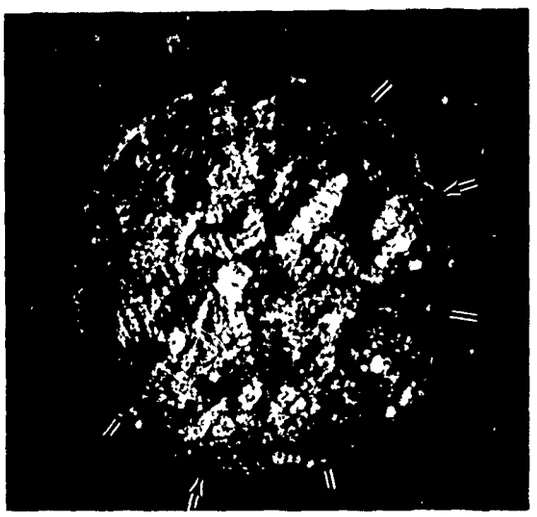

E 713C Alloy

G Coating
Failure at 1200 cycles, 111.8 ksi

Multiple fatigue origins as indicated by markers.

Magnification: 13X

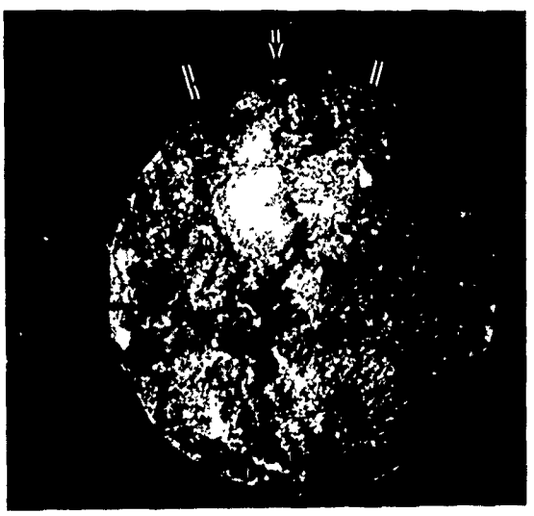

F SEL-15 Alloy

F Coating
Failure at 27,000 cycles, 99.2 ksi

Single fatigue origin near a casting defect.

Magnification: 13X

FIGURE 147. SURFACES OF SPECIMENS AFTER LOW-CYCLE FATIGUE TESTS
(Sheet 2 of 3)

G WI-52 Alloy

C Coating
Failure at 1 cycle, 69.8 ksi

No obvious fatigue origin evident.

Magnification: 13X

FIGURE 147. SURFACES OF SPECIMENS AFTER LOW-CYCLE FATIGUE TESTS (Sheet 3 of 3)

Of particular interest to this investigation was the nature of the fatigue origin and propagation prior to catastrophic overload failure. Figures 147A through 147G show typical examples of the fracture surfaces resulting from the low cycle fatigue tests.

Figure 147B is another example of MAR-M-246 alloy with the J coating. In this specimen the fatigue crack did not nucleate at a single point, but around almost half of the circumference of the test specimen as shown by the markers. This type of origin is indicative of a higher applied stress than that shown in Figure 147A and would act as a severe notch for the overload portion of the failure. The conditions for failure shown in Figures 147A and 147B further substantiate these observations.

Figures 147C through 147E are examples of multiple fatigue origins. All three of these alloy-coating systems also exhibit multiple cracking around the circumference of the test bar. The secondary cracks increase the effective applied stress on the specimen as well as acting as severe stress risers.

Figure 147F shows the F coating on SEL-15 alloy. Fatigue originated from one point on the surface which was near a casting defect. The casting defect would be expected to decrease the fatigue life of this part.

Figure 147G shows the C coating on WI-52 alloy. There is no obvious fatigue origin, or propagation region on the fracture surface, since this part failed during the first cycle. This failure is entirely intergranular and probably initiated at a grain boundary which was acting as a severe notch.

Figures 148 through 150 show alloy-coating systems which developed optically observable secondary cracks during fatigue testing. It is possible that all of the systems develop microscopic secondary cracks, but time limitations allowed only the obvious systems to be examined. Of particular interest is the extent to which the fatigue portion of these secondary cracks have propagated into the alloy matrix. The fatigue portion corresponds to the straight, transgranular cracked region. In some cases, this is 0.04 inch into the matrix. These secondary cracks which exist prior to complete failure considerably increase the effective applied stress by reducing the available load bearing cross-section. In many cases, the fatigue mode has already changed to overload as evidenced by the intergranular crack propagation. In addition, the tip of these secondary cracks act as severe stress risers. Generally under these temperatures, the grain boundaries in these alloys are weaker than the grains, and once a grain boundary is intersected by the fatigue crack, intergranular failure propagates rapidly. This phenomena is shown in Figures 149 and 150.

The results of this examination of the low cycle fatigue fracture surfaces has revealed that in general, the outside coating surface provides ample notches (stress risers) for initiation of fatigue cracks. These cracks once nucleated, increase the effective applied stress on the part by decreasing the load bearing area and acting as severe stress risers thereby decreasing the fatigue life of the coated (notched) part in comparison to the uncoated (unnotched) part.

4.3 TASK II - STRESS RUPTURE TESTS

The prime properties for selecting blade materials for use in a gas turbine engine are stress rupture, creep, and oxidation resistance at the operating temperatures. Secondary properties, e.g., fatigue strength and impact strength, must be measured, but they are less critical than the prime properties.

Development of improved turbine materials has been a challenging problem for a number of years with time-to-rupture at a critical stress the guiding criterion. Stress rupture performance has been gradually increased by alloy development and process refinement; therefore retention of this critical property after coating is imperative. In this task, the effect of the coatings, coating processing conditions, and stripping and recoating on the 100-hour rupture strength has been determined.

4.3.1 Test Procedures

The flow chart of the Task II Stress Rupture Program is shown in Figure 151.

Two batches of specimens of the two selected coatings on the eight nickel-base and the two cobalt-base alloys were subjected to furnace exposure for 500 hours duration in air atmosphere. The coated nickel-base alloys were exposed at 1800°F;

Text Continued on Page 204.

A

Secondary cracks characteristic of this alloy-coating system.

Magnification: 3.5X

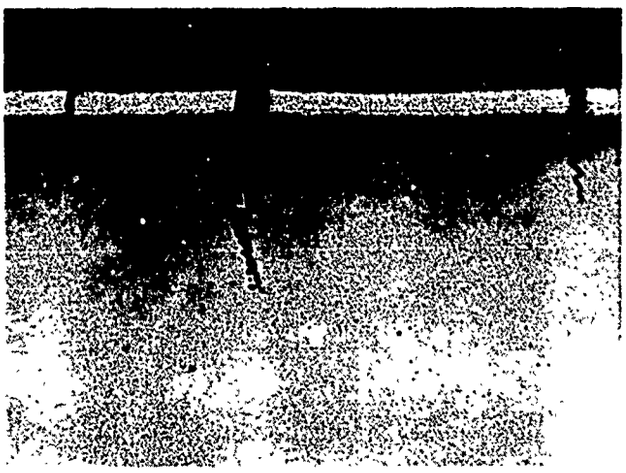

B

Cross-section of above specimen showing extent of secondary cracking and notches in coating surface.

Magnification: 40X

C

Higher magnification of secondary crack and notches.

Magnification: 200X

FIGURE 148. SURFACE CRACKS AND MICROSTRUCTURE OF A COATING ON U-710 ALLOY AFTER FATIGUE TESTING

A

Secondary cracks characteristic of this alloy-coating system.

Magnification: 3.5X

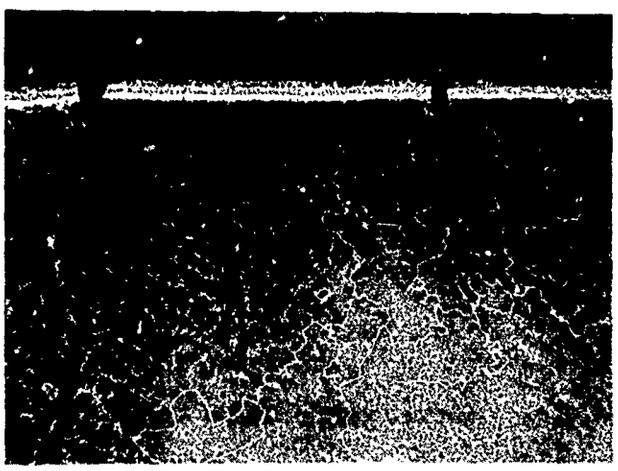

B

Cross-section of above specimen showing extent of secondary cracking and notches in coating-surface.

Magnification: 40X

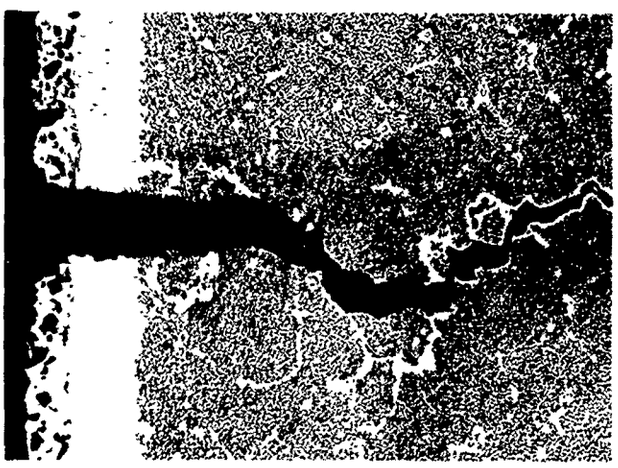

C

Higher magnification of secondary crack and notches.

Magnification: 200X

FIGURE 149. SURFACE CRACKS AND MICROSTRUCTURE OF G COATING ON 713C ALLOY AFTER FATIGUE TESTING

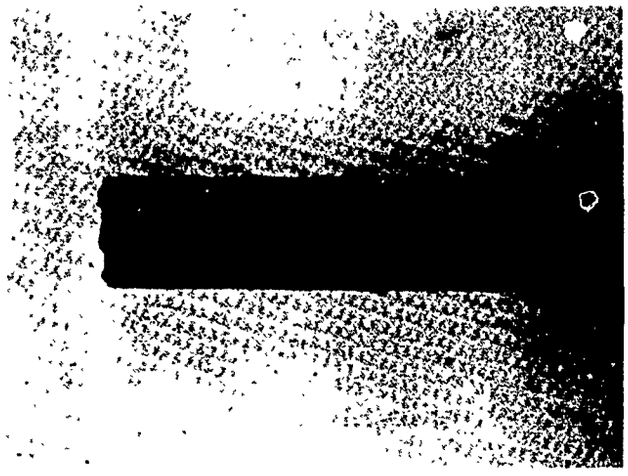

A

Secondary crack characteristic of this alloy-coating system.

Magnification: 3.5X

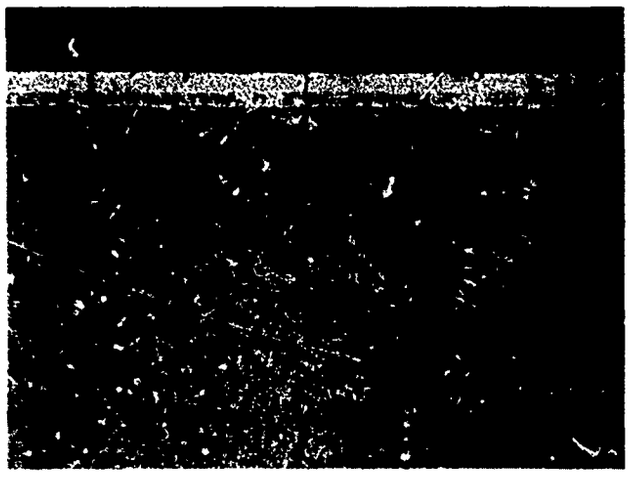

B

Cross-section of above specimen showing extent of secondary cracking and notches in coating surface.

Magnification: 40X

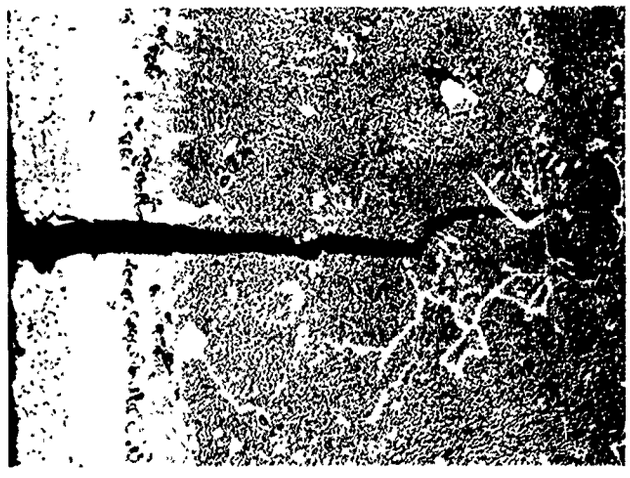

C

Higher magnification of secondary cracks and notches.

Magnification: 200X

FIGURE 150. SURFACE CRACKS AND MICROSTRUCTURE OF A COATING ON IN-100 ALLOY AFTER FATIGUE TESTING

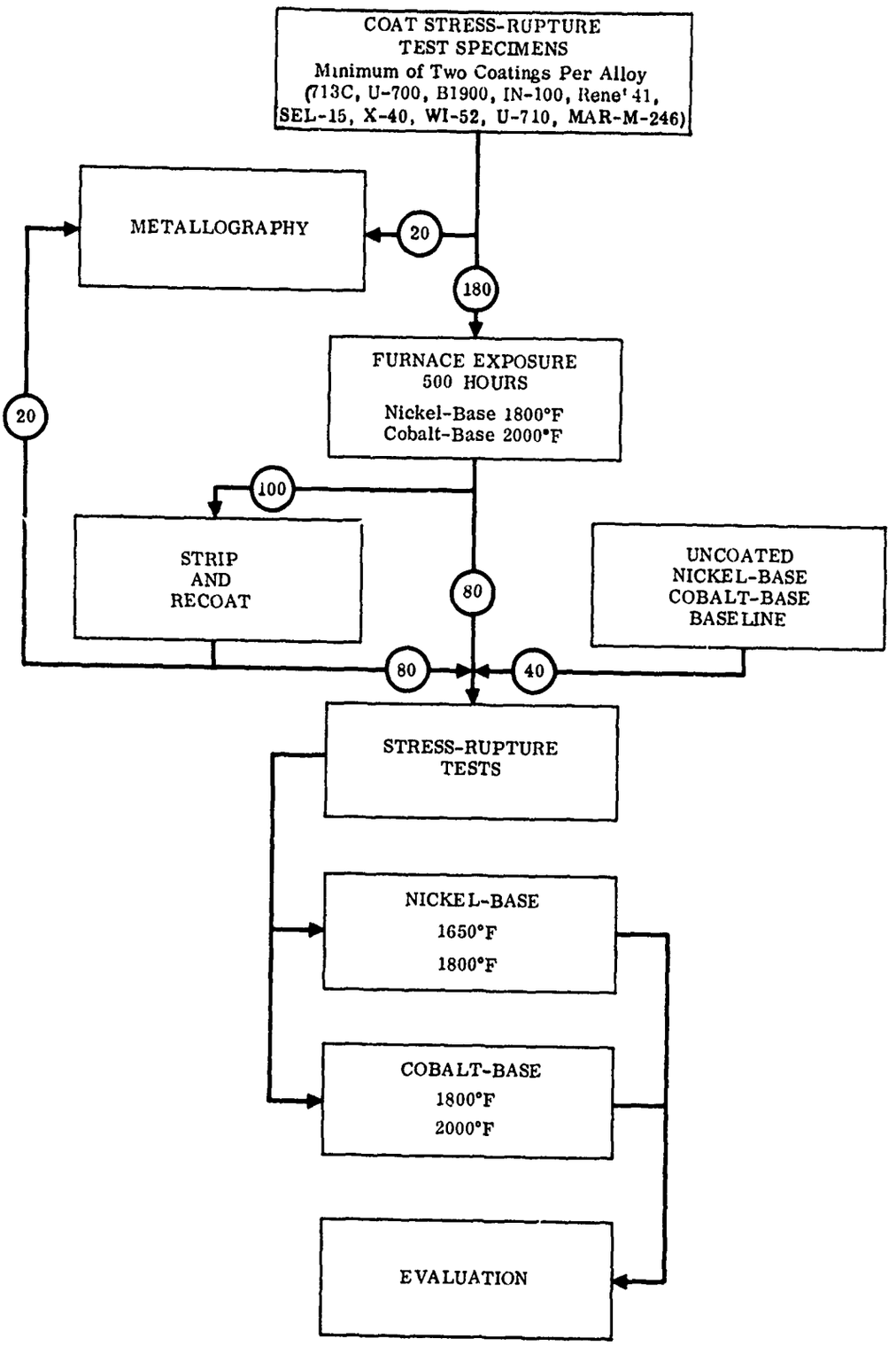

FIGURE 151. FLOW CHART OF PHASE II STRESS-RUPTURE TESTS

the cobalt-base alloys at 2000°F. Following the 500 hour exposure, one batch of specimens (duplicate specimens of all coating-alloy combinations) were returned to the coating vendor for stripping and recoating with the same coating system. After recoating; the specimens were subjected to the 100-hour stress rupture tests along with the uncoated alloys for baseline data.

Tests were performed at 1650°F and 1800°F for the nickel-base alloys; the cobalt-base alloys were tested at 1800°F and 2000°F.

The stress rupture tests were performed using Satec Corporation stress rupture test frames. Figure 152 shows a portion of Solar's stress rupture facility. Specimens were heated to the appropriate test temperature by means of standard Kanthal A-1 resistance wire furnaces.

4.3.2 Test Results

The results of the stress rupture tests on the uncoated and coated alloys are shown in Figures 153 through 162. The test data are summarized in the tables in Appendix III.

The stress levels for each alloy, at each temperature level, were selected to produce rupture in 100 hours maximum from the data presented in References 6 through 10. These stresses were also verified, where possible, against Larson-Miller stress-rupture parameter curves published by the alloy developers.

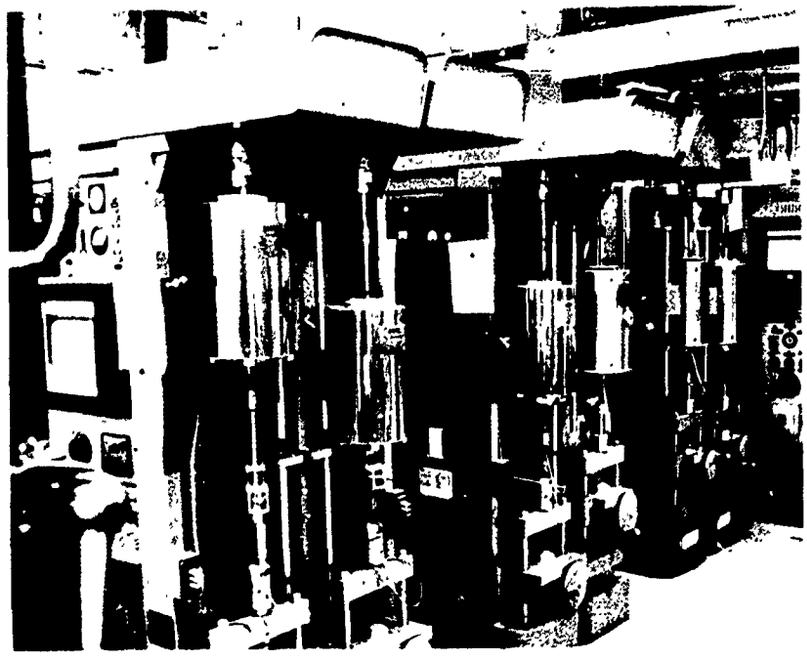

FIGURE 152. STRESS RUPTURE TEST FACILITY

Text Continued on Page 215.

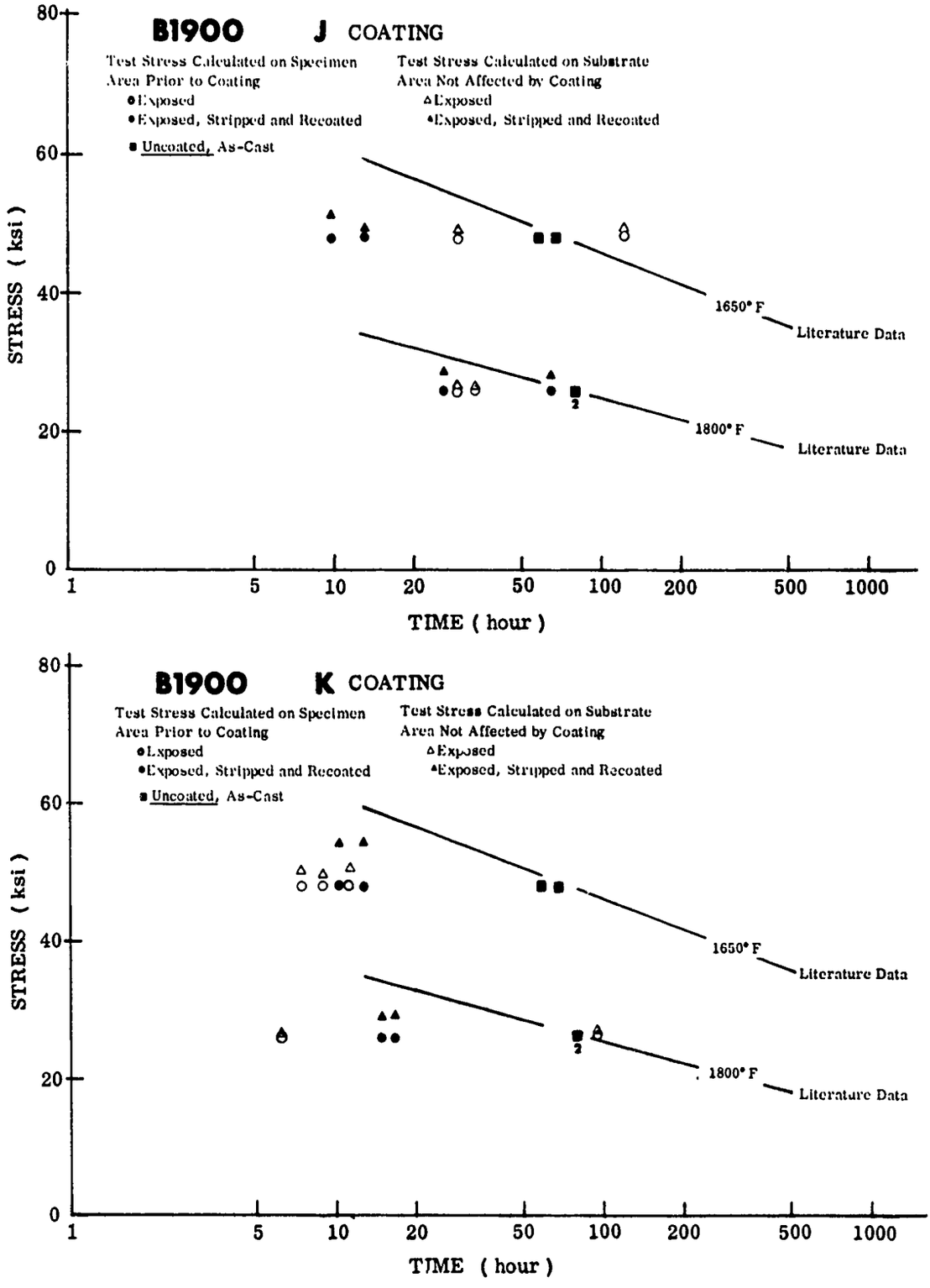

FIGURE 153. STRESS RUPTURE PROPERTIES OF B1900 ALLOY

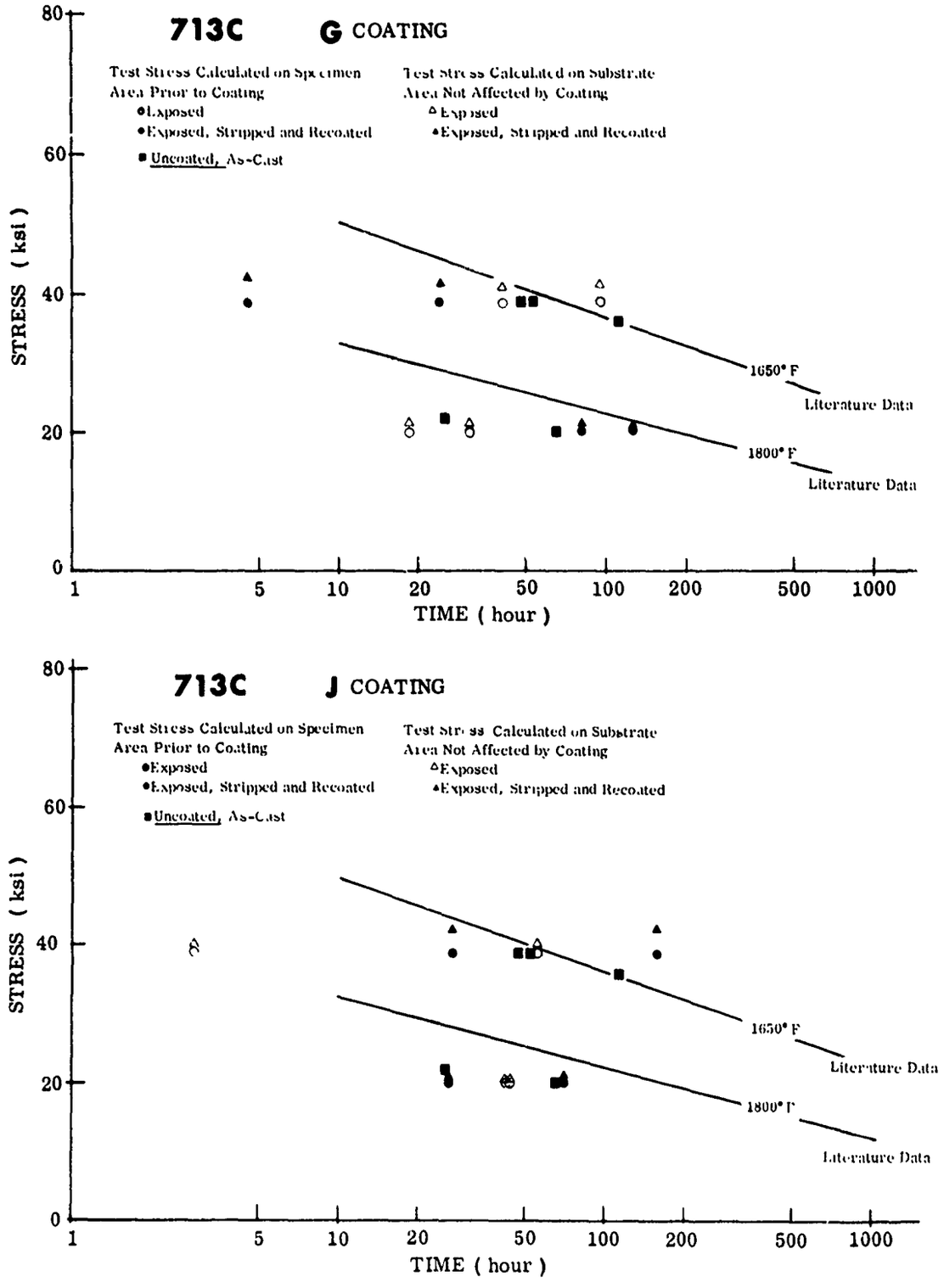

FIGURE 154. STRESS RUPTURE PROPERTIES OF 713C ALLOY

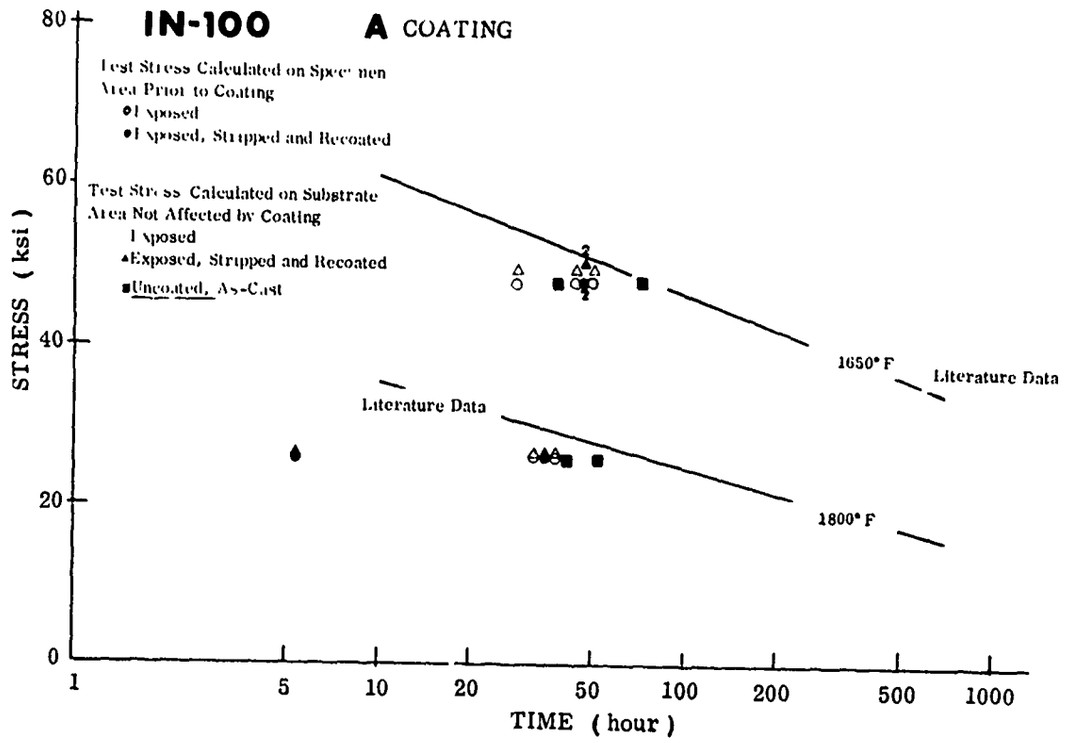

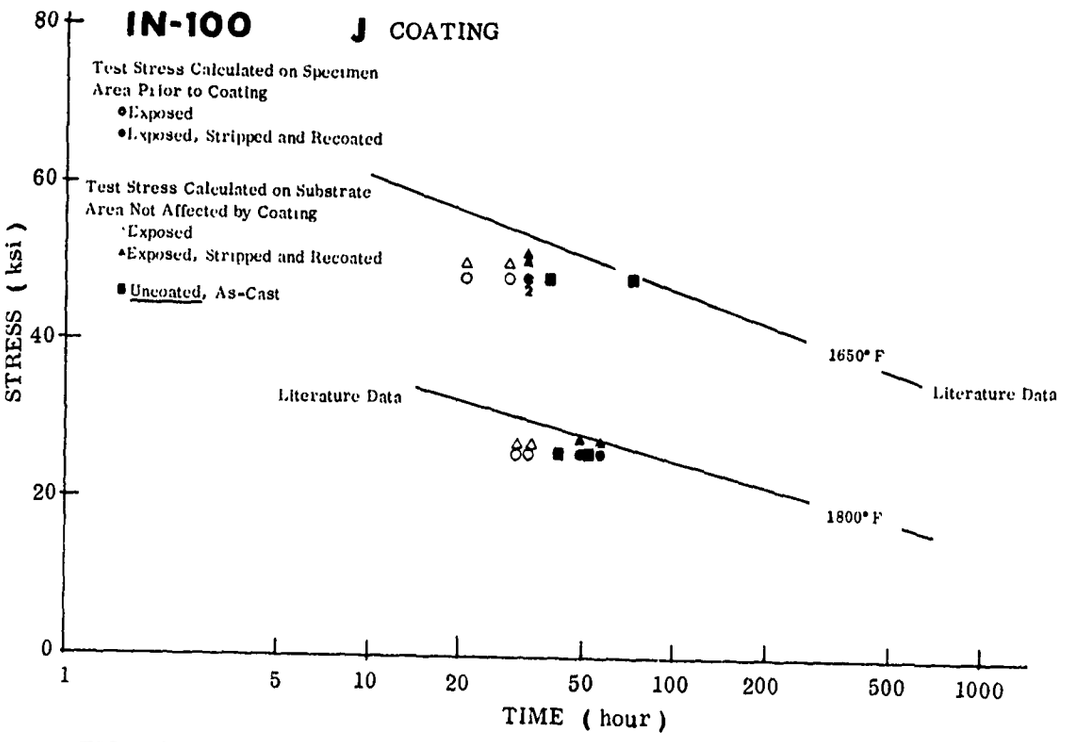

FIGURE 155. STRESS RUPTURE PROPERTIES OF IN-100 ALLOY

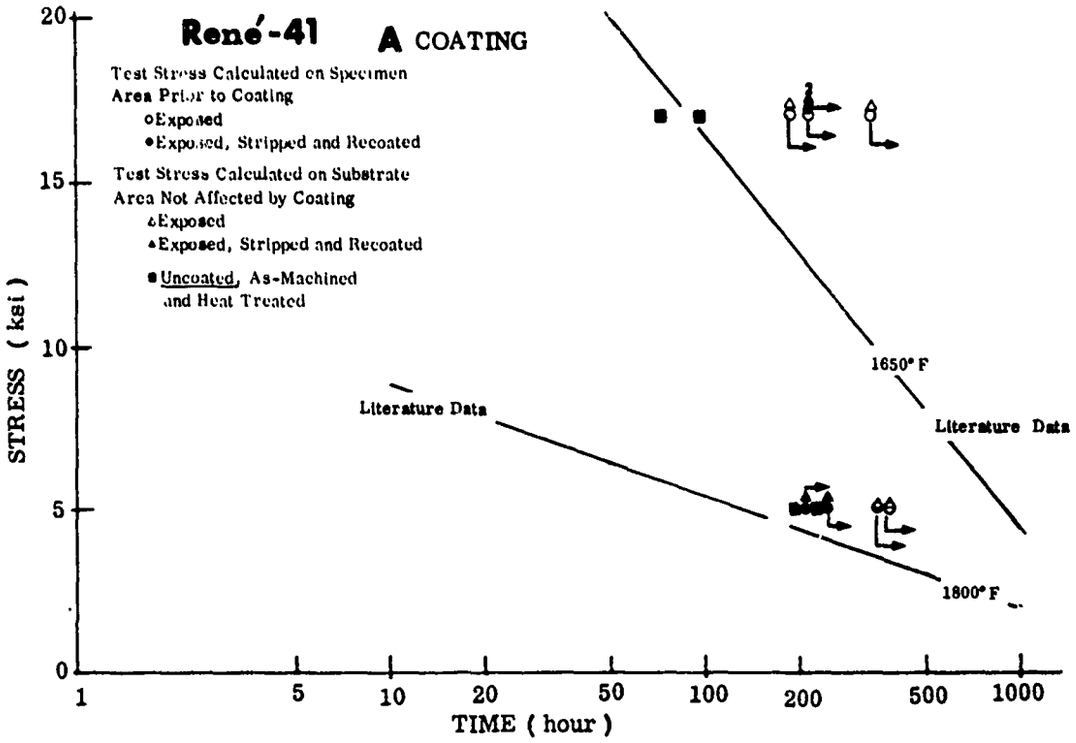

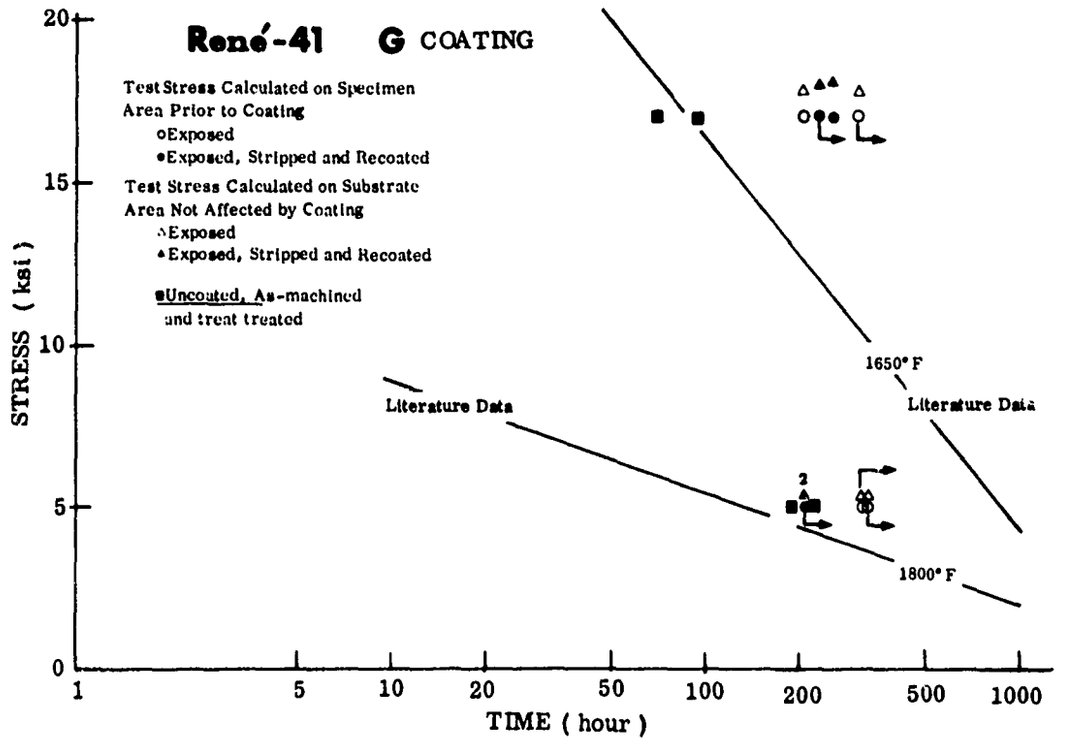

FIGURE 156. STRESS RUPTURE PROPERTIES OF RENE' 41 ALLOY

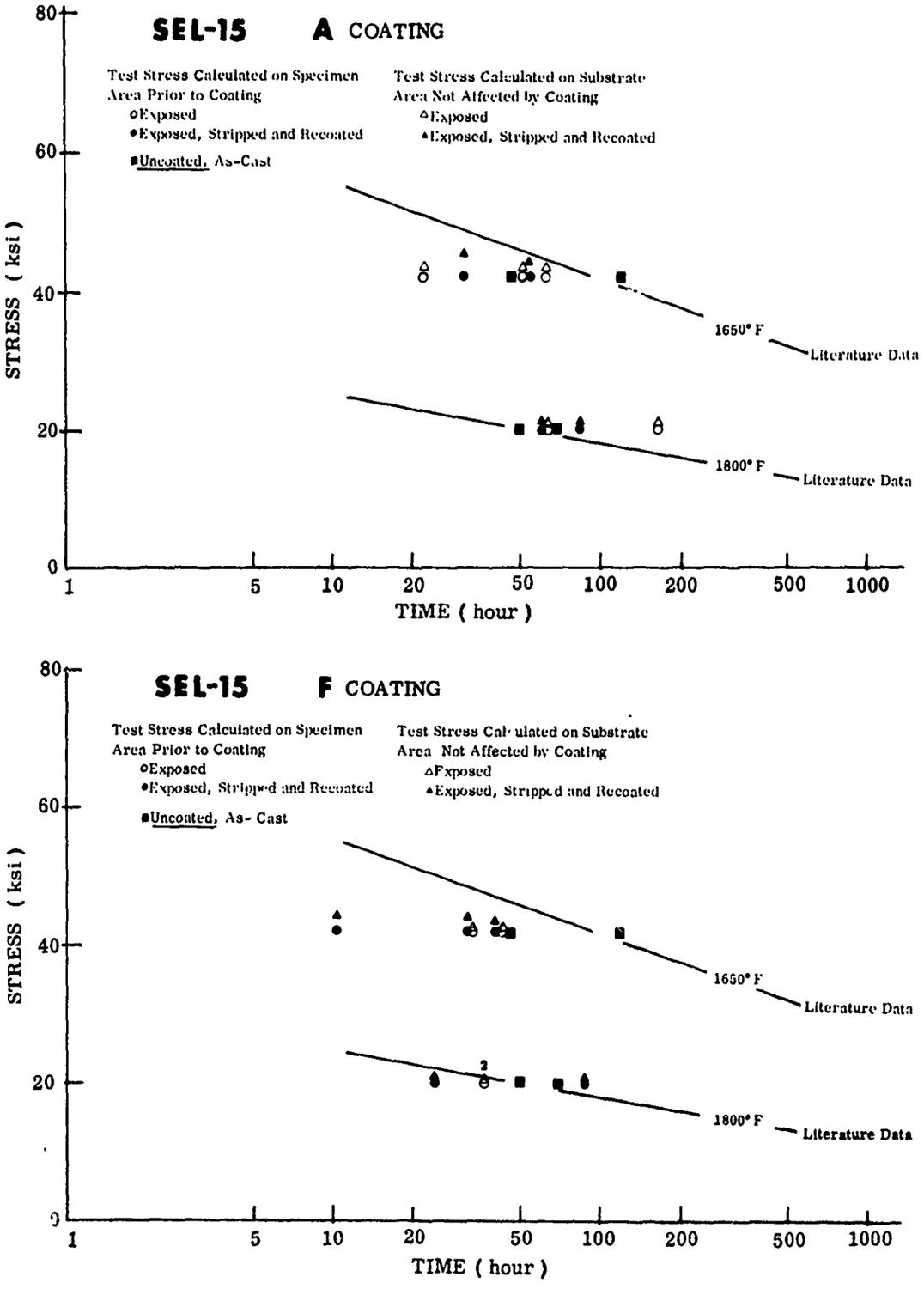

FIGURE 157. STRESS RUPTURE PROPERTIES OF SEL-15 ALLOY

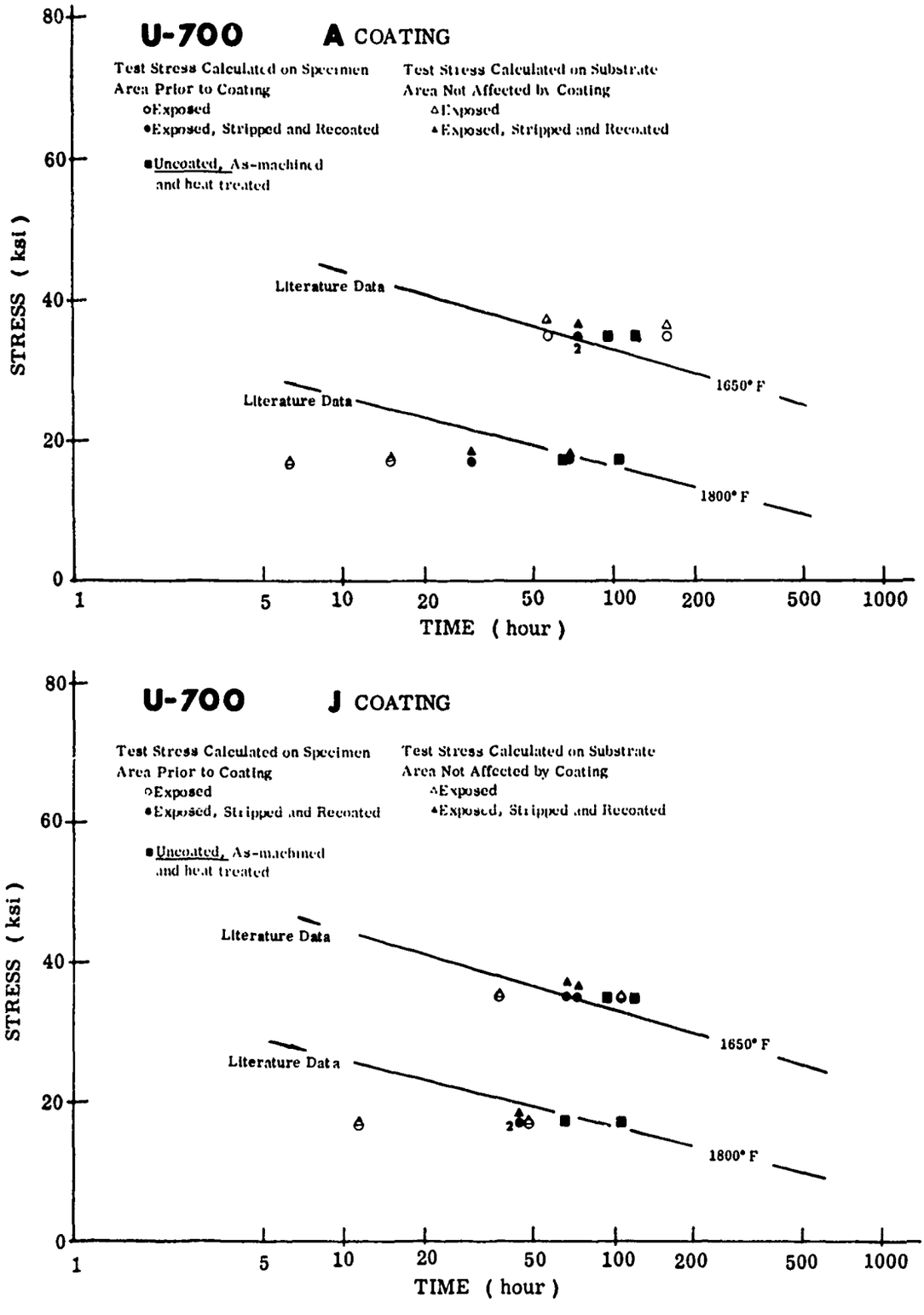

FIGURE 158. STRESS RUPTURE PROPERTIES OF U-700 ALLOY

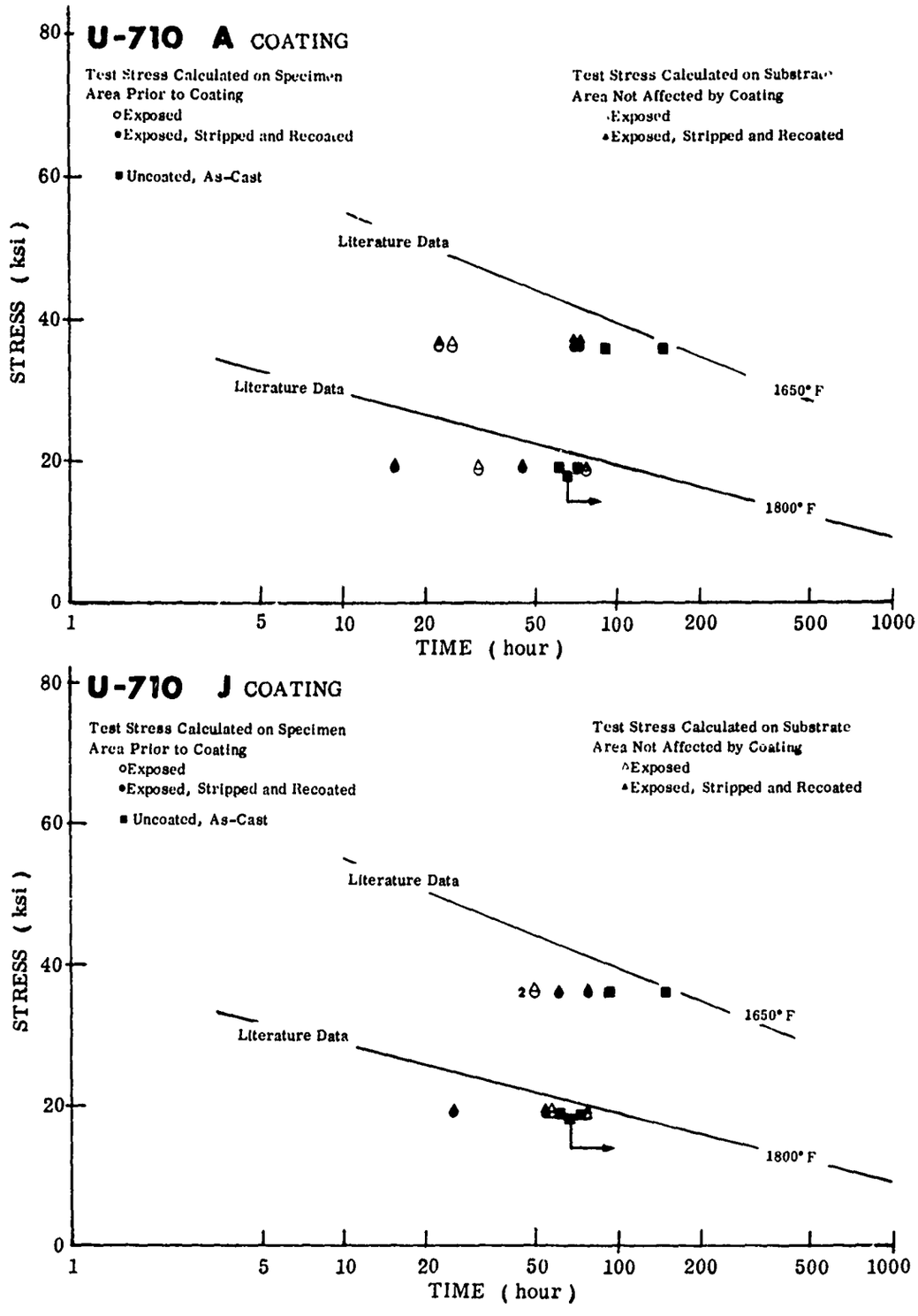

FIGURE 159. STRESS RUPTURE PROPERTIES OF U-710 ALLOY

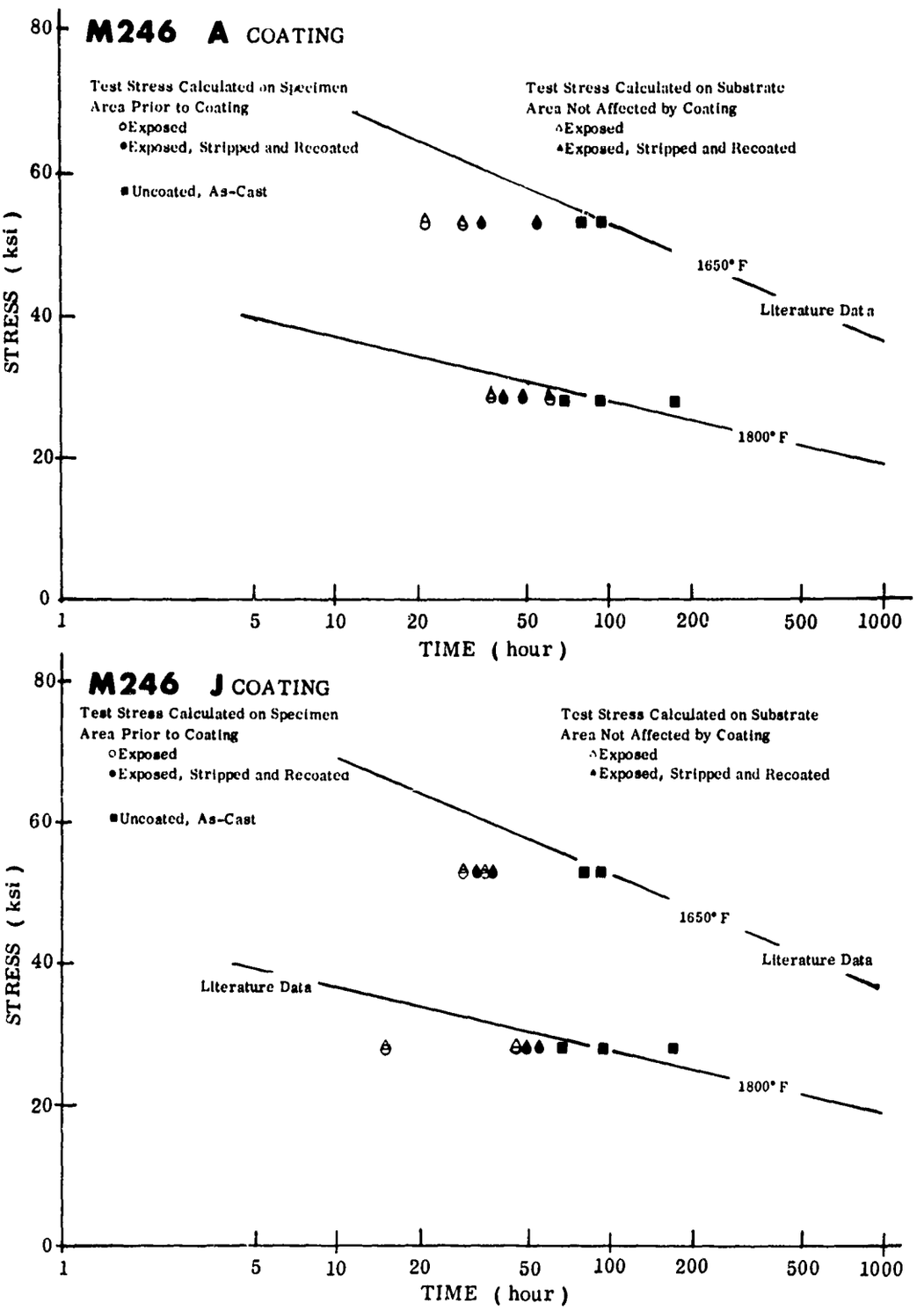

FIGURE 160. STRESS RUPTURE PROPERTIES OF MAR-M-246 ALLOY

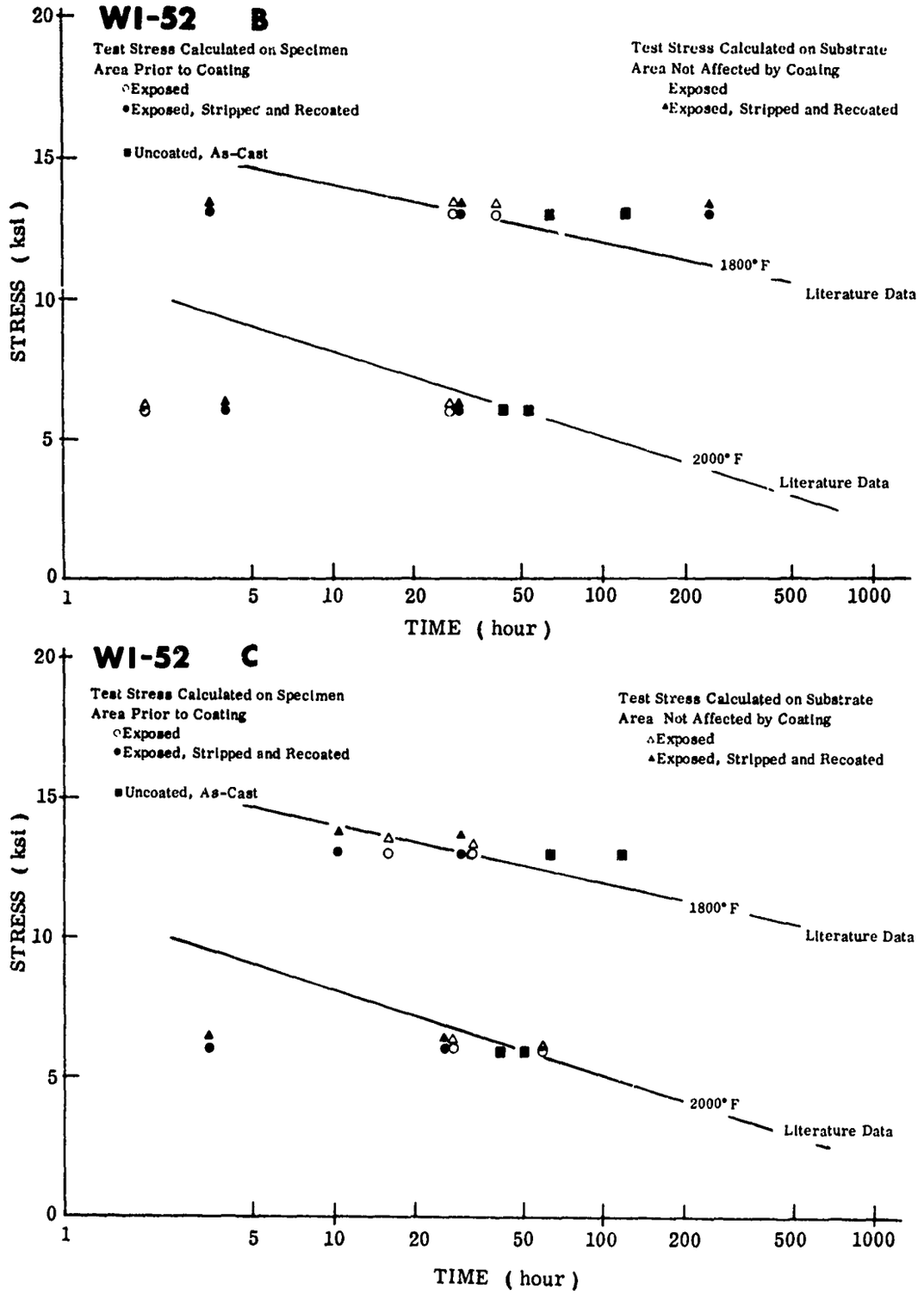

FIGURE 161. STRESS RUPTURE PROPERTIES OF WI-52 ALLOY

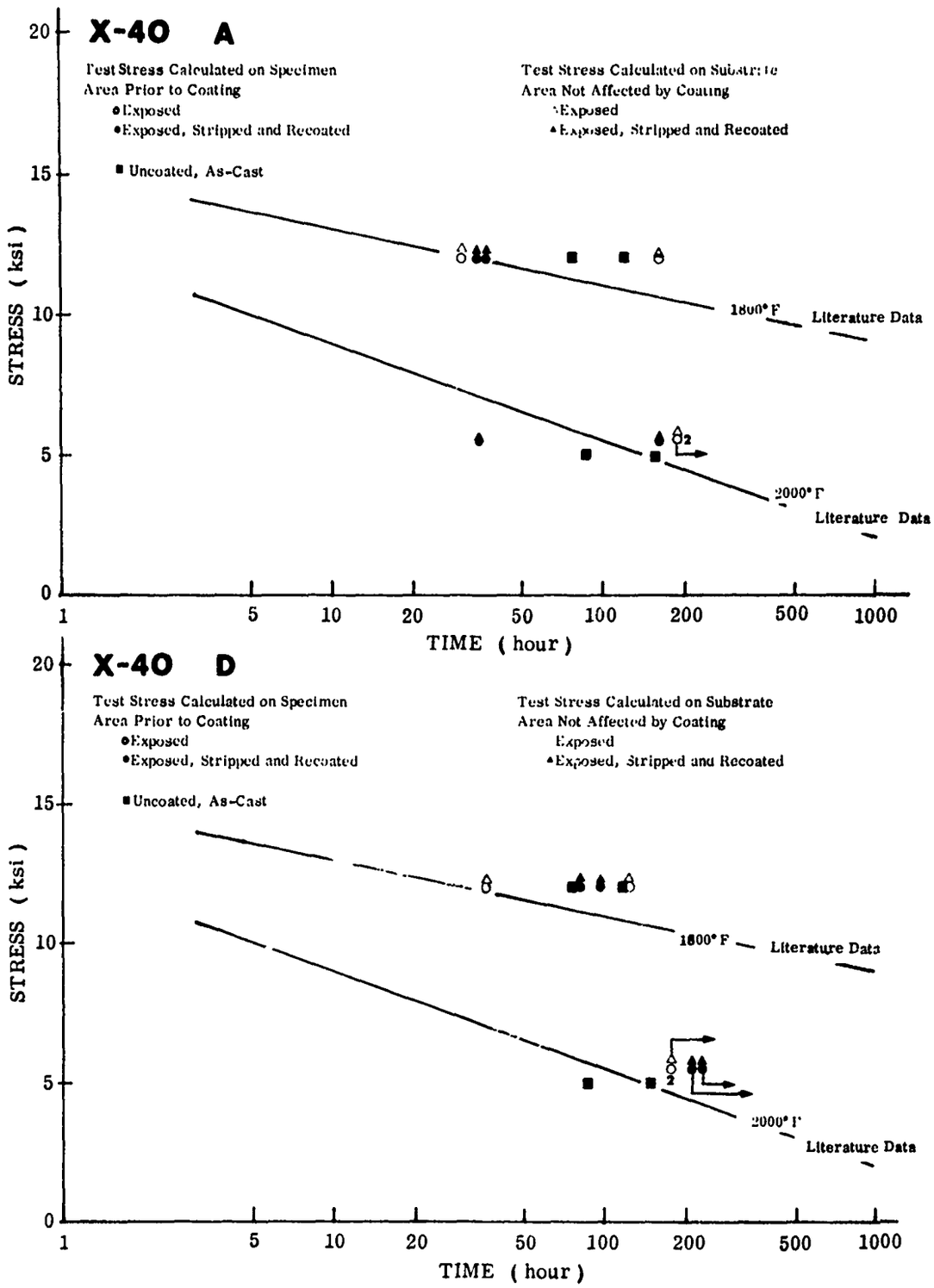

FIGURE 162. STRESS RUPTURE PROPERTIES OF X-40 ALLOY

On each graph, the following data are shown:

- Data points for the uncoated, as-received alloys at 1650°F and 1800°F (shown as solid square symbols)
- Data points for the coated specimens exposed for 500 hours (open symbols)
- Data points for the coated specimens exposed for 500 hours, stripped and recoated (solid symbols)

For comparison purposes, curves are drawn on each graph showing the published data on the stress-rupture properties of the uncoated as-received superalloys.

Uncoated Alloys

The test data for the uncoated nickel-base alloys are in good agreement with the published values. Most of the test points are on, or quite close to, the standard curves with very little scatter between the duplicate test specimens.

The WI-52 and X-40 cobalt-base alloys exhibited a slightly higher stress rupture strength at the 1800°F test temperature. Stress rupture strengths for both alloys at the 2000°F temperature level, however, were very close to the published literature values.

Coated Alloys - Thermally Exposed

Most of the nickel-base alloys exhibited a decrease in stress rupture life due to the long term exposure. At 1650°F, the U-710, MAR-M-246, SEL-15 and In-100 alloys showed a definite decrease in life for both coating systems. The decrease in rupture life was greatest for the U-710 and MAR-M-246 alloys (approximately 70 percent of baseline). The U-700, B1900 and 713C alloys exhibited a decrease in rupture life with only one of the two applied coating systems and an increase with the other coating, but this apparent increase in strength is undoubtedly due to scatter in the test data. Neither of the two coatings on Rene' 41 alloy caused a reduction in stress rupture life at either 1650°F or 1800°F. The stress rupture tests were terminated after exposures ranging up to 329 hours at 1650°F and 364 hours at 1800°F. Only one G coated Rene' 41 specimen failed after 206 hours exposure at 1650°F. Total elongation was approximately 30 percent which was in good agreement with the results of the tests on the uncoated, unexposed alloy.

At 1800°F, all of the coated nickel-base alloys except Rene' 41 exhibited a decrease in the stress rupture life due to the long term exposures. The decrease in average stress rupture life was greatest for the coated U-700 alloy (approximately 75 percent), followed closely by the coated MAR-M-246 alloy (65 percent). The 713C and B1900 alloys also exhibited a large decrease in stress rupture life after coating and exposing, with the average time to rupture for the two coatings dropping to approximately 50 percent of baseline data. The two coatings on IN-100 alloy decreased the rupture life by 28 percent whereas the U-710 alloy showed only a drop of about 10 percent. The SEL-15 alloy exhibited a decrease in rupture life with only the F coating (30 percent). The A coating on this alloy did not cause the usual drop in life as shown by this coating on U-710, U-700, MAR-M-246, and IN-100 alloys.

The B1900 alloy with the K coating showed a severe drop of 85 percent in stress rupture life after coating and exposing for 500 hours. The average life dropped from 61 to 9 hours when tested at 1650°F. At 1800°F, one specimen failed at 6 hours and another at 93 hours. However, all specimens stripped and recoated failed within 10 to 16 hours total exposure at both 1650°F and 1800°F.

The cobalt-base alloys both exhibited a decrease in stress rupture life after coating and exposing in air for 500 hours. When tested at 1800°F, both coatings on WI-52 alloy decreased the time to rupture by more than 65 percent. The decrease in stress rupture life was not as great, however, for the two coatings on X-40 alloy; average time to rupture was decreased by only 13 percent.

At 2000°F, the decrease in rupture life for the coated WI-52 alloy was not as great as at 1800°F (30 percent). Neither coating had an adverse affect on X-40 alloy at 2000°F. Tests were terminated without failure after approximately 180 hours total exposure for both the A and D coatings.

Coated Alloys - Exposed, Stripped and Recoated

All coating vendors were able to strip the coatings, either partially or completely, and recoat satisfactorily with the original coating system. The stripping and recoating operations on the nickel-base alloys after the 500-hour thermal exposures did not appear to have any appreciable added detrimental effects on the stress rupture lives. Some coating-alloy combinations exhibited an increase in the stress rupture life after the stripping and recoating (IN-100, U-710), and others showed a decrease in the rupture life after this recoating operation. No real trend however was apparent to show that the one additional thermal cycle from recoating was significantly harmful to the alloys. The two cobalt-base alloys however, both exhibited an additional small decrease in the stress rupture life at 1800 and 2000°F. For example, the average time to rupture for the exposed-stripped and recoated B and C coatings on WI-52 alloy was 19 hours compared to approximately 30 hours average life for the specimens coated and exposed only.

5

SELECTION OF BEST COATINGS

A summary of the best coatings for each substrate alloy based on its performance in hot corrosion, stress rupture and low-cycle fatigue tests is shown in Table XIV. In selecting the best coating, more emphasis was placed on the performance of the coatings in tests at 1650°F for the nickel-base alloys and 1800°F for the cobalt-base alloys.

The J coating was selected as the best performing coating on six of the eight nickel-base alloys. (The coating vendor declined to apply the coating to Rene' 41 and SEL-15 alloys due to lack of performance data on these two alloys.) The hot corrosion resistance was excellent on U-710, U-700, MAR-M-246, and 713C alloys and good on IN-100 and B1900 alloys. The coating also had the lease affect on the mechanical properties of the alloys.

The A coating, which was initially selected and tested on all ten of the program alloys, provided very good protection in the hot corrosion test environment (probably due to the fact that it was thicker than the other coatings). However, diffusion instability was more severe than with the other coatings evaluated in the program, also extensive formation of sigma phase was also apparent after long term oxidation exposure. The A coating caused the largest drop in fatigue life of the six nickel-base alloys on which it was evaluated. Performance was best in the hot corrosion and stress rupture tests and rated good in the low-cycle fatigue tests on SEL-15 alloy only.

The G coating was selected for Rene' 41 alloy based mainly on performance in the low-cycle fatigue tests. The coating caused less reduction in mechanical properties than the A coating system.

On the cobalt-base alloys, the D coating was selected for the X-40 alloy and the B or C coatings for the WI-52 alloy. The D coating on X-40 was below the specified minimum thickness, only 0.0011 inch, however, performance in the hot corrosion test environment was rated fair to good. The coating had less influence on the mechanical properties of the alloy than the A coating and was therefore selected as the better coating system.

TABLE XIV

SELECTION OF BEST COATING SYSTEMS

Alloy	Best Coating			Consensus
	Hot Corrosion Tests	Stress Rupture Tests	Low-Cycle Fatigue Tests	
B1900	J	J	J	J
713C	J	J	J	J
IN-100	J	A	J	J
Rene' 41	A	(1)	G	G
SEL-15	A	A	F	A
MAR-M-246	J	J	J	J
U-700	J	A	J	J
U-710	A	J	J	J
WI-52	C	B	B or C	B or C
X-40	A	D	D	D

Notes: (1) Uncertain

Both the B and C coatings were selected as the best coatings for WI-52 alloy. Performance in the hot corrosion tests was slightly better for the C coating, but in the stress rupture tests the B coating was rated somewhat higher. In low-cycle fatigue, neither coating had an adverse effect on the fatigue life of the alloy. Both B and C coated WI-52 alloy specimens exhibited approximately the same fatigue strength as the uncoated-exposed alloy specimens.

REFERENCES

1. Blade, O. C., Aviation Fuel. Petroleum Product Survey, No. 4, 9, 14, 19, 24, 20 and 34, Bartlesville, Oklahoma. Petroleum Research Center, Bureau of Mines, 265, Department of Interior (1958-1964).

2. Kriege, O. H. and Baris, J. M., "The Chemical Portioning of Elements in γ' Separated From Precipitation-Hardened, High Temperature Nickel Base Alloys". Trans. ASM. Vol. 62 (1969).

3. Stetson, A. R., et al., "Evaluation of Coatings for Cobalt- and Nickel-Base Superalloys", NASA CR-72359, Contract NASA-9401, Vol. I, Solar RDR 1474-2 (January 1969), NASA CR-72714, Vol. II, Solar RDR 1474-3 (July 1970).

4. Redden, T. K., "Ni-Al Coating Base Metal Interactions in Several Nickel Base Alloys", Trans. AIME (January 23, 1968).

5. Colby, J. W., "Magic-A Computer Program for Quantitative Electron Microprobe Analysis", Bell Telephone Laboratories, Inc., Allentown, Pa.

6. High Temperature, High Strength Nickel-Base Alloys. The International Nickel Company, Inc., Copyright 1964, Revised Edition.

7. Metal Progress Data Sheet, June 1967, pp. 86-86A.

8. Biever, C. G., Kiholgren, T. E., "A New Cast 1850-1900°F Turbine Blade Alloy, IN-100", The International Nickel Company, Inc., New York, N.Y., (February 1961).

9. Simmons, Ward F., Preliminary Properties of Udimet 710 Alloy. Defense Metals Information Center, Batelle Memorial Institute, Columbus, Ohio, (July 23, 1969).

10. Alloy Performance Data - Udimet 700. Special Metals, Inc., New Hartford, New York.

APPENDIX I

SYNTHETIC SEA WATER

FEDERAL TEST METHOD STANDARD NO. 151

Method 812, May 6, 1959

Synthetic Sea Water

Stock Solution

KCl (c.p.)	10 gm
KBr (c.p.	45 gm
$MgCl_2 \cdot 6H_2O$ (c.p.)	550 gm
$CaCl_2 \cdot 6H_2O$ (c.p.)	110 gm

Sterile distilled H_2O to make 1 liter

Spray Solution

NaCl (c.p.)	23 gm
$Na_2SO_4 \cdot 10H_2O$	8 gm
Stock solution	20 ml

Distilled H_2O to make 1 liter

APPENDIX II

TABLES

WEIGHT CHANGE

WEIGHT CHANGE DURING HOT-CORROSION TEST
1650°F MAXIMUM TEST TEMPERATURE
35ppm SEA SALT
UNCOATED NICKEL ALLOYS

Exposure Time (Hours)	Cumulative Weight Change (mg) Specimen Number											
	B1	B2	I1	I2	S1	S2	C1	C2	U1	U2	R1	R2
10	+17.4	+54.6	+6.9	-14.0	-0.4	-7.2	+ 4.9	+ 8.9	+ 7.4	+ 8.1	+3.3	+ 2.6
20	-	-	-	-	-	-	+ 6.4	+ 11.8	+10.6	+ 8.9	+3.7	+ 2.5
30	-	-	-	-	-	-	+ 7.2	+ 11.6	+11.0	+ 9.5	+3.4	+ 2.7
40	-	-	-	-	-	-	+12.8	+ 18.2	+20.4	+23.7	+8.0	+ 7.9
50	-	-	-	-	-	-	+12.8	- 17.6	+19.4	+19.5	+3.4	+ 1.0
60	-	-	-	-	-	-	+14.9	-104.7	+19.7	+20.7	-4.3	- 8.2
70	-	-	-	-	-	-	-	-	+19.8	+20.9	-6.3	-10.3
80	-	-	-	-	-	-	-	-	+22.1	+22.5	-4.7	-10.1
90	-	-	-	-	-	-	-	-	+20.0	+21.4	-8.2	-10.4
100	-	-	-	-	-	-	-	-	+12.9	+23.2	-8.0	- 9.7
110	-	-	-	-	-	-	-	-	+10.6	+ 3.2	-6.7	- 9.3
120	-	-	-	-	-	-	-	-	-	-	-7.6	- 8.4
150	-	-	-	-	-	-	-	-	-	-	-9.3	-11.4

WEIGHT CHANGE DURING HOT-CORROSION TEST
1800°F MAXIMUM TEST TEMPERATURE
35ppm SEA SALT
UNCOATED NICKEL ALLOYS

Exposure Time (Hours)	Cumulative Weight Change (mg) Specimen Number							
	C3	C4	B29	B30	I24	I25	S3	S4
10	-418	-81.3	- 363	- 387	- 777	- 860	-	-
17	-	-	-1470	-1610	-1960	-2280	-	-
20	-	-	-	-	-	-	-4895	-3673

Exposure Time (Hours)	Cumulative Weight Change (mg) Specimen Number			
	R3	R4	U3	U4
10	-	-	+15.2	+ 5.3
20	-16.9	-16.4	+14.4	+21.8
30	-	-	+20.8	+42.4
40	-39.0	-37.0	+20.4	+43.2
50	-55.0	-52.4	+20.7	+24.4
70	-77.8	-53.0	+25.1	+21.9
80	-	-	+19.0	+17.6
100	-	-	+18.9	+17.6
120	-	-	+24.4	+17.4
140	-	-	+25.2	+12.0
150	-	-	+25.0	+35.7

Note: - denotes weight loss

WEIGHT CHANGE DURING HOT-CORROSION TEST
1800°F MAXIMUM TEST TEMPERATURE
35ppm SEA SALT
UNCOATED COBALT ALLOYS

Exposure Time (Hours)	Cumulative Weight Change (mg)			
	Specimen Number			
	W24	W25	X68	X88
10	-305	-324	-174	-194
17	-484	-511	-328	-311

Note: - denotes weight loss

WEIGHT CHANGE DURING HOT-CORROSION TEST
2000°F MAXIMUM TEST TEMPERATURE
35ppm SEA SALT
UNCOATED COBALT ALLOY

Exposure Time (Hours)	Cumulative Weight Change (mg)			
	Specimen Number			
	W26	W23	X98	X93
10	-1251	-1434	- 385	- 421
20	-	-	- 710	- 784
30	-	-	-1124	-1215
40	-	-	-	-
50	-	-	-2006	-2087

Note: - denotes weight loss

WEIGHT CHANGE DURING HOT-CORROSION TEST
1650°F MAXIMUM TEST TEMPERATURE
35ppm SEA SALT
COATED IN-100 ALLOY

Exposure Time (Hours)	Cumulative Weight Change (mg) Specimen Number									
	IA3	IA6	IC3	IC2	IF2	IF4	IG1	IG2	IJ3	IJ2
30	+ 3.6	+ 4.5	+ 21.6	+ 2.6	+0.3	0.3	+ 2.3	+1.6	+10.5	+ 9.5
60	+ 5.6	+ 7.4	-273.6	-315.6	-7.4	- 7.4	-23.4	- 1.7	+14.7	+13.9
90	+ 7.9	+10.3	-	-	+0.7	-36.6	-	-	+15.8	+15.2
120	+ 9.4	+10.7	-	-	-	-	-	-	+19.3	+17.5
150	+10.9	+12.1	-	-	-	-	-	-	+19.2	+19.3

Note: - denotes weight loss

WEIGHT CHANGE DURING HOT-CORROSION TEST
1800°F MAXIMUM TEST TEMPERATURE
35ppm SEA SALT
COATED IN-100 ALLOY

Exposure Time (Hours)	Cumulative Weight Change (mg) Specimen Number									
	IA1	IA4	IC5	IC6	IF5	IF6	IG5	IG6	IJ4	IJ5
30	+ 7.4	+5.4	-45.4	-8.5	+29.2	+25.0	+ 1.9	+ 1.5	+10.8	+11.5
60	+14.4	+9.0	-	-	-	-	+10.5	+10.7	+13.4	+14.1
90	+19.7	+3.2	-	-	-	-	+ 9.1	+ 9.1	(2)	
120	(2)						+ 9.8	-30.8		
	IA5								IJ6	
30	+ 5.6								+ 8.8	
60	+ 8.0								+10.6	
90	+13.3								+31.8	
120	-17.2								-	

Note: 1 - denotes weight loss
2 - specimens melted due to a malfunction of a temperature controller. One new specimen of each coating system added to the test.

WEIGHT CHANGE DURING HOT-CORROSION TEST
1650°F MAXIMUM TEST TEMPERATURE
35ppm SEA SALT
COATED IN-713C ALLOY

Exposure Time (Hours)	Cumulative Weight Change (mg) Specimen Number									
	CA3	CA1	CC3	CC5	CF3	CF6	CG4	CG5	CJ4	CJ5
30	+ 1.7	-0.1	+ 5.6	+10.7	+3.4	+ 2.3	+1.8	+0.4	+ 7.3	+ 6.9
60	+ 2.2	+1.3	+ 9.4	+15.0	+5.0	+ 7.1	+4.1	+4.6	+10.2	+10.2
90	+ 0.6	+1.7	+ 9.7	+18.0	-3.7	+18.7	+5.1	+5.0	+ 9.6	+11.5
120	+11.1	-4.8	+12.8	+17.3	-	-	+7.1	+8.6	+10.3	+14.3
150	+15.7	+5.7	-	-	-	-	+8.5	+7.4	+ 6.5	+13.8

Note: - denotes weight loss

WEIGHT CHANGE DURING HOT-CORROSION TEST
1800°F MAXIMUM TEST TEMPERATURE
35ppm SEA SALT
COATED IN-713C ALLOY

Exposure Time (Hours)	Cumulative Weight Change (mg) Specimen Number									
	CA4	CA5	CC1	CC4	CF1	CF2	CG1	CC..	CJ1	CJ2
30	+4.2	+5.0	+10.4	+9.0	- 13.2	- 0.9	-0.1	-0.1	+12.4	+12.7
60	+7.9	+8.9	+12.8	+4.9	-214.8	-78.0	+2.9	+2.6	+17.6	+ 13.7
90	+4.4	-1.0	-	-	-	-	+6.4	+5.3	+23.2	+19.1
120	-	-	-	-	-	-	+6.4	+6.9	+28.5	+24.4
150	-	-	-	-	-	-	+9.2	+9.5	+35.1	+30.0

Note: - denotes weight loss

WEIGHT CHANGE DURING HOT-CORROSION TEST
1650°F MAXIMUM TEST TEMPERATURE
35ppm SEA SALT
COATED B1900 ALLOY

Exposure Time (Hours)	Cumulative Weight Change (mg) Specimen Number									
	BA1	BA2	BF3	BF4	BI4	BI5	BK38	BK39	BJ1	BJ3
30	+10.3	+4.1	-162.9	-13.5	-42.5	-3.5	+ 4.9	+5.3	+ 8.3	+10.3
60	+ 5.8	+5.6	-	-	-	-	- 7.5	- 2.0	+16.2	+18.3
90	-	-	-	-	-	-	-31.0	- 2.3	+16.0	+18.7
120	-	-	-	-	-	-	-39.1	- 6.9	+11.7	- 10.4
150	-	-	-	-	-	-	-	-	-	-
Note: - denotes weight loss										

WEIGHT CHANGE DURING HOT-CORROSION TEST
1800°F MAXIMUM TEST TEMPERATURE
35ppm SEA SALT
COATED B1900 ALLOY

Exposure Time (Hours)	Cumulative Weight Change (mg) Specimen Number									
	BA4	BA6	BF5	BF6	BI1	BI3	BK51	BK53	BJ4	BJ2
20	-	-	-	-	-	-	+11.4	+17.9	-	-
30	+ 7.4	+ 7.2	- 31.2	+ 5.4	+5.9	-37.9	-	-	+11.1	+10.1
40	-	-	-	-	-	-	- 3.8	+ 1.1	-	-
60	+ 9.7	+13.0	-385.5	-98.7	-	-	- 5.1	- 0.8	+15.6	+16.2
90	+10.7	+36.4	-	-	-	-	- 5.3	- 0.4	+15.2	+16.5
120	+10.6	-34.5	-	-	-	-	-20.0	-17.3	+10.6	+17.4
140	-	-	-	-	-	-	-	-	+24.0	+29.6
150	-26.7	-48.8	-	-	-	-	-33.1	-30.6	-	-
160	-	-	-	-	-	-	-	-	+18.7	+21.0
Note: - denotes weight loss										

WEIGHT CHANGE DURING HOT-CORROSION TEST
1650°F MAXIMUM TEST TEMPERATURE
35ppm SEA SALT
COATED RENE' 41 ALLOY

Exposure Time (Hours)	Cumulative Weight Change (mg) Specimen Number							
	RA3	RA5	RC1	RC5	RF1	RF2	RG2	RG3
20	+ 4.2	+ 4.7	+4.3	+ 4.7	+1.0	+0.6	+ 1.0	+0.3
40	+ 6.3	+ 6.7	+1.9	+ 5.3	+3.0	+2.6	+ 3.3	+1.9
60	+ 7.5	+ 9.0	+3.7	+12.3	+4.6	+4.1	+ 7.1	+5.5
80	+ 8.0	+ 8.8	+3.4	+11.5	+4.5	+3.6	+ 6.3	+5.3
100	+ 8.6	+ 9.4	+4.8	+14.8	+5.7	+5.6	+ 8.2	+6.1
120	+ 9.4	+ 9.9	+3.8	+ 8.6	+4.9	+5.1	+ 8.1	+7.0
150	+10.7	+11.3	+5.4	+10.1	+6.2	+7.1	+10.1	+8.9

Note: - denotes weight loss

WEIGHT CHANGE DURING HOT-CORROSION TEST
1800°F MAXIMUM TEST TEMPERATURE
35ppm SEA SALT
COATED RENE' 41 ALLOY

Exposure Time (Hours)	Cumulative Weight Change (mg) Specimen Number							
	RA1	RA6	RC2	RC4	RF3	RF4	RG4	RG5
30	+14.1	+23.4	+ 5.1	+5.7	+ 19.0	+13.2	+1.6	+1.4
60	+13.4	+12.6	+ 7.7	+8.1	+ 28.8	+18.1	(2)	
90	+19.5	+21.1	(2)		+ 35.2	+22.8	-	-
120	+22.6	+30.1	-	-	- 28.4	- 2.9	-	-
150	+25.7	+25.8	-	-	-159.8	- 3.3	-	-

	RC6	RG6
30	+ 5.5	0
60	+ 3.6	-5.0
90	+ 7.9	-0.6
120	+17.3	+9.2
150	+16.9	+6.2

Note: 1) - denotes weight loss
2) - specimens melted due to a malfunction of a temperature controller. One new specimen of each coating system added to the test.

WEIGHT CHANGE DURING HOT-CORROSION TEST
1650°F MAXIMUM TEST TEMPERATURE
35ppm SEA SALT
COATED SEL-15 ALLOY

Exposure Time (Hours)	Cumulative Weight Change (mg) Specimen Number							
	SA1	SA2	SC5	SC6	SF1	SF2	SGI	SG2
30	+3.2	+2.2	+4.4	-56.5	-7.0	-23.0	-315.0	-440.0
60	+6.8	+4.8	-	-	-	-		
90	+6.9	+5.2	-	-	-	-		
120	+7.1	+5.4	-	-	-	-		
150	+8.6	+8.1	-	-	-	-		

Note: - denotes weight loss

WEIGHT CHANGE DURING HOT-CORROSION TEST
1800°F MAXIMUM TEST TEMPERATURE
35ppm SEA SALT
COATED SEL-15 ALLOY

Exposure Time (Hours)	Cumulative Weight Change (mg) Specimen Number							
	SA5	SA6	SC3	SC4	SF3	SF4	SG4	SG5
30	+10.1	+ 6.1	-158.3	+4.0	+3.1	+3.1	+ 0.4	+ 0.6
60	+ 3.8	+ 5.2	-	-	+7.7	+1.8	+ 7.8	+ 6.5
90	+ 3.7	+ 7.0	-	-	-	-	+15.5	+12.7
120	+ 8.7	+11.5	-	-	-	-	+14.2	+12.8
150	+14.6	+11.2	-	-	-	-	- 3.7	-14.2

Note: - denotes weight loss

WEIGHT CHANGE DURING HOT-CORROSION TEST
1650°F MAXIMUM TEST TEMPERATURE
35ppm SEA SALT
COATED U-700 ALLOY

Exposure Time (Hours)	Cumulative Weight Change (mg) Specimen Number									
	UA2	UA5	UC1	UC3	UF1	UF3	UI1	UI2	UJ1	UJ6
30	+1.9	+ 3.4	+ 8.9	+14.4	+ 3.5	+ 2.1	+ 7.8	+ 5.6	+ 9.5	+ 7.8
60	+3.4	+ 6.1	- 6.9	+ 9.5	+ 2.2	+ 1.1	+ 9.3	+ 7.7	+10.9	+10.8
90	+5.7	+ 9.2	- 47.5	- 9.4	0	+ 9.1	+10.2	+ 8.6	+12.4	+10.9
120	+6.3	+11.5	-251.8	- 60.6	-24.0	-93.9	+12.0	+14.0	+13.1	+13.5
150	+8.1	+15.3	-	-	-	-	+13.4	+12.2	+13.4	+12.2

Note: - denotes weight loss

WEIGHT CHANGE DURING HOT-CORROSION TEST
1800°F MAXIMUM TEST TEMPERATURE
35ppm SEA SALT
COATED U-700 ALLOY

Exposure Time (Hours)	Cumulative Weight Change (mg) Specimen Number									
	UA3	UA4	UC4	UC5	UF4	UF5	UI4	UI6	UJ3	UJ4
30	+ 4.5	+ 8.1	-13.9	-5.4	+14.8	+12.8	+ 9.8	+5.4	+10.6	+ 9.6
60	+19.9	+ 8.5	-	-	+11.8	+ 5.8	+11.7	+5.7	+20.3	+17.5
90	+22.5	+12.2	-	-	-	-	-	-	+21.6	+16.5
120	+ 2.7	+15.5	-	-	-	-	-	-	+22.8	+17.8
150	-	-	-	-	-	-	-	-	+19.8	-32.6

Note: - denotes weight loss

WEIGHT CHANGE DURING HOT-CORROSION TEST
1800°F MAXIMUM TEST TEMPERATURE
35ppm SEA SALT
COATED WI-52 ALLOY

Exposure Time (Hours)	Cumulative Weight Change (mg) Specimen Number									
	WA2	WA3	WB1	WB6	WC1	WC2	WD1	WD2	WH1	WH2
20	-	-	-	-	+5.4	+4.3	-	-	-	-
30	+12.1	+ 3.7	+11.4	+12.7	-	-	+15.4	+17.6	+15.7	+18.7
40	-	-	-	-	+4.9	+7.7	-	-	-	-
60	+11.8	+ 4.2	+12.9	+13.2	+3.9	+6.2	+14.0	+14.3	+14.2	+24.6
80	-	-	-	-	+4.8	+7.2	-	-	-	-
90	+16.0	+ 6.6	+15.5	+17.0	-	-	+17.3	+17.2	+ 8.9	+25.0
100	-	-	-	-	+6.0	+8.1	-	-	-	-
120	+19.6	+10.4	+18.0	+20.0	+6.5	+7.9	+19.8	+20.8	- 1.4	+26.5
140	-	-	-	-	+6.7	+9.2	-	-	-	-
150	+15.6	+ 6.3	+12.3	+14.9	+6.7	+8.5	+13.5	+14.6	-22.3	+26.1

Note: - denotes weight loss

WEIGHT CHANGE DURING HOT-CORROSION TEST
2000°F MAXIMUM TEST TEMPERATURE
35ppm SEA SALT
COATED WI-52 ALLOY

Exposure Time (Hours)	Cumulative Weight Change (mg) Specimen Number									
	WA4	WA5	WB2	WB3	WC4	WC5	WD3	WD4	WH3	WH6
30	- 42.7	+18.2	+ 3.0	+9.0	+6.4	+32.5	+10.3	+12.3	- 13.2	- 6.3
60	-139.6	- 18.6	-16.0	- 5.0	+2.4	- 33.8	- 11.7	- 12.1	-275.8	-197.6
90	-	-	-	-	-	-	-	-	-	-
120	-	-	-	-	-	-	-	-	-	-
150	-	-	-	-	-	-	-	-	-	-

Note: - denotes weight loss

WEIGHT CHANGE DURING HOT-CORROSION TEST
1800°F MAXIMUM TEST TEMPERATURE
35ppm SEA SALT
COATED X-40 ALLOY

Exposure Time (Hours)	Cumulative Weight Change (mg) Specimen Number									
	XA1	XA2	XB1	XB2	XC1	XC6	XD1	XD2	XH1	XH4
20	+ 6.4	+4.8	+4.1	+ 5.9	-	-	+ 5.9	+6.6	+31.4	+28.7
30	-	-	-	-	+ 8.7	+11.3	-	-	-	-
40	+ 8.0	0.0	+4.9	+ 7.9	-	-	+ 9.1	+8.0	+34.0	+25.9
60	+ 8.8	+5.4	+6.1	+ 8.1	+10.1	+19.2	+ 9.9	+7.7	+31.3	+18.3
80	+19.7	+5.9	+8.8	+11.0	-	-	+10.8	+7.7	-	-
90	-	-	-	-	+14.4	+11.0	-	-	+46.3	+13.9
100	+10.5	+7.0	+8.7	+13.1	-	-	+10.7	+8.2	-	-
120	+10.0	+6.4	+9.7	+13.4	+16.9	+14.3	+10.3	+8.4	+35.1	+18.4
140	+10.9	+7.5	+6.1	+17.3	-	-	+11.7	+9.2	-	-
150	+10.4	+6.9	+1.1	+17.1	+14.9	+13.8	+11.4	+9.6	+22.7	- 1.8

Note: - denotes weight loss

WEIGHT CHANGE DURING HOT-CORROSION TEST
2000°F MAXIMUM TEST TEMPERATURE
35ppm SEA SALT
COATED X-40 ALLOY

Exposure Time (Hours)	Cumulative Weight Change (mg) Specimen Number									
	XA3	XA4	XB3	XB5	XC2	XC4	XD3	XD5	XH5	XH6
30	+24.4	+18.6	+29.2	+22.4	+19.7	+20.8	+32.5	+34.3	-112.1	- 3.4
60	+28.4	+18.9	+34.5	+26.0	+10.2	+26.6	+27.6	+32.7	-726.3	-114.7
90	+20.7	+19.3	+36.1	+12.8	-47.5	- 1.6	+23.2	+ 2.4	-	-
120	0.0	- 0.3	-	-	-	-	-	-	-	-
150	- 1.0	- 4.0	-	-	-	-	-	-	-	-

Note: - denotes weight loss

WEIGHT CHANGE DURING HOT-CORROSION TESTS
1650°F MAXIMUM TEST TEMPERATURE
35 ppm SEA SALT
MAR-M-246 ALLOY

Exposure Time (Hours)	Cumulative Weight Change (mg) Specimen Number							
	MA1	MA2	MG1	MG2	MJ1	MJ3	M1	M2
20	-	-	-18.3	-24.4	+ 4.8	+ 5.3	-16.1	-65.9
30	+3.8	+3.5	-	-	-	-	-	-
40	-	-	- 7.8	-65.9	+ 9.5	+ 9.1	-	-
60	+4.5	+5.2	-	-	+23.3	+19.4	-	-
80	-	-	-	-	+15.6	+18.4	-	-
90	+4.5	+5.8	-	-	-	-	-	-
100	-	-	-	-	+14.4	+19.7	-	-
120	+7.5	+6.7	-	-	+16.7	+24.6	-	-
140	-	-	-	-	+22.1	+26.0	-	-
150	+6.4	+8.2	-	-	+23.8	+28.0	-	-

Note: - denotes weight loss

WEIGHT CHANGE DURING HOT-CORROSION TESTS
1650°F MAXIMUM TEST TEMPERATURE
35 ppm SEA SALT
U-710 ALLOY

Exposure Time (Hours)	Cumulative Weight Change (mg) Specimen Number							
	DA1	DA2	DG1	DG2	DJ1	DJ2	D1	D2
20	-	-	- 1.9	-4.5	+ 7.1	+ 5.7	+ 4.2	+ 2.5
30	+2.7	+3.2	-	-	-	-	-	-
40	-	-	+ 5.7	+4.2	+13.1	+ 6.1	+ 5.7	+ 4.3
60	+5.1	+5.5	+ 2.4	+2.2	+18.1	+26.9	+10.3	+ 8.2
80	-	-	+ 4.9	-0.6	+16.6	+15.8	+13.6	+12.6
90	+6.4	+5.7	-	-	-	-	-	-
100	-	-	+11.5	+4.3	+17.7	+16.2	+18.8	+22.2
120	+7.0	+7.6	+16.1	+8.3	+20.9	+20.5	+18.2	+16.6
150	+7.6	+7.5	+14.5	+9.9	+26.5	+28.5	+26.0	+22.5

Note: - denotes weight loss

WEIGHT CHANGE DURING HOT-CORROSION TESTS
1800°F MAXIMUM TEST TEMPERATURE
35 ppm SEA SALT
MAR-M-246 ALLOY

Exposure Time (Hours)	Cumulative Weight Change (mg) Specimen Number									
	M4	M5	MA3	MA4	MA5	MG3	MG4	MJ2	MJ4	MJ5
20	+173	+109	-	-	-	-	-	-	-	-
30	-	-	+2.2	-599	-186	-0.3	+1.0	+ 4.4	+ 1.3	+ 4.3
60	-	-	+3.5	-	-	-0.4	+4.4	+ 8.2	+ 9.8	+10.8
90	-	-	+3.6	-	-	+3.3	+5.0	+10.1	+ 7.8	+10.6
120	-	-	+6.6	-	-	+5.5	+6.8	+10.4	+ 9.1	+11.5
150	-	-	-	-	-	+8.5	+9.8	-	+16.2	+13.7

Note: - denotes weight loss

WEIGHT CHANGE DURING HOT-CORROSION TESTS
1800°F MAXIMUM TEST TEMPERATURE
35 ppm SEA SALT
U-710 ALLOY

Exposure Time (Hours)	Cumulative Weight Change (mg) Specimen Number							
	D4	D5	DA3	DA4	DG4	DG5	DJ4	DJ5
20	+11.4	+ 7.2	-	-	-	-	-	-
30	-	-	+ 5.8	+ 5.5	+ 8.4	+ 6.8	+12.2	+16.2
40	+14.3	+10.4	-	-	-	-	-	-
60	+11.9	+16.6	+ 9.7	+ 9.1	+13.2	+12.2	+12.4	+15.0
80	+12.2	+19.4	-	-	-	-	-	-
90	-	-	+12.6	+11.1	+13.9	+12.9	+20.0	+22.2
100	+13.4	+25.0	-	-	-	-	-	-
120	+ 9.9	+13.7	+16.3	+13.8	+18.9	+16.7	+20.4	+22.3
150	+ 5.2	+ 8.9	+19.8	+16.4	+21.2	+19.6	+23.3	+25.3

APPENDIX III

STRESS RUPTURE TABLES

FATIGUE TEST TABLES

SUMMARY OF LOW-CYCLE FATIGUE TESTS ON UNCOATED ALLOYS

As-Received Alloys				As-Thermaliy Exposed for 500 Hours[1]		
Specimen Identification Code		Maximum Stress (ksi)	Fatigue Life, N (cycles x 10^3)	Specimen Identification Code	Maximum Stress (ksi)	Fatigue Life, N (cycles x 10^3)
B1900 Alloy	B-1	118	4.0	B-5	106	3.5
	B-2	118	3.0	B-6	106	2.8
	B-3	112	6.5	B-7	95	12.5
	B-4	106	10.5	B-8	95	16.0
713-C Alloy	C-1	120	3.5	C-5	114	13.5
	C-2	117	6.0[2]	C-6	114	21.0
	C-3	117	6.5	C-7	118	5.3
	C-4	114	8.3	C-8	118	4.0
IN-100 Alloy	I-1	127	2.0	I-5	114	13.3
	I-2	123	5.0	I-6	118	6.0
	I-3	118	9.5	I-7	114	18.0
	I-4	114	14.0	I-8	123	3.5
Rene' 41 Alloy	R-1	138	2.2	R-5	115	10.5
	R-2	123	11.0	R-6	115	4.5
	R-3	100	+110.0[3]	R-7	110	8.6
	R-3A	115	15.0	R-8	110	+50.0[3]
	R-4	120	36.0[4]			
SEL-15 Alloy	S-1	119	3.0	S-5	110	9.8
	S-2	116	8.0	S-6	110	16.5
	S-3	110	22.0	S-7	115	2.0
	S-4	110	18.5	S-8	115	4.3
U-700 Alloy	U-1	138	6.6[2]	U-5	128	2.0
	U-2	128	6.0	U-6	128	1.8
	U-3	128	8.0[2]	U-7	118	4.4
	U-4	128	26.0	U-8	108	16.4
	U-20	130	10.5			
	U-22	125	18.0			
	U-23	132	11.0			
	U-21	128	25.0			
WI-52 Alloy	W-1	53	+50.0[3]	W-5	68	0[6]
	W-1A	67	11.0	W-6	60	14.5
	W-2	70	13.5	W-7	60	28.5
	W-3	72	0.5	W-8	65	7.1
	W-4	68	22.6			
X-40 Alloy	X-1	53	+50.0[3]	X-5	60	4.3
	X-1A	57	18.0	X-6	60	3.5
	X-2	(5)	--	X-7	50	+50.0[3]
	X-3	65	2.0	X-7A	55	36.0
	X-4	60	8.4	X-8	57	23.0

(Cont)

SUMMARY OF LOW-CYCLE FATIGUE TESTS ON UNCOATED ALLOYS

As-Received Alloys				As-Thermally Exposed for 500 Hours(1)		
	Specimen Identification Code	Maximum Stress (ksi)	Fatigue Life, N (cycles x 10^3)	Specimen Identification Code	Maximum Stress (ksi)	Fatigue Life, N (cycles x 10^3)
M246 Alloy	M-1	135	2.80	M-1	120	6.50
	M-2	130	5.96	M-2	110	13.06
	M-3	125	9.25	M-3	125	2.00
	M-4	120	17.17	M-4	115	6.85
U-710 Alloy	D-1	90	+50.00(3)	D-1	105	7.00
	D-1	125	3.00	D-2	95	24.50
	D-2	120	2.50	D-3	100	4.50
	D-3	115	3.60	D-4	100	4.80
	D-4	105	9.80			

Notes: Temperature: 1400° F Stress Ratio R = 0.15, Frequency 20 cps

(1) Nickel alloys exposed at 1800° F, cobalt alloys exposed at 2000° F
(2) Thread root failure 0.25 inch diameter test area
(3) No failure - specimen re-run at higher stress
(4) Thread root failure 0.185 inch diameter test area
(5) Specimen broke during machining
(6) Specimen failed on start-up

SUMMARY OF LOW-CYCLE FATIGUE TESTS ON COATED ALLOYS THERMALLY EXPOSED FOR 500 HOURS(1)

Specimen Identification Code		Maximum Stress (ksi)(4)	Life (cycles x 10^3)	Specimen Identification Code		Maximum Stress (ksi)	Life (cycles x 10^3)
B1900 Alloy	K	92	0.50	SEL-15 Alloy	A	110	<0.001 (3)
		90	9.00			102	1.20
		87	6.00			100	2.20
		85	9.50			97	7.00
		80	+50.00 (2)			95	13.50
	J	106	0.90		F	100	2.00
		100	2.10			98	7.80
		96	6.30			96	27.00
		92	9.80			95	30.00
713-C Alloy	G	114	<0.001 (3)	U-700 Alloy	A	105	1.10
		109	0.05			100	1.70
		100	1.20			95	2.00
		95	8.20			90	2.50
		92	5.20			85	3.50
	J	101	1.00		J	102	2.10
		100	0.70			100	2.00
		97	2.80			95	2.50
		95	40.00			90	5.00
						85	+50.00 (2)
IN-100 Alloy	A	106	1.50				
		104	1.00	WI-52 Alloy	B	68	1.20
		100	1.20			65	5.60
		95	2.20			62	12.80
		90	3.80			60	+50.00 (2)
	J	110	1.20		C	68	<0.001 (3)
		105	14.00			68	0.90
		102	4.40			62	4.50
		100	1.80			61	6.60
		95	+50.00 (2)			60	+50.00 (2)
		92	27.00				
				X-40 Alloy	\	60	1.50
Rene' 41 Alloy	A	110	<0.001 (3)			55	3.50
		100	0.05			52	4.70
		90	1.00			47	9.50
		80	2.40		D	70	5.00
		76	3.10			70	2.10
	G	102	1.10			65	5.50
		100	1.40			62	11.00
		90	2.60			55	+50.00 (2)
		85	2.50				
		80	7.50				

Notes: (1) Nickel alloys exposed in air atmosphere at 1800°F; cobalt alloys exposed in air atmosphere at 2000°F.
(2) No failure.
(3) Specimens failed on start-up.
(4) Stress calculated based on specimen area prior to coating.

(Cont)

SUMMARY OF LOW-CYCLE FATIGUE TESTS ON COATED ALLOYS THERMALLY EXPOSED FOR 500 HOURS

Specimen Identification Code		Maximum Stress (ksi)	Life (cycles x 10^3)
U-710 Alloy	A	100	1.00
		90	2.00
		80	4.20
		77	6.80
		75	+50.00
	J	90	2.10
		80	8.00
		77	13.50
		75	+50.00
MAR-M246 Alloy	A	115	4.50
		110	10.00
		105	9.80
		100	13.00
		97	14.40
	J	115	0.60
		110	6.90
		105	12.80
		102	13.50

SUMMARY OF STRESS RUPTURE RESULTS OF UNCOATED ALLOYS

Alloy	Test Number	Test Temperature (° F)	Stress (ksi)	Time To Rupture (hrs)	Elongation (%)
713C	1	1650	39.0	53.3	10.0
	2	1650	39.0	48.7	9.0
	3	1650	36.0	114.9	12.0
	4	1800	22.0	25.5	15.0
	5	1800	20.0	65.9	16.0
Rene' 41	1	1650	17.0	70.2	56.0
	2	1650	17.0	95.6	34.0
	3	1800	5.0	193.2	37.0
	4	1800	5.0	227.8	39.0
SEL-15	1	1650	42.0	119.6	4.0
	2	1650	42.0	48.9	4.0
	3	1800	20.0	46.1	1.0
	4	1800	20.0	67.1	2.0
U700	1	1650	35.0	116.9	8.0
	2	1650	35.0	92.3	9.0
	3	1800	17.0	64.7	41.0
	4	1800	17.0	106.4	10.0
WI-52	1	1800	13.0	66.7	11.0
	2	1800	13.0	122.5	9.5
	3	2000	6.0	44.8	11.0
	4	2000	6.0	56.8	9.0
X-40	1	1800	12.0	77.2	(1)
	2	1800	12.0	116.5	10.0
	3	2000	5.5	88.4	12.0
	4	2000	5.5	149.6	6.6
B1900	1	1650	48.0	64.9	4.0
	2	1650	48.0	56.3	6.0
	3	1800	26.0	79.8	10.0
	4	1800	26.0	79.4	7.0
IN-100	1	1650	48.0	71.9	5.0
	2	1650	48.0	35.2	7.0
	3	1800	26.0	51.6	11.0
	4	1800	26.0	40.7	10.0

(Cont)

SUMMARY OF STRESS RUPTURE RESULTS OF UNCOATED ALLOYS

Alloy	Specimen Number	Temperature °F	Stress (ksi)	Time (hour)	Elongation (%)
MAR-M246	M1	1650	53.0	92.9	5.0
	M3	1650	53.0	80.0	6.3
	M2	1800	28.0	183.0	3.5
	M4 (2)	1800	28.0	68.3	7.2
	M5	1800	28.0	91.8	3.1
UD-710	D1	1650	36.0	149.9	10.0
	D3	1650	36.0	89.6	14.4
	D2 (3)	1800	18.0	>66.0	---
	D4	1800	19.0	70.6	7.2
	D5	1800	19.0	61.6	10.1

Notes: (1) Failed outside gage marks.
(2) Threads in grip pulled loose at 27.7 hours. Shut off machine. Test restarted.
(3) Test terminated at 66.0 hours due to temperature controller malfunction.

SUMMARY OF STRESS RUPTURE RESULTS AT 1650°F ON COATED ALLOYS

Alloy and Stress[2]	Coating	Thermally Exposed for 500 Hours[1]		Thermally Exposed for 500 Hours, Stripped and Recoated[1]	
		Time to Rupture (Hours)	Elongation (%)	Time to Rupture (Hours)	Elongation (%)
B1900	J	115.9	5.0	13.0	5.0
48.0 ksi	J	29.9	10.0	9.8	2.0
	K	11.1	8.5	12.2	3.5
	K	9.0	6.5	10.1	4.0
	K	7.5	5.5	--	--
713C	G	96.3	8.2	24.3	11.5
39.0 ksi	G	41.0	18.5	4.5	12.0
	J	55.2	13.0	152.2	12.0
	J	31.6	14.0	26.8	10.0
	J	2.9	19.0	--	--
IN-100	A	49.2	10.5	49.1	13.0
48.0 ksi	A	43.8	10.5	44.2	11.5
	A	27.7	9.0	--	--
	J	30.1	12.0	37.5	11.0
	J	20.4	13.0	36.2	11.0
MAR-M-246	A	29.4	7.0	53.7	9.0
53.0 ksi	A	21.4	8.5	34.0	8.0
	J	33.8	8.0	33.5	13.0
	J	28.8	6.5	31.7	6.0
	J	--	--	16.1	9.0
Rene' 41	A	>329	>1.0	>213	>2.5
17.0 ksi	A	>210	>2.0	>213	>1.0
	A	>184	>3.5	--	--
	G	>302	>2.3	259.1	31.0
	G	206.7	29.5	>232	>5.0
SEL-15	A	63.1	3.5	53.6	2.0
42.0 ksi	A	51.0	4.5	32.3	7.0
	A	22.9	4.0	--	--
	F	43.7	3.5	41.3	3.5
	F	36.4	4.5	35.3	--
	F	--	--	10.1	4.0
U-700	A	156.0	4.0	70.5	6.5
35.0 ksi	A	57.1	9.0	70.0	8.5
	J	104.4	10.0	71.1	12.0
	J	37.0	8.5	67.4	9.0
U-710	A	24.6	10.0	74.7	9.0
36.0 ksi	A	22.8	12.0	72.5	6.0
	J	49.8	10.5	77.8	15.0
	J	48.7	15.0	59.8	16.0

Notes:

1. Nickel base alloys exposed at 1800°F, cobalt base alloys exposed at 2000°F, air atmosphere.
2. Stress calculated based on specimen areas prior to coating.
3. >Denotes specimen did not fail. Test terminated at hours shown.

SUMMARY OF STRESS RUPTURE RESULTS AT 1800°F ON COATED ALLOYS

Alloy and Stress(2)	Coating	Thermally Exposed for 500 Hours(1)		Thermally Exposed for 500 Hours, Stripped and Recoated(1)	
		Time to Rupture (Hours)	Elongation (%)	Time to Rupture (Hours)	Elongation (%)
B1900	J	35.7	9 0	64 0	13 0
26 0 ksi	J	28.9	10.5	26.4	13.5
	K	92 6	10.0	16.5	13 5
	K	6 2	13.0	15 3	12.0
	K	---	---	14.8	11 0
713C	G	32 3	12 0	126 4	18.0
20 0 ksi	G	18.5	10.1	80.4	20.0
	J	44 1	16.0	67.0	13.0
	J	43 2	15 0	26 6	17 0
IN-100	A	39 5	6 0	34 4	10.5
26 0 ksi	A	32.2	7.0	5 4	13.0
	J	31.9	13.0	58.2	12.0
	J	28 6	13.0	49 1	12.0
MAR-M-246	A	62.4	6 0	49.4	7 0
28 0 ksi	A	37.3	7 0	41.6	9.0
	J	46.1	7.0	52.5	4.0
	J	14 9	7.0	49.4	4 0
Rene' 41	A	>363.0	>2.5	>258.0	>2.0
5.0 ksi	A	>356 0	>1 2	>209.0	>1 5
	G	>335 0	>2 0	>211.0	>2.0
	G	>322.0	>2.0	>209.0	>2 5
SEL-15	A	164 5	1 5	85.6	4.0
20 0 ksi	A	65.9	3.5	64.2	5 5
	F	38.9	12.5	88.9	2.5
	F	37.0	11.5	24.2	2.0
U-700	A	15.5	8 5	68 0	12 0
17 0 ksi	A	6.4	10.0	30 4	8.0
	J	49 1	12 5	46.1	10.0
	J	42.6	9 0	44.1	12.0
	J	11.1	13 0	---	---
U-710	A	72.8	12 0	46 0	13.0
19 0 ksi	A	31.4	10.0	15.4	5.0
	J	75 5	10 0	54 1	11 0
	J	56 3	14 5	25 3	11.0
WI-52	B	40 1	19.0	253.5	7.0
13.0 ksi	B	28.9	12.0	29.6	24.0
	B	---	---	3 5	31.0
	C	33 7	33.0	30.7	25.0
	C	15.7	19.5	10.5	9.0
X-40	A	152.3	31.0	36.4	45.0
12 0 ksi	A	30.0	48.0	32.4	52.0
	D	119 3	33.5	95.8	29.0
	D	36.4	34 0	78.2	29.5

Notes

1 Nickel-base alloys exposed at 1800° F, cobalt-base alloys exposed at 2000° F, air atmosphere.

2 Stress calculated based on specimen area prior to coating

3. > Denotes specimen did not fail Test terminated at hours shown

SUMMARY OF STRESS RUPTURE RESULTS AT 2000°F ON COATED ALLOYS

Alloy and Stress[2]	Coating	Thermally Exposed for 500 Hours[1]		Thermally Exposed for 500 Hours, Stripped and Recoated[1]	
		Time to Rupture (Hours)	Elongation (%)	Time to Rupture (Hours)	Elongation (%)
WI-52 6.0 ksi	B	55.6	12.0	27.8	15.0
	B	26.8	10.8	4.0	14.0
	B	2.1	20.0	---	---
	C	60.6	14.0	27.1	17.0
	C	27.8	18.5	16.8	21.5
	C	---	---	3.3	20.0
X-40 5.5 ksi	A	>183.0	>4.5	164.1	25.0
	A	>183.0	>6.5	35.4	39.5
	D	>183.0	>2.0	>232.0	>3.5
	D	>179.0	>1.5	>209.0	>6.0

Notes:

1. Alloy exposed at 2000° F in air atmosphere.
2. Stress calculated based on specimen area prior to coating.
3. > Denotes specimen did not fail. Test terminated at hours shown.

Unclassified

Security Classification

DOCUMENT CONTROL DATA - R&D

(Security classification of title, body of abstract and indexing annotation must be entered when the overall report is classified)

1 ORIGINATING ACTIVITY (Corporate author)	2a REPORT SECURITY CLASSIFICATION
Solar Division of International Harvester Company 2200 Pacific Highway, San Diego, California 92112	Unclassified 2b GROUP --

3 REPORT TITLE

Hot Corrosion of Coated Superalloys in a Gas Turbine Environment

4 DESCRIPTIVE NOTES (Type of report and inclusive dates)

Final Report - 3 July 1968 through 30 November 1970

5 AUTHOR(S) (Last name, first name, initial)

Moore, V. S., Stetson, A. R.

6 REPORT DATE	7a TOTAL NO. OF PAGES	7b NO. OF REFS
15 December 1970	246	10

8a CONTRACT OR GRANT NO	9a ORIGINATOR'S REPORT NUMBER(S)
N00019-68-C-0532 b PROJECT NO	Research Department Report No. 1626-5
c d	9b OTHER REPORT NO(S) (Any other numbers that may be assigned this report)

10 AVAILABILITY/LIMITATION NOTICES

~~Distribution of this document is unlimited~~

11 SUPPLEMENTARY NOTES	12 SPONSORING MILITARY ACTIVITY
	Department of the Navy Naval Air Systems Command (AIR-53674) Washington, D. C. 20360

13 ABSTRACT

The final results of a Hot Corrosion Rig Test Evaluation of 45 coating-alloy combinations are presented. Alloys included in the program were B1900, 713C, IN-100, Rene' 41, SEL-15, U-700, U-710, MAR-M-246, WI-52 and X-40. Rig tests were performed for up to 150 hours at 1650°F and 1800°F on nickel-base alloys and 1800°F and 2000°F on cobalt-base alloys in a high-velocity environment obtained from the combustion of JP-5 fuel and air and ingestion of 35 parts sea salt per one million parts air.

The coatings tested were commercially available and were essentially βNiAl or βCoAl with numerous secondary phases, some of which were formed from the reaction of coating elements and substrate and some of which were formed by elements codeposited with aluminum.

Under the conditions of the test, protection could be afforded by at least one of the coatings on the nickel-base alloys for 150 hours at 1650°F and 100 hours at 1800°F. At 1800°F the relatively thin coatings on cobalt-base alloys exhibited poorer protection than coated nickel-base alloys at this temperature. At 2000°F the coatings on WI-52 could not afford protection beyond 60 hours. Performance was only slightly better on the higher-chromium X-40 alloy. The life of coatings closely correlated with thickness on both nickel- and cobalt-base alloys and was strongly influenced by the chromium content of the substrate. Minor additives to the aluminides, notably silicon, also significantly enhanced the performance of the aluminide coatings on nickel-base alloys.

The effects of coatings, processing conditions, and long-term high temperature exposures on the mechanical properties of the nickel- and cobalt-base alloys were also evaluated. Data are presented on (1) the low-cycle fatigue life of the ten alloys uncoated as-received, uncoated and coated after 500 hours exposure at high temperature, and (2) the elevated temperature stress rupture properties of the coated alloys after long term exposures and after coating stripping and recoating operations to simulate repair of used blades and vanes.

DD FORM 1 JAN 54 1473

Unclassified

Security Classification

14 KEY WORDS	LINK A		LINK B		LINK C	
	ROLE	WT	ROLE	WT	ROLE	WT
Sulfidation-erosion tests						
Hot corrosion						
Turbine blades and vanes						
Commercially available coatings						
Nickel-base alloys						
Cobalt-base alloys						
1650°F						
1800°F						
2000°F						
Mechanical Properties						
Low-Cycle Fatigue Tests						
Stress Rupture Tests						

INSTRUCTIONS

1. ORIGINATING ACTIVITY: Enter the name and address of the contractor, subcontractor, grantee, Department of Defense activity or other organization *(corporate author)* issuing the report.

2*a*. REPORT SECURITY CLASSIFICATION: Enter the overall security classification of the report. Indicate whether "Restricted Data" is included. Marking is to be in accordance with appropriate security regulations.

2*b*. GROUP: Automatic downgrading is specified in DoD Directive 5200.10 and Armed Forces Industrial Manual. Enter the group number. Also, when applicable, show that optional markings have been used for Group 3 and Group 4 as authorized.

3. REPORT TITLE: Enter the complete report title in all capital letters. Titles in all cases should be unclassified. If a meaningful title cannot be selected without classification, show title classification in all capitals in parenthesis immediately following the title.

4. DESCRIPTIVE NOTES: If appropriate, enter the type of report, e.g., interim, progress, summary, annual, or final. Give the inclusive dates when a specific reporting period is covered.

5. AUTHOR(S). Enter the name(s) of author(s) as shown on or in the report. Enter last name, first name, middle initial. If military, show rank and branch of service. The name of the principal author is an absolute minimum requirement.

6. REPORT DATE: Enter the date of the report as day, month, year, or month, year. If more than one date appears on the report, use date of publication.

7*a*. TOTAL NUMBER OF PAGES: The total page count should follow normal pagination procedures, i.e., enter the number of pages containing information.

7*b*. NUMBER OF REFERENCES: Enter the total number of references cited in the report.

8*a*. CONTRACT OR GRANT NUMBER: If appropriate, enter the applicable number of the contract or grant under which the report was written.

8*b*, 8*c*, & 8*d*. PROJECT NUMBER: Enter the appropriate military department identification, such as project number, subproject number, system numbers, task number, etc.

9*a*. ORIGINATOR'S REPORT NUMBER(S): Enter the official report number by which the document will be identified and controlled by the originating activity. This number must be unique to this report.

9*b*. OTHER REPORT NUMBER(S): If the report has been assigned any other report numbers *(either by the originator or by the sponsor)*, also enter this number(s).

10. AVAILABILITY/LIMITATION NOTICES: Enter any limitations on further dissemination of the report, other than those imposed by security classification, using standard statements such as:

(1) "Qualified requesters may obtain copies of this report from DDC."

(2) "Foreign announcement and dissemination of this report by DDC is not authorized."

(3) "U. S. Government agencies may obtain copies of this report directly from DDC. Other qualified DDC users shall request through

_____."

(4) "U. S. military agencies may obtain copies of this report directly from DDC. Other qualified users shall request through

_____."

(5) "All distribution of this report is controlled. Qualified DDC users shall request through

_____."

If the report has been furnished to the Office of Technical Services, Department of Commerce, for sale to the public, indicate this fact and enter the price, if known.

11. SUPPLEMENTARY NOTES: Use for additional explanatory notes.

12. SPONSORING MILITARY ACTIVITY: Enter the name of the departmental project office or laboratory sponsoring *(paying for)* the research and development. Include address.

13. ABSTRACT: Enter an abstract giving a brief and factual summary of the document indicative of the report, even though it may also appear elsewhere in the body of the technical report. If additional space is required, a continuation sheet shall be attached.

It is highly desirable that the abstract of classified reports be unclassified. Each paragraph of the abstract shall end with an indication of the military security classification of the information in the paragraph, represented as *(TS), (S), (C), or (U)*

There is no limitation on the length of the abstract. However, the suggested length is from 150 to 225 words.

14. KEY WORDS: Key words are technically meaningful terms or short phrases that characterize a report and may be used as index entries for cataloging the report. Key words must be selected so that no security classification is required. Identifiers, such as equipment model designation, trade name, military project code name, geographic location, may be used as key words but will be followed by an indication of technical context. The assignment of links, rules, and weights is optional.